

UNIVERSITY OF LATVIA
FACULTY OF CHEMISTRY

DISSERTATION

Synthesis of novel cationic 1,4-dihydropyridine and 3,4-dihydropyridone based fluoros amphiphiles for possible transmembrane delivery applications

RUFUS SMITS

Supervisor

Dr.chem. BRIGITA VĪGANTE

Advisor

Dr.chem. prof. G.W. BUCHANAN

RĪGA

2012

The practical work of this dissertation was carried out at the Latvian organic synthesis institute in the time frame from 2007 to 2012.

Reviewers: Dr. Chem. Habil. G. Veinbergs
Dr. Chem. Habil. Prof. A. Zicmanis

Supervisor Dr. Chem. Brigita Vigante

Advisor Dr. Chem. Prof. G.W. Buchanan

ABSTRACT

Synthesis of novel 1,4-dihydropyridine and 3,4-dihydropyridone based fluorous cationic amphiphiles for possible transmembrane delivery applications. Smits R., Dr. Chem. Prof. G.W. Buchanan, Dr. Chem. Vigante B., Doctor's Thesis , 163 pages, 48 figures, 54 schemes, 6 tables, 266 references. In English language.

1,4-DIHYDROPYRIDINE, 3,4-DIHYDROPYRIDONE, FLUOROUS ESTERS, CATIONIC AMPHIPHILES, DNA TRANSFECTION, DRUG DELIVERY, BROMINATION, OXIDATION, CHLORO-FORMYLATION, HYDROGEN BONDING, SELF-ASSEMBLY, X-RAY DIFFRACTION, ¹⁹F-MRI.

In this work both the pharmacologically and synthetically versatile 1,4-dihydropyridines and 3,4-dihydropyridones in combination with the unique properties of fluorous long chain alkyl esters allow the generation of novel putative transmembrane delivery agents, addressing the self-assembly, stability, toxicity and gene transfection problems of current systems with the added advantage that these carriers can be tracked *in vivo* by non-invasive ¹⁹F-magnetic resonance imaging. Along the way some fundamental chemistry aspects, such as stereo-specific bromination, hydrogen bonding and oxidation of the 1,4-dihydropyridine and 3,4-dihydropyridone heterocycles are explored. X-ray diffraction is used throughout the work to provide molecular interaction data and unequivocal structural proofs of the synthesized compounds.

KOPSAVILKUMS

Fluorsaturošu katjono 1,4-dihidropiridīna un 3,4-dihidropiridona amfifīlu sintēze transmembrānu nogādes pētījumiem.

Smits R., Dr. Ķīm. Prof. G.W. Buchanan, Dr. Ķīm. Vīgante B., Doktora disertācija, 163 lappuses, 48 attēli, 54 shēmas, 6 tabulas, 266 atsauces. Angļu valodā.

1,4-DIHDROPIRIDĪNS, 3,4-DIHDROPIRIDONS, FLUORĒTIE ESTERI, KATJONIE AMFIFĪLI, DNS TRANSFEKCIJA, ZĀĻU PĀRNESE, BROMĒŠANA, OKSIDĒŠANA, HLORO-FORMILĒŠANA, ŪDEŅRAŽA SAITES VEIDOŠANA, PAŠAGREGĒŠANĀS, RENTGENSTARU DIFRAKCIJA, ¹⁹F-KMR.

Šajā darbā apskatīta 1,4-dihidropiridīnu un 3,4-dihidropiridonu farmakoloģiskā un sintētiskā daudzveidība. Kombinācijā ar garu fluorētu alkilesteru unikālajām īpašībām veidoti iespējami transmembrānu aģenti, risinot līdz šim zināmo sistēmu pašagregēšanās, stabilitātes, toksicitātes un gēnu transfekcijas problēmas ar būtisku priekšrocību – šie nesēji var tikt izsekoti *in vivo* ar maz agresīvu ¹⁹F-magnētisko rezonansi. Darba gaitā izskaidroti vairāki fundamentāli 1,4-dihidropiridīnu un 3,4-dihidropiridonu ķīmijas aspekti, tādi kā stereospecifiska bromēšana, ūdeņraža saites veidošanās un heterocikla oksidēšanās. Lai neapšaubāmi pierādītu sintezēto savienojumu struktūru un iegūtu molekulāro iedarbību datus, izmantota rentgenstruktūras analīze.

CONTENTS

INTRODUCTION	10
1. LITERATURE REVIEW	14
1.1. Gene transfection	14
1.2. siRNA-mediated gene silencing	17
1.3. siRNA delivery systems for in vivo application	18
1.4. Lipid-based siRNA delivery	19
1.5. Cationic amphiphiles	20
1.6. 1,4-Dihydropyridine as linker	23
1.7. 3,4-Dihydropyridone as linker	27
1.8. Fluorinated carriers	30
1.9. ¹⁹ F-imaging	32
2. RESULTS AND DISCUSSION	35
2.1. Synthesis of perfluorinated 1,4-dihydropyridine amphiphiles.....	35
2.2. Synthesis of 3,4-dihydro-2(1 <i>H</i>)-pyridones (DHPODs).....	49
2.3. Bromination of 3,4-dihydro-2(1 <i>H</i>)-pyridones	58
2.4. Oxidation potential determination of DHP and DHPOD derivatives using CV.72	
2.5. The 6-bromomethyl-3,4-dihydro-2(1 <i>H</i>)-pyridones as versatile synthons	81
2.6. Vilsmeier-Haack chloroformylation of DHPOD and subsequent reactions	85
2.7. The unexpected 4 <i>H</i> -pyran synthesis under solvent-free and grinding.....	89
conditions	
2.8. Biological activities	95
2.9. ¹⁹ F-MRI of fluorinated sucrose octaoleate-F104	99
3. CONCLUSION.....	102
4. EXPERIMENTAL.....	104

Publications.....	146
References.....	148
Additions.....	161

ABBREVIATIONS

Å	Angstrom
Ac	acetyl
AcOH	acetic acid
AIBN	azobisisobutyronitrile
AFM	atomic force microscopy
Ar	aromatic group
Bn	benzyl
°C	degrees Celsius
cm ⁻¹	wavenumbers
DCM	dichloromethane
DHP	dihydropyridine
DHPOD	dihydropyridone
DLS	dynamic light scattering
DMAP	4-(dimethylamino)pyridine
DMF	dimethylformamide
DMSO	dimethylsulfoxide
DNA	deoxyribonucleic acid
E ⁺	generic electrophile
EDC	1-ethyl-3-(3-dimethylaminopropyl) carbodiimide
Et	ethyl
<i>et al.</i>	<i>et alii</i> (Latin: and others)
EtOAc	ethylacetate
EW	electron withdrawing

g	grams
h	hours
HPLC	high performance liquid chromatography
i.e.	<i>id est</i> (Latin: that is)
IR	infra-red (spectroscopy)
L	litre
m	milli (prefix 10^{-3})
Mp.	melting point
m/z	mass to charge ratio
MeOH	methanol
min	minute(s)
mol	moles
MRI	magnetic resonance imaging
MS	mass spectrometry
<i>n</i>	normal
NBS	<i>N</i> -bromosuccinimide
nm	nanometer
NMR	nuclear magnetic resonance (spectroscopy)
NP	nanoparticle
Nu ⁻	generic nucleophile
<i>p</i> -	para
pH	$-\log_{10}[\text{H}^+]$
Ph	phenyl
ppm	part per million

Py	pyridine
rac	racemic
RB	round bottom
R _f	retention factor
R _F	perfluoroalkyl
RT	room temperature
T	temperature
<i>t, tert</i>	tertiary
TFA	trifluoroacetic acid
THF	tetrahydrofuran
TLC	thin layer chromatography
TMS	trimethylsilyl
δ	chemical shift, ppm
Δ	heated at reflux
μ	micro (prefix: 10 ⁻⁶)
v _{max}	infra-red absorption maximum, cm ⁻¹

INTRODUCTION

Great hopes are placed in the use of cationic lipids for gene transfection and drug delivery therapy to combat a myriad of inherited or acquired diseases. These vectors possess a notable potential compared with those of biological origin, since they are much safer, less toxic and are able to incorporate larger payloads. As concerns *in vivo* transfection, the most severe limitations of the current non-viral gene delivery systems are the relatively low efficiency of gene transfection into the target cells, the physico-chemical instability of the DNA/vector complexes and the induced cytotoxicity. The major obstacles encountered during the transfer of foreign genetic material into the body involve in particular interactions with blood components and vascular endothelial cells and uptake by phagocytosis [1]. It should be borne in mind, however, that the use of such delivery systems are still in the initial stages of development.

This present work seeks to build on the exceptional *in vitro* gene transfection efficiency displayed by doubly charged 1,4-dihydropyridine (1,4-DHP) cationic amphiphiles developed at the Latvian Organic Synthesis Institute (LOSI) Membrane Active and β -Diketone laboratory (MAS). It has been determined, that pyridinium and alkylammonium cationic (1,4-DHP) amphiphiles self-assemble in aqueous solutions and as a result form nano-aggregates. This research led to the development of an original gene transfection agent, whose transfection efficiency is higher than the currently available commercial non-viral cationic transfection vectors [2-3].

On the other hand highly fluorinated molecular materials, fluorocarbons and fluorinated amphiphiles, constitute new promising components of emulsions, vesicles and other colloidal systems. Fluorocarbons possess high biological inertness, gas solubility, low surface tension, and other valuable characteristics. Fluorous amphiphiles are highly surface-active, they have a strong hydrophobic character, and are lipophobic as well. Therefore, they constitute unique components of supramolecular assemblies, especially when segregation between hydrophilic and lipophilic domains is desired. Their strong tendency to self-assemble result in the formation of highly stable vesicles, tubules and other colloidal systems. The internal fluorinated film that forms within bilayer membranes made from fluorinated amphiphiles reduces the permeability of this membrane [4]. Moreover ^{19}F -MRI is presented as an alternative and emerging method to assess the fluorinated drug carrier movement and quantity, since the concentration of a fluorine compound is directly proportional to the ^{19}F signal in density weighted ^{19}F -MRI. ^{19}F provides a

strong NMR signal due to the large gyromagnetic ratio, minimal background signal and exquisite sensitivity to changes in the microenvironment [5]. The ability to combine ^1H and ^{19}F -MRI offers anatomical localization as well as definitive and quantitative mapping of nanoparticle uptake [6].

The research objective of this work is the synthesis of novel potential transmembrane transport agents, by uniting in one molecule pyridinium and alkylammonium cationic 1,4-DHP or 3,4-dihydropyridone (3,4-DHPOD) structures with the unique physico-chemical properties of amphiphilic fluorinated alkyl esters. The 1,4-DHP heterocycle is considered as one of privileged structures with a wide pharmacological profile. The most extensive research and applications of 1,4-DHPs have been in cardiovascular system regulation. However, in the past decade it has been determined that 1,4-DHPs possess a wide pharmacological spectra of activity: antioxidant, neuroprotective, anticancer, antidiabetic, and antimicrobial etc. characteristics. Therefore, fluorinated cationic 1,4-DHP or 3,4-DHPOD amphiphiles may function not only as passive DNA or small molecule drug delivery agents but, they may at the same time fulfill some desirable pharmacological activity in the target cells.

Aim of this dissertation: synthesis and characterization of novel cationic perfluorinated fatty acid ester containing 1,4-DHP and 3,4-DHPOD amphiphiles as potential lipido-mimetics, obtaining new types of transmembrane transport agents.

The following tasks have been proposed to reach the above objectives:

- To work out synthetic methods for obtaining perfluorinated β -ketoesters and β -aminocrotonic acid esters using perfluorinated alcohols as substrates.
- Synthesize and characterize perfluorinated fatty acid ester containing cationic 1,4-DHP amphiphilic compounds.
- To work out synthetic methods for obtaining new types of fluorinated ester containing cationic 3,4-DHPOD amphiphiles.
- To determine the direction of dihydropyridine bromination reaction depending on the substrate structure and brominating agent.
- Synthesize cationic 3,4-DHPOD-triphenylphosphonium amphiphiles.
- Investigate the cationic 1,4-DHP and 3,4-DHPOD amphiphile self-assembly in aqueous solution and characterize the obtained structure dependent aggregates.

- Compile and analyse the cytotoxicity data of the newly synthesized compounds, and their structure activity relationship in gene transfection.

The scientific novelty of this research: The theme of this dissertation, the development of novel transmembrane drug delivery vehicles is important and actual in medicinal chemistry. As a result of the work on this dissertation, new types of cationic lipids- long perfluoroalkyl ester containing dihydroazine compounds have been synthesized, for the further structure activity relationship study in gene transfection research. A preliminary study has indicated that these types of compounds can be useful in further transmembrane drug delivery research. The perfluoro groups in these carriers provide a means of non-invasive *in vivo* tracking of the delivery and drug uptake using ^{19}F -magnetic resonance imaging. For the first time dynamic light scattering and atomic force microscopy has been used to characterize the fluorinated cationic 1,4-DHP and 3,4-DHPOD amphiphile self-assembled aggregates in aqueous solutions. Fundamental chemistry aspects in the 3,4-DHPOD series have been explored by a study on the importance of a substituent in position 4 in directing the stereospecific bromine and methoxide addition in this heterocycle. For the first time a 3,4-DHPOD-6-methylenetriphenylphosphine derivative has been synthesized and employed in a Wittig reaction with pyridine-2-carboxaldehyde providing a compound with an ultra short $\text{NH}\cdots\text{N}$ bond. For the first time a 3,4-DHPOD-6-methyleneazide derivative has been synthesized and used in „click chemistry” to provide a 3,4-DHPOD triazole derivative. These two reactions provide opportunities for the generation of large 3,4-DHPOD-6-methylene substituted libraries for further research. Single crystal X-ray diffraction has been used to disprove a recently published synthesis of 2-amino-1,4-DHP derivatives proving unambiguously that the reported derivatives were actually 4*H*-pyrans.

Acknowledgements

Firstly, I want to thank professor G.Duburs for the opportunity to work in his group and my supervisor Dr. B.Vigante. Special thanks to professor G.W.Buchanan who introduced me to the chemistry of fluorine and his support. Thanks to Dr. S.Belyakov for X-ray analysis, Dr. B. Turovska for CV measurements, Dr. M.Petrova for NMR, Dr. D.Erts and P.Birjukov of the University of Latvia physics dept. for allowing the use of AFM and B. Skrivele for taking the AFM measurements, Dr. I. Sestakova for cytotoxicity data, and Dr. Hab. Biol. T.Kozlovskaja of the Latvian Biomedicine research center for gene transfection data. I want to thank my

colleagues I.Vesere and Y.Goncharenko and ESF project leader Dr. A.Plotniece for including me in the project.

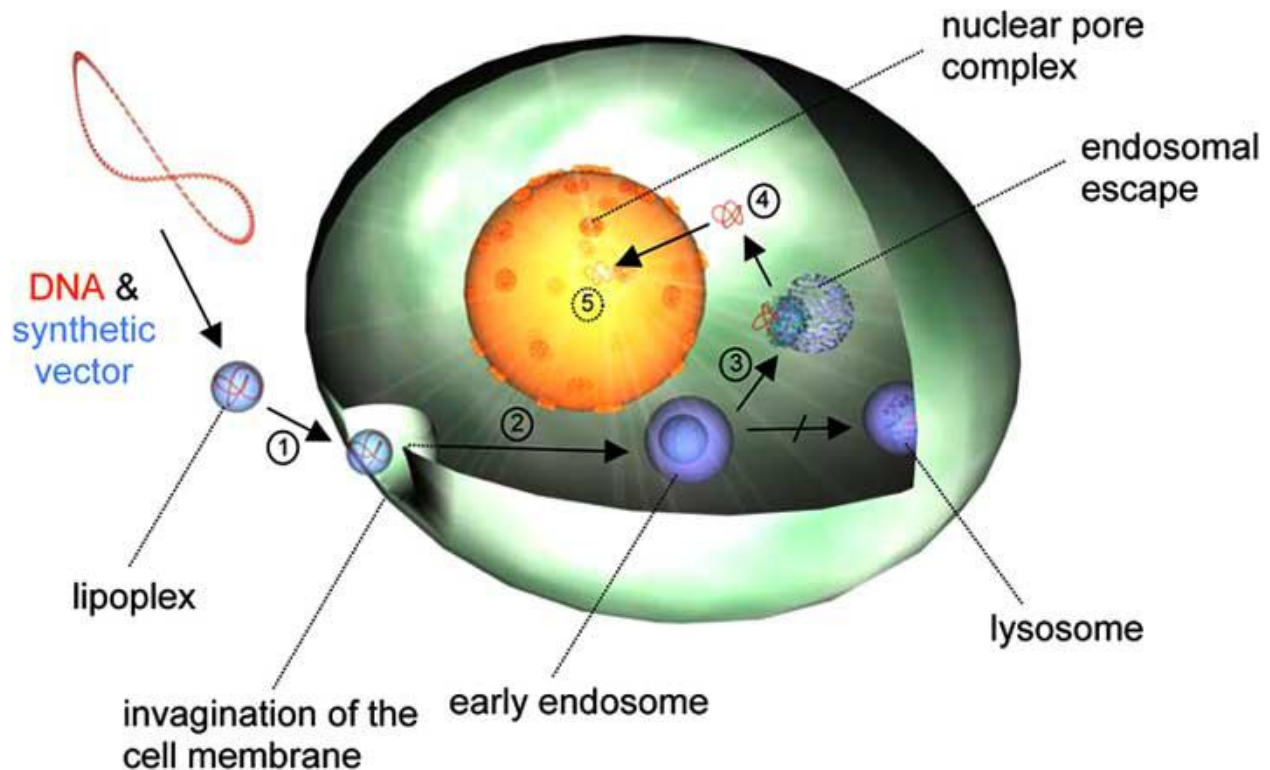
Financial support was provided by **ESF project :2009/0197/1DP/1.1.1.2.0/09/APIA/VIAA/014**

1. LITERATURE REVIEW

1.1. Gene transfection

The clinical success of gene therapy, the modality to combat a myriad of inherited diseases, continues to remain critically dependent on the availability of safe and efficacious gene delivery reagents, popularly known as transfection vectors [7]. Broadly speaking, contemporary transfection vectors are classified into two major categories: viral and non-viral. Viral vectors, although remarkably efficient in transfecting our body cells, suffer from numerous biosafety related disadvantages. For instance, viral vectors are capable of the following: generating a potentially replication competent virus through various recombination events with the host genome; inducing inflammatory and adverse immunogenic responses; and producing insertional mutagenesis through random integration into the host genome; etc., [8]. More recently, it has been reported that retrovirus vector insertion near the promoter of the proto-oncogene LMO2 in 2 human patients with X-linked severe combined immunodeficiency (SCID-XI) is capable of triggering deregulated premalignant cell proliferation with unexpected frequency [9]. In addition, viral vectors have a low insert size limit for the therapeutic genes they can pack inside. Consequently, an increasing number of investigations are being reported on the development of safe and efficacious nonviral alternatives including cationic amphiphiles (also known as cationic transfection lipids) [10], cationic polymers [11], dendrimers [12], etc. Because of their lesser immunogenic nature, robust manufacture ability to deliver large pieces of DNA, and ease of handling and preparation techniques, an upsurge of global interest has recently been witnessed in developing efficacious cationic transfection lipids for delivering genes into our body cells [13,14]. However, transfer to the nucleus of target cells of either a functional gene, or a structure capable of interfering with a cellular gene, is a daunting task when considering the number of barriers the vector/DNA complexes must overcome. Numerous roles are required of the vector which include protection of the DNA from the extracellular environments, facilitated uptake into the target cells, escape from intracellular compartments and finally release of the plasmid, which must subsequently pass across the nuclear membrane before transgene expression can occur [15-17]. Currently believed intracellular pathways (Fig. 1.1) involved in cationic lipid mediated gene transfer (lipofection) include the condensation of the large DNA molecule, driven by an electrostatic interaction between the cationic lipid and the polyanionic DNA. Spontaneous self-

assembly into nanometric particles termed lipoplexes results (stage 1), leading to shielding of the DNA from the nucleases of the extracellular medium. Use of an excess of cationic amphiphile (quantified by the lipid/DNA ratio resulting in a mean theoretical charge ratio of the lipoplex (+/-)) equips the lipoplex surface with a positive charge, which is presumed to mediate subsequent cellular uptake *via* interaction with negative cell surface structures such as heparin sulphates and other proteoglycans [18-20].



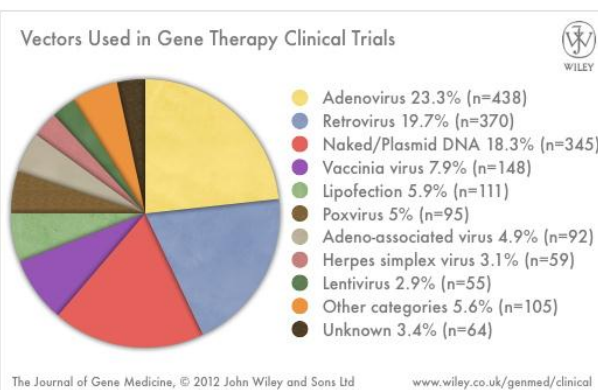
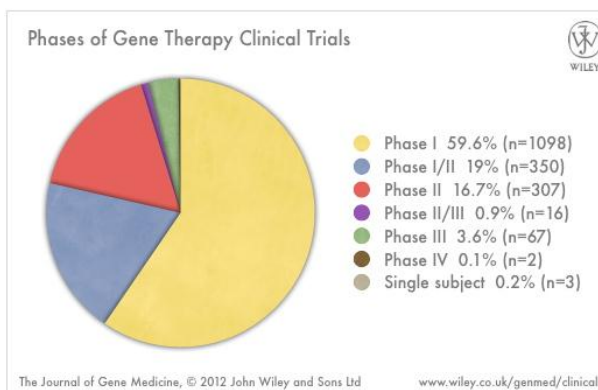
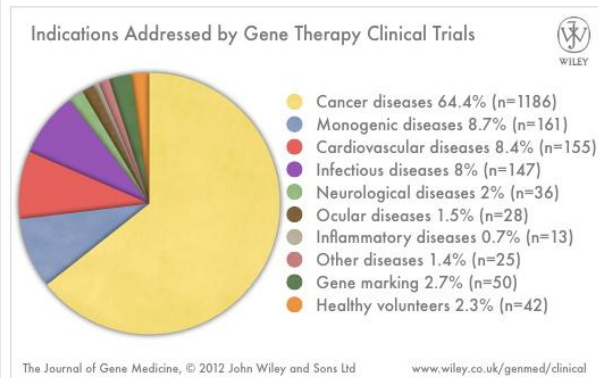
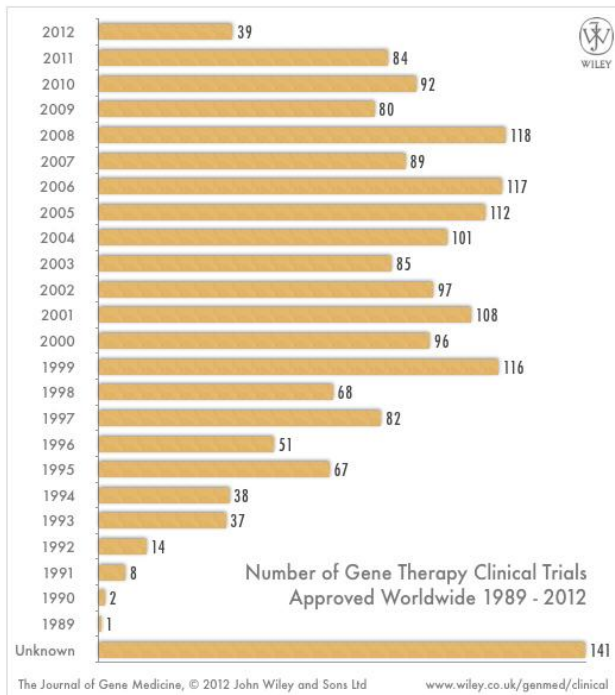
1. Formation (*via* self-assembly) of vector/DNA complexes (lipoplexes).
2. Cellular uptake *via* endocytosis.
3. Endosomal escape to avoid DNA degradation in lysosomes (barred arrow).
4. Trafficking through the cytoplasm and nuclear entry.
5. Transgene expression in the nucleus.

Figure 1.1. A representation of the various steps involved in gene transfection by cationic lipids [32].

As a result of non-specific endocytosis, the lipoplex is encapsulated in intracellular vesicles [15] (stage 2), though fusion-based cellular uptake cannot be totally excluded [17]. The DNA must then avoid degradation in the late endosome/lysosome compartment (barred arrow) by escaping from the (early) endosome into the cytoplasm (stage 3) [15, 21]. Trafficking of the DNA through the cytoplasm precedes uptake by the nucleus of the target cell (stage 4), and subsequent transgene expression therein (stage 5). In the nucleus, the DNA appears to be separated from its vector [22]

and microinjection experiments [15] have suggested that gene expression does not occur if the DNA remains condensed in intact lipoplexes. It should be stressed here that the efficiency of cationic lipids for gene transfection can be studied in various ways. First, their efficacy can be evaluated in terms of gene delivery (percentage of transfected cells) or gene expression (amount of transgene protein produced). Second, the efficiency of any transfection reagent also strongly depends on the cell system chosen for its evaluation (transformed cell lines or primary cells *in vitro*, *in vivo* administration *via* various routes), efficiency gains *in vitro* therefore not automatically lead to higher efficiencies *in vivo* [32].

Advances in the field of non-viral vectors are now made in two distinct structural categories: cationic polymers and cationic lipids, both of which must face the barriers to gene



delivery, which are becoming ever clearer on both a chemical and biological level [15, 23-25].

A great number and an impressive variety of synthetic vectors have been prepared and their transfection efficiency evaluated not only in experimental studies, but also in clinical trials for treatment of diseases such as cancer [26, 27] and cystic fibrosis [28-31]. An exhaustive list of clinical trials can be found at www.wiley.co.uk/genmed/clinical.

1.2. siRNA-mediated gene silencing

RNA interference (RNAi) refers to the ability of doublestranded RNA (dsRNA) to cause sequence-specific degradation of complementary mRNA molecules. Since its discovery in *Caenorhabditis elegans* in 1998 [33], it has rapidly attracted attention from researchers in fields ranging from genetics to clinical medicine. A natural intracellular process likely involved in cell-based defence against mobile genetic elements such as viruses and transposons [34], RNAi promises to be an invaluable tool for gene function analysis as well as a powerful therapeutic agent that can be used to silence pathogenic gene products associated with diseases including cancer, viral infections and autoimmune disorders [35–40].

A central component of RNAi is a double-stranded siRNA molecule that is 21–23 nt in length with 2 nt long 3' overhangs [41]. These siRNA effector molecules can be introduced into cells directly as synthetic siRNAs or indirectly as precursor long dsRNAs or short-hairpin RNAs (shRNAs). RNA polymerase II- or III-driven expression cassettes can be used for constitutive expression of shRNA molecules [42]. Both the long dsRNAs and shRNAs are cleaved by Dicer (RNase III family of endonucleases) into the appropriately sized siRNA effectors. Although the presence of dsRNA >30 nt can elicit an interferon response in mammalian cells [43], Elbashir and co-workers demonstrated that synthetic 21mer siRNAs evaded the interferon response and yet were still effective mediators of sequence-specific gene silencing in mammalian cells [41].

Because synthetic siRNA molecules must be transported into the cells before they can function in RNAi, successful delivery of siRNA is of central importance (Fig. 1.2.). Delivery vehicles must protect the siRNA from nucleases in the serum or extracellular media, enhance siRNA transport across the cell membrane and guide the siRNA to its proper location through interactions with the intracellular trafficking machinery. While naked siRNA molecules have been shown to enter cells, significantly more siRNA can be delivered using carrier vehicles [44, 45]. Both viral and nonviral vectors deliver siRNA into cells, although viral vectors are limited

to delivering siRNA-expressing constructs such as shRNA. Commercially available cationic lipids such as Oligofectamine can effectively deliver siRNA molecules into cells *in vitro* with

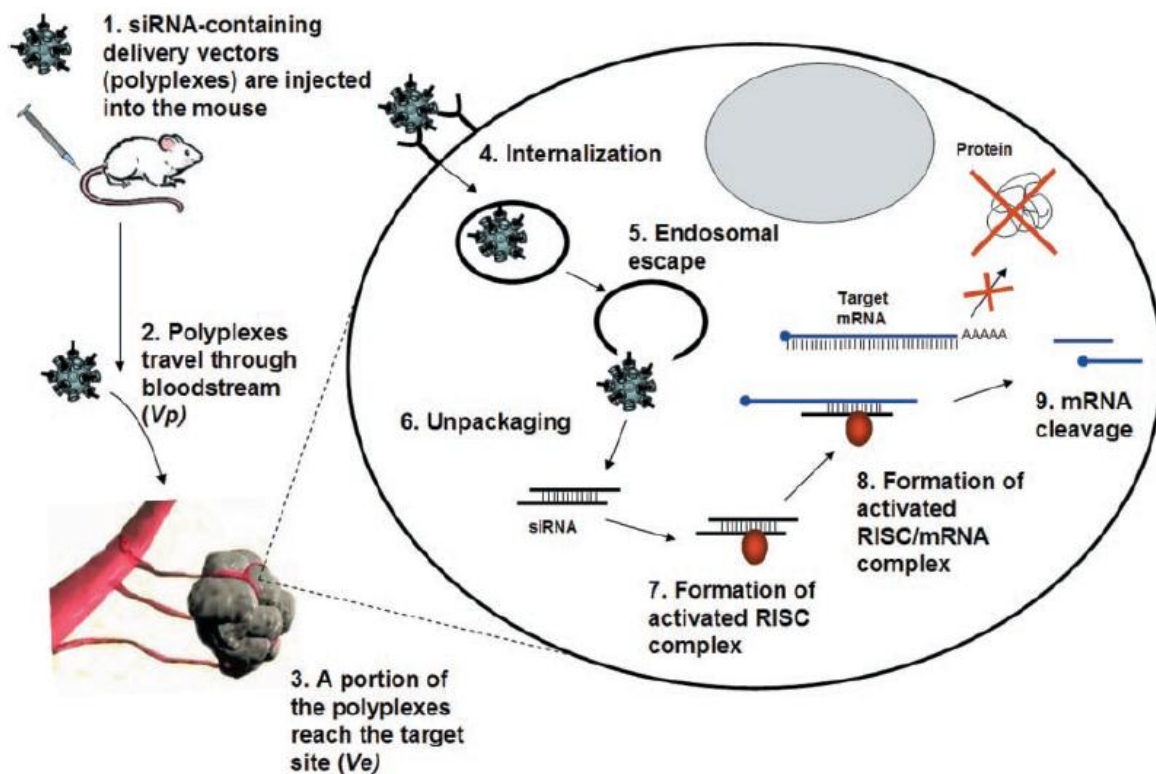


Figure 1.2. Simplified schematic of the key steps required for siRNA delivery to and function within mammalian cells. Steps 1–3 are unique to *in vivo* application of siRNA, whereas steps 4–9 represent the general processes on the level of an individual cell and are therefore common to both *in vivo* and *in vitro* application of siRNA [47].

transfection efficiencies approaching 90%. However, the high toxicity of cationic lipids limits their use for systemic delivery *in vivo*. Recent studies have shown that cyclodextrin-containing polycations (CDPs) can achieve safe and effective systemic delivery of siRNA in mice [46].

1.3. siRNA delivery systems for *in vivo* application

Although researchers and biotechnology companies have reported many siRNA vectors for delivery into the cytoplasm of cells, and although these are satisfactory for most *in vitro* applications, these delivery technologies are usually inappropriate for *in vivo* use [48]. Currently, siRNAs in clinical trials are directly administered to local target sites such as the eye and lung, thereby avoiding the complexity of systemic delivery. However, it is necessary to introduce siRNA by a systemic route to treat most cancers and other diseases. The optimal *in vivo* systemic

delivery systems for siRNA should have the following characteristics. First, the delivery systems should be biocompatible, biodegradable, and nonimmunogenic. Second, the systems should provide efficient delivery of siRNA into target cells or tissues with protection of the active double-stranded siRNA products from attack by serum nucleases. Next, the delivery systems must provide target tissue-specific distribution after systemic administration, avoiding rapid hepatic or renal clearance. Finally, after delivery into target cells via endocytosis, the systems should promote the endosomal release of siRNA into the cytoplasm, allowing the interaction of siRNA with the endogenous RISC [49,50]. To confer drug-like properties such as stability, cellular delivery, and tissue bioavailability to siRNAs, various strategies that range from chemical modification of siRNA to design of different non-viral vectors have been developed and validated.

1.4. Lipid-based siRNA delivery

Various lipid-based delivery systems have been developed for *in vivo* application of siRNA. Lipid-based systems include liposomes, micelles, emulsions, and solid lipid nanoparticles. For the delivery of siRNA using lipid-based systems, lipid composition, drug-to-lipid ratio, particle size, and the manufacturing process should be optimized. Among synthetic delivery systems for siRNA, cationic liposomes have emerged as one of the most attractive vehicles owing to the simple manner in which such liposomes form complexes with negatively charged siRNA, their high transfection efficiency, their enhanced pharmacokinetic properties, and their relatively low toxicity and immunogenicity. Moreover, cationic liposomes can protect siRNA from enzymatic degradation, and provide reduced siRNA renal clearance.

One key factor in the success of lipid-based siRNA delivery systems is the development of cationic lipids. Since N-[1-(2,3-dioleoyloxy) propyl]-N,N,N-trimethylammonium chloride (DOTMA), a synthetic cationic lipid, was first used to transfer plasmid DNA into mammalian cells in the late 1980s, many other cationic lipids have been developed [51]. Cationic lipids can be readily mixed and complexed with negatively charged DNA or RNA to form nanoparticles by electrostatic interaction. Until the early 2000s, most cationic lipid-based systems were used to transfer plasmid DNA into targeted cells or tissues. Since the advent of siRNAs as potential innovative drugs, the use of cationic liposomes has shifted from delivery of plasmid DNA to delivery of siRNA.

The structure of cationic lipids is known to affect transfection efficiency and toxicity of cationic lipid-based delivery systems [52]. Different lengths of hydrocarbon chain influence the cytotoxicity of cationic lipids [53,54]. Given the importance of cationic lipids as core components of lipid-based systems, numerous cationic lipids generated by combinatorial synthesis have been screened for optimal siRNA delivery [55].

Although most lipid-based systems for delivery of siRNA have used liposomal formulations, other types of lipid-based systems have also been developed for efficient delivery of siRNA. A cationic solid lipid nanoparticle composed of cholesteryl ester, triglyceride, cholesterol, dioleoyl phosphatidylethanolamine (DOPE), and 3-[N-(N',N'-dimethylaminoethane)-carbamoyl]-cholesterol, was complexed with a reducible conjugate of siRNA and polyethylene glycol (siRNA-PEG) via electrostatic interactions. Park et al. reported that the delivery of siRNA using solid lipid nanoparticles resulted in efficient target gene silencing and serum stability, with a minimal level of cytotoxicity [56].

For *in vivo* siRNA delivery, stable nucleic acid–lipid particles (SNALPs) have been formulated and evaluated in mice, guinea pigs, and non-human primates. A SNALP consists of a lipid bilayer containing a mixture of cationic and fusogenic lipids that enables the cellular uptake and endosomal release of siRNA. The surfaces of SNALPs were coated with a polyethylene glycol–lipid conjugate that provides a neutral, hydrophilic, exterior and stabilizes the particle during formulation [57]. SNALPs were first used to deliver HBV-specific siRNA in diseased mouse models. Three daily intravenous injections of SNALPs encapsulating siRNA, at a total dosing schedule of 3 mg/kg/day, resulted in substantial reduction of serum HBVDNA in mice. The SNALPs also showed an RNAi effect after *in vivo* delivery to guinea pigs [58]. In that study, Ebola virus polymerase L-specific siRNA in SNALPs or in polyethyleneimine (PEI) complexes was intraperitoneally administered 1 h after challenge of guinea pigs using lethal Ebola virus. The PEI/siRNA complexes partially protected the animals from death, but treatment with SNALPs containing the siRNA completely protected guinea pigs against viremia and death.

1.5. Cationic amphiphiles

The molecular architectures of cationic amphiphiles (Fig. 1.3.) consist of a positively charged water-loving (hydrophilic) polar head group region and a nonpolar hydrophobic tail region (usually consisting of either two long aliphatic hydrocarbon chains or a cholesterol

skeleton) often tethered together via a linker functionality such as ether, ester, amide, amidine group, etc. Understanding the structural parameters capable of influencing the gene delivery efficiencies of cationic amphiphiles is essential for rational design of efficient cationic

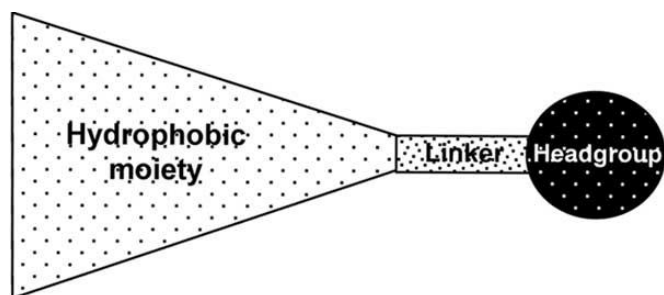


Figure 1.3. The three basic domains of any cationic lipid: hydrophobic moiety, linker and head group [32].

transfection lipids. To this end, the focus of many prior structure-activity investigations have been centered around probing the influence of each of these three lipid structural components in modulating the gene transfer efficacies of cationic amphiphiles. For instance, a number of prior reports have demonstrated that the gene transfer efficiencies of cationic amphiphiles critically depends on their molecular architectures including hydrophobic alkyl chain lengths, [60] nature of head groups [59,61] as well as on the nature of linker and spacer functionalities used in covalent tethering of the polar head groups and the nonpolar tails of cationic amphiphiles [61-64].

Cationic lipids were first introduced by Felgner *et al.*, following early attempts to transfer DNA *via* encapsulation in liposomes [65, 66]. Thus, the first reported lipid was DOTMA (N-(1-(2,3-dioleoyloxy)propyl)-N,N,N-trimethylammonium chloride), which consists of a quaternary amine connected to two unsaturated aliphatic hydrocarbon chains *via* ether groups [67] (Fig. 1.4.). Synthesis of the multivalent lipopolyamine DOGS (dioctadecylamido-glycylspermine) was reported soon afterwards [68] and the efficiency of the vector DC-Chol (3b-[N-(N',N'-dimethylaminoethyl)carbonyl]cholesterol) with cholesterol as the hydrophobic portion was subsequently reported [69] (Fig. 1.4.). It is noteworthy that the transfection activity of cationic lipids (especially those which are incapable of forming bilayers alone) can be increased by their formulation as stable liposomes with the neutral co-lipid DOPE (dioleoyl phosphatidylethanolamine), (Fig. 1.4.) [70]. Inclusion of DOPE is presumed to enhance

endosomal escape of the lipoplexes into the cytoplasm as DOPE is thought to have fusogenic properties important for endosomal membrane disruption [70-72].

The use of these initial lipids demonstrated the transfection ability of cationic lipids. However, progress in improving the level of transfection efficiency up to that required for therapeutic use has been slow. Progress has been made in the design of cationic head groups, hydrophobic domain, and linkers. In brief, the choice of cationic head groups has expanded into

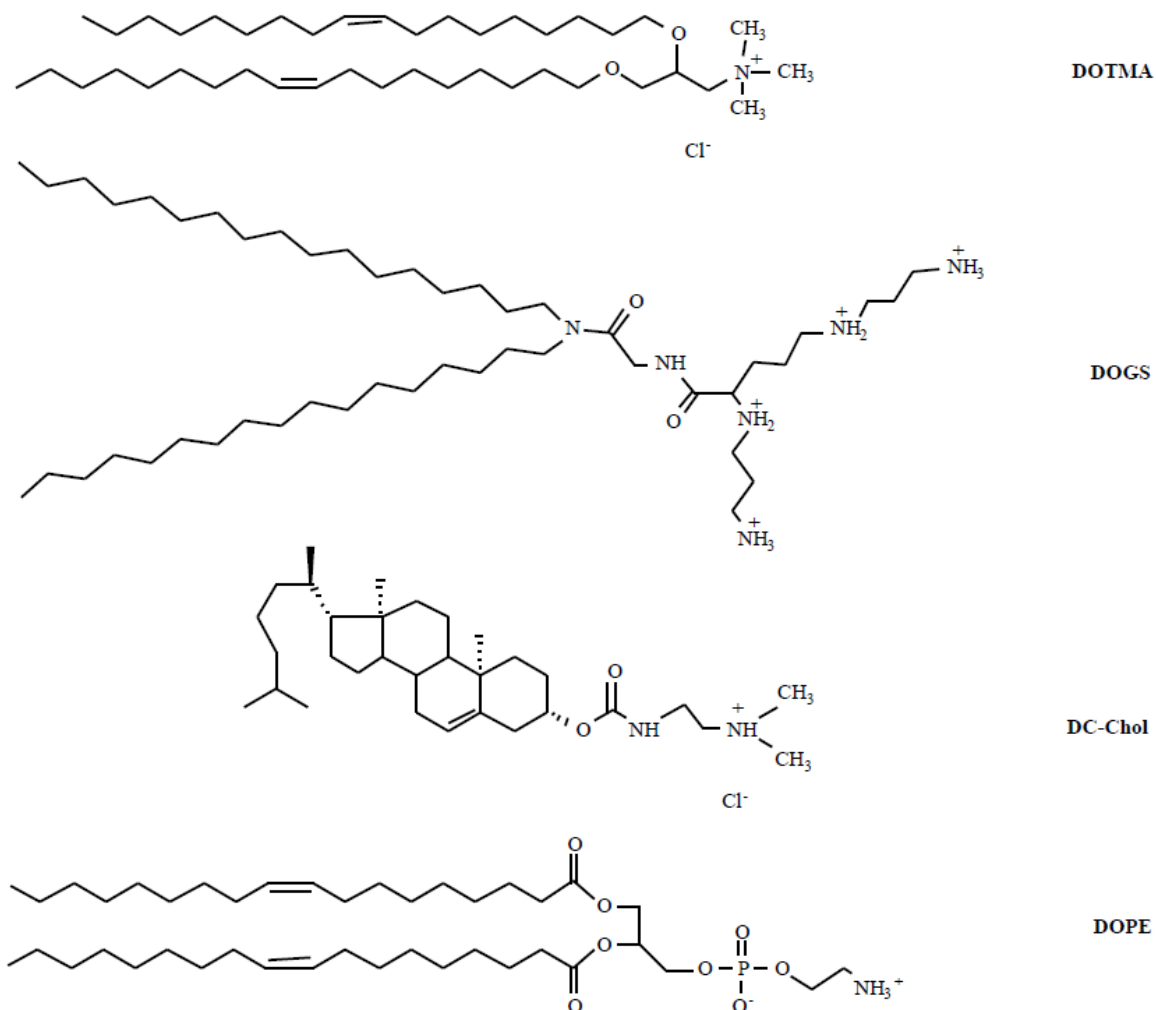


Figure 1.4. Structures of the ‘early’ cationic lipids and of the co-lipid DOPE [32].

the use of natural architectures and functional groups with recognized DNA binding modes as well as non-amino-based cationic moieties. Modifications of the hydrophobic domain have shown that optimal vector structure is often dependant on this moiety, which can fall into various

structural classes and variants. Finally, labile linkers have been introduced which are sensitive to various biological stimuli, inducing DNA release at defined time-points during the intracellular trafficking of the lipoplex.

1.6. 1,4-Dihydropyridine as linker

Despite the huge potential of the 1,4-DHP heterocycle for modification there is only one group (OSI in collaboration with Kuopio University) who have published [2] on its utilization as linker in pyridinium and alkylammonium cationic (1,4-DHP) amphiphile (Fig. 1.5.) synthesis and gene transfection studies.

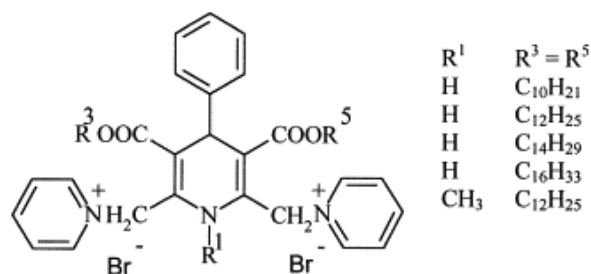


Figure 1.5. Cationic amphiphiles with a 1,4-DHP linker [2].

The closest analogs to this system are the SAINT vectors (Fig. 1.6.) [32].

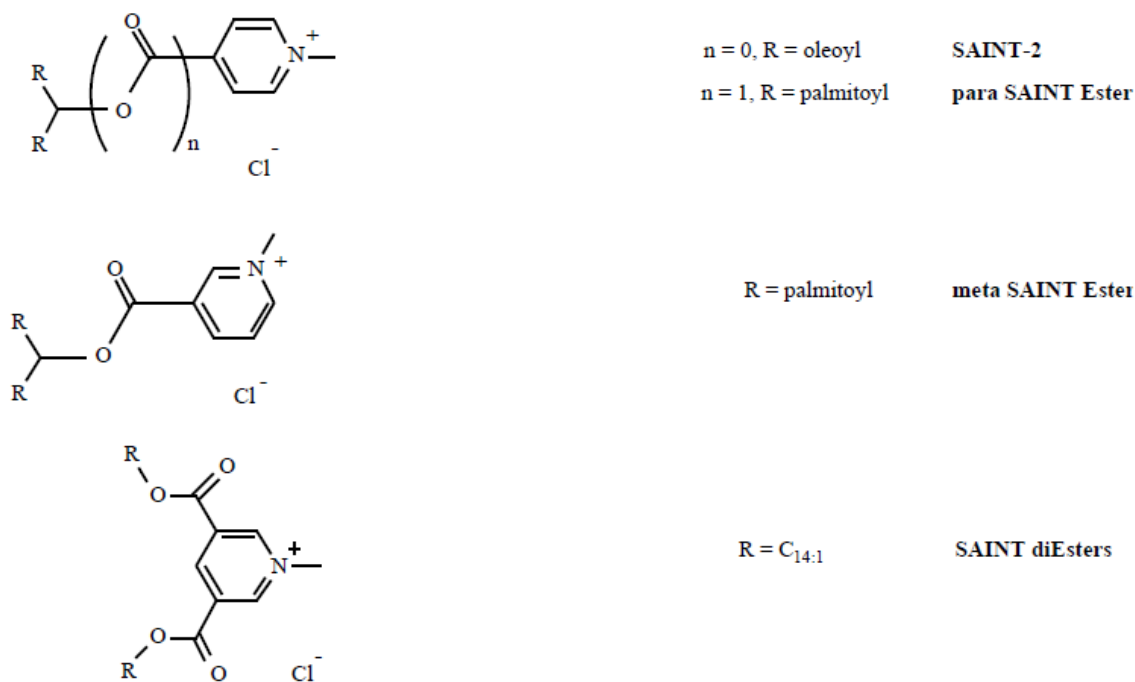


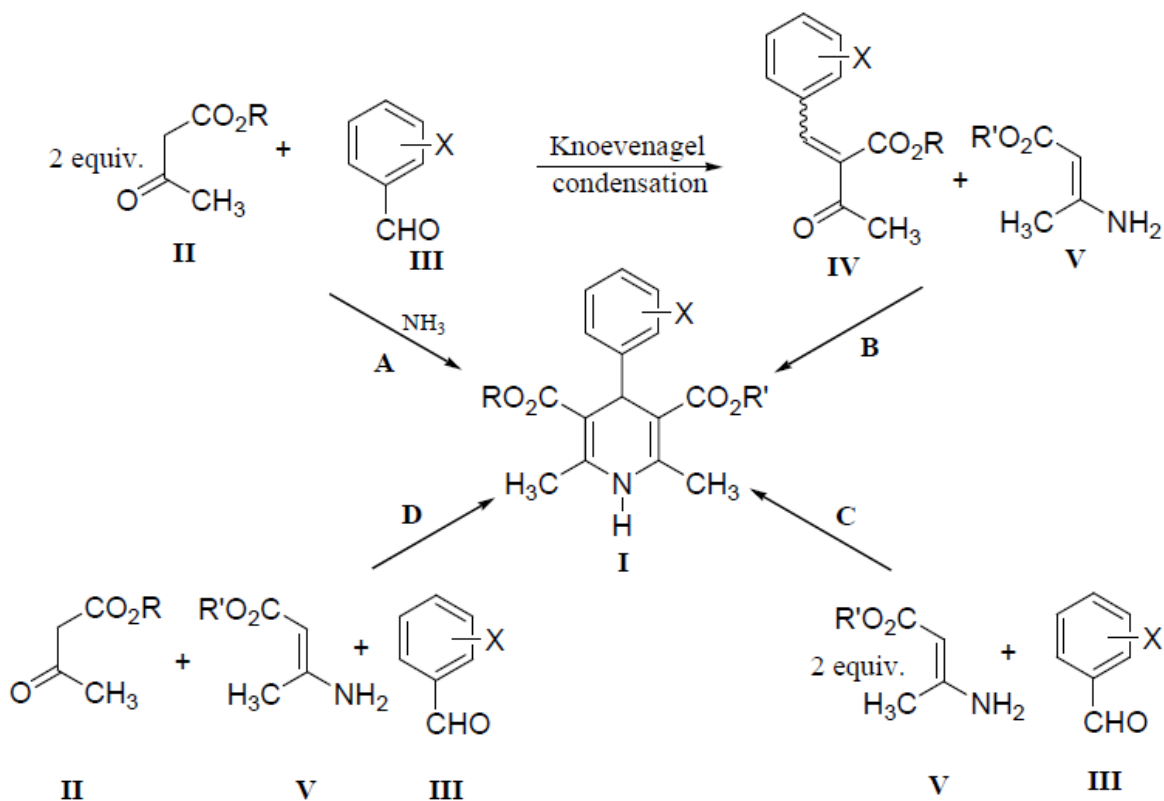
Figure 1.6. Incorporation of ester functions into the linker: esterases and/or pH-sensitive vectors.

These vectors incorporating ester groups are designed to be cleaved by endogenous esterases, although pH variations may also serve as trigger to hydrolysis. Indeed, the fragility of the ester function in certain environments has been recognised by numerous groups [73,74]. The site of attachment of the ester group to the pyridinium heterocycle of the resulting SAINT Esters had a significant impact on the transfection efficiency (meta > para) which however, was in each case greater than that of the non-ester control SAINT-2 [75]. As foreseen, the toxicity of the ester analogues was also lower. However, contrary to initial expectations, the SAINT Ester vectors were found to be most stable at low pH, with increasing instability on increasing basicity, thereby confusing any mechanistic predictions for the observed increase in transfection levels based on pH alone. The same pH profile was observed for the latest generation of SAINT vectors, which incorporate an ester group between each of the two aliphatic chains (SAINT diEster of (Fig. 1.6.)) [76].

Nowadays it is clear that the 1,4-DHP nucleus is a privileged scaffold since, when appropriately substituted, it can selectively modulate diverse receptors, channels and enzymes. Therefore, the 1,4-DHP scaffold could be used to treat various diseases by a single-ligand multi-target approach [77]. Dihydropyridines have attracted increasing interest due to their diverse therapeutic and pharmacological properties such as insecticidal, bactericidal and herbicidal effects [78]. DHP drugs, namely nifedipine, nicardipine and amlodipine, are cardiovascular agents for the treatment of hypertension [79]. A number of DHP calcium antagonists have been introduced as potential drugs for the treatment of congestive heart failure [80]. Further, cerebrocrast, a dihydropyridine derivative, has been introduced as a neuroprotective agent [81]. Together with calcium channel blocker and neuroprotective activity, a number of dihydropyridine derivatives have been found as vasodilators, antihypertensive, bronchodilators, antiatherosclerotic, hepatoprotective, antitumour, antimutagenic, geroprotective, antidiabetic and antiplatelet aggregation agents [82-86]. In a recent article, 4-[5-chloro-3-methyl-1-phenyl-1H-pyrazol-4-yl]-dihydropyridines have been shown to possess significant antimicrobial activity [87]. In addition to the above, aromatization of 1,4-DHP has also attracted considerable attention in recent years as Böcker has demonstrated that metabolism of the above drugs involves a cytochrome P-450 catalysed oxidation in the liver [88]. Dihydropyridines find applications in stereo specific hydrogen transfer reduction of phenylglyoxylic and pyruvic acid to biomimetic

models of lactase dehydrogenase [89]. Recently, DHPs are used as organocatalysts for asymmetric reactions such as hydrogenation of quinolines in the synthesis of alkaloids [90], asymmetric reductive amination of aldehydes [91] and hydrogenation of α,β -unsaturated aldehydes and ketones [92].

The first synthesis of a 1,4-DHP *via* a three component cyclocondensation reaction of acetoacetic ester, aldehyde and ammonia was reported by Arthur Hantzsch in 1882 [93]. Since then a lot of new variants of the original method have been developed, allowing synthesis of different substituted 1,4-DHPs (Scheme 1.1). Classical Hantzsch synthesis of these compounds is carried out in acetic acid or by refluxing in alcohol for a long time [94]. Several other methods are reported including use of micro-waves [95], molecular iodine [96], cyanuric chloride [97], ionic liquids [98], silica gel/NaHSO₄ [99], TMSCl-NaI [100], metal triflates [101] and ultrasound irradiations [102]. As can be seen from the (Scheme 1.1), methods **A** and **C** are only convenient for the synthesis of symmetrical, nonchiral 1,4-DHPs (R=R') [104-106], while methods **B** (two step synthesis via Knoevenagel intermediate **IV**) and **D** (three component



Scheme 1.1. Most common variants of the Hantzsch 1,4-DHP synthesis [103].

cyclocondensation) are usually used for the synthesis of 1,4-DHPs having different ester moieties ($R \neq R'$) [107-110].

As one might predict, symmetrical 1,4-DHPs are always formed as impurities in synthesis of nonsymmetrical 1,4-DHPs. However, formation of impurities other than intermediates leading to the 1,4-DHP ring is rarely described in Hantzsch condensations [111]. Thus, Angeles *et. al.* [112] have isolated four different compounds **1-4** (Fig. 1.7.) from the Hantzsch condensation of 2-nitrobenzaldehyde, NH_4OH and acetoacetic acid ethyl ester. The formation of 1,2-DHP **2**, cyclic amide **3** and substituted hydroxamic acid **4** is possibly due to steric hindrance as well as the oxidative ability of the nitro group in the *ortho*- position. Similar observations have not yet been published for other substituents (OCH_3 , Cl , CH_3 etc.).

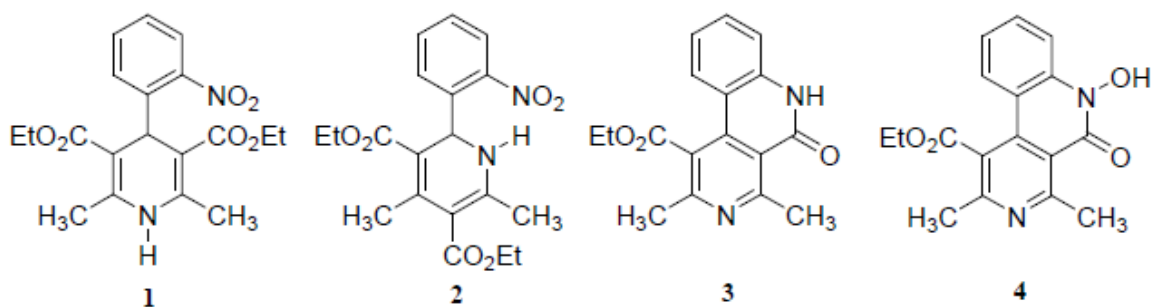
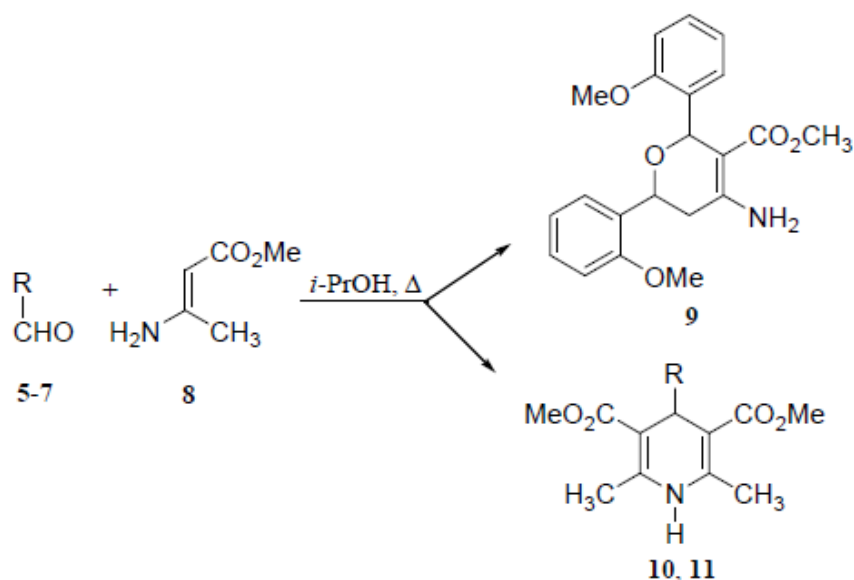


Figure 1.7. Products formed in Hantzsch condensation using 2-nitrobenzaldehyde.

Görlitzer *et. al.* [113] have studied the dimerisation of *o*-nitrobenzylideneacetic acid esters and isolated two diastereomeric substituted hexenes which could also be present as impurities in the classical Hantzsch condensation. Recently another impurity which is formed in substantial amounts was reported [103] when reaction path **C** of the 1,4-DHP synthesis was followed using the sterically hindered *o*-methoxybenzaldehyde (Scheme 1.2.).

This type of side product formation is characteristic of Hantzsch condensations employing two equivalents of alkyl-3-aminocrotonates and substituted benzaldehydes, but the amounts formed may vary drastically, depending on the nature of the substituents present on the aromatic ring [103]. Also, noteworthy are the low yields in entries 2 and 3 even with long refluxing times. However, by using the right choice of solvent, catalyst, and reaction conditions it's possible to get very reasonable yields in 1,4-DHP synthesis.



Scheme 1.2. Hantzsch condensation of (*o*-, *m*- and *p*-)methoxybenzaldehydes **5-7** with methyl-3-aminocrotonate (**8**) [103].

Entry	R	Product	Reaction time[h] ^a	Yields after crystallisation [%]	mp	R _f (TLC)
1	<i>o</i> -MeOC ₆ H ₄	9	84	25.6	170.0 - 171.5	0.11 ^b
2	<i>m</i> -MeOC ₆ H ₄	10	23	28.8	168.0 - 170.5	0.39 ^c
3	<i>p</i> -MeOC ₆ H ₄	11	17	15.3	172.5 - 175.0	0.47 ^c

^a Determined by TLC; ^b CH₂Cl₂/MeOH, 9:1 as eluent; ^c CH₂Cl₂/AcOEt, 9:1 as eluent.

By using 1,4-DHP as a linker for constructing cationic amphiphiles has an additional benefit which is not present in conventional carriers. As already indicated above, the wide pharmacological profile of this linker may serve not only as a construction element in DNA or small molecule drug delivery but, may at the same time fulfill some desirable pharmacological activity in the target cells.

1.7. 3,4-Dihydropyridone as linker

There are no published reports of 3,4-dihydropyridones being used as a linkers (Fig. 1.8)

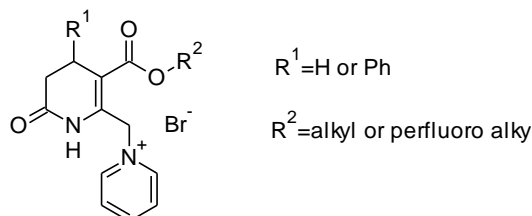


Figure 1.8. Example of cationic amphiphiles with a 3,4-dihydropyridone linker.

in cationic amphiphile synthesis. This linker is similar to the 1,4-DHP heterocycle, except with one less methyl group, one less carboxyl group, and an additional keto group at carbon 2. This 3,4-DHPOD scaffold provides an opportunity for a single cation to be placed on the methyl group at carbon 6 and also one ester group at carbon 5 and the physico/chemical differences between the 1,4-DHP analogs to be compared.

Dihydropyridones are important intermediates for the synthesis of natural products, particularly alkaloids [114,115] and they have been extensively investigated as valuable building block for the construction of piperidines, perhydroquinolines, indolizidines, quinolizidines and other alkaloid systems, with a wide range of biological and pharmacological activities. These compounds are known for their antiproliferative and antitubolin activities [116] and as potential selective inhibitors of receptor tyrosine kinase [117,118]. Rho-associated kinase (ROCK1) is a serine/threonine kinase that has been implicated in a variety of cellular processes including vascular smooth muscle contraction, stress-fiber formation, cell migration, and gene expression. In vascular smooth muscle contraction, ROCK1 plays a central role in the calcium-sensitization pathway. Activation of ROCK1 indirectly regulates the phosphorylation state of myosin light chain, leading to increased vascular smooth muscle contraction. Inhibition of this pathway represents a promising strategy for the treatment of a variety of cardiovascular diseases, including hypertension. The 3,4-DHPOD-indazole amide (Fig. 1.9) was identified as a potent and selective ROCK1 inhibitor with improved pharmacokinetic parameters [119] and might have

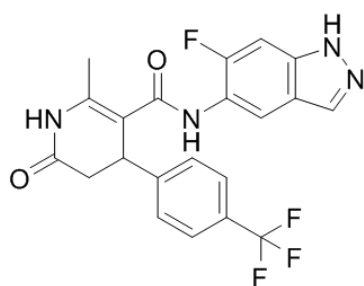
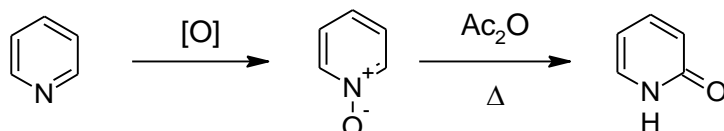


Figure 1.9. GSK429286A a 3,4-DHPOD based potent ROCK inhibitor [119].

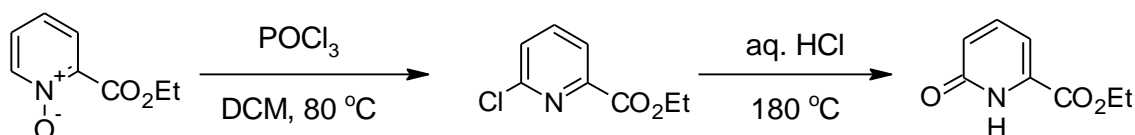
utility in treating Parkinson's disease [120]. Their ability to induce leukaemic cell differentiation has been demonstrated. In addition they have potent antimalarial activity [121] and good anticonvulsant activity against acutely elicited Seizures [122].

Manipulation of pyridines has long been recognized as a convenient avenue to 2-pyridones [123,124]. For instance, conversion of 2-unsubstituted pyridines to pyridones can be accomplished by a Polonovski-type oxidation via a pyridine N-oxide intermediate (Scheme 1.3).



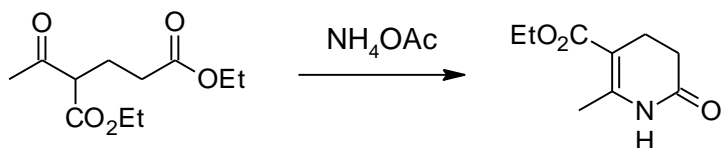
Scheme 1.3. Polonovski rearrangement.

Similarly, 2-pyridones can be accessed through hydrolysis of 2-halopyridines, which in turn, can be obtained from a pyridine N-oxide (Scheme 1.4) [125].



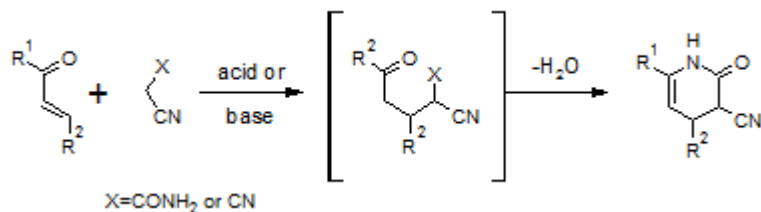
Scheme 1.4. Synthesis of 2-pyridone via 2-chloropyridine.

Construction of 3,4-dihydropyridones via cyclization of linear systems can be found in many natural product synthesis. For example condensation between 2-acetylglutarate derivatives and ammonium acetate provide 3,4-dihydropyridones (Scheme 1.5) [126].



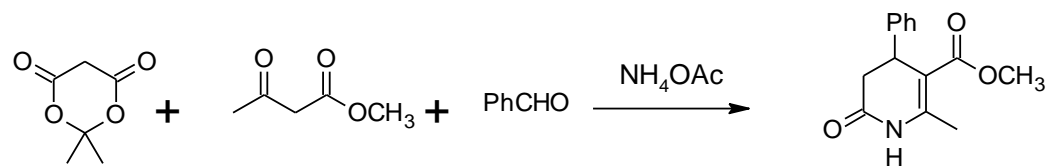
Scheme 1.5. Synthesis of 3,4-DHPOD from 1,5-dicarbonyl.

Alternatively, 3,4-DHPODs can also be accessed through the merging of an enecarbonyl compound and cyanoacetamide or malonitrile (Scheme 1.6) [124]. Mechanistically, such [3+3] annulations generally involve an initial Michael addition of the activated methylene compound to give an acyclic adduct, which undergoes dehydration to furnish the corresponding 3,4-DHPOD.



Scheme 1.6. [3+3] annulation to form 3,4-DHPODs.

The 4-aryl substituted 3,4-DHPOD synthesis has received the most attention due to the many works published by M. Suarez and N. Martin *et. al.*, using a multicomponent facile one-pot condensation reaction of Meldrum's acid, methyl acetoacetate and the appropriate benzaldehyde in the presence of ammonium acetate (Scheme 1.7).



Scheme 1.7. Multicomponent 4-phenyl-3,4-DHPOD synthesis.

Many reaction conditions of the above reaction have been reported including solid phase [127], microwaves [128], ultrasound in glacial acetic acid [129], and solvent-free infrared irradiation [130] in order to increase yields and provide greener protocols for the 4-aryl-3,4-DHPOD synthesis.

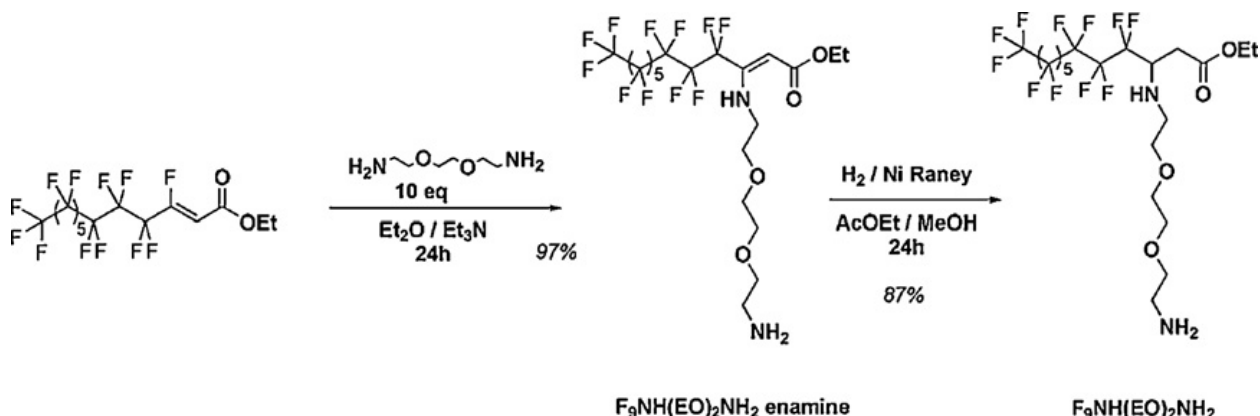
1.8. Fluorinated carriers

A perfluorinated group has peculiar physical and chemical properties. It is both hydrophobic and lipophobic at the same time. As a matter of fact, perfluorocarbons prefer to form a separated fluoruous phase rather than mix with either hydrophilic or hydrophobic molecules. This phenomenon, known as the fluorophobic effect, allows the self-assembly of highly fluorinated molecules in strict analogy to the hydrophobic effect [131,132].

Cationic liposomes [133-138] have been suggested as possible agents for non-viral gene delivery since they offer several advantages: (i) positively charged interfaces which can efficiently complex ssDNA through electrostatic interactions, (ii) due to their membranous nature, they can assist the delivery of ssDNA inside the cells. However, when designing novel vectors for nucleic acids one should take into account not only the hydrophilic part, usually responsible for the ssDNA complexation, but also the hydrophobic domain [139] responsible for the physical features of the bilayer (i.e. phase transition temperature, fluidity) and influencing the stability of the lipoplexes. From this point of view, fluorinated surfactants are of particular interest and many cationic fluorinated amphiphiles have been developed as transfecting agents [140-148]. It was suggested that the enhanced transfection efficiency was related to the fluoruous tags, more hydrophobic and more lipophobic and therefore less damaged by biomolecules *in vivo*. Fluorinated vesicles are more stables than hydrogenated ones and are less recognizable by

macrophages [146,149]. Moreover, the biophysical behavior of these compounds seems to be related not only to the presence of the fluorinated domain in the molecule but also to its position with respect to the hydrophilic part [150].

The recently reported [151] synthesis of a novel monocatener fluorinated surfactant bearing a diamino-diethoxylated head group (Scheme 1.9), provides an example of an amphiphile that was designed in order to respond to three criteria: (i) a fluorinated hydrophobic tag responsible for self-assembling and suited for spontaneous-vesicle-formation, (ii) an ethylene oxide moiety sufficiently hydrophilic so that the compound would be soluble at high concentration, up to 1 mM, and avoiding the precipitation of the surfactant–ssDNA complex and (iii) a protonated at physiological pH primary amine responsible for binding. Thus, the ssDNA-fluorous surfactant interaction is made through electrostatic interactions between the external primary amine and the phosphate groups. By externalizing the binding site, the repulsions between the bulky ethylene oxide moiety and the anionic ssDNA could be avoided, whereas the



Scheme 1.9. Synthesis of fluorinated surfactant $\text{F}_9\text{NH}(\text{EO})_2\text{NH}_2$ [151].

flexibility of the polar head allowed conformational changes for an optimum complexation. The authors' have provided an elegant study of ss-DNA interactions with a fluorinated surfactant based on the surfactant concentration, which is monitored using static light scattering (Fig. 1.10) the inflection points in the graph represent critical aggregate concentration (CAC). Compared to the formation of micelles, formation of vesicles requires a significantly higher number of surfactant molecules, which are partly supplied from the exterior and partly provided from previously generated micelles.

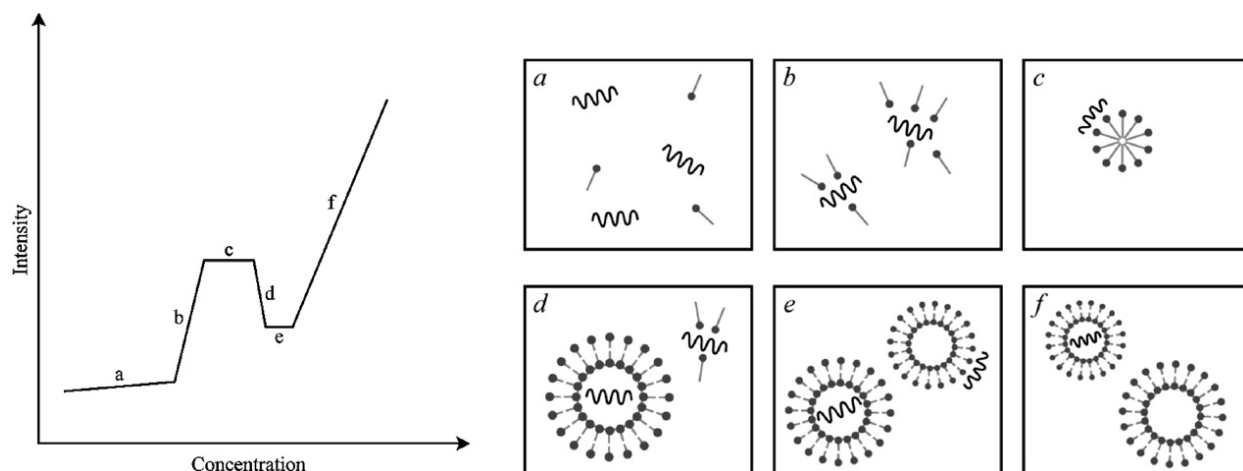


Figure 1.10. ssDNA/ $F_9NH(EO)_2NH_2$ interactions as monitored by static light scattering (left), schematic mechanism (right): (a) the surfactant is in a monomeric form and ssDNA/ $F_9NH(EO)_2NH_2$ interactions are weak, (b) micellization of the surfactant on the ssDNA matrix occurs (c) maximum of monomers micellizing onto ssDNA, (d) demicellization and vesicle ssDNA-loading (e) only ssDNA-loaded fluorinated vesicles and (f) mixture of empty and ssDNA-loaded fluorinated vesicles [151].

Moreover, the combination of the spontaneously formed vesicle properties, oligonucleotide complexation and the non-toxicity of the fluorinated surfactant demonstrate the great potential of these amphiphiles for biomedical applications such as gene therapy or RNA interference.

1.9. ^{19}F -imaging

Of the myriad of particles that have emerged as prospective candidates for clinical translation, perfluorocarbon (PFC) nanoparticles offer great potential for combining targeted imaging with drug delivery, much like the “magic bullet” envisioned by Paul Ehrlich 100 years ago. Perfluorocarbon nanoparticles, once studied in Phase III clinical trials as blood substitutes, have found new life for molecular imaging and drug delivery. The particles have been adapted for use with all clinically relevant modalities and for targeted drug delivery. In particular, their intravascular constraint due to particle size provides a distinct advantage for angiogenesis imaging and antiangiogenesis therapy [152]. MRI offers several advantages over other clinical modalities for molecular imaging, including high resolution, noninvasiveness, high anatomical contrast, and lack of ionizing radiation. ^{19}F presents an excellent probe for quantitative MRI, which is highly enriched in perfluorocarbon nanoparticles. ^{19}F has 100% natural abundance, a spin of $\frac{1}{2}$, and a gyromagnetic ratio of 40.08 MHz/T close to the that of 1H (42.58 MHz/T), resulting in 83% of the sensitivity of 1H [153]. In addition, the chemical shift of ^{19}F , due to its

seven outershell electrons, is sensitive to the molecular environment of the nucleus, including oxygen tension. The ^{19}F spectroscopic signature manifests a range of >200 ppm, [154,155] which permits unambiguous identification of distinctive ^{19}F -containing compounds even at low field strengths. Moreover, no background exists for the ^{19}F signal *in vivo*, since there is negligible endogenous ^{19}F MRI signal from the body, as the physiological concentrations of detectable

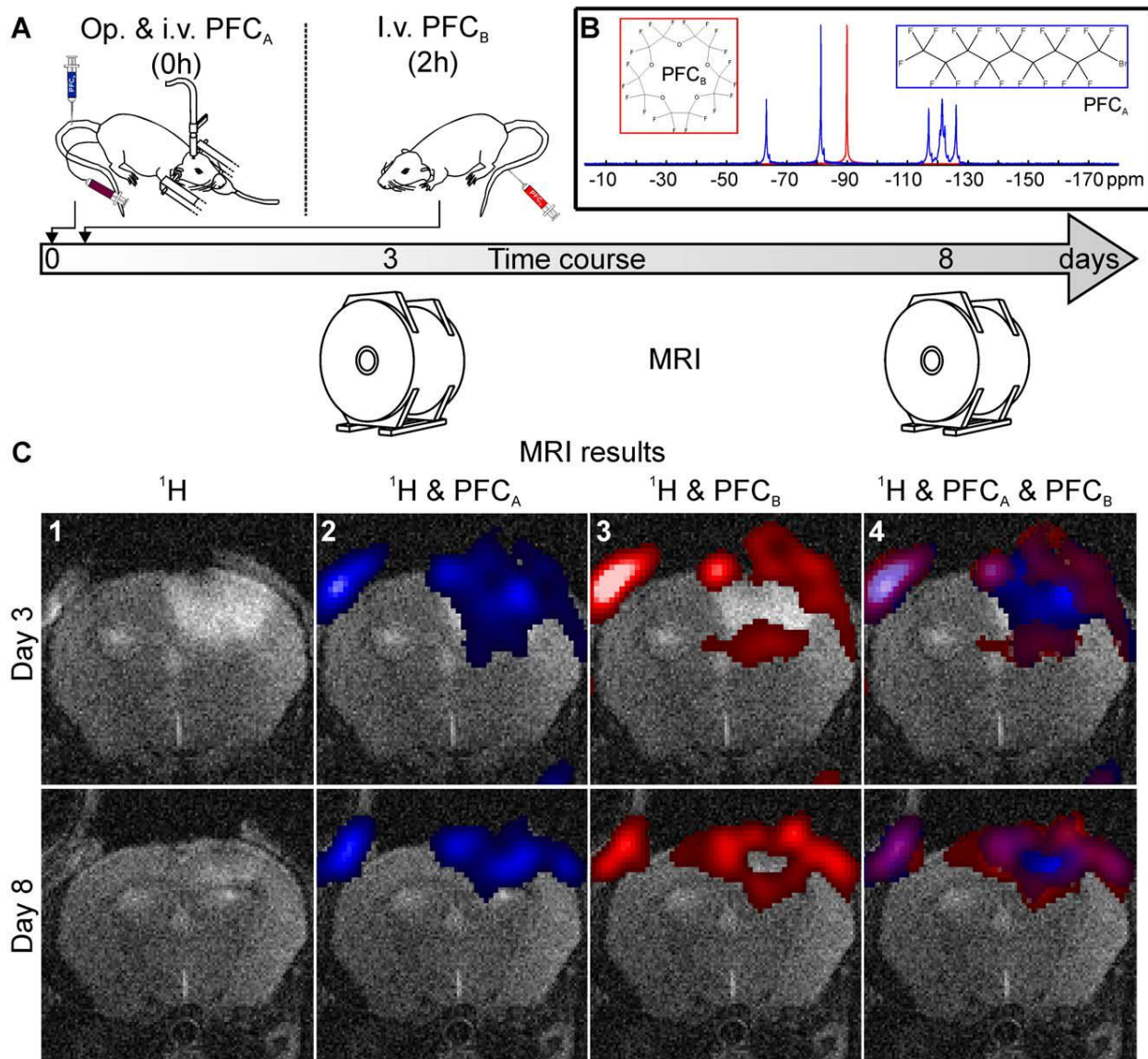


Figure 1.11. *In vivo* visualization of ongoing vessel occlusion. A subgroup of animals received two chemically shifted PFC compounds sequentially. PFC_A with a multi-resonant perfluorooctylbromide was administered immediately after the end of illumination while single-resonant PFC_B with a peak at -90 ppm was injected with two hours delay (A,B). [157].

mobile fluorine are below the detection limit (usually less than 10–3 $\mu\text{mol/g}$ wet tissue weight) [156], providing a unique spectroscopic signature for quantitative MRI.

PFC nanoparticles uniquely support both ^1H and ^{19}F imaging, which now may be performed simultaneously, and which offers many benefits in image registration, motion correction, and quantitative data calibration. 3D CSI experiments with two chemically shifted PFC compounds were recently performed [157] which allowed differentiation of both markers and thus visualization of ongoing vessel occlusion in a single MRI measurement (Fig. 1.11). Administration of the first emulsion (PFC_A) directly after induction of photothrombosis (PT) led to a fluorine signal throughout the cortical infarction (Fig. 1.11C). The second ^{19}F marker (PFC_B) that was applied two hours later, however, accumulated at the outer margins sparing the center of the infarcted zone. By merging the signals on a ^1H background image the different spatial distribution of the compounds could be identified in a single measurement. Thus, the ^{19}F -MRI is presented as an alternative and emerging method to assess the fluorinated drug carrier movement and quantification.

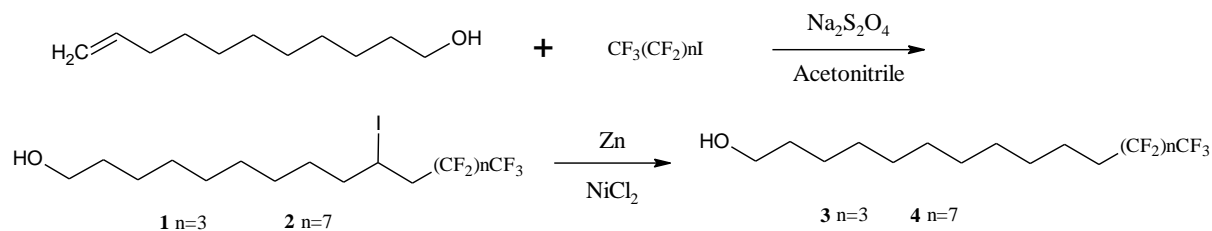
2. RESULTS AND DISCUSSION

2.1. Synthesis of perfluorinated 1,4-dihydropyridine amphiphiles

The 1,4-dihydropyridine scaffold having long chain alkyl esters in the 3,5 positions and bearing a double positive charge via two pyridinium bromides on the 2 and 6 methyl groups has shown exceptional gene transfection efficiency in *in vitro* experiments [2]. To elaborate this promising cationic amphiphile in hopes of further decreasing its cytotoxicity and enhancing transfection efficiency, replacement of the alkyl esters with perfluoro alkyl esters was envisioned as a viable option since perfluoro groups beside having toxicity lowering properties are chemically and biologically inert, have remarkable self-assembly properties forming stable aggregates. Indeed, by preventing DNA from interactions with lipophilic and hydrophilic biocompounds and, from degradation, fluorinated lipoplexes have been found to exhibit a higher *in vitro* and *in vivo* transfection potential than conventional lipoplexes or even than PEI polyplexes [158].

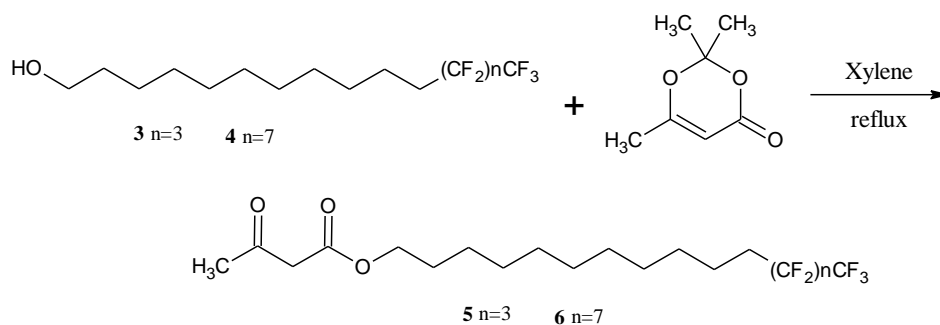
Long chain alcohols **3** and **4** with fluorinated tails were synthesized using perfluoro iodides reacted with 10-undecenol and $\text{Na}_2\text{S}_2\text{O}_4$ as a free radical initiator to give alkyl iodide **1** as a light yellow oil in 92% yield and **2** in 94% yield as an oily solid, which were then deiodinated with Zn in the presence of NiCl_2 catalyst to give alcohol **3** as a white solid mp. 33.5°C in 78% yield and **4** as a white solid mp. 77.2°C in 86% yield.

Scheme 2.1: Synthesis of long chain alkyl alcohols with perfluorinated tails.



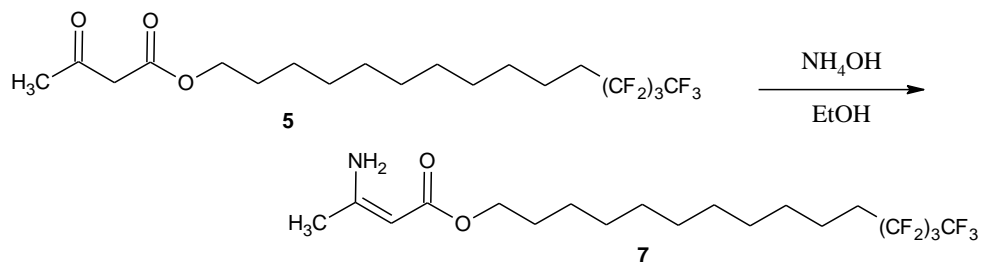
These alcohols were used to obtain esters of 3-oxobutanoic acid **5** and **6** by reaction with 2,2,6-trimethyl-4-H-1,3-dioxine-4-one in refluxing xylene. Ester **5** was obtained in 80% yield as an oily solid and ester **6** was obtained as a white solid mp. $50\text{-}51^\circ\text{C}$ in 96% yield.

Scheme 2.2: Synthesis of fluorinated acetoacetyl esters.



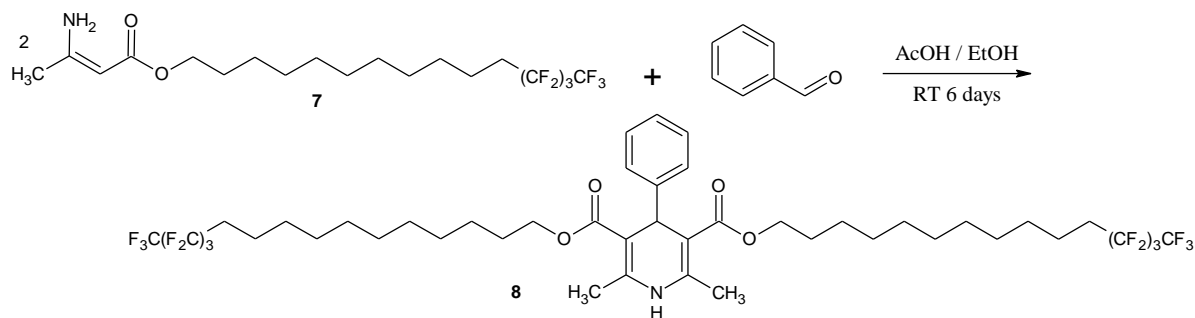
5 was reacted with concentrated aqueous ammonia in ethanol to give enamine **7** as a white solid mp. 33-35°C in 65% yield.

Scheme 2.3.



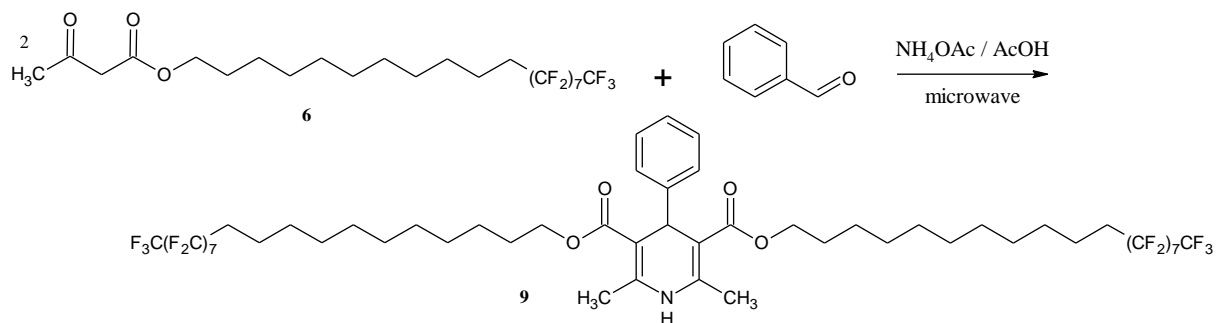
Two equivalents of **7** were reacted with one equivalent of benzaldehyde in ethanol at room temperature for six days to give after silica gel column the 1,4-dihydropyridine **8** as a clear oil in 15% yield.

Scheme 2.4: Synthesis of DHP **8** at room temperature.



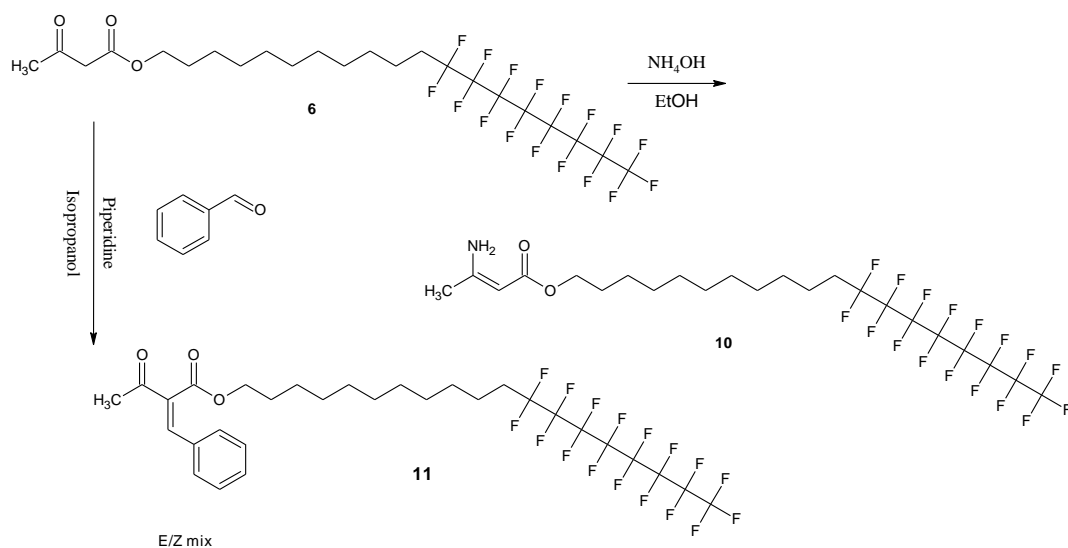
In an effort to improve on the very low yield of the DHP **8** the next reaction, (Scheme 2.5) was carried out using microwave irradiation. Two equivalents of ester **6**, one equivalent of benzaldehyde and one equivalent of ammonium acetate were reacted in ethanol under microwave irradiation at 120°C for 30 minutes to give 1,4-dihydropyridine **9** as a light yellow solid with a broad melting range 82-87°C in 25% yield.

Scheme 2.5: Synthesis of DHP **9** using microwave irradiation.

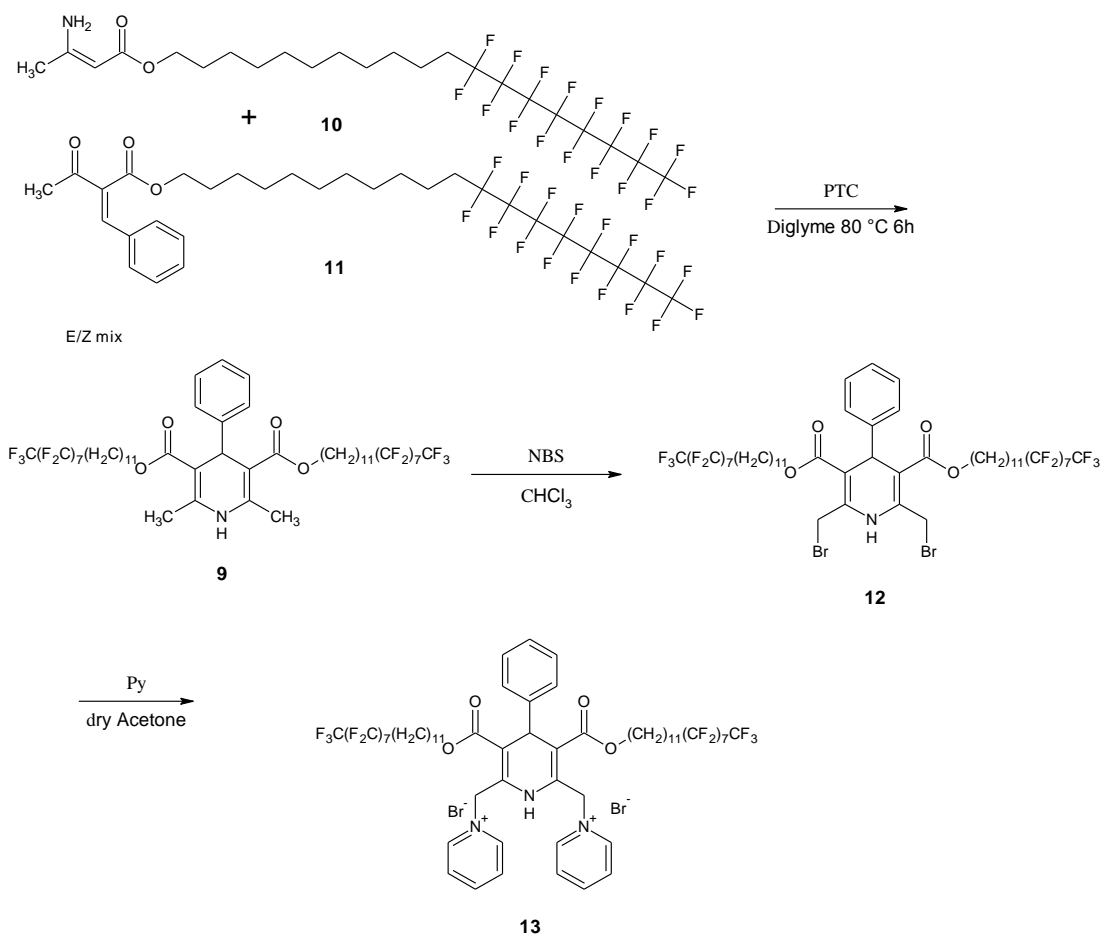


By using microwaves the yield of the 1,4-dihydropyridine **9** was improved, although not optimized but all the same quite low which may indicate that the reacting species may be entrapped in the long alkyl chains of the acetoacetate derivative and thus prohibiting the reaction from taking place. Another attempt at improving the product yield was to do the reaction using a phase transfer catalyst (PTC). In this route the perfluorinated enamine **10** was obtained by the

Scheme 2.6: Synthesis of enamine **10** and benzylidene derivative **11**.



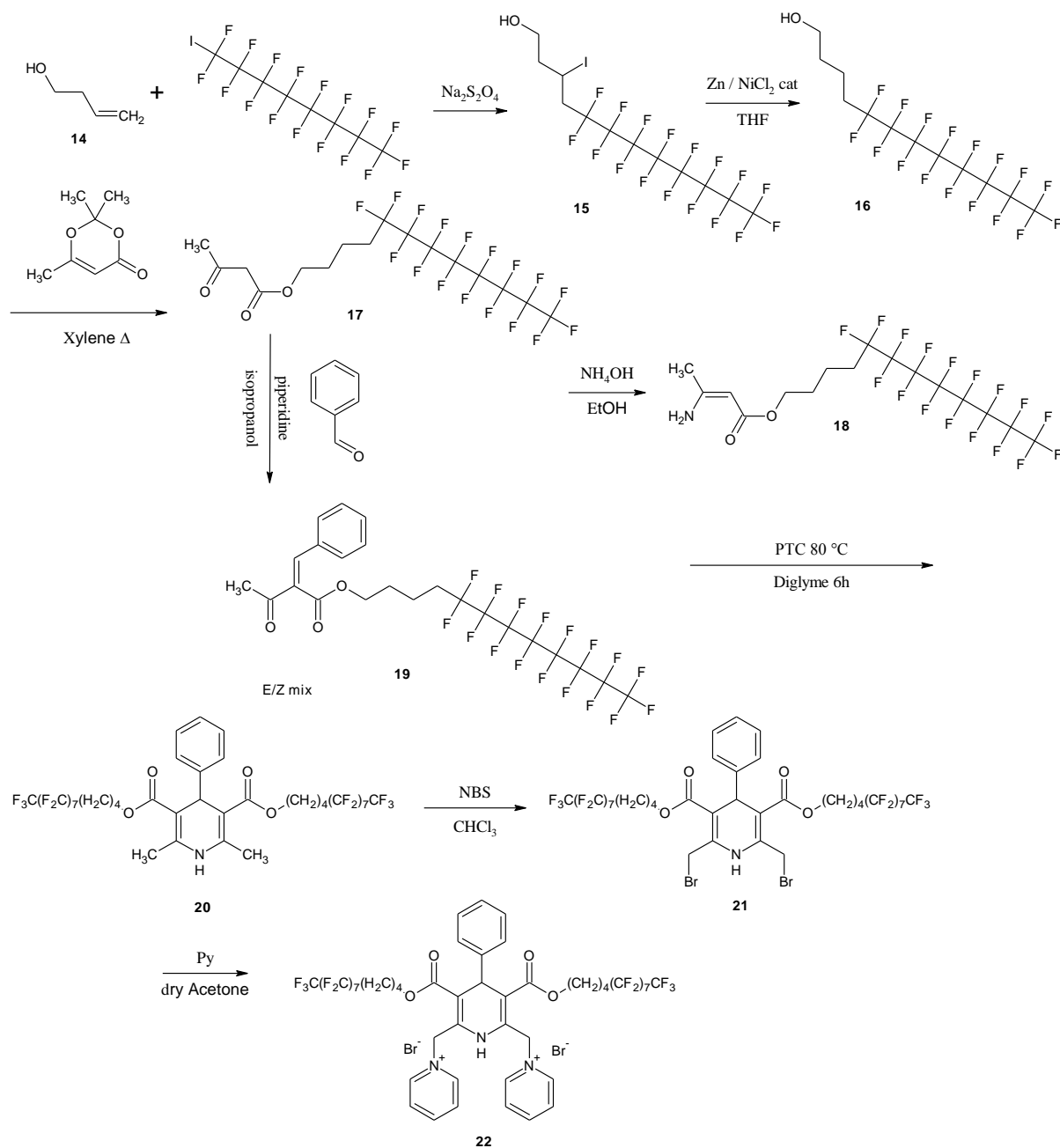
ammonium hydroxide reaction with acetoacetate **6** and the benzylidene derivative **11** was generated by reacting benzaldehyde and acetoacetate **6** with a catalytic amount of piperidine in isopropanol to give an E/Z mixture of products. When the enamine **10** and benzylidene **11** were reacted in diglyme at 80°C for 6 hours using n-butylpyridinium bromide as PTC the DHP **9** was obtained in 45% yield. The DHP **9** was further reacted with NBS in chloroform to give the dibromo derivative **12** which without purification was reacted with pyridine to give the charged DHP pyridinium compound **13** as a light yellow solid with a broad melting point 85-105°C.



Scheme 2.7: Synthesis of DHP **9** under PTC conditions.

The DHP **13** was tested at the Latvian Organic Synthesis Institute's pharmacology laboratory chemotherapy group, lead by Dr. I.Sestakova for cytotoxicity on HT-800 and MG-22A cancer cells where it showed no activity and on normal 3T3 cell where this compound was found to be totally nontoxic. Also a test was run by Kupio University, Finland to test its ability to complex

DNA and transfect cells. The test indicated that compound **13** does form a complex with DNA, but the complex showed no transfection of cells. Encouraged by the nontoxicity results research was continued to increase the transfection efficiency of these DHP amphiphiles. Thus work was carried on to synthesize DHPs with shorter ester groups according to (Scheme 2.8).



Scheme 2.8. Synthesis of DHP **22** with shortened ester groups.

This time 3-Buten-1-ol **14** was used as the alkene to which the perfluorooctyl iodide was added via a radical reaction to give a perfluorinated iodo alcohol **15** from which the iodine was removed with Zn powder using a NiCl₂ catalyst. The perfluoroalcohol **16** was reacted with 2,2,6-trimethyl-4-H-1,3-dioxine-4-one in refluxing xylene to give the acetoacetyl ester **17** which was converted to the enamine **18** and benzylidene **19** and reacted in diglyme with *n*-butylpyridinium chloride as a PTC catalyst at 80°C for 6 hours to furnish after recrystallization the DHP **20** in 45% yield as an almost white powder mp. 107-108°C. This compound was dibrominated with NBS in chloroform to give the dibromo DHP **21** and after addition of pyridine in dry acetone the DHP dipyrindinium bromide **22** as a pale yellow compound. The compound was placed in water 1 mg/ml and sonicated with a probe type sonicator to form aggregates which were imaged by atomic force microscopy (AFM) in tapping mode (Fig. 3.1) at the Institute of Chemical Physics, University of Latvia. The free energy of transferring an amphiphile from water into a micelle depends linearly on chain length, so the critical micelle concentration (cmc) depends exponentially on chain length [159]. Vesicles are closed bilayer structures with an aqueous compartment. Whether micelles or vesicles are formed can be explained largely by packing considerations [160,161]. The balance of attractive interactions and repulsive interactions gives an optimal interfacial area per molecule. Amphiphiles self-assemble into structures having area exposed to solvent (*a*) close to this optimum. Spherical micelles have the greatest interfacial area, in which $v/a = l/3$ (where *v* = volume and *l* = hydrophobic chain length), cylindrical micelles have $v/a = l/2$, and vesicles have $v/a = l$. To a first approximation, the presence of two chains on an amphiphile doubles *v* whereas the optimal *a* and *l* are constant, so a consequence of these considerations is that single-chain amphiphiles tend to form micelles whereas double-chain amphiphiles tend to form cylindrical micelles or vesicles. Vesicle formation is also favored by factors that reduce the optimal interfacial area. For example, fatty acids form micelles at high pH when their head groups are negatively charged, but they form vesicles at lower pH when their head groups interact more favorably [162]. As seen in the image the average diameter of the aggregates are 100-200 nm which is a very good size for cell transport applications.

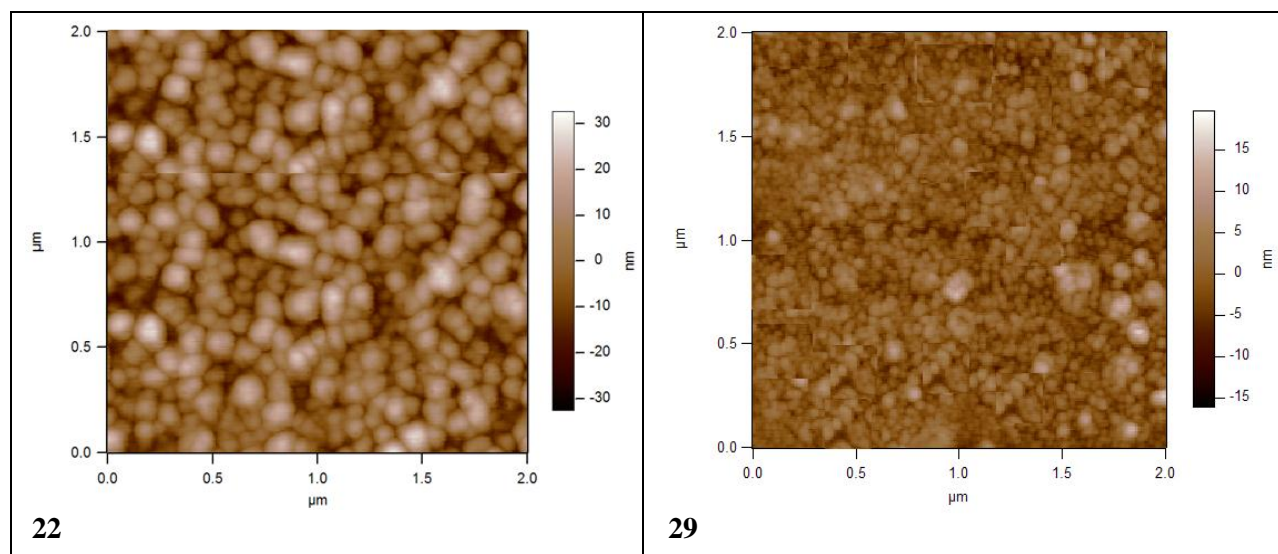
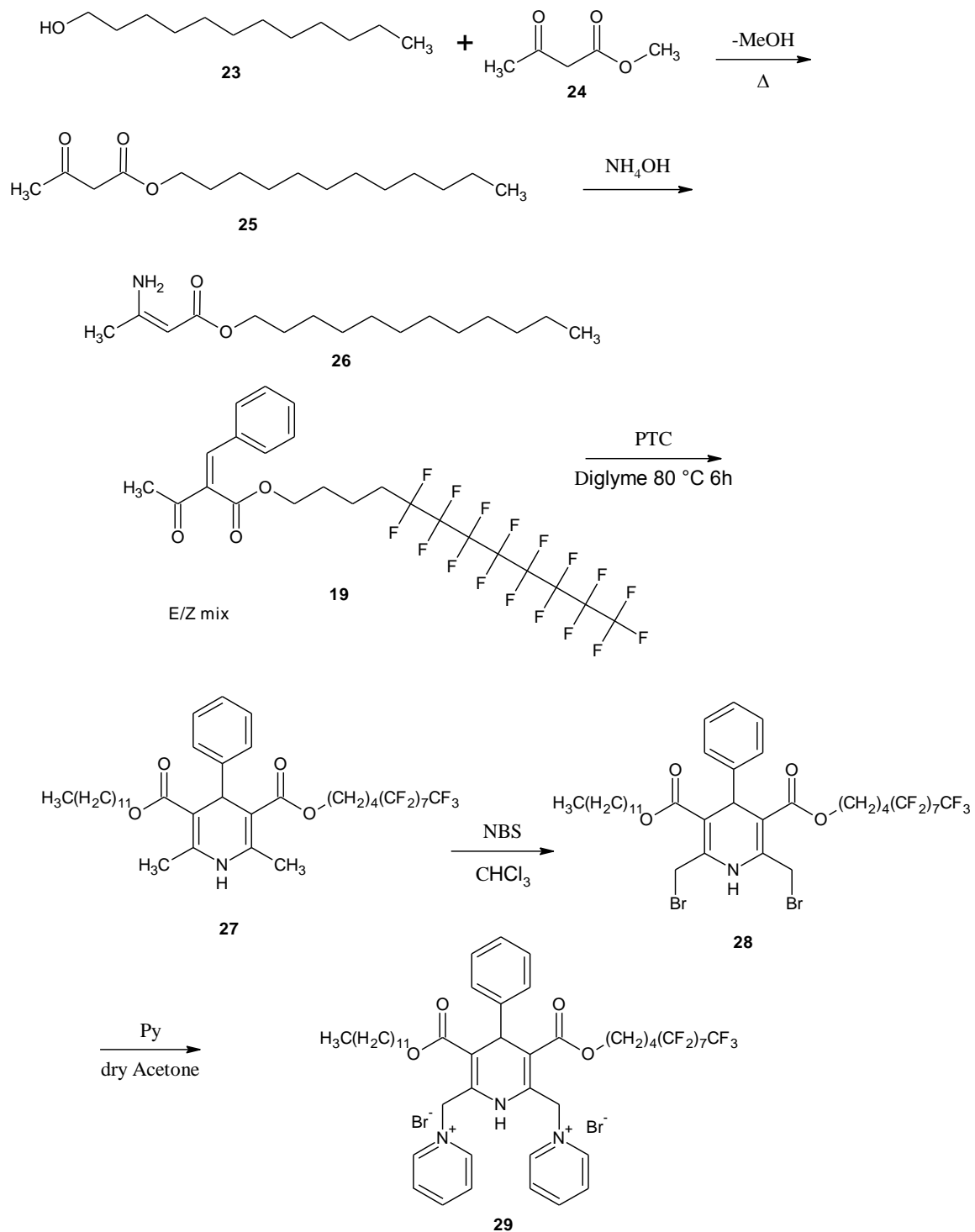
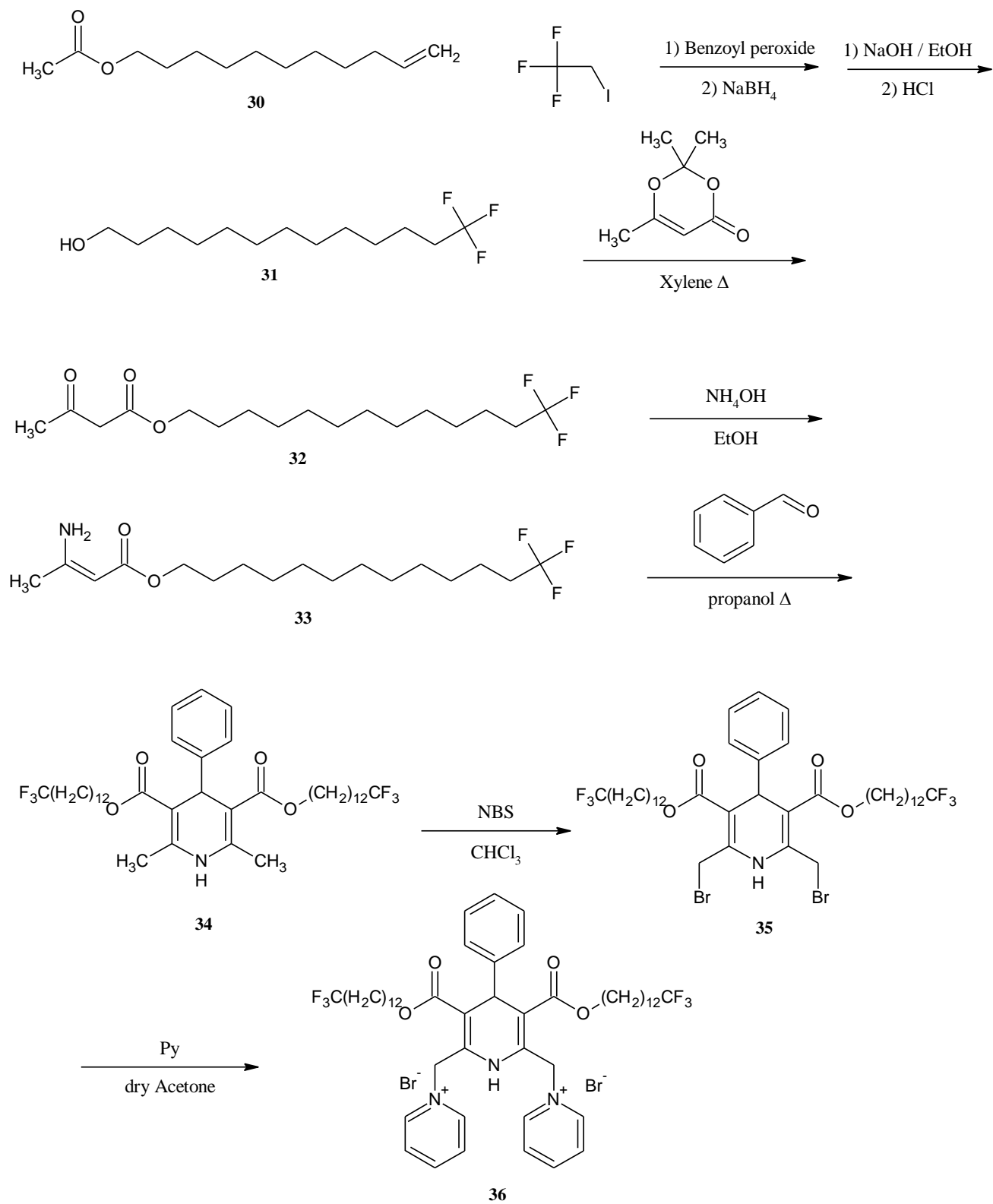


Figure 2.1. AFM images of self-assembled aggregates of DHP **22** and **29** in aqueous solution.

Since perfluorinated hydrocarbon chains are hydrophobic and also lipophobic there is a need to find the right balance of the perfluorinated content which confers stability and self-assembly properties to the amphiphiles and the nonfluorinated content which confers lipophilicity and may aid in the transport through lipid bilayer membranes. To increase the lipophilicity of the esters an unsymmetrical DHP was synthesized where only one of the ester group's contains a perfluorinated tail (Scheme 2.9). Dodecanol **23** was heated together with methyl acetoacetate **24** while methanol slowly distilled off to form the transesterified, dodecyl acetoacetate **25** which on reaction with aqueous ammonia yielded the enamine **26** as a white solid. The optimized conditions for the synthesis of **25** and **26** were worked out by K. Pajuste [3]. The enamine **26** and benzylidene **19** were reacted in diglyme at 80°C with n-butylpyridinium chloride as a PTC to yield the DHP **27** as a yellowish solid, which on bromination with NBS formed the dibromo DHP **28** and further with pyridine gave the unsymmetrical DHP pyridinium bromide **29** as a yellowish solid with a broad mp. 145-160°C with decomposition.

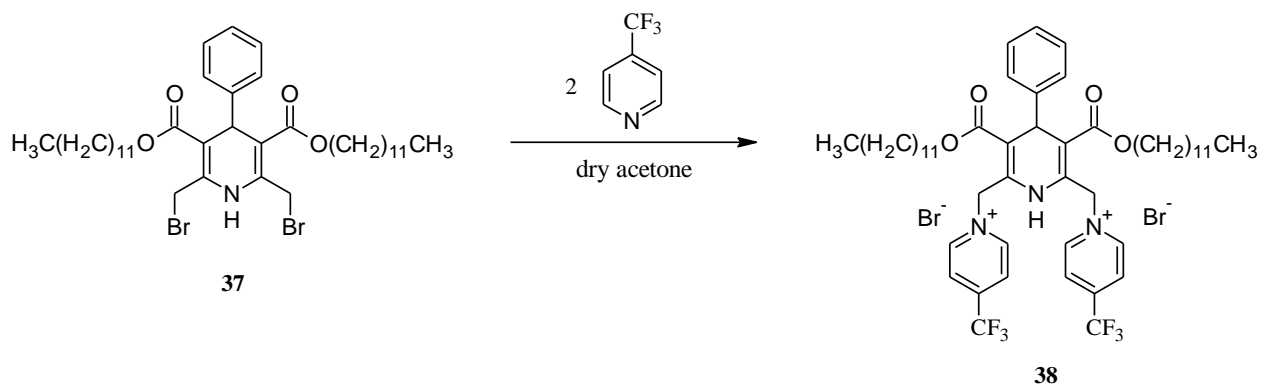
Scheme 2.9. Synthesis of unsymmetrical DHP **29** containing only one ester with a perfluorinated tail.





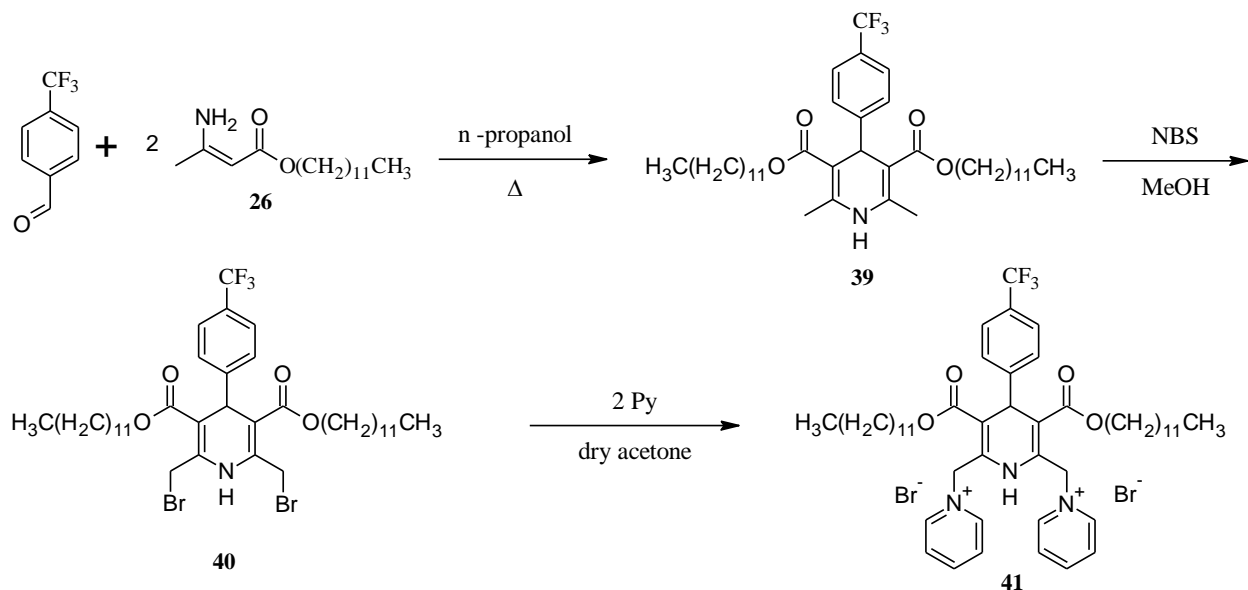
Scheme 2.10. Synthesis of a DHP amphiphile having esters with terminal CF_3 groups.

To decrease still further the fluorine content in the alkyl esters, 13,13,13-trifluoro-1-tridecanol was synthesized and used to construct a DHP derivative with 3,5 alkyl esters containing terminal CF_3 groups (Scheme 2.10). The 13,13,13-trifluoro-1-tridecanol (**31**) wasn't as straight forward to synthesize as the 5,5,6,6,7,7,8,8,9,9,10,10,11,11,12,12,12-heptafluorododecan-1-ol (**16**) since the trifluoroethyl iodide doesn't form radicals as efficiently as the perfluorooctyl iodide. Using the same procedure with $\text{Na}_2\text{S}_2\text{O}_4$ as a free radical initiator there was obtained only 22% of the CH_2CF_3 addition product, therefore a different reaction sequence was tried. Undecenyl acetate, trifluoroethyl iodide and benzoyl peroxide (2 mol %) were placed in a pressure tube since the boiling point of trifluoroethyl iodide is 55°C and the pressure tube was sealed with a screw cap. The pressure tube was placed in an oil bath and heated to 80°C . Every 3h the tube was cooled down in ice and more benzoyl peroxide was added until an H-NMR probe indicated that most of the double bond had reacted (six cycles). The iodine was deiodinated with sodium borohydride in dimethyl formamide and the acetate hydrolyzed with sodium hydroxide and after addition of acid the 13,13,13-trifluoro-1-tridecanol was obtained as a clear oil in good yield. The rest of the scheme was carried out without complications to yield the DHP **34** in 32% yield and after bromination with NBS and reaction with pyridine in dry acetone gave the DHP amphiphile **36** containing 3,5-alkyl esters with terminal CF_3 groups in 52% yield. The CF_3 group can be used as a convenient molecular label since the ^{19}F -NMR spectra shows only a single peak (a triplet) at $\delta = -66.42$ ppm for compound **36**. Thus, two other CF_3 labeled molecules were synthesized which could yield information concerning the self-assembled structures of the DHP amphiphiles (Scheme 2.11 and Scheme 2.12).



Scheme 2.11. Synthesis of a DHP amphiphile with CF_3 substituted pyridines.

Previously substitution of the bromines in DHP **37** were tried with 2-fluoropyridine but, after two days of reaction no substitution took place. Apparently the fluorine in the 2 position withdraws the electrons from the nitrogen to such an extent that it renders the nitrogen totally non-nucleophilic. The 4-trifluoromethylpyridine is also quite an electron withdrawn heterocycle, yet it was possible after 24 hours of reaction to obtain the bis-4-trifluoromethylpyridinium DHP **38** in 29% yield giving a single peak for the ^{19}F -NMR spectrum $\delta = -65.25$ ppm.



Scheme 2.12. Synthesis of DHP amphiphile with 4-p- CF_3 benzene group.

The DHP cationic amphiphile having a p-trifluoromethylbenzene group in the 4 position was synthesized in a straightforward manner starting with p-trifluoromethylbenzaldehyde and dodecyl 3-aminobut-2-enoate (**26**) in refluxing n-propanol to give the 4-trifluoromethylbenzene DHP **39** in 41% yield which was brominated with NBS and after reaction with pyridine provided the 4-p-trifluoromethylbenzene DHP dipyridinium bromide **41** in 73% yield as a white powder with a single peak in the ^{19}F -NMR spectrum with $\delta = -62.41$ ppm.

In (Fig. 2.2) are depicted the types of micelles and unilamellar liposomes that would be expected to form in aqueous solution from cationic DHP amphiphiles containing the CF_3 groups. Compound **36** would show only one ^{19}F -NMR signal if either micelles or liposomes formed as the self-assembled aggregates. For compounds **38** and **41** if micelles formed then only one signal would be observed in the ^{19}F -NMR spectrum but, if unilamellar liposomes formed then most

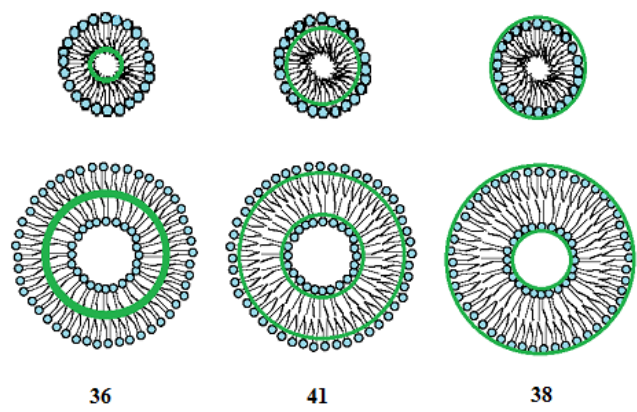


Figure 2.2. Micelles and unilamellar liposomes which could form from the CF_3 (green color) labeled DHP amphiphiles **36**, **38**, and **41** in water.

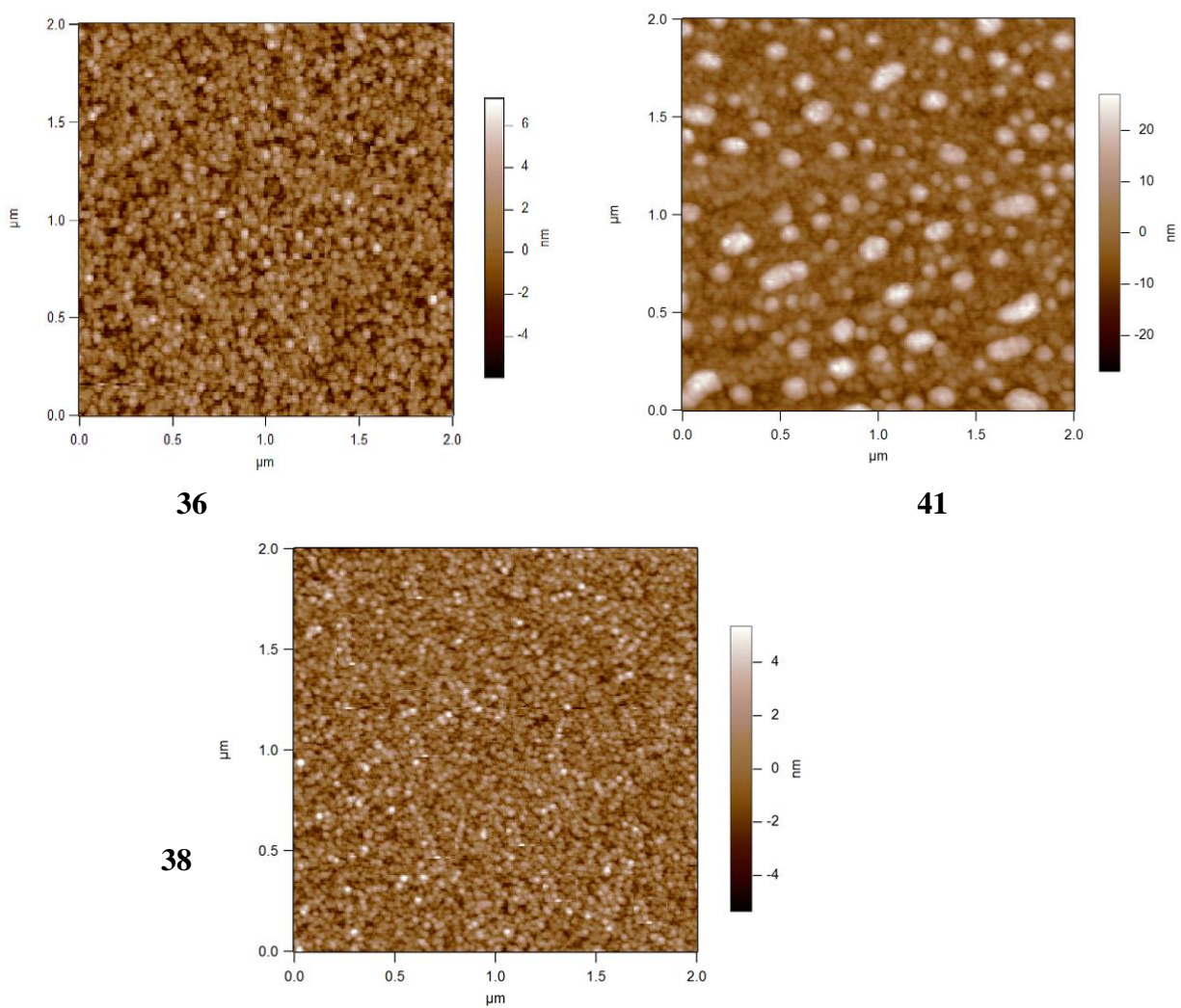
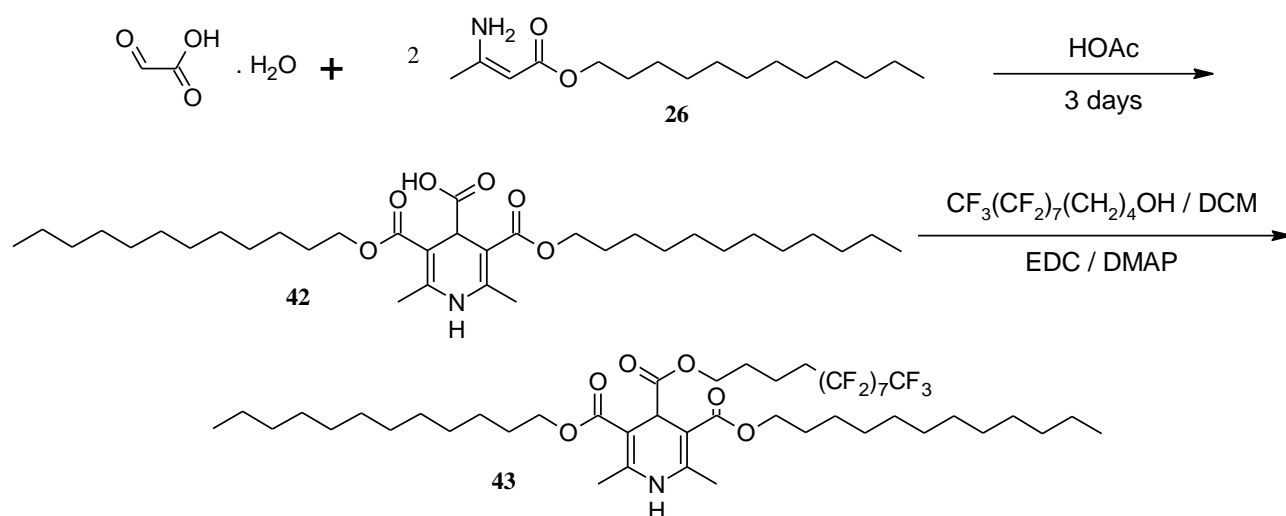


Figure 2.3. AFM images of self-assembled aggregates of **36**, **41**, and **38** in aqueous solution.

likely one would observe two signals, since the CF_3 groups inside the liposome are in a different environment than the CF_3 groups on the outside of the liposome.

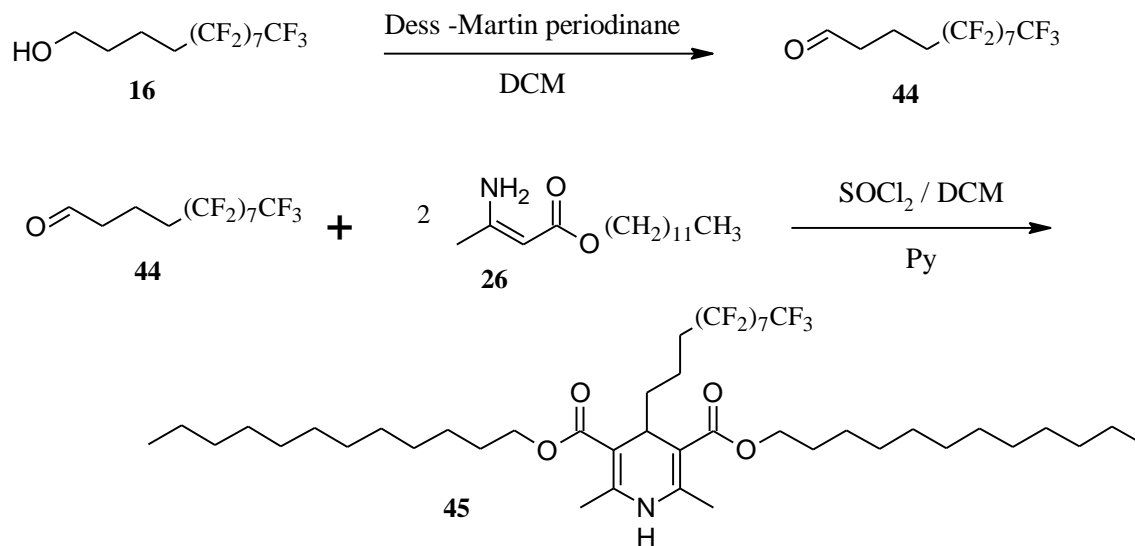
The AFM images of the self-assembled aggregates in aqueous solution of the three CF_3 amphiphiles (Fig. 2.2) indicate that the aggregates have a spherical shape and the diameters for aggregates from compounds **36** and **38** have a uniform distribution in the 50 nm range. The aggregates which formed from compound **41** show a more dispersed diameter range from about 80-160 nm.

To add more variation to the cationic 1,4-DHP amphiphile series the 4-phenyl group was replaced by a carboxylic acid group (Scheme 2.13) and alkyl groups (Scheme 2.14).



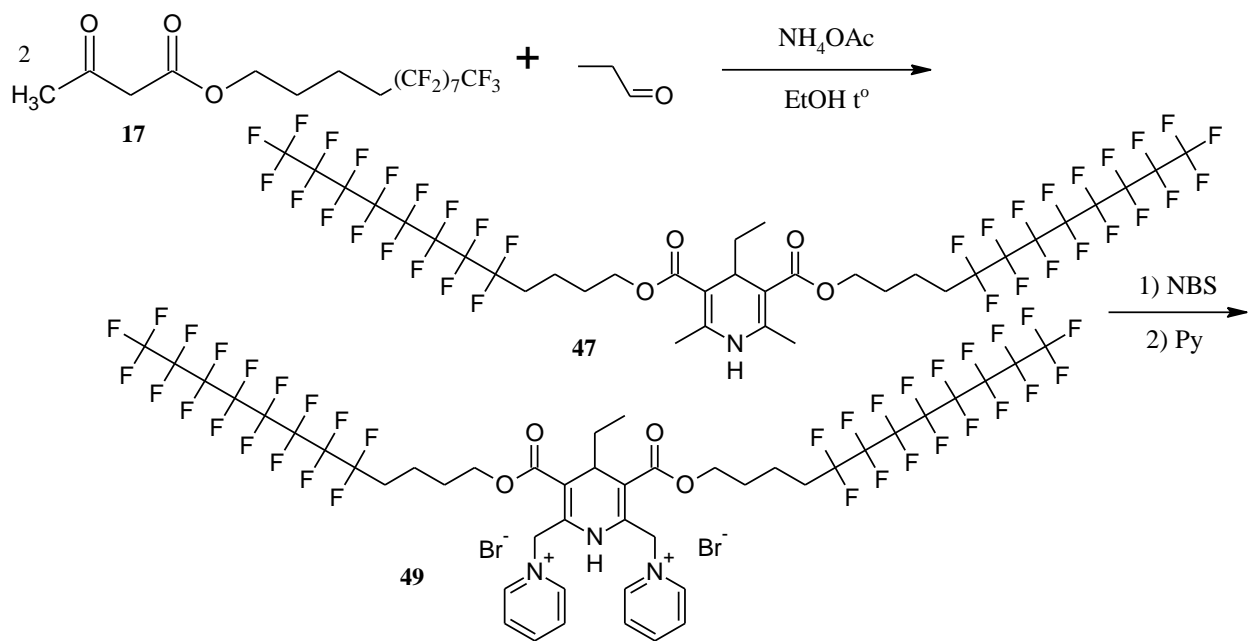
Scheme 2.13. Synthesis of DHP with a carboxylic acid group at position 4.

The 1,4-DHP 4-carboxylic acid **42** was synthesized from glyoxylic acid monohydrate and dodecyl 3-aminobut-2-enoate (**26**) by stirring these components in glacial acetic acid for three days. After pouring the reaction mixture in ice water the precipitate was recrystallized from ethanol to give the compound as a pale yellow powder in 24% yield. An attempt was made to introduce a perfluorinated ester in position 4 by using 5,5,6,6,7,7,8,8,9,9,10,10,11,11,12,12,12-heptafluorododecan-1-ol (**16**) and EDC as a coupling agent but, when the reaction was carried out in DCM and DMAP as catalyst no reaction took place. This reaction should be reinvestigated with fresh EDC (since this reagent is very hygroscopic) or tried by another route, perhaps through the acid chloride.



Scheme 2.14. Synthesis of DHP **45** which contains a perfluoro alkyl chain in position 4.

Synthesis of DHP **45** which contains a perfluoro alkyl chain in position 4, started with the Dess-Martin oxidation of the perfluorinated alcohol **16** in DCM solution at room temperature [163]. The reaction had gone to completion in 2 hours and after work up gave a yellow oil of the perfluorinated aldehyde **44** in 93% yield which solidified in the fridge. Further, the aldehyde was reacted with two equivalents of enamine **26** in the presence of thionyl chloride and pyridine in DCM at room temperature overnight. After removing the solvent and silica gel flash chromatography purification there was obtained the DHP **45** as a yellow syrup in 64% yield. An attempt was made to brominate the 2,6-dimethyl groups using NBS however, judging by the H-NMR spectrum it seems that the DHP was oxidized to the pyridine without any bromination of the methyl groups. Therefore, reaction conditions still need to be found (perhaps by lowering reaction temperature) which would yield the dibrominated DHP. Finally an ethyl group was introduced in the 4-position of a DHP containing 3,5-perfluorinated alkyl esters (Scheme 2.15) by using propionaldehyde, 2 equivalents of 5,5,6,6,7,7,8,8,9,9,10,10,11,11,12,12,12-heptafluorododecyl 3-oxobutanoate and ammonium acetate in refluxing ethanol to give the 4-ethyl DHP **27** in 56% yield. The 2,6-dimethyl groups were brominated with NBS in chloroform and reaction with pyridine in dry acetone yielded the 4-ethyl DHP amphiphile **49** as a pale yellow powder in 48% yield.



Scheme 2.15. Synthesis of a DHP amphiphile with an ethyl group at position 4.

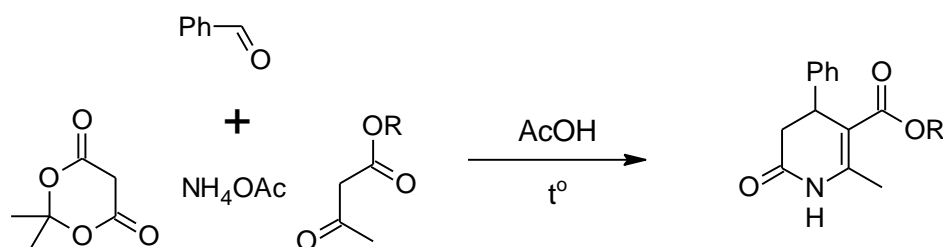
In summary a series of perfluoroalkyl ester 4-phenyl and 4-alkyl substituted 1,4-DHP cationic amphiphiles have been synthesized with greatly reduced cytotoxicity but in rather modest yields. The best yield was obtained a reaction where DCM was used as solvent and the Hantzsch condensation was catalyzed by *in situ* generated pyridinium chloride, giving a respectable 63% of the 1,4-DHP derivative.

2.2. Synthesis of 3,4-dihydro-2(1H)-pyridones (DHPODs)

The 3,4-dihydropyridone is a convenient scaffold for attaching cationic head groups and fluorous long chain esters for the construction of cationic amphiphiles. Also it is relatively straight forward to synthesize from Meldrum's acid as the second dicarbonyl component in a Hantzsch-like reaction [164,165] and recently by employing microwaves the yields have been boosted substantially [129]. The 2-pyridones possess interesting pharmacological properties such as reverse transcriptase inhibition of human immunodeficiency virus-1 (HIV-1) [166,167]. Milrinone, Amrinone [168] and their analogs are cardiotoxic agents for the treatment of heart failure. They have also been reported to possess antitumor [169,170], antibacterial [171] and other biological activities [172-174].

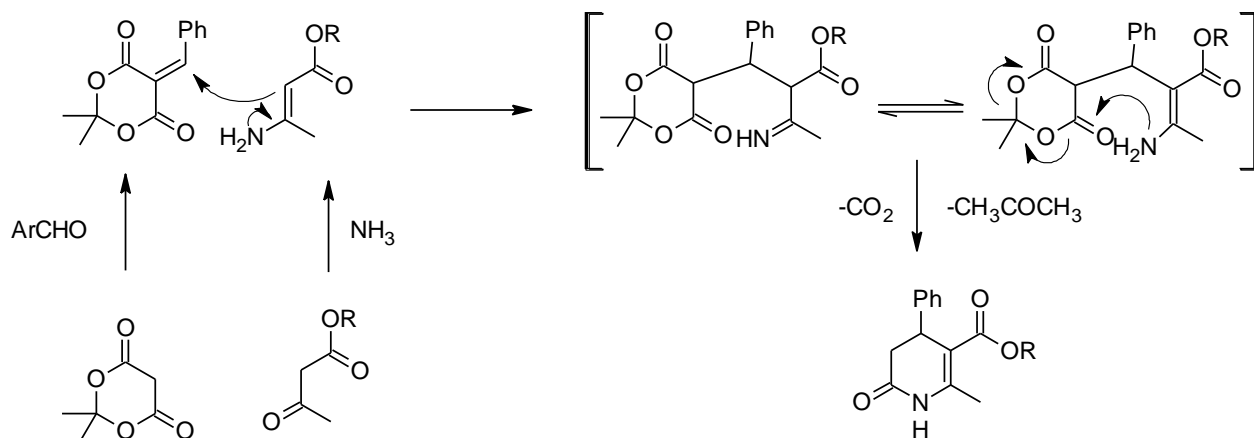
Previously Hyvonen et al. [175] have tested a series of symmetrical cationic amphiphilic double-charged didodecyl 1,4-dihydropyridine-3,5-dicarboxylate derivatives (1,4-DHP), which have self-associating properties in aqueous media forming liposomes with a mean diameter in the 50–130 nm range. The aim of this present study is to combine the properties of DHP derived cationic amphiphiles with the stability imparted by fluoros groups and to synthesize novel charged fluoros 6-methyl-3,4-dihydro-2(1H)-pyridone-5-carboxylates which are 1,4-DHP analogs having a single alkyl ester group. The formation of bilayers and vesicles usually requires bicaudal (double chain) amphiphiles but, organized supramolecular systems can be obtained from a single pure monocaudal nonrigid amphiphile by reinforcing the hydrophobic interactions in the surfactant film through the use of a highly perfluorinated tail, without recourse to classical steric effects or intermolecular associations [176]. The force of this self-assembling capacity is illustrated by the ability of single chain F-surfactants to form stable vesicles rather than micelles in water and as a rule, films and membranes made of F-surfactants are more stable than those of their hydrogenated analogs [177].

The general synthetic method used in this work for 4-phenyl-3,4-dihydro-2(1H)-pyridone synthesis employed a four component reaction using Meldrum's acid by a heterocyclization with a β -ketoester and an aromatic aldehyde in the presence of ammonium acetate in refluxing glacial acetic acid [165], (Scheme 2.16). After pouring the reaction mixture in ice-water the resulting solids were isolated by filtration and recrystallized from ethanol to provide white crystalline compounds.



Scheme 2.16. General 4 component synthesis of 3,4-dihydro-2-pyridones.

Under the reaction conditions the Meldrum's acid forms a Knoevenagel condensation product with the aromatic aldehyde and the β -ketoester with ammonium acetate form an enamine which then react together in a heterocyclization reaction with elimination of carbon dioxide and acetone to form the dihydropyridone (Scheme 2.17).



Scheme 2.17. Mechanism for the 4 component 3,4-dihydro-2-pyridone synthesis [128].

By using the above general method variously substituted DHPODs were synthesized in reasonable yields (Table 2.1).

The X-ray diffraction structure of the Cerebrocrast analogue, compound **53** revealed an interesting aspect concerning the 2-difluoromethoxy group, which interacts with the ether oxygen of the 5-ester group and forms an intramolecular CF₂H...O hydrogen bond, (Fig. 2.4).

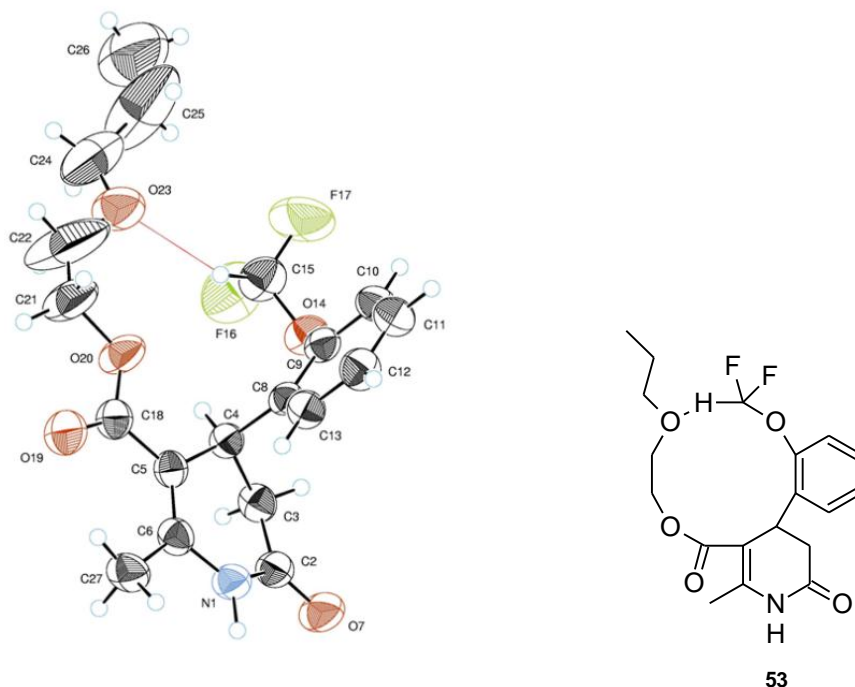


Figure 2.4. X-ray structure of compound **53** indicating a hydrogen bond (red line) between a difluoromethoxy hydrogen and an oxygen from the ester ether group.

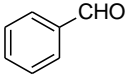
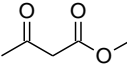
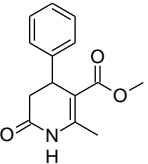
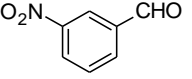
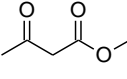
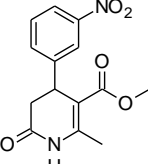
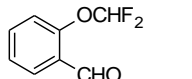
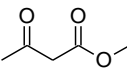
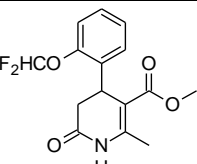
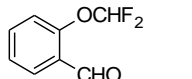
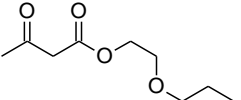
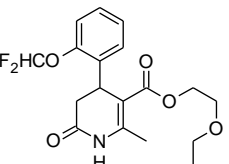
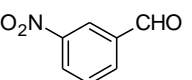
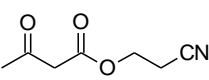
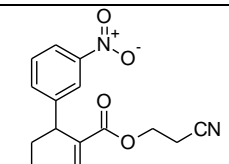
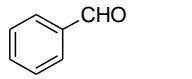
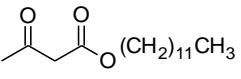
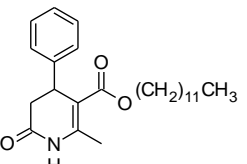
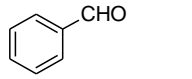
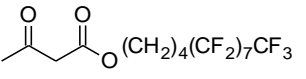
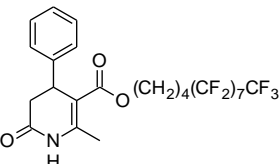
Aldehyde	Acetoacetate	Entry	DHPOD	Yield %	Mp. °C
		50		59	[178] 197-198
		51		63	[178] 204-205
		52		56	206-208
		53		43	136-138
		54		33	165-168
		55		23	79-80
		56		31	114-120

Table 2.1. DHPOD's obtained by the general method with various aryl aldehydes and acetoacetates.

Apparently the two methoxy fluorines polarize the carbon to an extent which makes it sufficiently positive to act as a hydrogen donor and form this rare hydrogen bond extending from a methyl group with $r_{\text{HO}} = 2.388 \text{ \AA}$ $\text{CF}_2\text{H}\cdots\text{O}$ hydrogen bond judging by the distance this is a weak interaction. This compound crystallizes as a hydrogen bonded dimer forming two $\text{NH}\cdots\text{O}$ bonds with $r_{\text{HO}} = 1.893 \text{ \AA}$.

Compounds with long-chain alkyl groups are very difficult to crystallize in monocrystals which would be of sufficient quality for X-ray diffraction since the thermal energy causes these molecules to be in continuous motion and disorder and require cryogenic methods to slow the motion. Therefore, it came as a great delight that at room temperature the dodecyl 4-phenyl-3,4-dihydro-2-pyridone compound **55** deposited crystals from ethanol from which the X-ray single crystal diffraction structure could be solved. As the ORTEP representation shows the crystals contain 2 molecules per unit cell which are the stereo antipodes of compound **55** (Fig. 2.5).

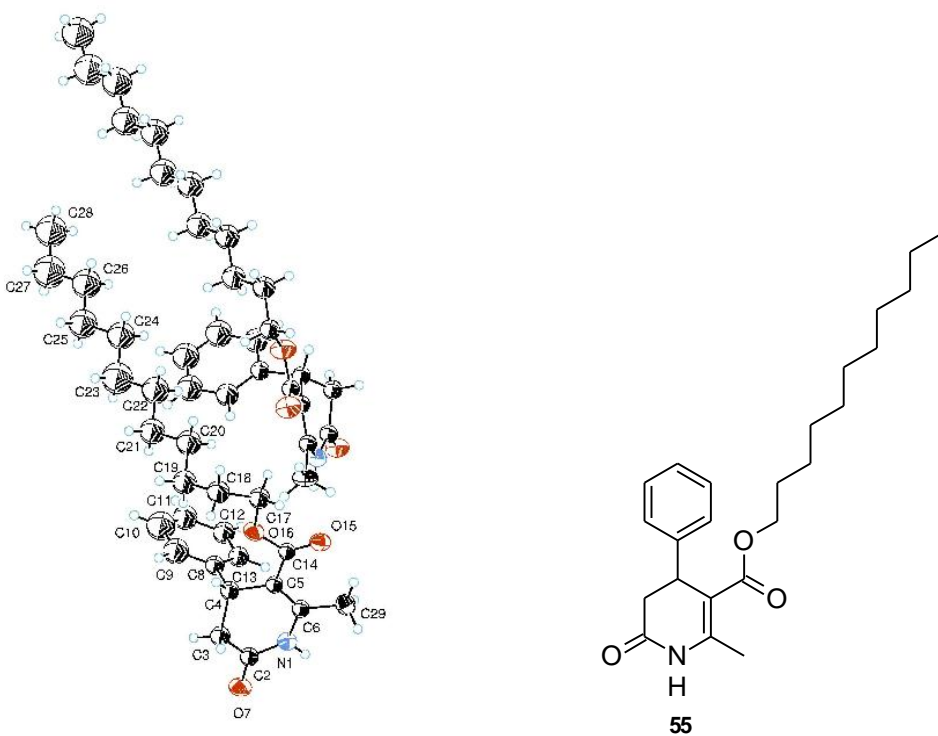


Figure 2.5. Ortep representation of compound **55**.

All attempts to grow dense X-ray quality crystals from the perfluoroalkyl ester compounds so far have failed since the crystals are very thin and not suitable for X-ray diffraction. In a recent

publication however, Hans-Joachim Lehmler *et al.* [179] have reported on the X-ray diffraction structures of perfluorinated sulfonamides. Although (partially) fluorinated compounds are often very difficult to crystallize [180], typically forming exceedingly thin, poorly stacked platelets, they were able to determine the crystal structure of *N,N*-diethyl-perfluorooctane-1-sulfonamide (Fig. 2.6). Flaky platelet crystals were obtained by recrystallization from reagent alcohol/dichloromethane at 4°C. These crystals proved far too small for analysis on conventional small-molecule diffraction equipment but gave recordable, albeit weak, diffraction using Cu K α X-rays on a specially configured hybrid small/macromolecule diffraction system.

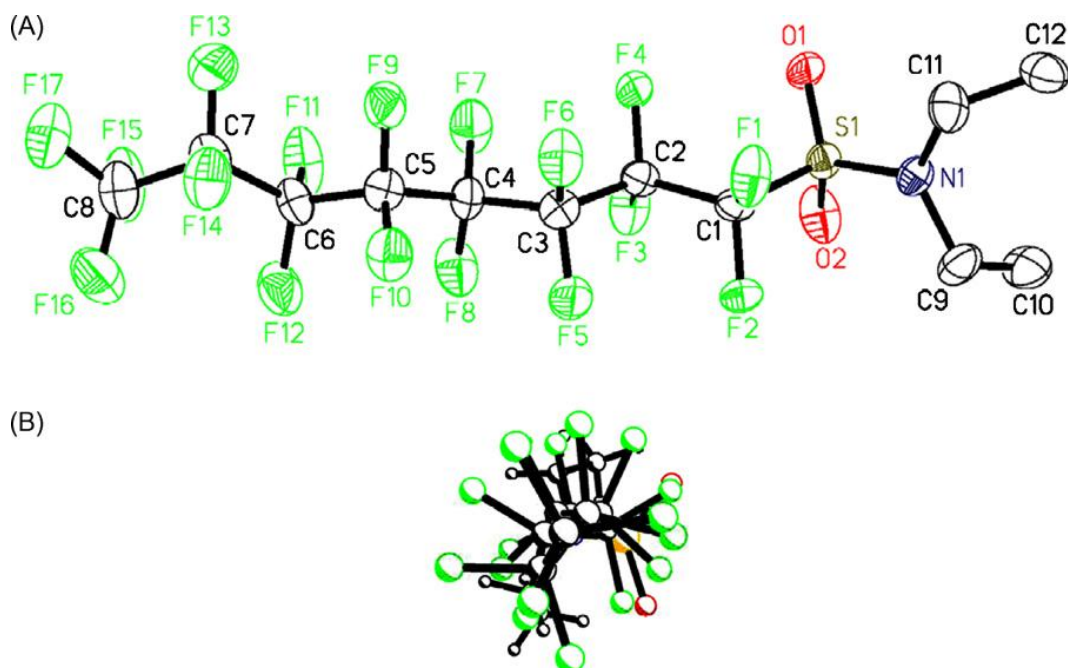


Figure 2.6. ORTEP view of *N,N*-diethyl-perfluorooctane-1-sulfonamide (A) showing the atom-labelling scheme. (B) View along the carbon backbone to illustrate the helical conformation of the perfluorooctyl chain of the major component in the crystal. Displacement ellipsoids are drawn at the 50% probability level [179].

An interesting feature of this crystal structure is that the perfluorooctyl chains of the disorder components are enantiomeric—they spiral around both ways, thus resulting in a disordered crystal. This is not surprising because perfluoroalkane chains typically adopt a helical conformation resulting from the larger van der Waals radius of fluorine relative to hydrogen [181]. As illustrated in (Fig. 2.7), the packing diagram of the crystal structure shows segregation of the electronically different parts of the perfluorooctanesulfonamide molecules to form bilayers with a perfluoroalkyl core which are separated by the sulfonamide groups.

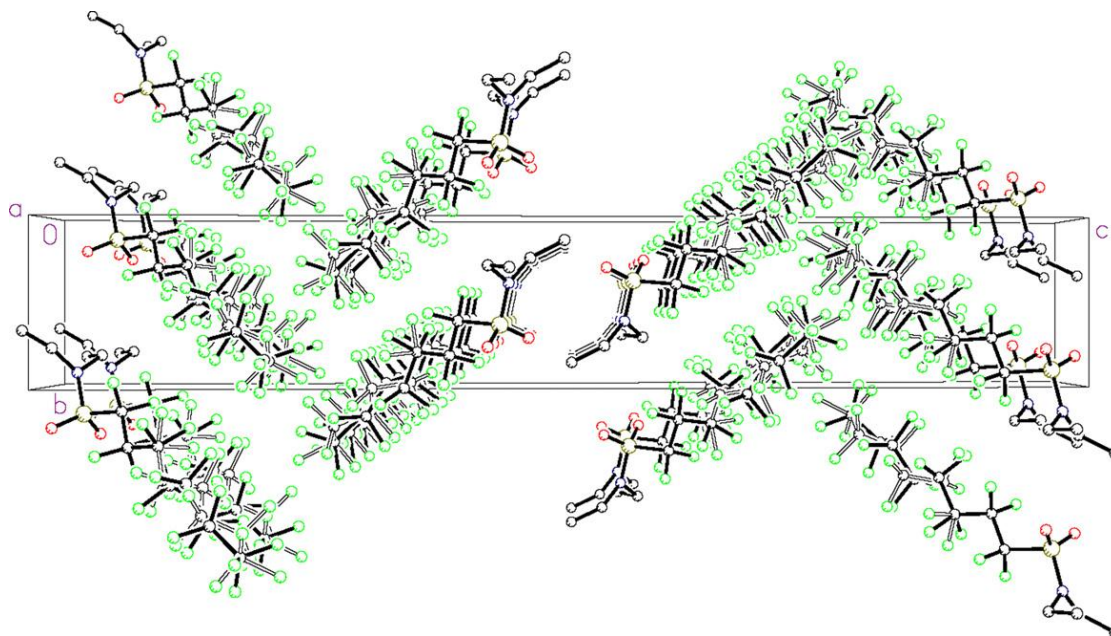
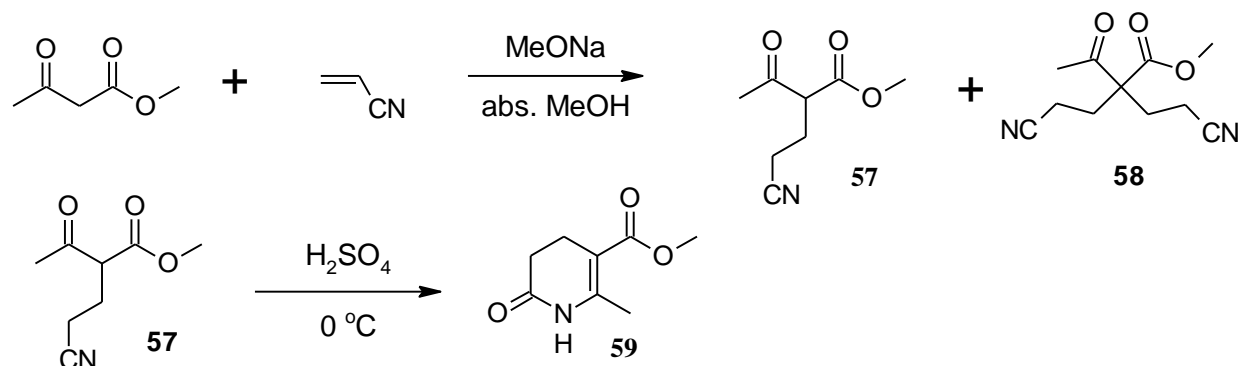


Figure 2.7. Packing diagram of *N,N*-diethyl-perfluorooctane-1-sulfonamide, viewed down the *b* axis, illustrating the bilayers of oriented parallel to the *a*–*b* plane. H atoms have been omitted for clarity.

Specifically, *N,N*-diethyl-perfluorooctane-1-sulfonamide forms bilayers parallel to the *a*–*b* plane and the perfluorooctanesulfonamides molecules are tilted within the bilayer by approximately 35°. The formation of bilayers by the perfluorooctanesulfonamides is not a surprising observation because *A*⋯*B* interactions (e.g., interactions between different parts of a molecule) are usually less favorable than the mean of *A*⋯*A* and *B*⋯*B* interactions (i.e., interactions between similar parts of a molecule) [180]. This is particularly true for the hydrophobic and lipophobic perfluoroalkyl chains [179].

The 4-unsubstituted 3,4-dihydropyridone was synthesized by a literature method [182] from methyl 2-(2-cyanoethyl)-3-oxobutanoate (**57**) by condensation in concentrated sulfuric acid. The methyl 2-(2-cyanoethyl)-3-oxobutanoate was in turn synthesized from methyl acetoacetate and sodium ethoxide in ethanol as solvent with the drop-wise addition of acrylonitrile. Two products formed, the wanted mono substituted or methyl 2-(2-cyanoethyl)-3-oxobutanoate and the doubly substituted methyl 2,2-bis(2-cyanoethyl)-3-oxobutanoate product **58**. It was not possible to get only one product, even by very slow acrylonitrile addition or by lowering the temperature. The bis-ethylcyano product was a solid and precipitated from the

reaction mixture and after high vacuum distillation the mono substituted product **57** was isolated as an oil in 28% yield (Scheme 2.18).



Scheme 2.18. Synthesis of 4-unsubstituted 3,4-dihydro-2-pyridone **59**.

The methyl 2-(2-cyanoethyl)-3-oxobutanoate was added drop-wise with stirring to an ice cooled concentrated sulfuric acid and after stirring for half an hour at room temperature the syrupy mixture was poured into ice water. The white precipitated product was filtered and washed with cold water and dried to give a white powder of methyl 6-methyl-3,4-dihydro-2(1H)-pyridone-3-carboxylate (**59**) in 62% yield. The single crystal X-ray diffraction analysis indicated that this compound crystallizes as a dimer (**a**), which is reminiscent of the hydrogen bonded base pair formation (**b**) and molecular recognition in RNA and DNA and can be used as their simple experimental or theoretical models (Fig. 2.8). Also several attempts were made to crystallize compound **59** and the highly toxic anticancer drug 5-fluorouracil (5-FU) as their hydrogen bonded dimers (**c**) but, so far these attempts have failed. The idea was to use hydrogen bonding

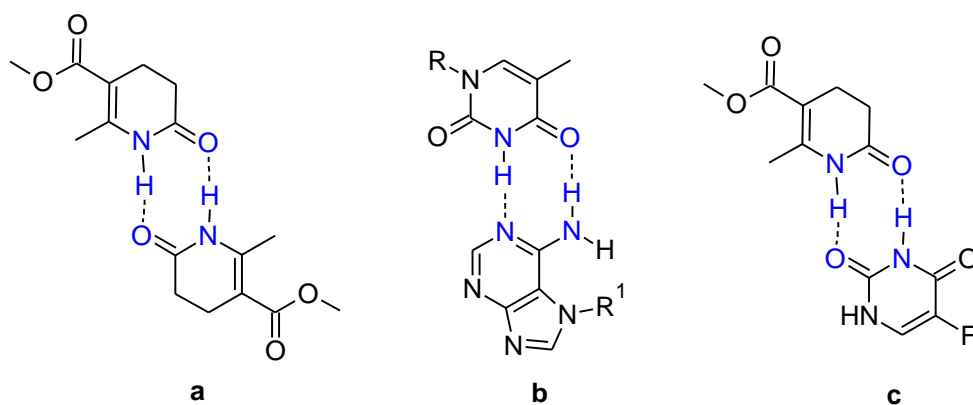
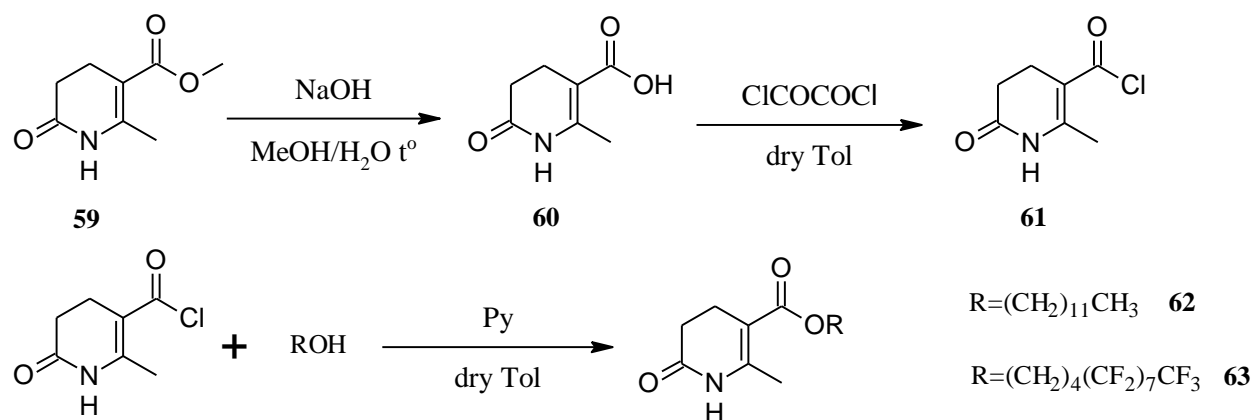


Figure 2.8. Representation of compound **59** as a hydrogen bonded dimer **a** from X-ray data, hydrogen bonded dimer of DNA base pairs **b** and hetero H-bonded pairs of **59** and fluorouracil **c**.

interactions of 5-FU to hold it inside some DHPOD derived aggregates, since in dipalmitoylphosphatidylcholine/cholesterol (DPPC/Chol) 5-FU entrapped liposomes there was observed extensive leaking of the drug from the liposomes [183].

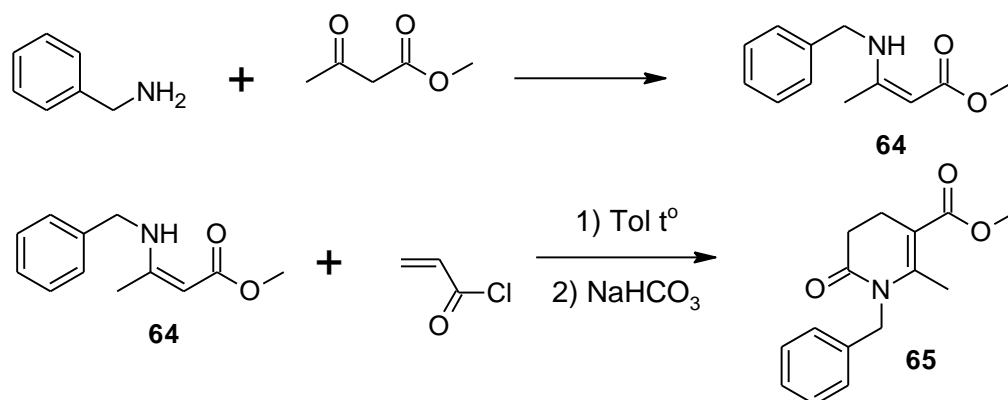
The methyl ester of dihydropyridone **59** was hydrolyzed with NaOH in refluxing aqueous methanol and after acidifying with HCl the 6-methyl-3,4-dihydro-2(1H)-pyridone-5-carboxylic acid (**60**) was isolated as a white powder in 80% yield. Oxalyl chloride was added dropwise to the dihydropyridone acid (**60**) in dry toluene to furnish the crude 6-methyl-3,4-dihydro-2(1H)-pyridone-5-carbonyl chloride (**61**) in almost quantitative yield as an orange solid. The dihydropyridone acid chloride was reacted further with dodecanol or 5,5,6,6,7,7,8,8,9,9,10,10,11,11,12,12,12-heptafluorododecanol in dry toluene with pyridine as base to provide the dodecyl 6-methyl-3,4-dihydro-2(1H)-pyridone-3-carboxylate (**62**) and 5,5,6,6,7,7,8,8,9,9,10,10,11,11,12,12,12-heptafluorododecyl 6-methyl-3,4-dihydro-2(1H)-pyridone-3-carboxylate (**63**) respectively as pale yellow solids (Scheme 2.19).



Scheme 2.19. Synthesis of dodecyl and its perfluoro analog 6-methyl-3,4-dihydro-2(1H)-pyridone-3-carboxylates.

N-benzyl-3,4-dihydro-2-pyridone (**65**) was synthesized from methyl 3-(benzylamino)but-2-enoate (**64**) and acryloyl chloride in refluxing toluene (Scheme 2.20). The N-benzyl-

dihydropyridone after purification was isolated as a yellow syrup.



Scheme 2.20. Synthesis of N-benzyl-3,4-dihydro-2-pyridone **65**.

2.3. Bromination of 3,4-dihydropyridine-2(1*H*)-ones

For further elaboration of the 3,4-dihydropyridin-2-one structure, the methyl group at carbon 6 stands out as a convenient handle. Thus following the previously well established procedure for 2,6-dimethyl DHP bromination with N-bromosuccinimide (NBS) in methanol, attempts were made to brominate the allylic 6-methyl group of a 3,4-dihydro-2-pyridone **52** (Scheme 2.21). The reaction took place readily and after workup gave an almost quantitative yield of a product. The product by NMR analysis didn't appear to be the desired 6-bromomethyl

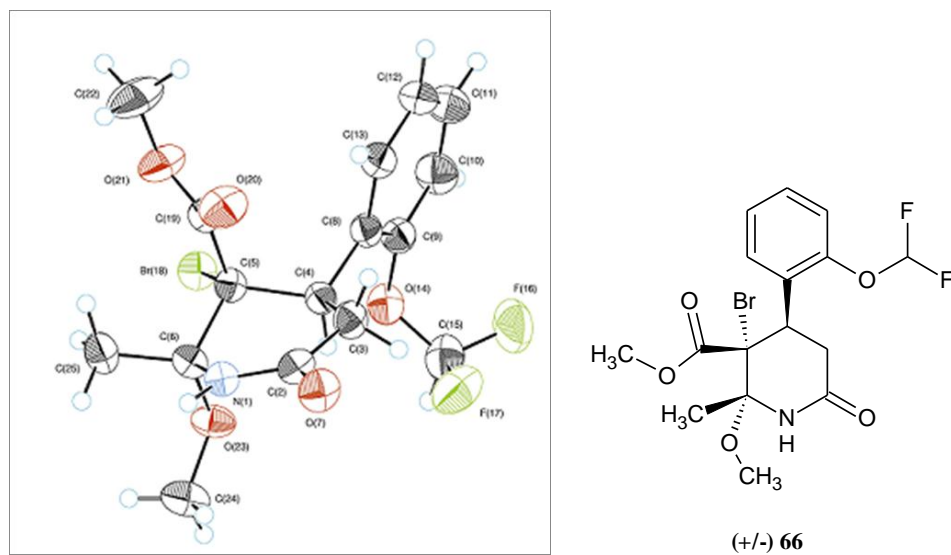
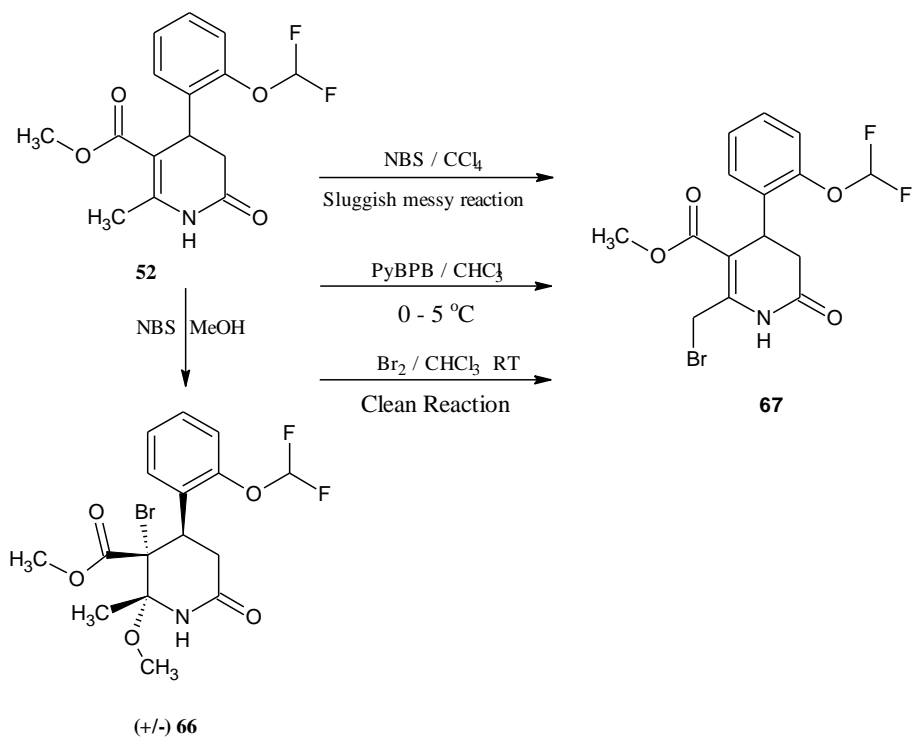


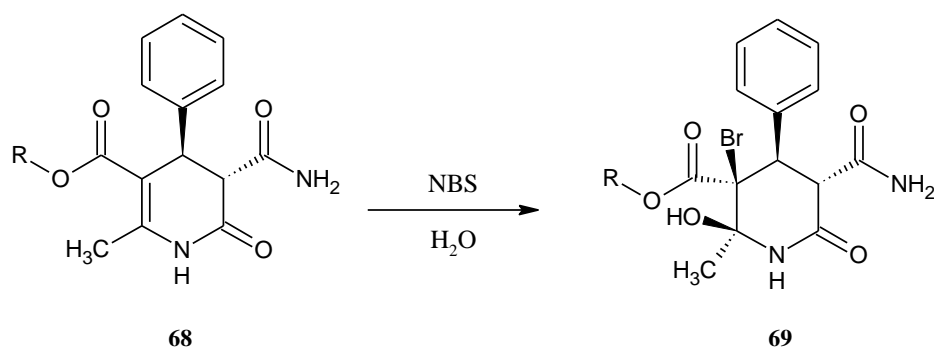
Figure 2.9. X-ray structure of compound **66**



Scheme 2.21. Bromination of 3,4-dihydro-2-pyridone **52**.

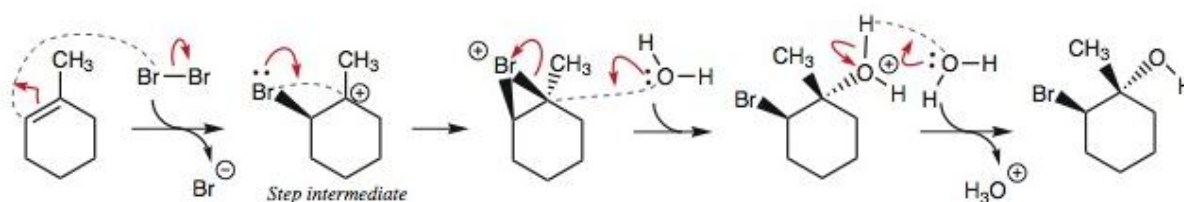
2-dihydropyridone **67**. After growing crystals and single crystal X-ray diffraction analysis the structure was ascertained to be an MeO and Br addition product across the double bond or compound **66** (Fig. 2.9).

A noteworthy aspect about structure **66** is that the MeO- and Br+ have added across the double bond in a cis fashion. This is a similar reaction which was reported by Z. Kalme *et al.* [184] (Scheme 2.22) where they observed that HO- and Br+ had added across the double bond also in a cis configuration.



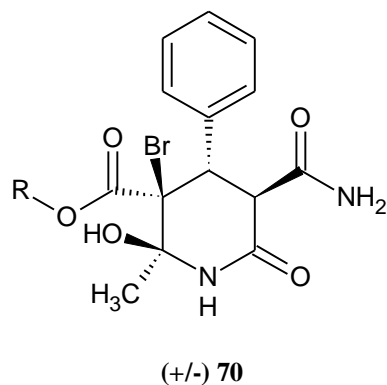
Scheme 2.22. The bromohydrin reaction with a dihydro-2-pyridone derivative [184].

This is a typical bromohydrin reaction, except that in the classical case the HO⁻ and Br⁺ add across the double bond in a trans fashion, due to the bromonium ion intermediate being attacked by the HOH nucleophile from the back side (Scheme 2.23).

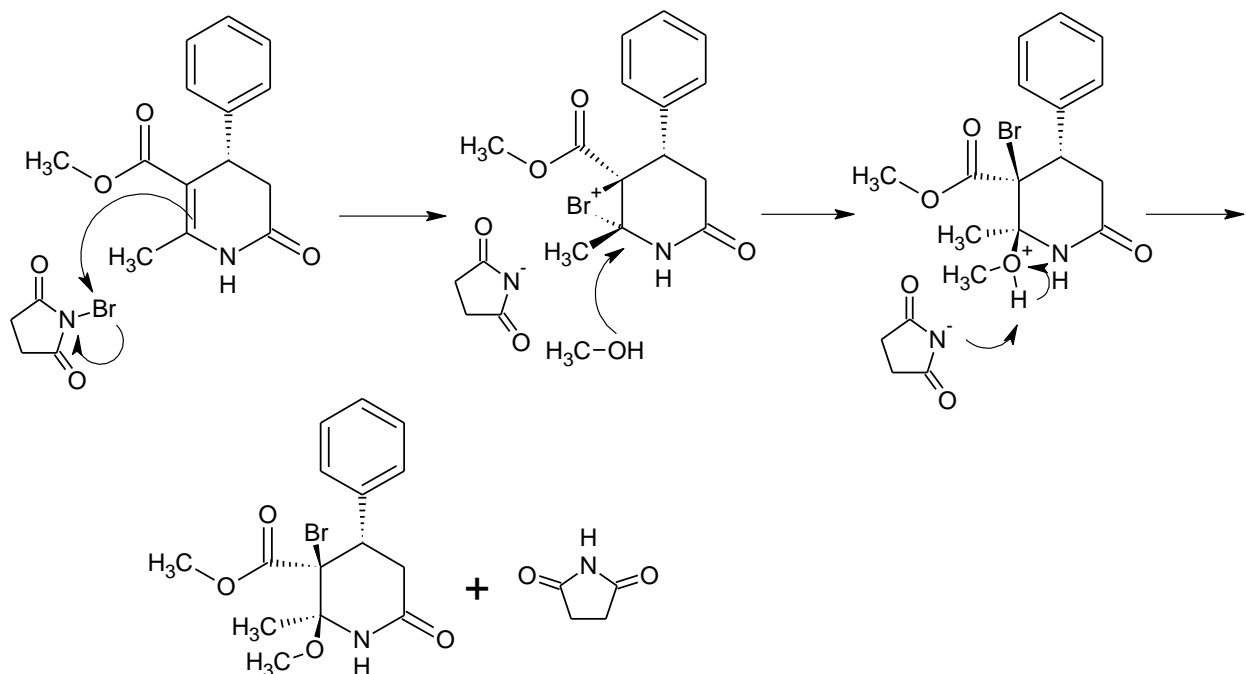


Scheme 2.23. Classical bromohydrin reaction of 1-methylcyclohexene giving the trans addition product.[185]

The spatial configuration of functional groups were assigned by ¹H-NMR based on the observed J_{34} being < 0.5 Hz which indicates that the Ph and amide groups have to be in a trans configuration. However, since they didn't have an X-ray structure for final proof, it is more logical that the structure would be drawn as compound **70** where the steric impediment from the Ph group for the incoming Br⁺ is minimized.



The MeO⁻ and Br⁺ addition across the double bond for compound **52** likely follows the mechanism depicted in (Scheme 2.24).



Scheme 2.24. A postulated mechanism whereby 3,4-dihydro-2-pyridone **52** adds MeO⁻ and Br⁺ across the double bond.

It is postulated that after the Br⁺ electrophile reacts at carbon 5, a bromonium ion forms where the CO₂Me and Me groups are trans with respect to each other, this is possible because the DHPOD heterocycle can assume a puckered conformation. The MeOH reacts at carbon 6 since carbon 5 is sterically crowded by the phenyl and the carboxy groups, finally deprotonation yields the cis substituted product. This reaction is depicted more clearly below using ACD/Chemsketch program providing the energy minimized structures based on molecular mechanics (Fig. 2.10).

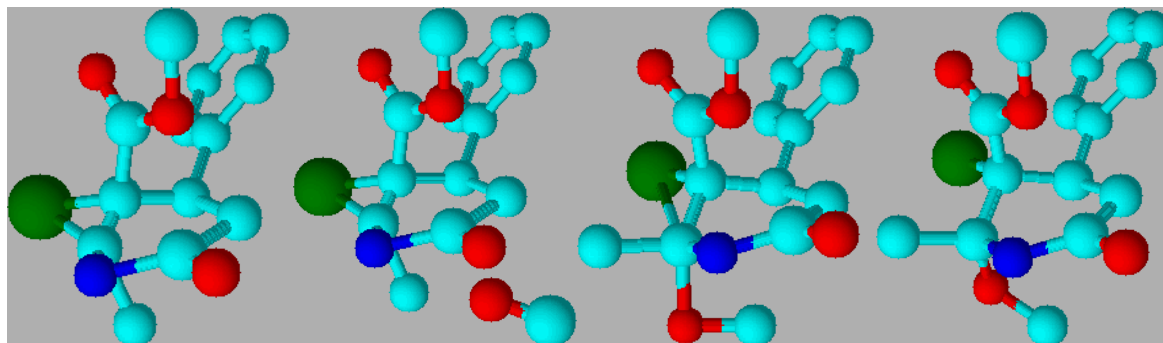


Figure 2.10. Addition of MeO to the bromonium intermediate.

When the bromination of the 6-methyl group of dihydropyridone **52** was attempted using NBS with 3-chloroperoxybenzoic acid (MCPBA) as a free radical initiator in carbontetrachloride, a

very sluggish and messy reaction took place, giving the desired 6-bromomethyl dihydropyridone **67** in addition to many byproducts (TLC). Bromination of the 6-methyl group of 4-aryldihydropyridones as described in the literature has been accomplished with NBS in refluxing chloroform for 10-14 hours [186]. Although the 6-bromomethyl compound was not isolated its presence as intermediate was suggested by the subsequent lactonization producing γ -lactone fused 3,4-dihydropyridones. Another report on the 6-methyl group bromination utilized bromine in chloroform and irradiation with a 500 W lamp, in this case only the crude compound was isolated and not further characterized [187]. To optimize the reaction, bromination was next tried with pyridinium bromide perbromide in dry chloroform at 0-5°C. After 30 minutes the reaction had gone to completion and after work up the 6-bromomethyl dihydropyridone **67** was isolated in 85% yield. Finally bromination of compound **52** in dry chloroform by the drop-wise addition of a bromine chloroform solution at room temperature gave a clean reaction producing compound **67** in 95% yield. Recrystallization from methanol deposited crystals which after single crystal X-ray diffraction confirmed the structure, (Fig. 2.11).

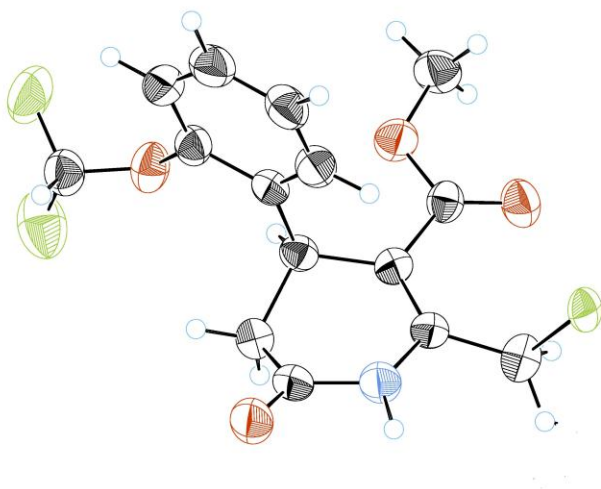
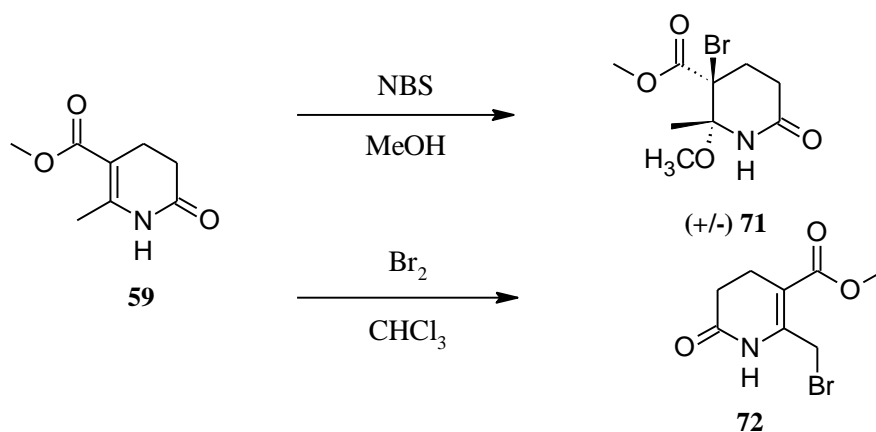


Figure 2.11. X-ray structure of compound **67**.

The $^1\text{H-NMR}$ spectrum has a doublet at $\delta=4.48$ ppm, $^2J=10.5$ Hz and a doublet at 5.03 ppm, $^2J=10.5$ Hz for the CH_2Br protons indicating the nonequivalence of the 2 protons. This phenomenon is also observed for the 4-substituted 2,6-bis(CH_2X) 1,4-DHP system as recently reported by M.Petrova *et al* [189], explaining how the CH_2X protons of symmetrically

substituted 1,4-dihydropyridine rings become diastereotopic in the presence of different substituents at position 4, thereby, providing an AB system in the corresponding $^1\text{H-NMR}$ spectra. The extent of the observed non-equivalence of the methylene protons should be influenced by the spatial conformation of side chains in the molecule and/or the anisotropy of the substituents.

There are two questions begging an answer to the above results: a) Is the phenyl group at position 4 responsible for the steric hindrance which dictates the syn addition of MeO^- and Br^+ across the double bond? b) Is the phenyl group at position 4 responsible for the diastereotopic effect of the CH_2X protons? The answer to these two questions can be provided by simply removing the phenyl group!



Scheme 2.25. Bromination of 4-unsubstituted 3,4-dihydro-2-pyridone.

Thus bromination of dihydropyridone **59** with one equivalent NBS in methanol yielded the MeO and Br substituted product **71** as the only isolated compound (Scheme 2.25). After growing crystals the X-ray diffraction analysis revealed (Fig. 2.13) that this time only the trans addition product had formed, indicating that if the 4-phenyl group is absent the classical bromohydrin

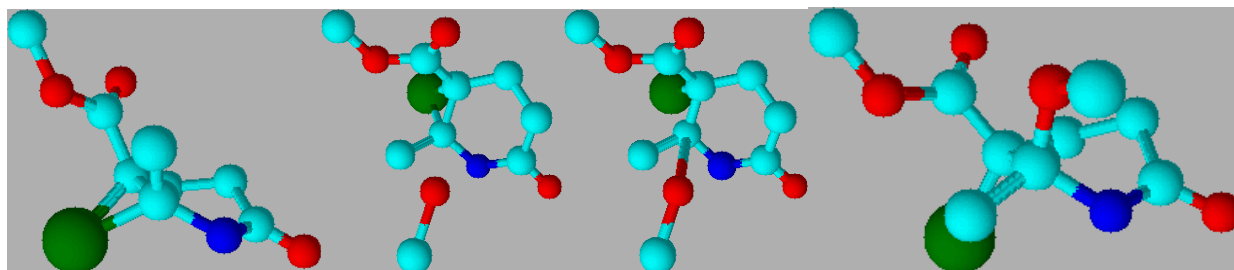


Figure 2.12. MeO addition to the bromonium ion resulting in trans product.

reaction mechanism is followed and the initial bromonium ion is attacked by MeOH from the back side resulting in the trans addition product (Fig 2.12).

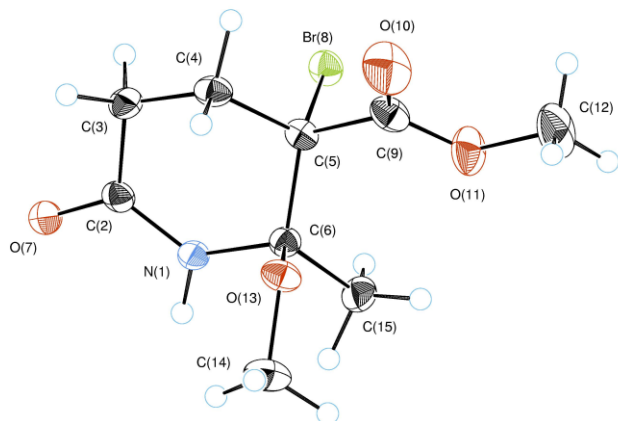


Figure 2.13. ORTEP representation of compound **71**.

The bromination of dihydropyridone **59** with 1 equivalent bromine in dry chloroform gave a high yield of 6-bromomethyl-3,4-dihydro-2-pyridone and after recrystallization from methanol deposited hexagonal crystals in 70% yield. The structure **72** was confirmed by X-ray diffraction analysis (Fig. 2.14).

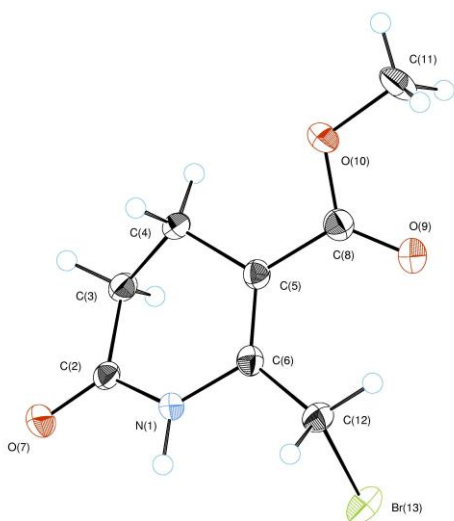
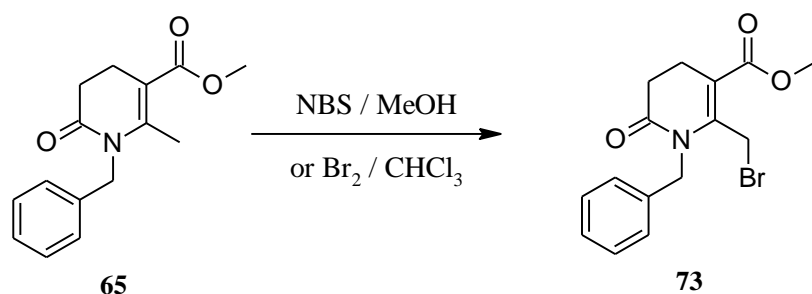


Figure 2.14. ORTEP representation of compound **72**.

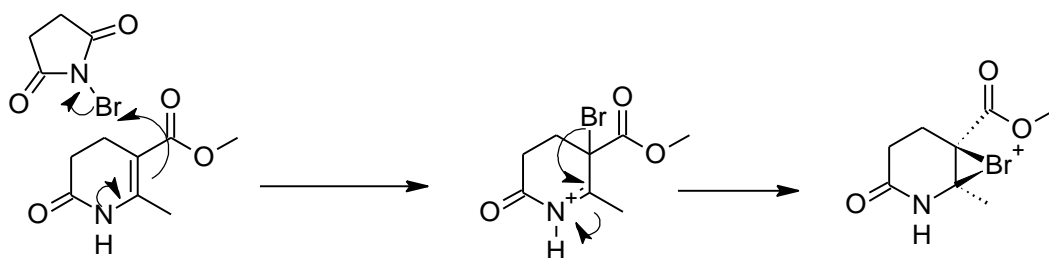
The $^1\text{H-NMR}$ spectrum shows only a singlet for the CH_2Br protons at $\delta=4.66$ ppm indicating that the substituent at position 4 is indeed the main factor responsible for the non-equivalence of the 2 protons, exerting steric hindrance through the 3-COOR and with additional hydrogen bonding augment the hinderance to free rotation about the 2-methyl bond.

Bromination was also tried on N-benzyl substituted dihydro-2-pyridone to see if this has any effect on the bromine addition to the double bond and stereochemistry according to (Scheme 2.26).



Scheme 2.26. Bromination of N-benzyl substituted dihydro-2-pyridone.

In this case using either NBS in methanol or bromine in chloroform the only product isolated was the 6-bromomethyl dihydro-2-pyridone **73**. This may indicate that in the N-unsubstituted case the electron pair on the N participates in the electrophilic addition of Br^+ according to the mechanism (Scheme 2.27).



Scheme 2.27. Electron pair on N can participate in the electrophilic Br^+ addition to the double bond forming the bromonium ion.

Apparently in the N-benzyl substituted case this mechanism is hindered and only the normal allylic radical bromination takes place.

Having optimized the bromination of the 6-methyl group by using bromine in chloroform, the following 6-bromomethyl substituted 3,4-dihydro-2-pyridones were synthesized in good yields (Fig. 2.15).

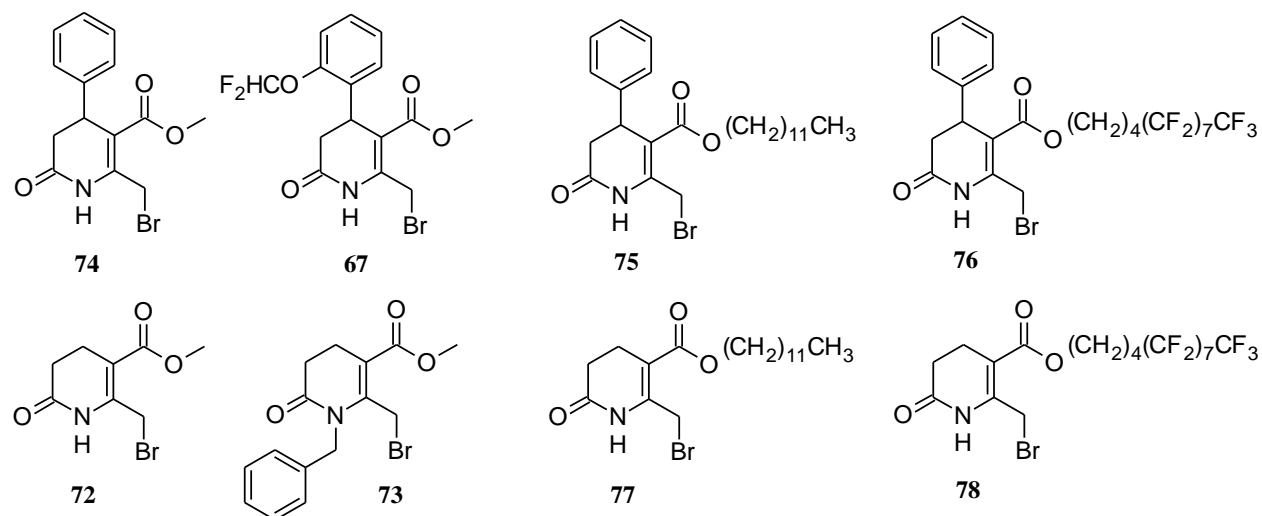
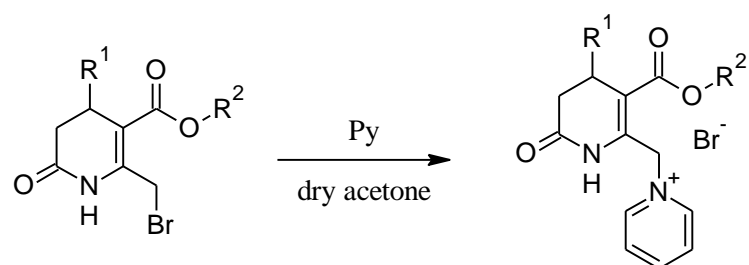


Figure 2.15. A series of 6-bromomethyl-3,4-dihydro-2(1H)-pyridones synthesized by the optimized bromination method.

2.3. Synthesis of 3,4-dihydro-2(1H)-pyridone amphiphiles and their self-assembly

The 6-bromomethyl-3,4-dihydro-2(1H)-pyridones were reacted with pyridine in dry acetone undergoing a facile pyridine nucleophilic substitution of the bromine providing 3,4-dihydro-2(1H)-pyridone-6-methylpyridinium bromides (Scheme 2.28).



Scheme 2.28. 6-Bromomethyl DHPOD reaction with pyridine, providing the pyridinium bromide salts.

Using the above procedure the following DHPOD pyridinium bromide salts and amphiphiles were synthesized in reasonable yields, (Fig. 2.16).

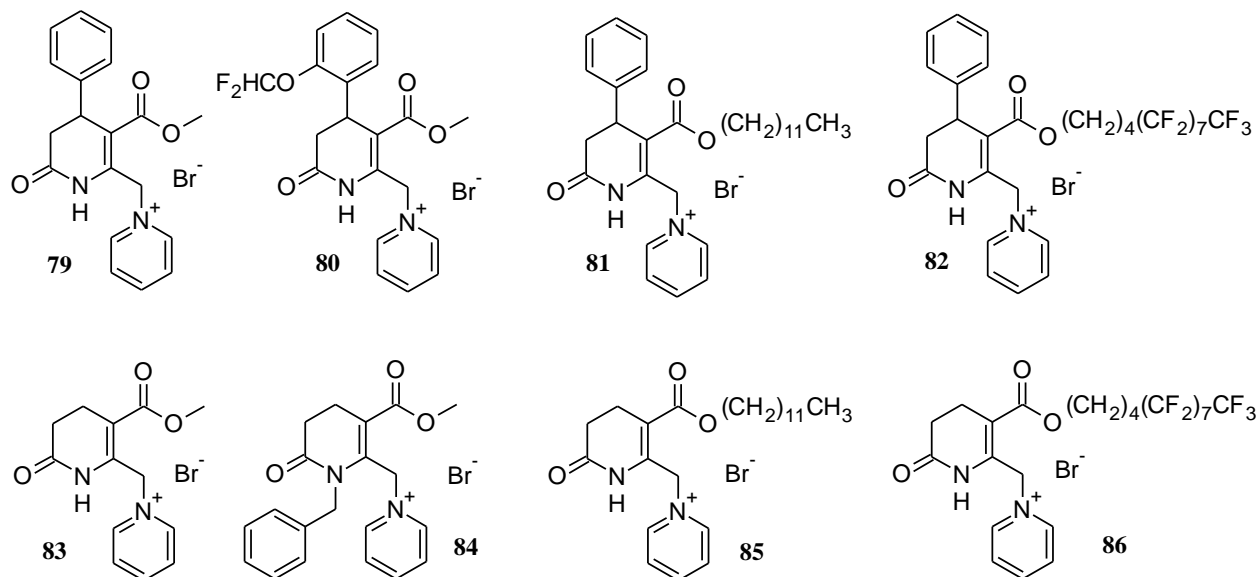


Figure 2.16. DHPOD pyridinium bromide salts and amphiphiles synthesized from the 6-bromomethyl DHPODs.

The 4- unsubstituted DHPOD pyridinium bromide **83** after recrystallization yielded quality crystals which after single crystal X-ray diffraction confirmed the structure (Fig. 2.17). Also noteworthy is the interaction which can be seen between the bromine and NH of the dihydropyridone forming an NH \cdots Br hydrogen bond.

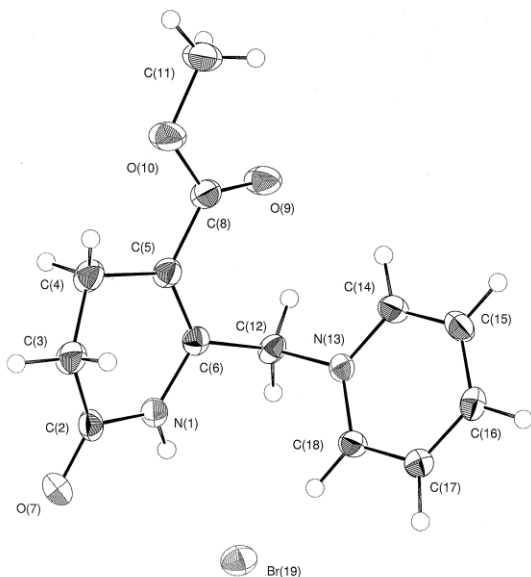


Figure 2.17. ORTEP representation of DHPOD pyridinium bromide **83** where the bromine is participating in NH \cdots Br hydrogen bonding.

By substituting *N,N*-dimethyldodecan-1-amine for the pyridine in the nucleophilic reaction with the 6-bromomethyl-3,4-dihydro-2(1*H*)-pyridones the following series of amphiphilic 3,4-dihydropyridone *N,N*-dimethyldodecan-1-aminium bromides were synthesized in good yields as white powders (Fig 2.18).

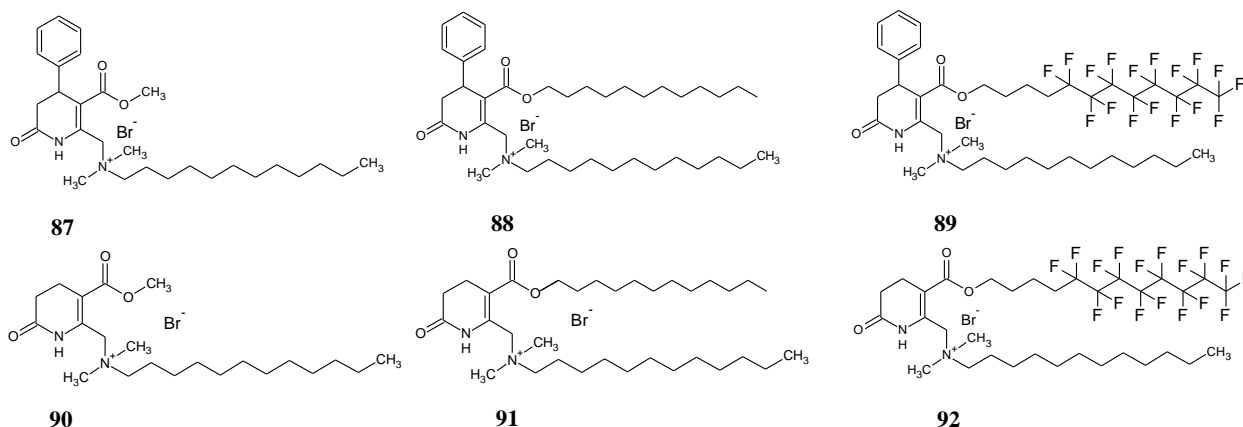
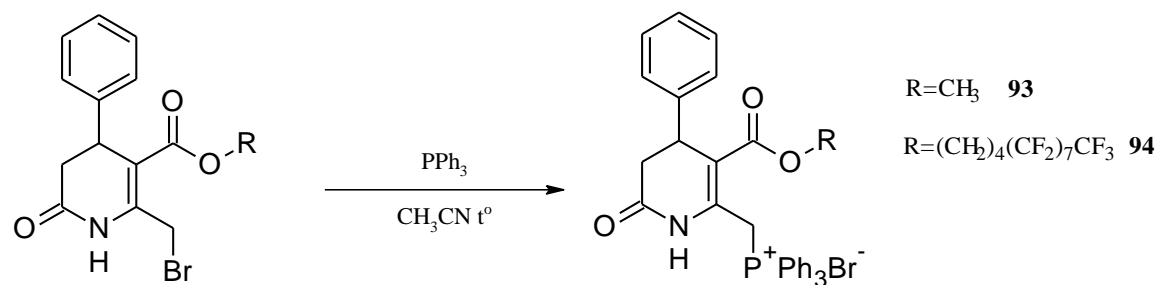


Figure 2.18. A series of cationic DHPOD amphiphiles synthesized by reaction of the respective DHPOD methylbromides with *N,N*-dimethyldodecylamine.

Finally two 3,4-dihydropyridone-2-methylphosphonium bromide salts were synthesized by substituting the bromine of the 2-bromomethyl DHPODs with triphenylphosphine in acetonitrile and heating at 40°C for two hours when noticeable amounts of the triphenylphosphonium bromides started precipitating from the solution. After cooling the reaction mixture the compounds were isolated by filtration as yellowish powders in 82% yield (Scheme 2.29).



Scheme 2.29. Synthesis of DHPOD triphenylphosphonium bromide salts.

Atomic force microscopy (AFM) and dynamic light scattering (DLS) were employed to observe the self-assembly of the cationic DHPOD amphiphiles (Fig. 2.19). The samples were prepared in a dilute (0.03%, w/v) aqueous dispersion by sonication using a probe type sonicator. Using a longer sonification time, it is possible to obtain nanoparticles (NPs) with a narrow size distribution, while after a short sonification time nanoparticles were quite different in their sizes

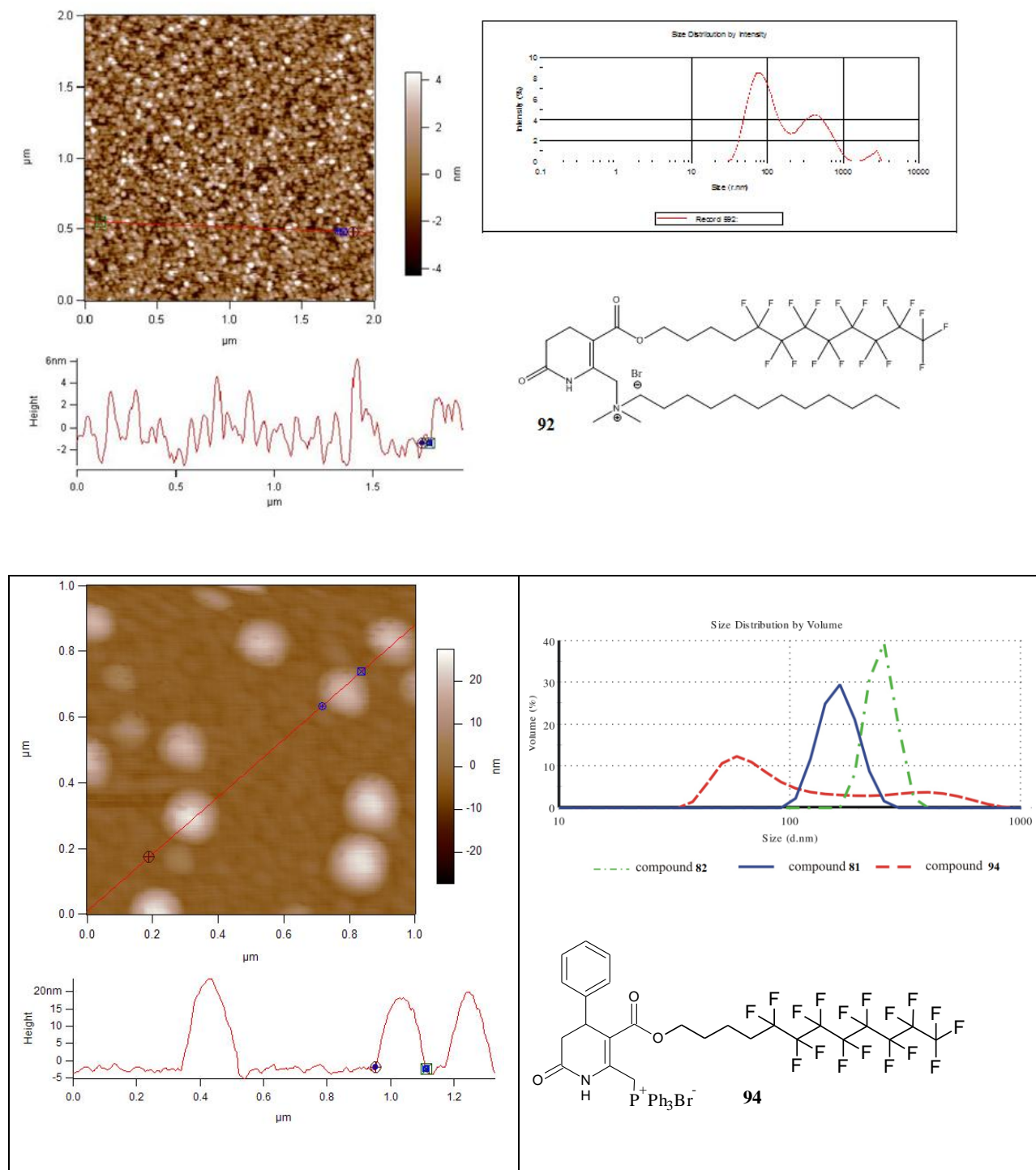


Figure 2.19. AFM images with corresponding height profiles of the self-assembled structures of representative cationic DHPOD amphiphiles adsorbed on a mica surface from aqueous solution and DLS data of the NPs in distilled water.

and shapes. For AFM observation freshly cleaved mica plates were dipped into the solution and kept for 30 s to allow the nanoaggregates to stick to the negatively charged surface. The mica samples were dried at room temperature and observed by AFM in tapping mode. AFM is a well established method for the characterization of nanoscale drug delivery systems (DDS) [189], enabling the direct observation of very small objects without the need of cumbersome and potentially contaminating sample preparation. Tapping mode AFM allows the investigation of soft samples with minimal sample alteration with a lateral resolution of several nanometers and height resolution of 0.1 nm [190].

The AFM and DLS data are summarized in (Table 2.2).

Table 2.2. AFM data and the corresponding DLS data of hydrodynamic diameters ($D_{[H]}$) with their % distribution of the self-assembled nanoaggregates in aqueous solutions.

Compound	AFM		DLS	
	Height (nm)	Diameter (nm)	$D_{[H]}$ peak 1 (nm) and % distr.	$D_{[H]}$ peak 2 (nm) and % distr.
81	6	80	165	
82	8	85	250	
88	20	150	300	
89	30	200	40 (30%)	200 (70%)
91	50	300	350	
92	6	100	80 (65%)	400 (35%)
94	20	150	90 (65%)	395 (35%)

The hydrodynamic diameters and their population percentages of the nanoparticles (NPs) suspended in water were determined by dynamic light scattering (DLS) and the values are presented in (Table 2.2). The advantages of DLS are rapidity of analysis, no requirement for calibration, and sensitivity [191]. The mean diameter represents the average diameter of all nanoaggregates in the sample and the most expected diameter depicts the diameter of the main population (or tip of the peak) of the nanoaggregate sample. The NPs with a single long chain fluorinated ester group (compound **82**) had a larger hydrodynamic diameter or approximately 250 nm and the nonfluorinated analog **81** had a smaller diameter of approximately 165 nm. Both of the compounds formed NPs in a relatively narrow size distribution range. For the

phosphonium amphiphile **94** which has a larger polar head group two populations of NPs were observed, one at about 90 nm and the other at 395 nm diameters in approximately 3:1 ratio. Since micelle diameters are usually not more than about 30 nm these NPs could not be micelles, they could be liposomes or some other nanoaggregates but, without freeze-fracture electron microscopy it cannot be proved conclusively. There is a diameter size discrepancy between the AFM and DLS methods as observed for example in compound **94**. This could be due to the fact that DLS is performed on NPs in water which makes them fully hydrated, whereas, in AFM the samples are dried on a mica slide surface and are flattened which may influence the size and shape of NPs. The polydispersity of the sample for compound **94** could be explained by recognizing that DLS measures average size ranges whereas AFM visualizes only a small number of NPs. In general given the higher atomic size of fluorine than hydrogen, the reduced conformational freedom of the perfluorinated tails leads to bulky and stiff chains, and to aggregate structures with less curvature which give rise to a larger diameter NPs. Fluorinated amphiphiles have then the property that even single chain amphiphiles can form bilayer aggregates or vesicles, although this is usually unfavorable for single chain hydrocarbon ones [192].

2.4. Oxidation potential determination of DHP and DHPOD derivatives using CV

The oxidation of 1,4-dihydropyridines and analogs to the corresponding pyridines is of interest because of its relevance to the biological NADH redox processes as well as to the metabolic studies pertaining to 1,4-DHPs [193,194]. The electrochemical oxidation of 1,4-DHPs has extensively been reported in different electrolytic media [195-206]. There are several in vitro findings that DHP calcium antagonists possess antioxidant properties, mainly during the development of atherosclerosis and some cardiovascular oxidative processes [207-213]. Furthermore, the Hantzsch 1,4-DHP is widely used as a safe, easy to handle and environmentally benign reagent for the reduction of organic functional groups [214], as antioxidant, antimutagenic, radical scavenger, and growth stimulator.

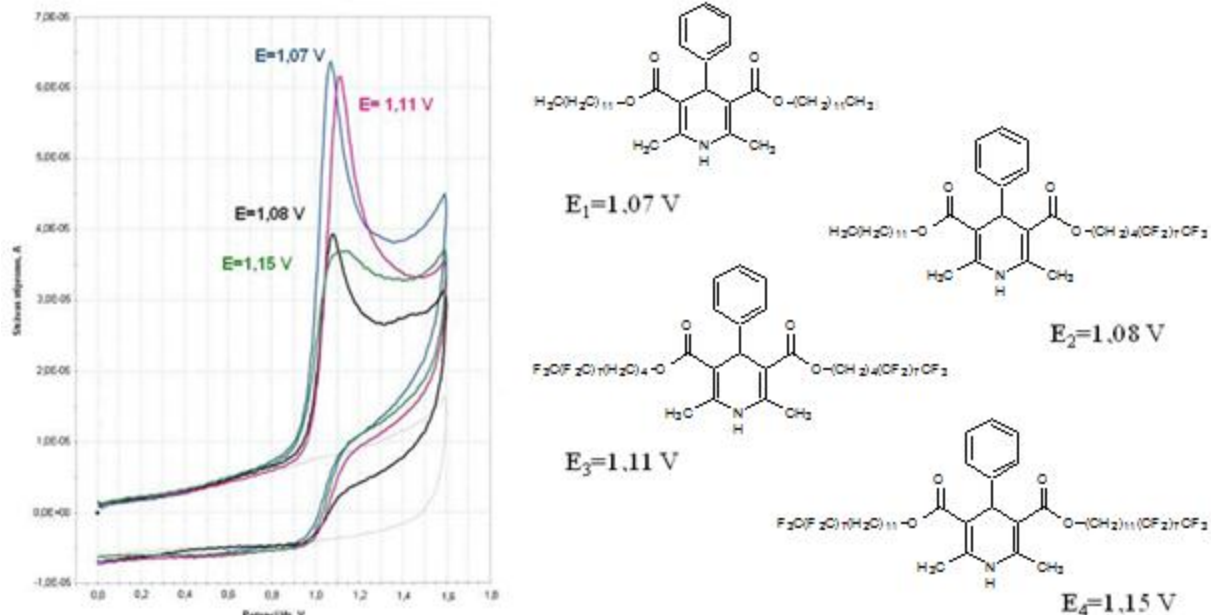
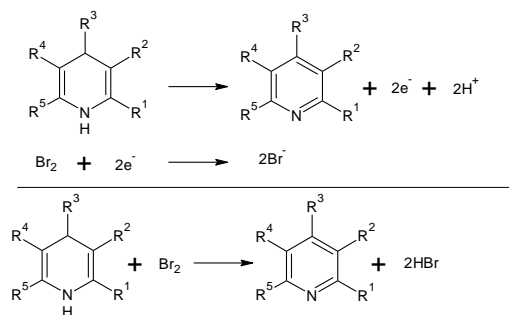


Figure 2.20. Cyclic voltammety traces showing the oxidation potentials of representative DHP's.

Due to the clean 2-methyl bromination of dihydropyridones with bromine in chloroform, consideration was given to the possibility of using this reaction to brominate the 2,6-dimethyl groups in 1,4-DHP's but since bromine can act as an oxidant, $\text{Br}_2 + 2\text{e}^- \rightarrow 2\text{Br}^-$ with a standard reduction potential of +1.09 volts it's possible that instead of bromination an oxidation of the DHP to pyridine would take place instead. Thus cyclic voltammety measurements were performed to determine the oxidation potentials of representative DHP's (Fig. 2.20).

These cyclic voltammety diagrams were obtained by B.Turovska, using a PARSTAT 2273 apparatus at the Latvian Organic Synthesis Institute. The oxidation of 1,4-DHP's with bromine would take place according to the following equation:



Indeed the DHP with oxidation potential of -1.07 volts would be oxidized with bromine spontaneously since the above overall reaction potential is +0.02 volts, but as more fluorines are added in the esters the oxidation becomes more difficult or higher potential is needed for oxidation, nevertheless this reaction was not tried since the potentials are low enough to cause oxidation as a side product. The CV diagrams also show that the oxidation occurs through a one irreversible step. The overall oxidation mechanism of 1,4-DHPs is depicted in (Figure 2.21). The transfer of the first electron is followed by elimination of a proton from position 4 and after the second electron transfer the pyridinium cation is formed which upon elimination of another proton generates the pyridine in an overall ECEC (E-electron transfer; C-proton transfer) mechanism.

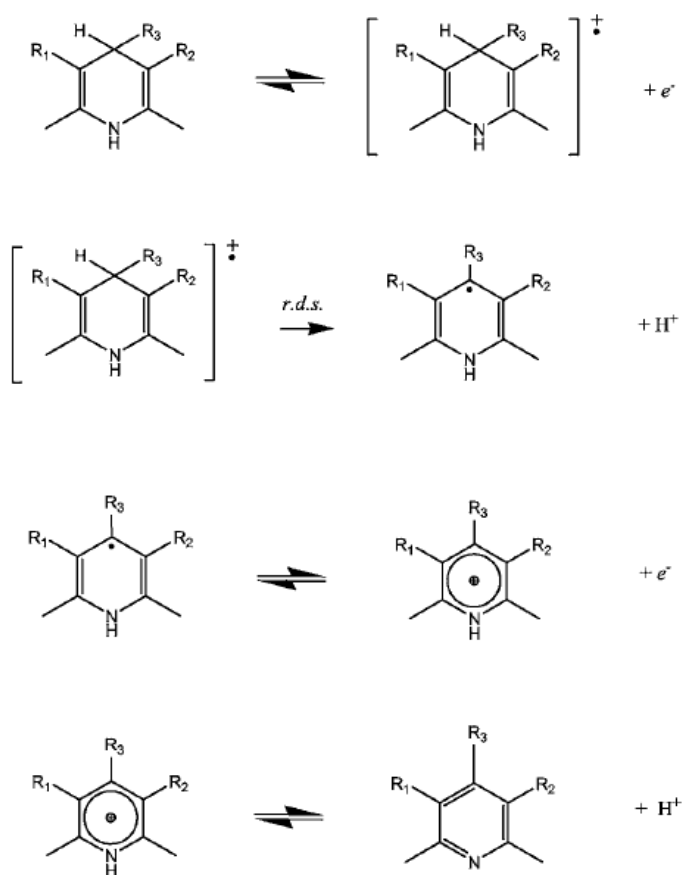


Figure 2.21. The overall electrochemical oxidation mechanism of 1,4-DHP in aprotic media indicating the ECEC sequence [215].

The oxidation is strongly pH dependent since if in the second step which is the rate determining step of the above reaction, there is a base present which could abstract the NH proton then the oxidation should proceed much more readily. (Figure 2.22) shows that the oxidation potentials of various DHP's in basic solution are almost half compared to the oxidation potentials obtained in acid solution. The oxidation is also influenced by electron withdrawing groups which are attached to the DHP heterocycle rendering the removal of electrons (oxidation) more difficult. The opposite effect or easier oxidation is attained by attaching electron donating groups to the DHP-heterocycle.

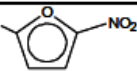
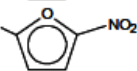
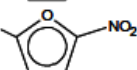
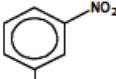
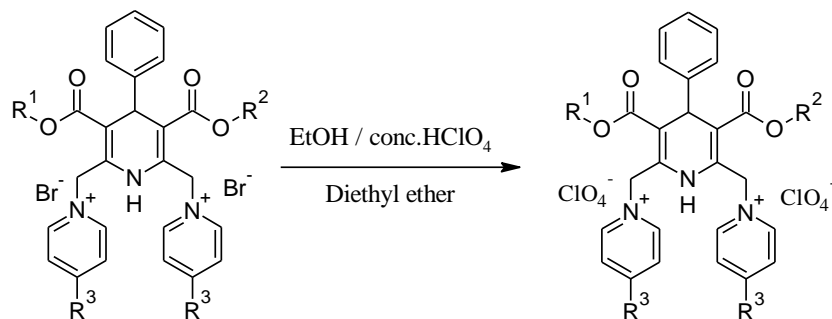
Compounds	R1	R2	R	Ep/mV (p H 3.0)	Ep/mV (pH 10.6)	
A	I	-CO ₂ Et	-CO ₂ Et		932	536
	II	-CN	-CO ₂ Et		956	484
	III	-CN	-CN		988	436
B	IV	-CO ₂ Et	-CO ₂ Et	-H	404	214
	V	-CO ₂ Et	-CO ₂ Et	-CH ₃	804	440
	VI	-CO ₂ Et	-CO ₂ Et		908	520

Figure 2.22. Chemical structures of 1,4-DHP's with their corresponding peak potential values in acidic and basic media [215].

To obtain CV measurements for the 1,4-DHP dipyridinium dibromides it was necessary to convert them to the perchlorates (Scheme 2.30) since at 1.08 V the bromine was observed to oxidize. The 1,4-DHP pyridinium dibromide was dissolved in ethanol and concentrated perchloric acid was added drop by drop until no more precipitate of the diperchlorates formed. The salts were filtered and washed with diethyl ether and dried. The oxidation potentials of the 1,4-DHP pyridinium diperchlorates are summarized in (Table 2.3). It can be seen that longer alkyl ester groups require slightly higher oxidation potentials as does the fluorine content in the ester groups but this is a very slight effect. The dipyridinium diperchlorates however, have a strong electron withdrawing effect on the DHP cycle raising the oxidation potential by about 0.5 V.



Scheme 2.30. Transformation of the 1,4-DHP dipyrindinium dibromides into diperchlorates.

Table 2.3. Oxidation potentials of 1,4-DHP dipyrindinium diperchlorates obtained by CV.

Entry	R ₁	R ₂	R ₃	E ^{ox} (V)
1.	C ₂ H ₅	C ₂ H ₅	H	1.57 ^[32]
2.	C ₁₂ H ₂₅	C ₁₂ H ₂₅	H	1.58
3.	C ₁₂ H ₂₅	C ₄ H ₈ C ₈ F ₁₇	H	1.70
4.	C ₄ H ₈ C ₈ F ₁₇	C ₄ H ₈ C ₈ F ₁₇	H	1.69
5.	C ₁₂ H ₂₅	C ₁₂ H ₂₅	CF ₃	1.63
6.	C ₁₂ H ₂₄ CF ₃	C ₁₂ H ₂₄ CF ₃	H	1.57

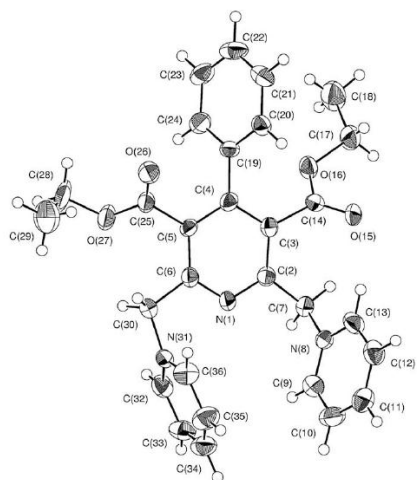
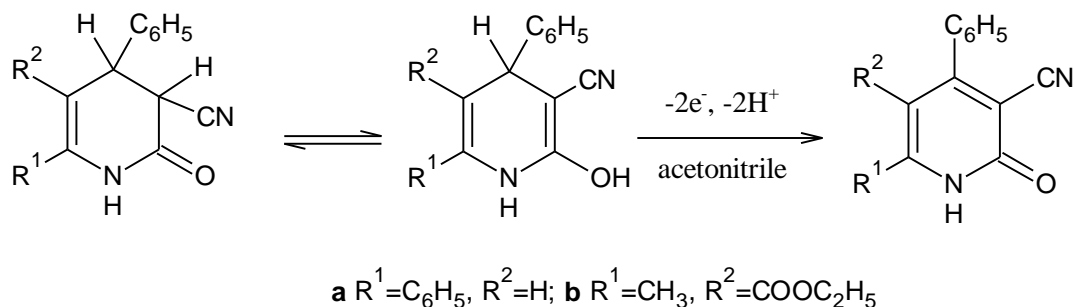


Figure 2.23. ORTEP representation of the oxidation product of entry 1. [216].

The first entry in the above table is from the published work of A. Plotniece *et al.* [216] where the electrochemical oxidation was done on a preparative scale and the product as a pyridine was confirmed by X-ray (Fig. 2.23).

In the 3,4-dihydropyridone series there is only one published report on their electrochemical oxidation at a rotating graphite electrode to obtain a quantitative characterization of the capacity of these compounds to undergo oxidation [217]. The DHPOD compounds can exist in two tautomeric forms- as derivatives of 2-oxo-1,2,3,4-tetrahydropyridine and 2-hydroxy-1,4-dihydropyridine. The NMR spectra taken in anhydrous acetonitrile show that these compounds at the selected experimental conditions for electrochemical study are in the undissociated oxo form. The $E_{1/2}$ value of the first, well-defined, wave was in the 0.9-1.5V range indicating that DHPOD's are oxidized with considerably greater difficulty than the 3,5-diethoxycarbonyl-1,4-dihydropyridines. The overall equation of the first stage of electrooxidation can be written as in (Scheme 2.31).



Scheme 2.31. 3,4-Dihydropyridone electrochemical oxidation in acetonitrile [217].

The electrochemical results indicate that the oxidation takes place monotypically by an ECEC mechanism but, they didn't permit an unambiguous prediction of either the position of the first detachment of an electron or of the sequence of detachment of protons and electrons from the various positions of the ring DHPOD's.

The oxidation potentials of DHPOD's synthesized in this work were obtained by CV at a glassy carbon electrode in dry acetonitrile (Figure 2.24) in a single irreversible oxidation wave and the results are summarized in (Table 2.4).

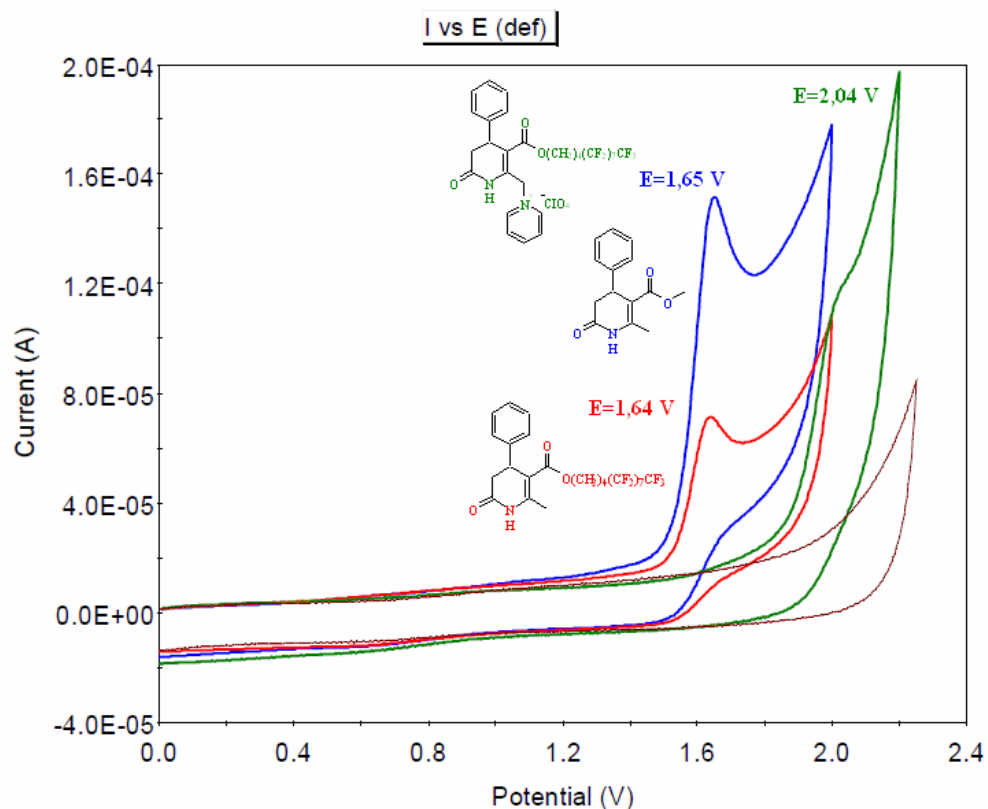
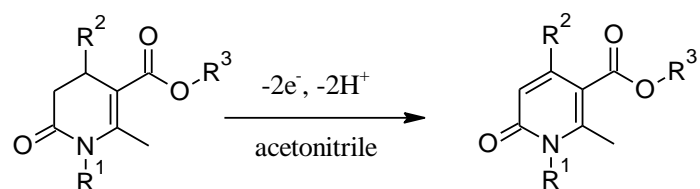


Figure 2.24. 3,4-Dihydropyridone electrochemical oxidation on glassy carbon (GC) electrode in $\text{CH}_3\text{CN}/0.1 \text{ M NaClO}_4$



Scheme 2.31. Electrochemical oxidation of substituted DHPODs in acetonitrile / 0.1M NaClO_4 .

Table 2.4. Oxidation potentials of substituted DHPODs.

Entry	R^1	R^2	R^3	E, V
1.	H	H	CH_3	1.63
2.	$\text{CH}_2\text{C}_6\text{H}_5$	H	CH_3	1.62
3.	H	H	$\text{C}_{12}\text{H}_{25}$	1.63
4.	H	H	$\text{C}_4\text{H}_8\text{C}_8\text{F}_{17}$	1.64
5.	H	Ph	CH_3	1.65
6.	H	Ph	$\text{C}_4\text{H}_8\text{C}_8\text{F}_{17}$	1.64

As can be seen in the above table the oxidation potentials for the substituted DHPODs are not influenced by the length of the ester or if there is a phenyl group at position 4 or not. The potentials are however, about 0.5 V higher than for the DHP series and this gives a clear answer as to why the DHPODs can be brominated with elemental bromine without any oxidation of the ring taking place. Compound in entry 5 was oxidized electrolytically on a preparative scale and after 24 hours at a 2.2 V potential the 4-phenyl-2-pyridone (**95**) was obtained quantitatively. The acetonitrile was evaporated and the compound was recrystallized from EtOH giving X-ray quality crystals which after X-ray diffraction confirmed the structure of the oxidized DHPOD (Figure 2.25).

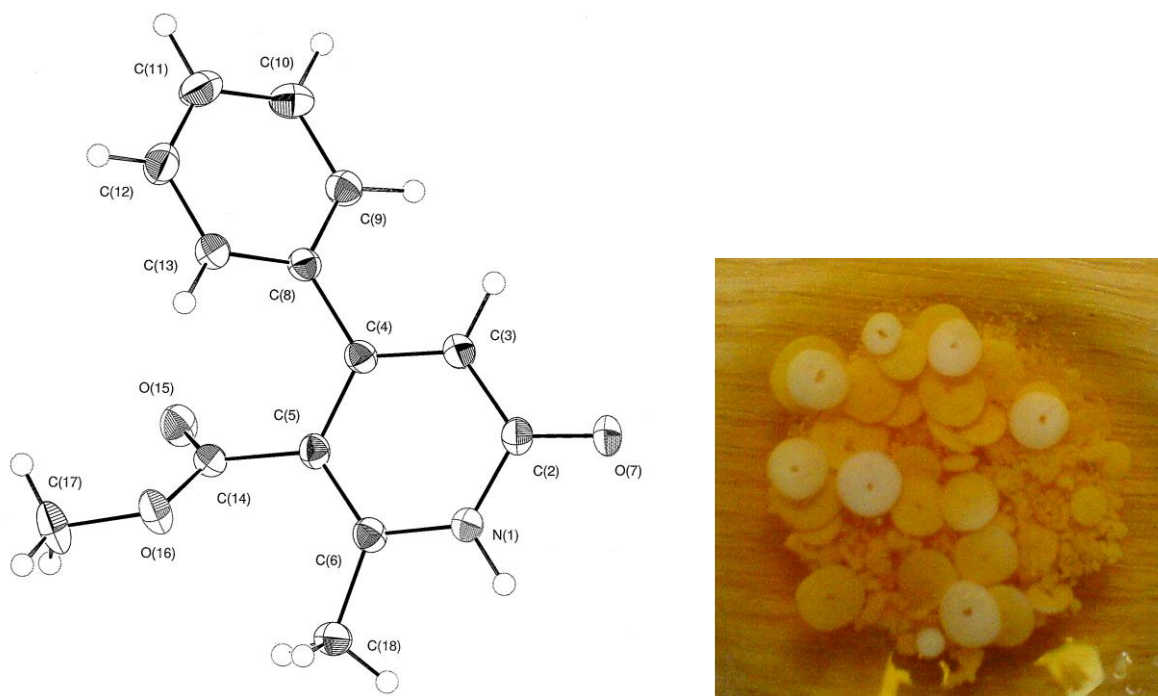
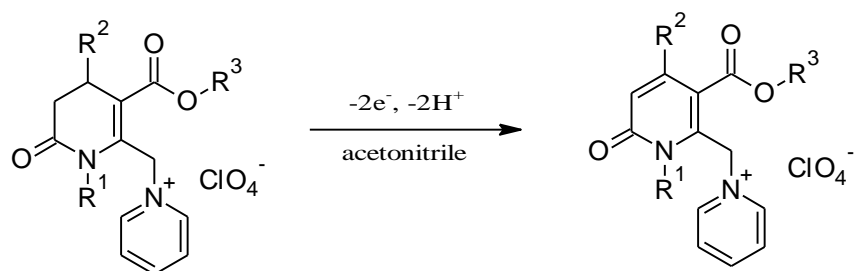


Figure 2.25. ORTEP representation of compound **95** and crystals in EtOH.

Compound **95** crystallized from ethanol in approximately 2-3mm diameter discs as the above photo indicates with a clear prismatic crystal in the center of the disc, these were taken and submitted for X-ray analysis. The X-ray analysis also indicated that the compound crystallizes as hydrogen bonded dimers with 1.810 Å NH \cdots O bond length. A series of DHPOD pyridinium perchlorates were again prepared from the pyridinium bromides and their oxidation potentials are summarized in (Table 2.5).



Scheme 2.32. Electrochemical oxidation of substituted DHPOD pyridinium perchlorates in acetonitrile / 0.1M NaClO₄.

Table 2.5. Oxidation potentials of DHPOD pyridinium perchlorates.

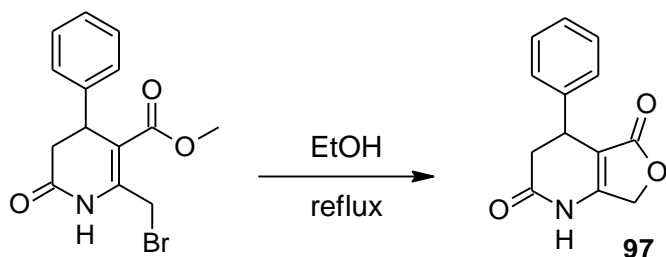
Entry	R ¹	R ²	R ³	E, V
1.	H	H	CH ₃	2.10
2.	CH ₂ C ₆ H ₅	H	CH ₃	2.35
3.	H	H	C ₁₂ H ₂₅	2.27
4.	H	H	C ₄ H ₈ C ₈ F ₁₇	2.22
5.	H	Ph	CH ₃	2.15
6.	H	Ph	C ₄ H ₈ C ₈ F ₁₇	2.04

In the DHPOD pyridinium perchlorate series there is a 0.6 V jump in the oxidation potentials compared to the DHPODs of the 6-methyl series, this is due to the strong electron withdrawing effect of the pyridinium cation on the dihydropyridone ring. The oxidation potential is lowest in the 4- unsubstituted case (entry 1) and is increased as the length of the ester group increases or when a phenyl substituent at position 4 is added. The highest oxidation potential is observed for N-benzyl substituted DHPOD (entry 2). Compound in entry 5 was oxidized electrolytically on a preparative scale and after 24 hours at a 2.2 V potential the 4-phenyl-2-pyridone pyridinium perchlorate (**96**) was obtained quantitatively as judged from the LC/MS chromatogram and after removal of solvent and recrystallization the structure was confirmed by NMR analysis. In summary the 1,4-DHP compounds in this work had oxidation potentials at 1.1-1.2 V and their pyridinium perchlorate salts at 1.6-1.7 V or 0.5 V higher due to their strong electron withdrawal from the DHP ring. The DHPOD series had oxidation potentials at 1.6 V and their pyridinium perchlorates at 2.0-2.4 V about 0.6 volts higher. The DHPODs oxidize at about 0.5 V higher than

the DHPs. The oxidation potentials also provide confirmation to why the DHP 2,6-methyl groups can't be brominated by bromine (V_{ox} 1.08) but, cause oxidation of the DHP to pyridine instead. The DHPOD with a substantially higher oxidation potential can be brominated with bromine without problems. The cationic DHP and especially DHPOD amphiphiles wouldn't function as good antioxidants based on their oxidation potentials since good antioxidants such as ascorbic acid (V_{ox} 0.42) and glutathione (V_{ox} 0.33) have substantially lower oxidation potentials. However, even though the antioxidant ability of antioxidants can be predicted quite accurately from the CV measurements, properties beside oxidation potential must be considered when antioxidation and prooxidation activity are evaluated [218].

2.5 The 6-bromomethyl-3,4-dihydro-2(1H)-pyridones as versatile synthons

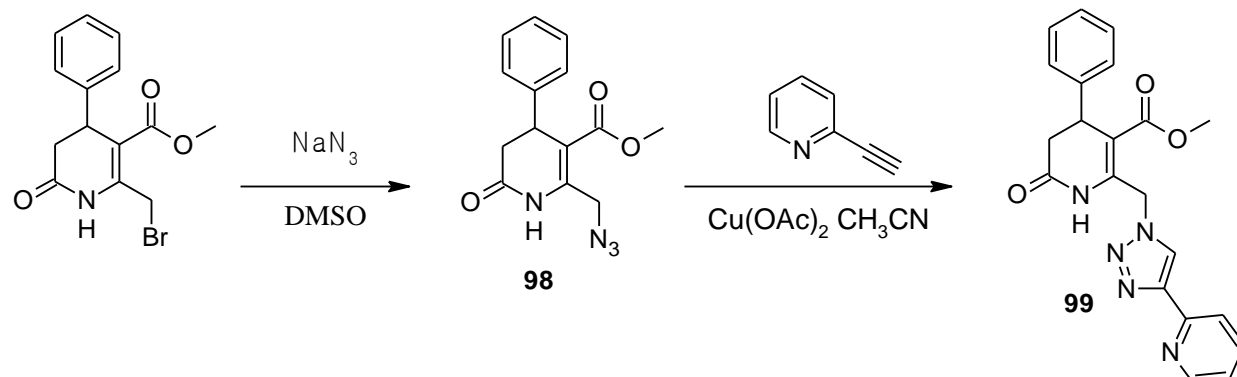
The bromine in the 6-bromomethyl-3,4-dihydro-2-pyridone systems reacts in nucleophilic reactions as normal allylic or benzylobromides and thus these compounds can be used as versatile synthons for elaboration of the 3,5-dihydropyridone heterocycle. As already mentioned in the previous section, the bromine can be displaced by an intramolecular acyl group and form dihydro-2-pyridone lactones spontaneously without isolation of the bromomethyl intermediate [128]. Thus refluxing methyl 4-phenyl-6-bromomethyl-3,4-dihydro-2-pyridone-5-carboxylate in ethanol for several hours resulted in the lactonization to the fused dihydropyridone lactone (Scheme 2.33).



Scheme 2.33. Lactonization of methyl 6-bromomethyl-3,4-dihydro-2-pyridone-5-carboxylate in refluxing ethanol [128].

The bromine was also substituted by azide by reacting the 6-bromomethyl DHPOD in DMSO with sodium azide overnight and after addition of water the DHPOD azide precipitated in 96% yield. The azide was reacted further with 2-ethynylpyridine according to the „click chemistry” protocol with $\text{Cu}(\text{OAc})_2$ and sodium ascorbate in acetonitrile to furnish the DHPOD triazole **99**

(Scheme 2.34) in 94% yield. The pyridine group can be replaced by a wide variety of groups providing a large library of substituted DHPOD triazoles.



Scheme 2.34. Synthesis of DHPOD azide which undergoes „click chemistry” with 2-ethynylpyridine to give the DHPOD pyridinyl triazole.

"Click Chemistry" is a term that was introduced by K. B. Sharpless in 2001 to describe reactions that are high yielding, wide in scope, create only byproducts that can be removed without chromatography, are stereospecific, simple to perform, and can be conducted in easily removable or benign solvents. This concept was developed in parallel with the interest within the pharmaceutical, materials, and other industries for generating large libraries of compounds for screening in drug discovery research. The mechanism of the copper catalyzed azide alkyne cycloaddition (CuAAC) is depicted in (Fig. 2.26).

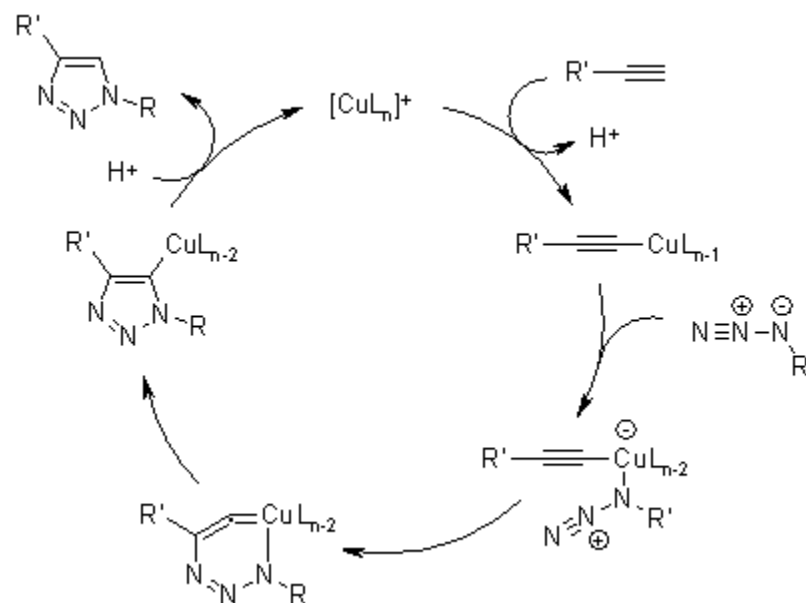
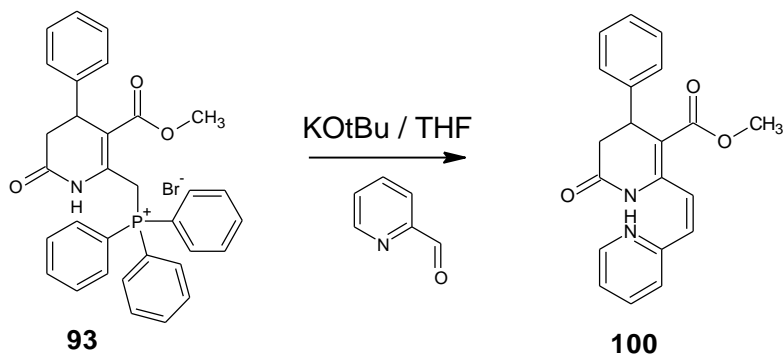


Figure 2.26. Proposed mechanism for the CuAAC reaction [219].

The active Cu(I) catalyst can be generated from Cu(I) salts or Cu(II) salts using sodium ascorbate as the reducing agent. Addition of a slight excess of sodium ascorbate prevents the formation of oxidative homocoupling products. Disproportionation of a Cu(II) salt in presence of a Cu wire can also be used to form active Cu(I). Coordination of Cu(I) to the alkyne is slightly endothermic in MeCN, but exothermic in water, which is in agreement with an observed rate acceleration in water. However, coordination of Cu to the acetylene does not accelerate a 1,3-dipolar cycloaddition. Such a process has been calculated to be even less favorable than the uncatalyzed 1,3-dipolar cycloaddition. Instead, a copper acetylide forms, after which the azide displaces another ligand and binds to the copper. Then, an unusual six-membered copper(III) metallacycle is formed. The barrier for this process has been calculated to be considerably lower than the one for the uncatalyzed reaction. The calculated rate at room temperature is 1 s^{-1} , which is quite reasonable. Ring contraction to a triazolyl-copper derivative is followed by protonolysis that delivers the triazole product and closes the catalytic cycle [219].

Finally by using the DHPOD 6-methyltriphenylphosphonium bromide in a Wittig reaction with 2-pyridinecarboxaldehyde in THF and tBuOK as base (Scheme 2.35) the cis addition product **100** was obtained.



Scheme 2.35. Wittig reaction with DHPOD 6-methyltriphenylphosphonium bromide and 2-pyridinecarboxaldehyde using KOtBu as base to generate the cis addition product **100**.

The product was isolated using preparative HPLC and after solvent removal was recrystallized from ethanol in light green needles which were submitted for single crystal X-ray diffraction analysis providing the structure confirmation (Fig. 2.27).

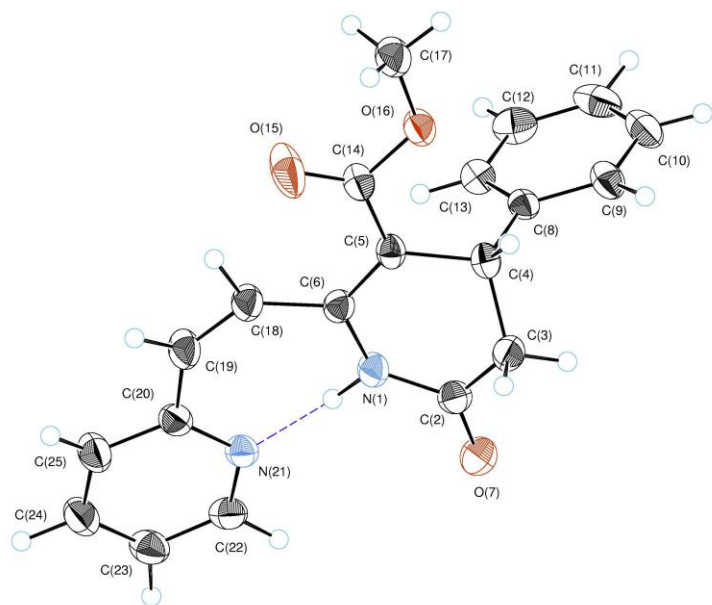
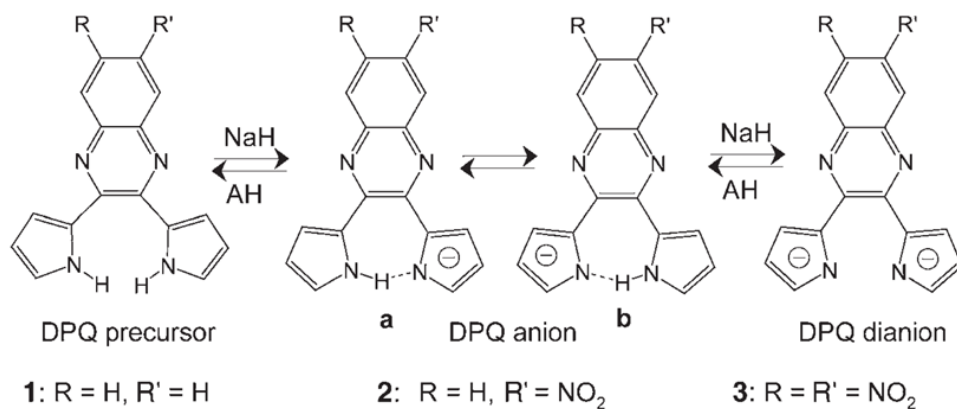


Figure 2.27. ORTEP representation of compound **100** having an ultra short NH \cdots N hydrogen bond.

The structure contains an ultra short intramolecular NH \cdots N hydrogen bond (forming a seven membered ring) measuring 1.765 Å which is also reflected in the $^1\text{H-NMR}$ spectra where the NH proton signal is shifted downfield from about 8 ppm in the parent DHPOD to almost 14 ppm in the product. A recent example of a compound with ultra short NH \cdots N bond was published by M.

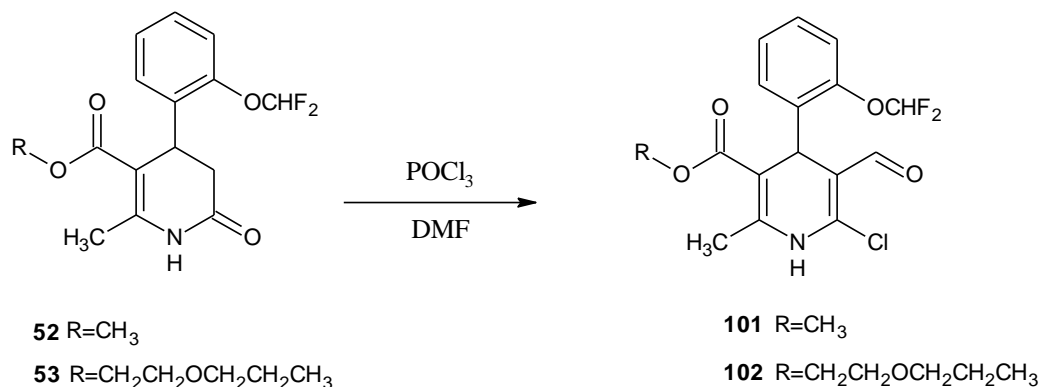


Scheme 2.36. Chemical structures of substituted 2,3-dipyrrol-2-ylquinoxalines (DPQ) and their deprotonated mono- and dianions. **1:** 2,3-dipyrrol-2-ylquinoxaline, **2:** 6-nitro-2,3-dipyrrol-2-ylquinoxaline, **3:** 6,7-dinitro-2,3-dipyrrol-2-ylquinoxaline. The monoanions are subject to a fast proton tautomerism between two forms labeled as **a** and **b**. AH = trifluoroacetic acid [220].

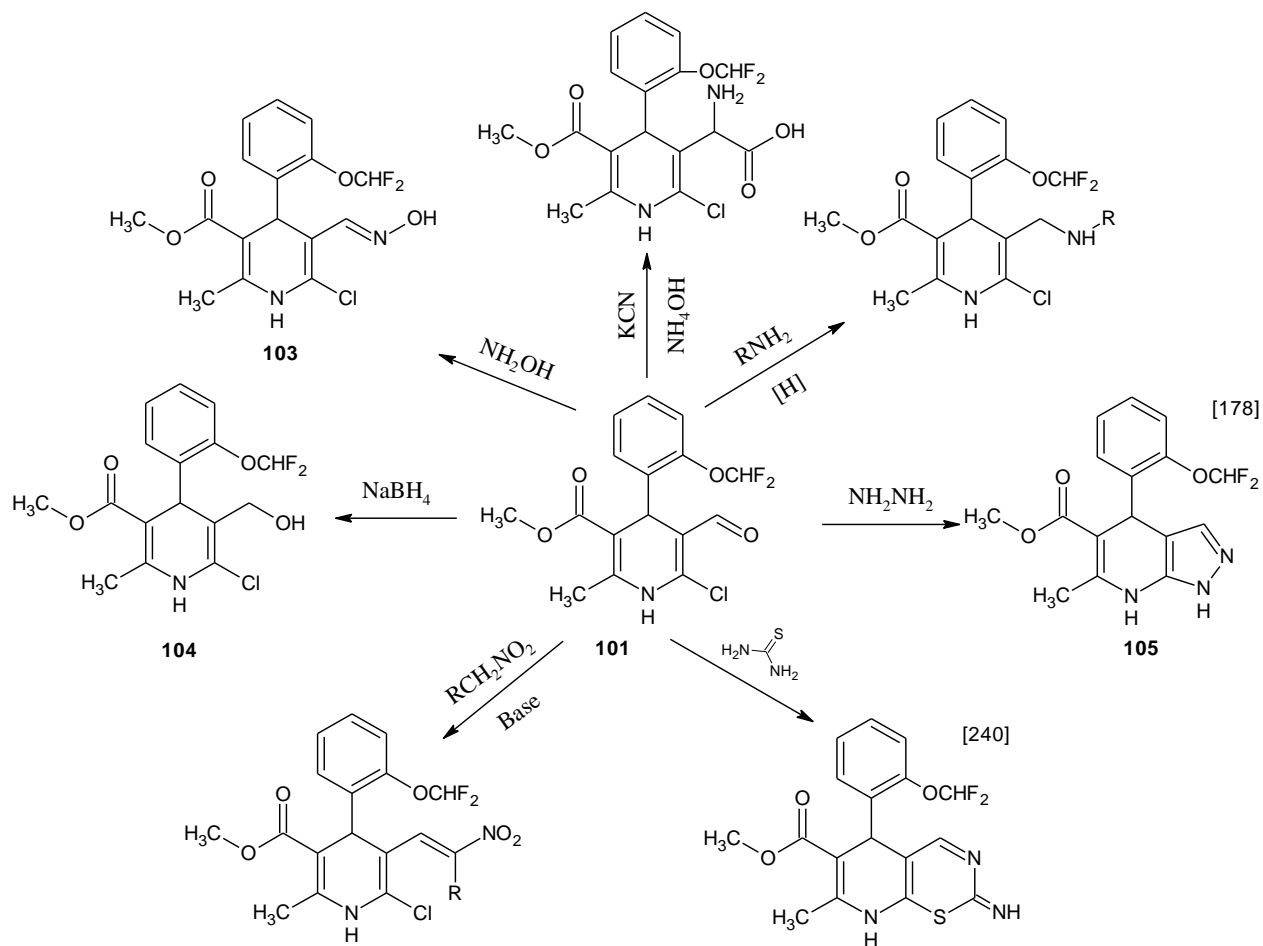
Pietrzak *et al.* [220] the bond was generated by deprotonation of one hydrogen from a dipyrrol (Scheme 2.36). DPQs have been synthesized and studied as colorimetric anion receptors for charge-dense species, such as fluoride [221]. However, their unusual geometry makes it likely that their monodeprotonated forms would have unusually short NHN hydrogen bonds and thus unusually large ^{15}N - ^{15}N coupling constants (more than 16 Hz). The equilibrium hydrogen-bond geometries of **1**⁻, **2**⁻, and **3**⁻ were calculated using DFT at the B3PW91/6-31 +G** level and determined to be between 1.49-1.52 Å.

2.6 Vilsmeier-Haack chloroformylation of DHPOD and subsequent reactions

The Vilsmeier-Haack reagent (halomethyleneiminium salt) formed from the interaction of dialkyl formamides such as DMF with POCl_3 has attracted the attention of synthetic organic chemists since its discovery in 1927.[222] It is one of the most commonly used reagents for the introduction of an aldehydic (CHO) group into aromatic and heteroaromatic compounds. [223] Acetanilides, particularly deactivated acetanilides, undergo Vilsmeier-Haack cyclisation in micellar media to afford the corresponding 2-chloro-3-formyl quinoline derivatives in good yields either by traditional methods [224-233] or by using microwaves [234] or ultrasonic irradiation [235]. In the present context the Vilsmeier-Haack reaction is a powerful tool for the rapid introduction of molecular diversity in the DHP heterocycle which is of relevance to medicinal and synthetic chemists alike. Some 6-chloro-5-formyl-1,4-dihydropyridine derivatives have been prepared by reaction of alkyl 2-methyl 6-oxo-1,4,5,6-tetrahydropyridine-3-carboxylates with Vilsmeier-Haack reagent (POCl_3 , DMF) [236-238]; however, these reactions require long times (18 h) to obtain moderate or good yields.



Scheme 2.37. Vilsmeier-Haack chloroformylation of DHPOD derivatives.



Scheme 2.38. Some possible reaction which the 6-chloro-5-formyl-DHPs can undergo.

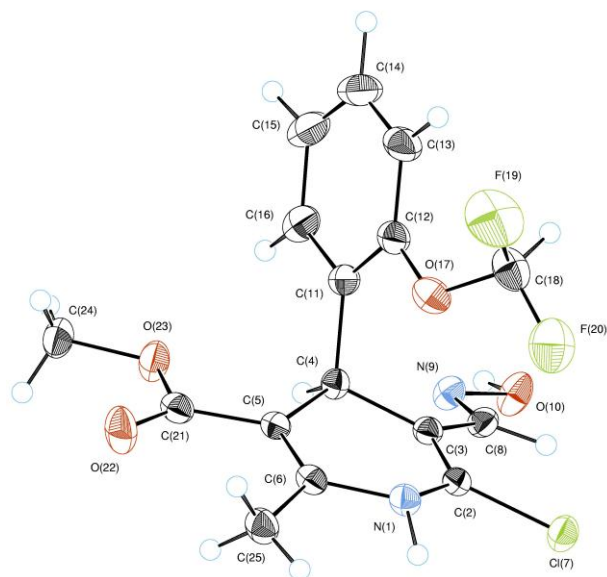
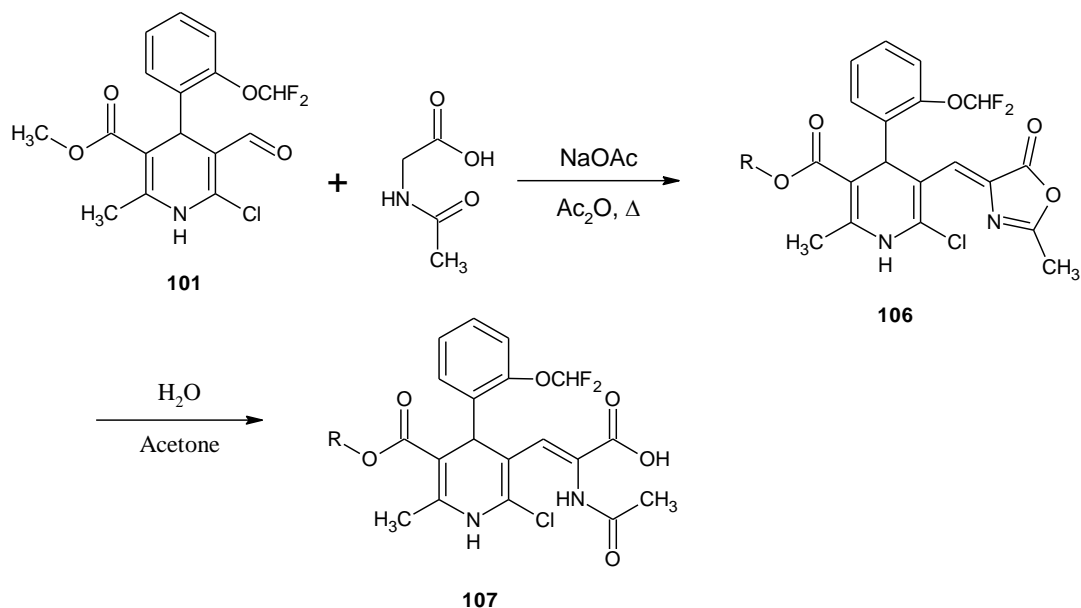


Figure 2.29. ORTEP representation of compound 103.

chlorine at position 6 can be displaced by nucleophiles this provides a route to further transformations into other heterocyclic-fused 1,4-DHPs. Thus in general when the 6-chloro-5-formyl-DHPs are refluxed in ethanol for 6 hours with equimolar amounts of hydrazine hydrate the fused DHP pyrazolo compounds are obtained in about 60% yield [178]. This reaction was tried with compound **101** and the desired compound **105** was obtained in 61% yield as a pale



Scheme 2.39. Erlenmeyer-Plöchl reaction with compound **101**.

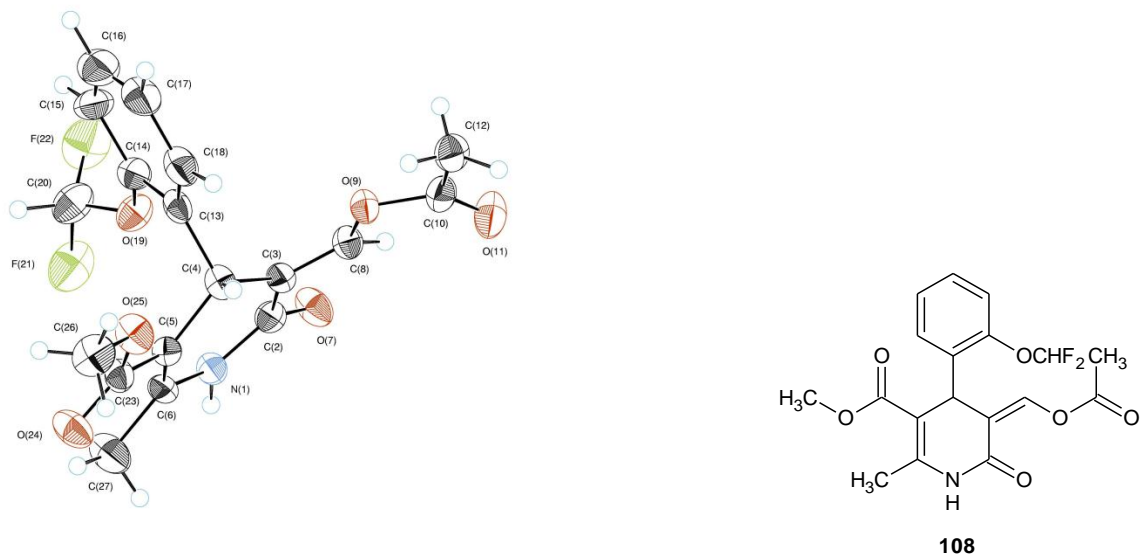
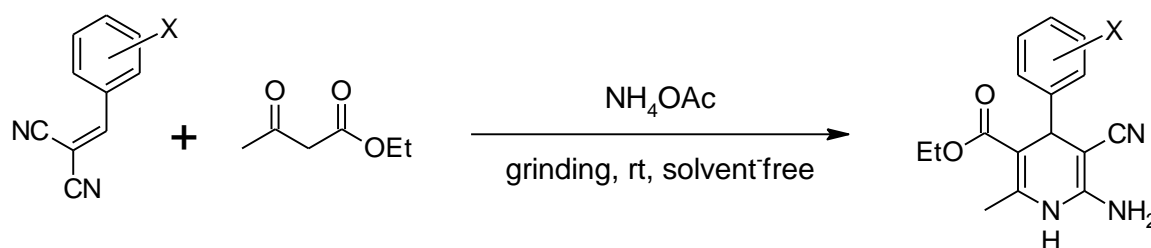


Figure 2.30. ORTEP representation of compound **108**.

yellow solid. As indicated in the scheme 6-chloro-5-formyl 1,4-DHPs can be used to introduce an amino acid in the 3 position using the Strecker reaction, hydantoin reaction and Erlenmeyer-Plöchl reaction. The latter was tried according to (Scheme 2.39). However, after growing crystals of the product from the reaction sequence the X-ray diffraction analysis indicated the structure as compound **108** (Figure 2.30) and not the expected compound **107**. This could result from the reaction of the aldehyde **101**, with acetic anhydride and hydrolysis of the chlorine to give the pyridone.

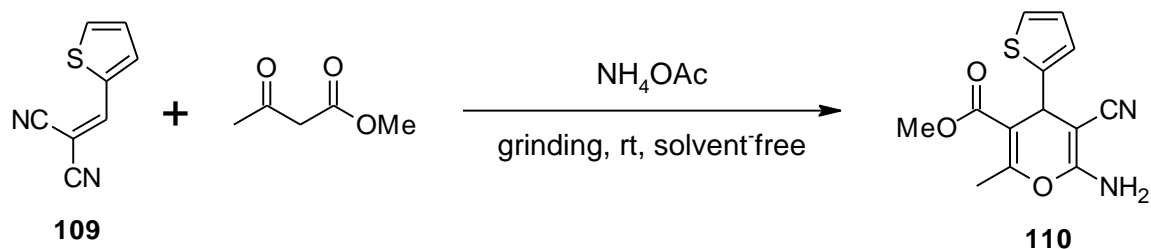
2.7. The unexpected 4*H*-pyran synthesis under solvent-free and grinding conditions

Finally in the continued efforts to provide molecular diversity in the 1,4-DHP heterocycle, an attempt was made to introduce an amino group in position 2. A survey of recent literature revealed an attractive environmentally friendly synthesis of ethyl 6-amino-5-cyano-4-aryl-1,4-dihydropyridine-3-carboxylate derivatives using a multicomponent room temperature grinding procedure of ethyl acetoacetate, [(2-aryl)methylene]malononitriles, and ammonium acetate (Scheme 2.40) [241].



Scheme 2.40. Reported synthesis of ethyl 6-amino-5-cyano-4-aryl-1,4-dihydropyridine-3-carboxylates under grinding and solvent-free conditions [241].

On repeating the above reported multicomponent grinding procedure with thiophene-2-carbaldehyde, malononitrile, and ammonium acetate to give the thiophenemethylene-malononitrile **109** and subsequent addition of methyl acetoacetate to generate the expected methyl 6-amino-5-cyano-2-methyl-4-(thiophen-2-yl)-1,4-dihydropyridine-3-carboxylate, it was surprising that the X-ray single crystal structure analysis of the recrystallized crystals (Fig. 2.31) proved that the compound was not a 1,4-DHP derivative, but a 4*H*-pyran derivative or methyl 6-amino-5-cyano-2-methyl-4-(thiophen-2-yl)-4*H*-pyran-3-carboxylate (**110**) (Scheme 2.41).



Scheme 2.41. Synthesis of methyl 6-amino-5-cyano-2-methyl-4-(thiophen-2-yl)-4*H*-pyran-3-carboxylate (**110**).

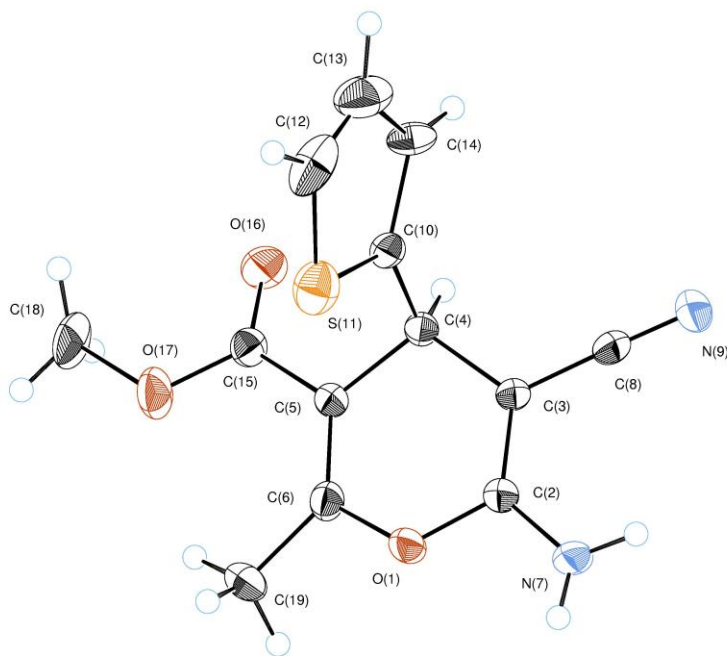


Figure 2.31. ORTEP representation of compound **110**.

The exact procedure from the publication was then carefully repeated with 3-nitrobenzaldehyde, malononitrile, and ammonium acetate to give the *m*-nitrophenylmethylenemalononitrile **111** with subsequent addition of ethyl acetoacetate and again the product which had the identical melting point of 187-188 °C and $^1\text{H-NMR}$ spectrum to the published compound when subjected to an X-ray single crystal structure analysis proved to be a 4*H*-pyran derivative **112** (Fig. 2.32).

Furthermore the literature melting points for 1,4-DHP derivatives differ significantly from the 4*H*-pyran derivatives, in particular for the above compound by more than 30°C.

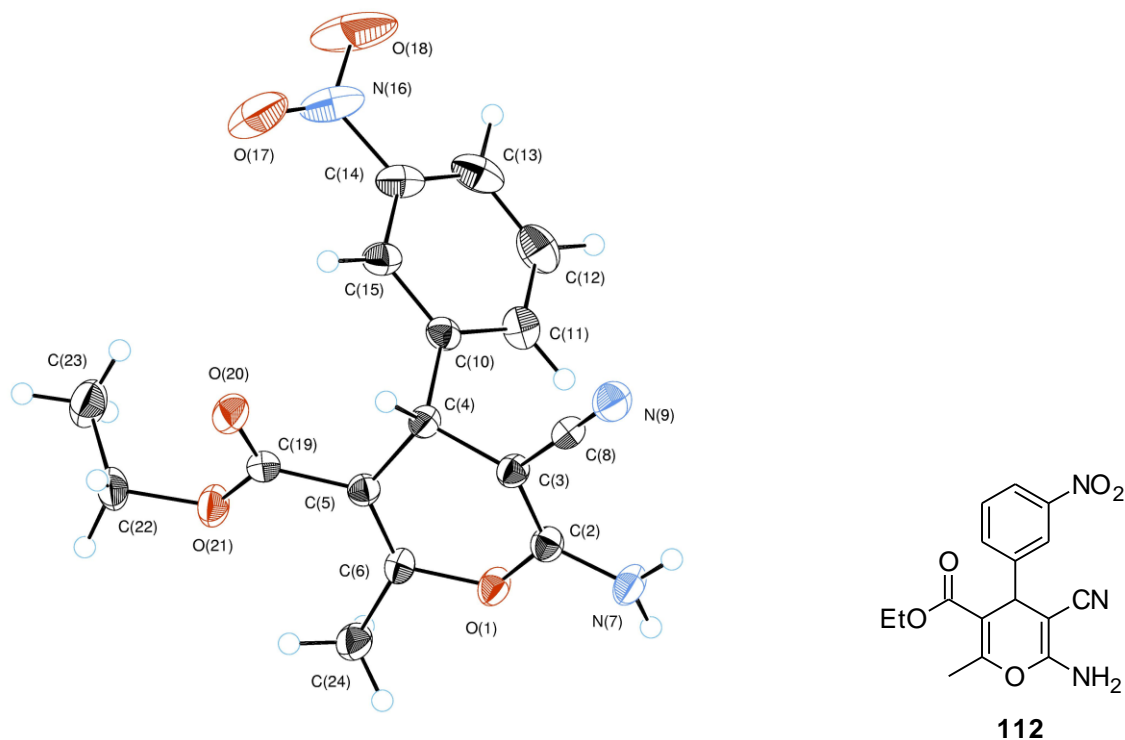
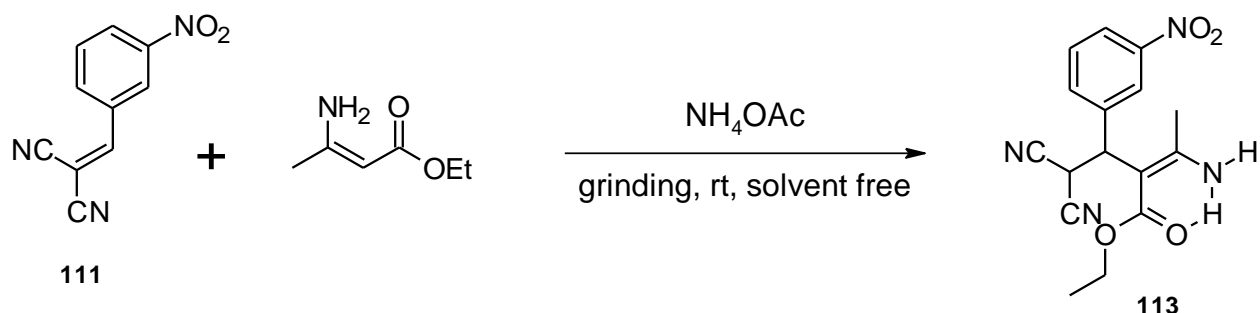


Figure 2.32. ORTEP representation of compound **112**.

In both structures the geometrical parameters of pyran systems are usual for *4H*-pyran heterocycles with the envelope conformation. The deviations of C(4) atom from the O(1), C(2), C(3), C(5), C(6) plane are equal 0.271(4) Å for methyl 6-amino-5-cyano-2-methyl-4-(thiophen-2-yl)-*4H*-pyran-3-carboxylate (**110**) and 0.359(3) Å for **112**. Both crystal structures are characterized by intermolecular hydrogen bonds of NH \cdots O and NH \cdots N types. The hydrogen bond lengths in **110** are 2.904(4) Å (N(7)–H(7A) \cdots O(16) bond) and 3.051(4) Å (N(7)–H(7B) \cdots N(9) bond). In **112** these bonds are stronger and the lengths are 2.820(3) Å (N(7)–H(7A) \cdots O(20) bond) and 2.987(3) Å (N(7)–H(7B) \cdots N(9) bond). The *4H*-pyrans exhibit an extensive range of biological and pharmacological activities, such as spasmolytic, diuretic, anti-coagulant, anti-cancer, and anti-anaphylactic properties. They may be useful in treatment of neurodegenerative disorders, including Alzheimer’s disease, amyotrophic lateral sclerosis, Huntington’s disease, and Parkinson’s disease.[242] Polyfunctionalized *4H*-pyrans also constitute a structural unit of many natural products,[243,244] having antiallergic,[245] antitumor,[246] and antibacterial [247-249] activities. *4H*-pyran derivatives are also potential calcium channel antagonists which are structurally similar to the biologically active 1,4-

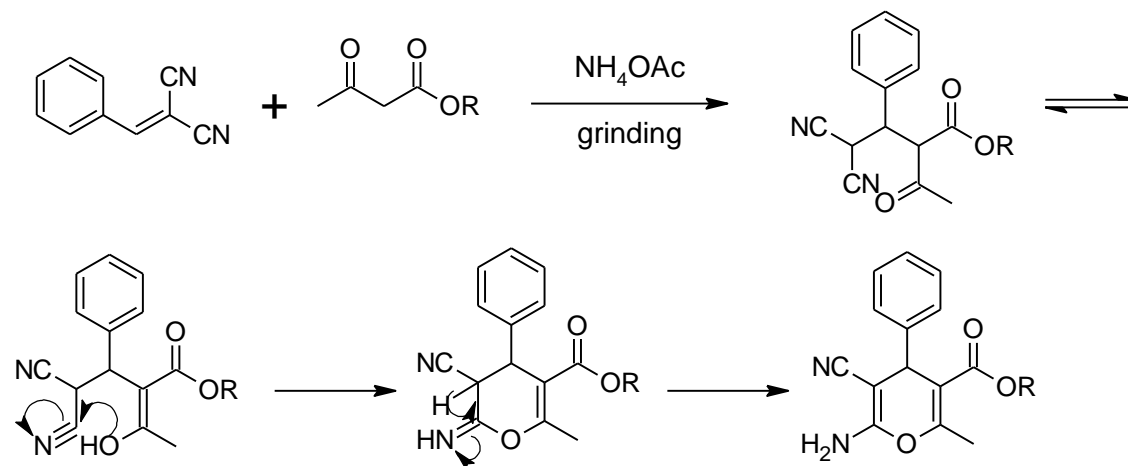
dihydropyridines[250]. Recent publications which report on the multicomponent synthesis of 4*H*-pyrans, use an aryl aldehyde, malononitrile, ethyl acetoacetate, and magnesium oxide as a basic catalyst, with grinding without solvent [249], another using silica nanoparticles as a catalyst and ethanol as solvent [251], and Cu(II) oxymetasilicate as a reusable catalyst in methanol as solvent [252]. In these reactions the catalyst had to be separated from the reaction medium. In the present work ammonium acetate was used as catalyst and after completion of the reaction was simply washed away with ethanol. The residual product was recrystallized to give high yields of the 4*H*-pyran derivatives.

Since the initial interest was to synthesize 1,4-DHP derivatives a reaction was tried where the ethyl acetoacetate in (Scheme 2.40) was substituted with ethyl 3-aminobut-2-enoate. Analysis of the product by NMR revealed that the compound formed was an intermediate (**113**), which has an acyclic structure, and an intramolecular NH \cdots O hydrogen bond (Scheme 2.42).



Scheme 2.42. Formation of intermediate **113** with an internal NH \cdots O bond.

The structure of intermediate **113** was further proved by single crystal X-ray diffraction (Fig. 2.33). The generation of this intermediate with a strong internal NH \cdots O bond with $r_{OH} = 1.903 \text{ \AA}$ in a six-membered ring configuration may explain why no further reaction takes place at room temperature to produce the dihydropyridine derivative. For the intermediate to react further the amino group must turn about the double bond and face the cyano group, which is possible through tautomerization, but apparently for this molecule the activation energy is rather high. Even when intermediate **113** was boiled in ethanol for 6 hours with DMAP as catalyst the starting material only slowly reacted to form a mixture of products which were not separated or further analysed. From this reaction it is also apparent that ethyl acetoacetate is deprotonated by the ammonium acetate catalyst and reacts in a Michael reaction first with compound **111** and then cyclizes to the 4*H*-pyran before it could form the enamine (Scheme 2.43).



Scheme 2.43. A plausible mechanism for 2-amino-4H-pyran synthesis indicating that during the grinding procedure the acetoacetate (not enamine) reacts with the phenylmethylenemalononitrile which then efficiently cyclizes to the 4H-pyran.

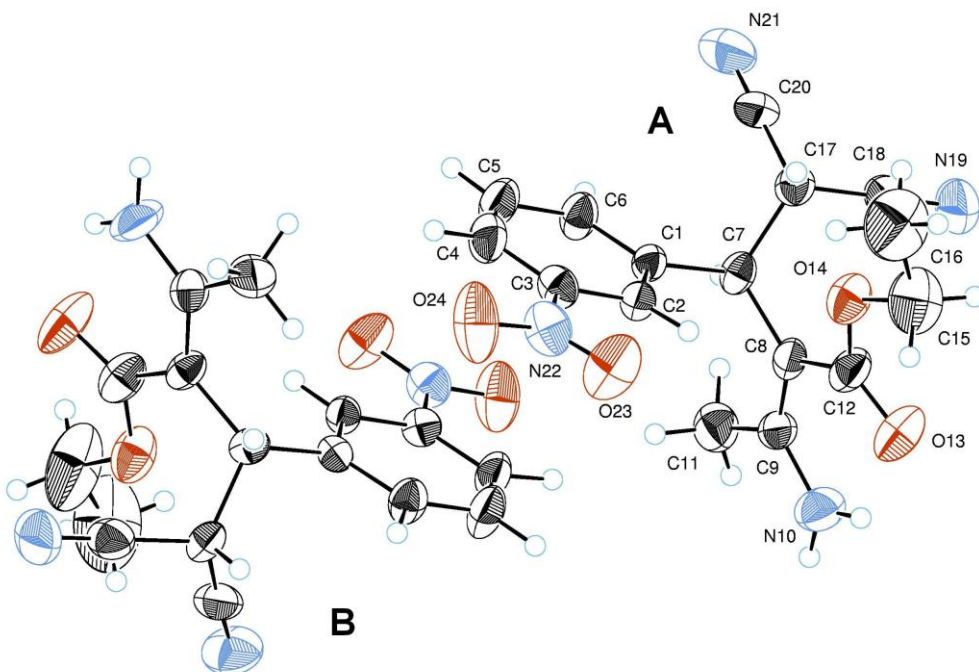


Figure 2.33 ORTEP representation on the intermediate **113**.

Intramolecular hydrogen bonding interactions are essential in biochemical reactions and enzymatic processes [253,254]. Malonaldehyde (MA) has been studied extensively not only because of the system's biological connections, but additionally because it is the prototypical

model that shows a short intramolecular hydrogen bonding for which proton transfer occurs between two oxygen atoms. In this study, a series of trends were examined to explore the effect of various substituents on the intramolecular hydrogen bonds. When placing substituents on the carbons, it was found that bulky electron donators on C1 and C3 and strong electron-withdrawing groups bonded to the unique carbon C2 created the strongest intramolecular hydrogen bonds. Thus the shortest hydrogen bond was found for NMe₂ groups at C1 and C3 and the strong electron-withdrawing group BH₂ on C2 with an O···O distance of 2.394 Å (Fig. 2.34) [255].

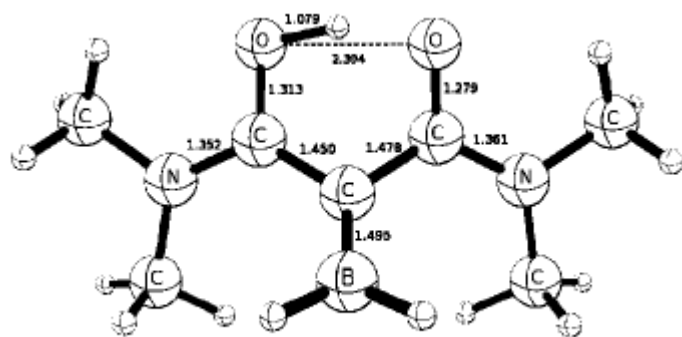
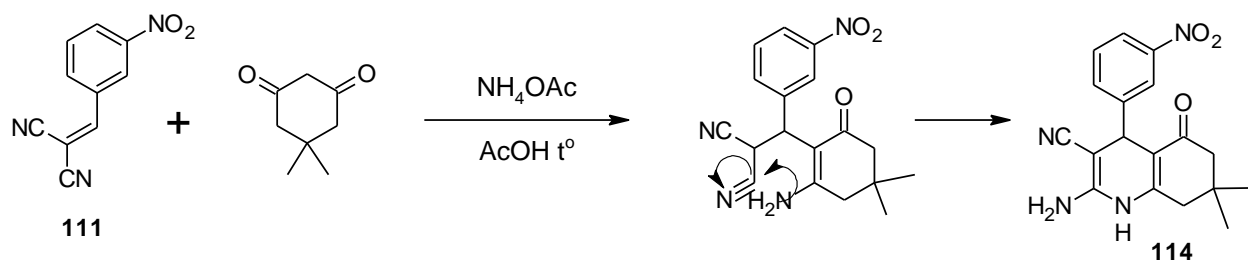


Figure 2.34. Malonaldehyde substituted with electron-donating NMe₂ on C1 and C3 and electron-withdrawing BH₂ on C2 resulting in a very short intramolecular hydrogen bond [255].

When the possibility of an internal hydrogen bonding is eliminated, as in the case of reacting compound **111** with dimedone in refluxing glacial acetic acid 5 hours,[256] the dihydropyridine structure **114** is formed readily in 70% yield (Scheme 2.44).



Scheme 2.44. Arylidene malononitrile reaction with dimedone and ammonium acetate in refluxing glacial acetic acid to form a 1,4-dihydropyridine derivative **114** [256].

This reaction was repeated except instead of refluxing in glacial acetic acid the reaction was carried out by grinding with mortar and pestle, the product was washed with ethanol and

recrystallized. When the crystals were analysed by X-ray diffraction the product again turned out to be a 4*H*-pyran derivative with dimedone **115** (Fig. 3.35) instead of the expected 1,4-DHP derivative. The X-ray structure reveals a molecule of ethanol which has crystallized along with the pyran and forms an OH⋯O hydrogen bond with the keto group $r_{\text{HO}}=1.860 \text{ \AA}$. This same reaction was carried out using microwaves in solvent-free conditions and in this case too only the 4*H*-pyran was isolated eventhough this exact reaction has been published by Shujiang Tu *et al.* [257] indicating that a 1,4-DHP derivative was obtained. These reactions warrant a closer reexamination. Thus it is apparent that the hydrogen bonding interaction is not the only

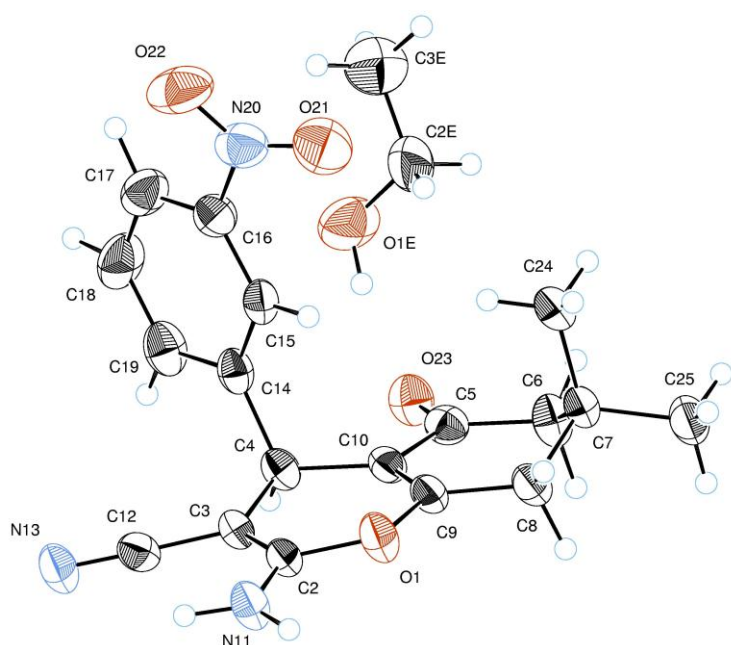


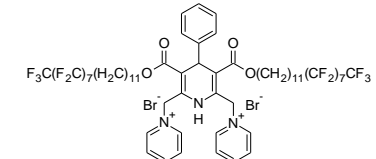
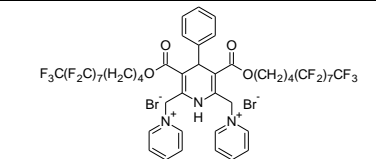
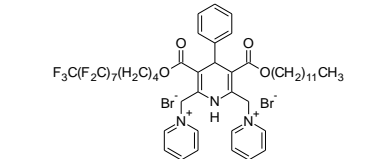
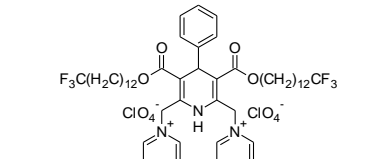
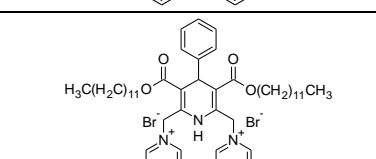
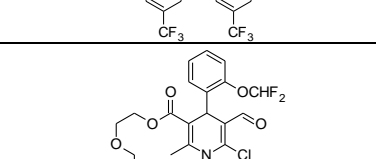
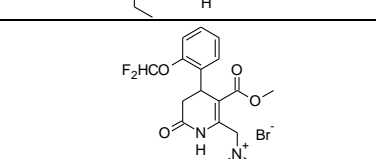
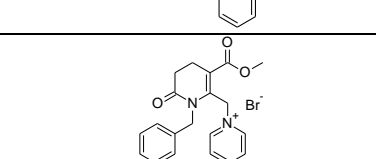
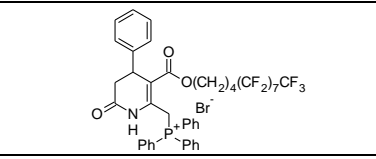
Figure 2.35. ORTEP representation of compound **115**.

determining factor in this reaction which leads to the 4*H*-pyran derivatives instead of to the desired 1,4-DHP derivatives.

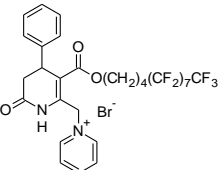
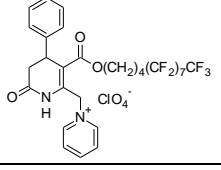
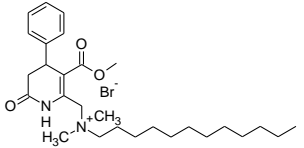
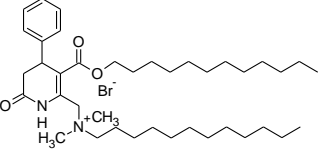
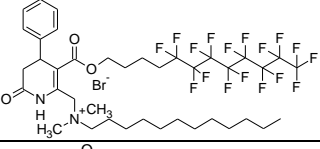
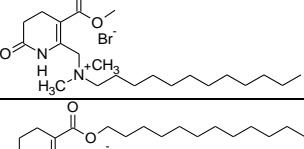
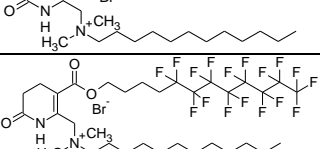
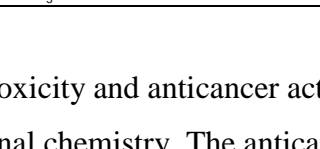
2.8 Biological activities

The first criterion for any drug, drug delivery vehicle, or gene trasfection agent to pass into the next phase of testing is their cytotoxicity. Thus the cytotoxicity data for various DHP amphiphiles and DHPOD amphiles on normal (3T3) cells, as well as their cytotoxicity on two cancer cell lines is provided in (Table 2.6).

Table 2.6. Cytotoxicity data obtained on HT-1080, MG-22A and 3T3 culture cell lines

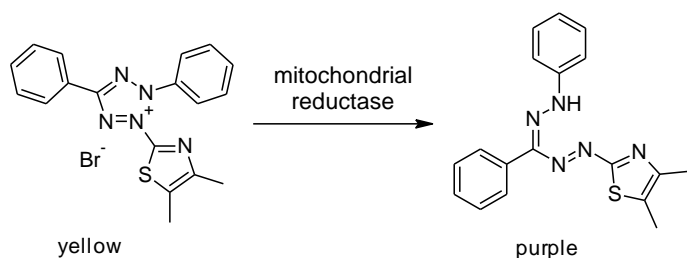
No.	Formula	HT-1080			MG-22A			3T3	
		IC ₅₀ CV	IC ₅₀ MTT	NO 100% CV	IC ₅₀ CV	IC ₅₀ MTT	NO 100% CV	IC ₅₀ NR	LD ₅₀ mg/kg
1	 F ₃ C(F ₂ C) ₇ (H ₂ C) ₁₁ O	*	*	8	*	*	6	*	>2000
2	 F ₃ C(F ₂ C) ₇ (H ₂ C) ₄ O	100	100	4	*	*	3	*	>2000
3	 F ₃ C(F ₂ C) ₇ (H ₂ C) ₄ O	50	47	9	47	75	6	477	3448
4	 F ₃ C(H ₂ C) ₁₂ O	18	10	75	10	19	50	16	771
5	 H ₃ C(H ₂ C) ₁₁ O	2	4	18	49	19	11	12	619
6	 OCHF ₂	*	100	5	5	56	61	300	1547
7	 F ₂ HCO	*	*	2	>100	*	4	1132	>2000
8	 Br ⁻	*	*	3	*	*	3	972	>2000
9	 Br ⁻	10	9	350	30	39	55	127	1779

Continuation of Table 2.6.

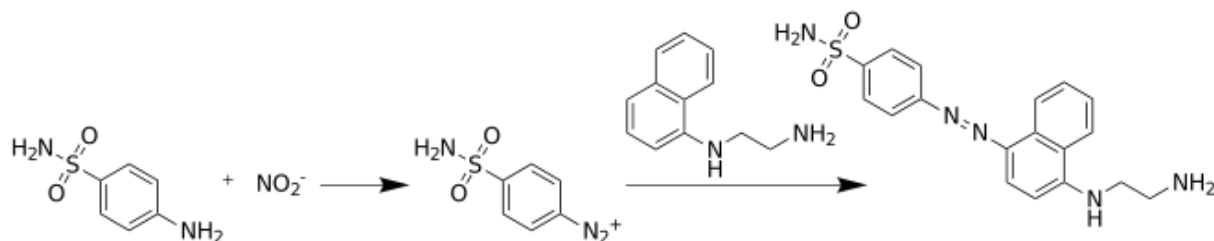
No.	Formula	HT-1080			MG-22A			3T3	
		IC ₅₀ CV	IC ₅₀ MTT	NO 100% CV	IC ₅₀ CV	IC ₅₀ MTT	NO 100% CV	IC ₅₀ NR	LD ₅₀ mg/kg
10		3	3	33	3	3	100	15	604
11		3	3	100	2	3	100	15	618
12		2	1	100	2	2	40	4	269
13		2	2	300	3	<1	150	6	346
14		3	30	200	26	30	100	27	898
15		2	1	100	18	16	67	63	831
16		2	3	150	3	1	200	7	369
17		3	2	100	4	<1	100	11	553

The cytotoxicity and anticancer activity of 17 compounds was determined at the OSI department of medicinal chemistry. The anticancer activity was tested on HT-1080 (human lung fibrosarcoma) and MG-22A (mouse hepatome) cell lines and the normal NIH 3T3 (mouse embryonic fibroblast) cell line. IC₅₀ is the compound concentration (µg/ml), at which 50% of the cells die. CV or crystal violet dye stains lipids in live cell membranes and thus is used to

determine the number of live cells based on the concentration of the dye which remains after staining. MTT is a standard colorimetric assay used to measure cellular proliferation. Yellow MTT (3-(4,5-dimethylthiazol-2-yl)-2,5-diphenyltetrazolium bromide is reduced to purple formazan in the mitochondria of living cells.



This reduction takes place only when mitochondrial reductase enzymes are active, and therefore conversion is directly related to the number of viable cells which can be quantified by the absorbance of the solution between ($\lambda=500$ to 600 nm) using a spectrophotometer. NO_2^- levels in the cell cultures were determined by the Greiss method.



Nitrite is detected and analyzed by formation of a red pink color upon treatment of a NO_2^- containing sample with sulphanilic acid the nitrites form a diazonium salt and when the azo dye (α -naphthylamine) is added a pink color develops. LD_{50} is determined using 3T3 cell culture based on the accepted Committee on the Validation of Alternative Methods (ICCVAM) protocol.

From the (Table 2.6) it is evident that the perfluorinated DHP amphiphiles (entries 1-3) are nontoxic and as the fluorine content in the esters is reduced the toxicity increases substantially (entries 4 and 5) also when the long ester groups are replaced with short ester groups like methyl for example, the cytotoxicity again is reduced (entries 7 and 8). The DHPOD series amphiphiles with a pyridinium polar head group are more toxic to normal cells than the DHP amphiphiles. The DHPOD amphiphile with a triphenylphosphonium polar head group (entry 9) is about 3 times less toxic than the analogous DHPOD with a pyridinium head group (entry 10). Some of

the DHPOD series cationic amphiphiles show a marked cytotoxicity towards cancer cells (entries 10-13, 15-17) this anti-cancer activity should be further explored which may lead to novel anti-cancer delivery or potentiation systems. A preliminary potentiation test with the fluoruous DHP amphiphile (entry 2) and anti-cancer drug 5-FU indicated a synergistic effect on the MDA-MB-435 (human breast cancer) cell lines.



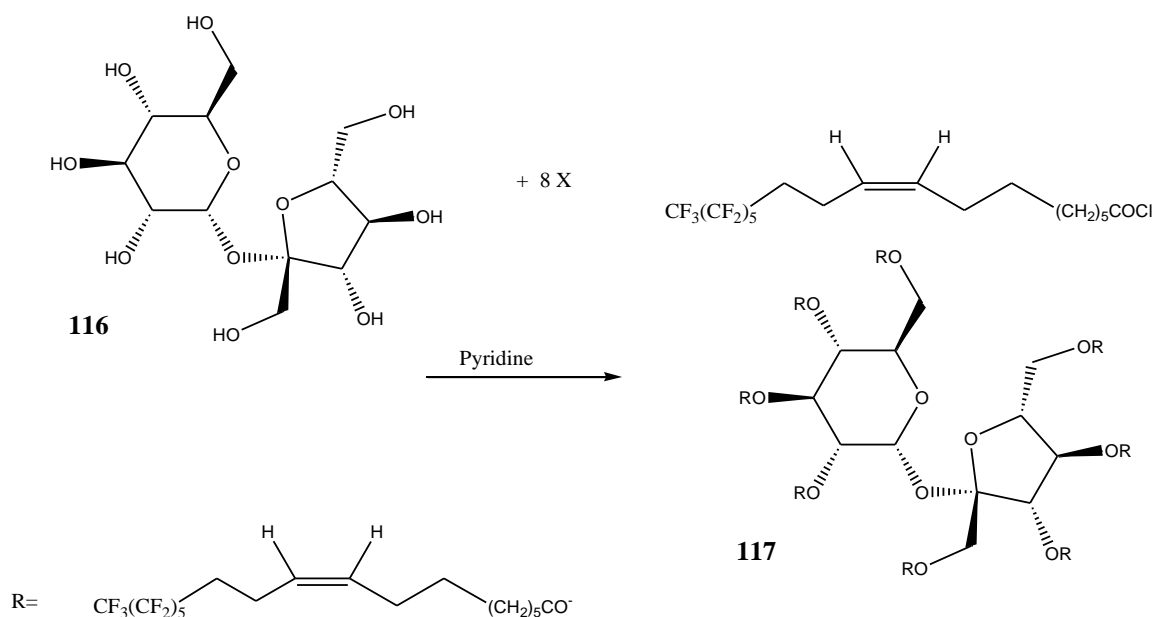
Figure 2.36. Gene transfection efficiency represented by the expressed green fluorescence gene at 80%, >50%, and no activity levels.

Gene transfection studies revealed that the fluoruous DHP amphiphile entry (2) and fluoruous DHPOD amphiphile (entry 10) had minimal transfection efficiencies but, the DHPOD amphiphiles (entries 13, 14, 16, 17) had greater than 50% gene transfection efficiencies (Fig 2.36).

2.9. ¹⁹F-MRI of Fluorinated Sucrose Octaoleate-F104

It is known [258] that the human lipase enzyme cannot metabolize sucrose polyesters in which more than five of the eight OH groups have been esterified with long-chain fatty acids. Indeed, the commercial non-caloric fat substitute OLESTRA is a mixture of hexa-, hepta- and octaesters of sucrose with a variety of unsaturated and saturated fatty acids [259]. Although no *in vivo* experiments have been done to prove the point, it is very likely that the corresponding fluorinated fatty acid esters will also pass unchanged through the human gastrointestinal tract. Hence these materials may have application in biocompatible delivery systems for magnetic resonance imaging (MRI) of gastrointestinal disorders.

We have synthesized perfluorinated oleic acid analogs [260,261] and utilized them to construct perfluorinated sucrose octaoleate-F104 [262], (Scheme 2.45), and used it in an emulsion containing egg yolk phospholipid (EYP) to encapsulate hyperpolarized xenon gas. In this work, we explored the possible use of this system *in vitro* as part of an eventual biocompatible *in vivo* delivery systems for hyperpolarized xenon in functional ¹²⁹Xe MRI [263,264].



Scheme 2.45. Synthesis of sucrose octaoleate-F104.

The success of hyperpolarized xenon imaging will depend ultimately on the rate of the xenon depolarization, hence long ^{129}Xe spin lattice relaxation times (T_1) are of critical importance. The observed T_1 value in above-mentioned EYP emulsion was 15 s [262], which would appear to present a substantial impediment for the eventual use of such a method for MRI applications. However, the high fluorine content of sucrose octaoleate-F104 and its likely physiological inertness make it an attractive candidate for use as a ^{19}F imaging agent, provided that a biocompatible delivery system can be devised. ^{19}F MRI has been reported previously, in particular the use of perfluorononane as a contrast agent for gastrointestinal imaging has been demonstrated [265]. There is, nevertheless, merit in examining other inert fluorinated imaging agents, since image resolution and sensitivity will depend on the agent employed. A number of vesicles of fat-like molecules have been approved for consumption, namely Intralipid (Pharmacia) in which aqueous suspensions of lipid vesicles of approximately 0.1 mm in diameter can be tolerated by humans and are used clinically as nutrient supplements.

We have prepared aqueous suspensions of lipid vesicles containing sucrose octaoleate-F104 and employed these vesicles to obtain high quality ^{19}F magnetic resonance images *in vitro* in time frames of the order of a few seconds. (Fig. 2.37) shows a typical image obtained from four scans using the spin-echo method with an echo delay of 6 ms and a repetition time of 1.2 s.

The internal diameter of the NMR tube containing the vesicles and the inner glass capillary can be estimated from the dimension bar on the right hand side of the image. With such an intense

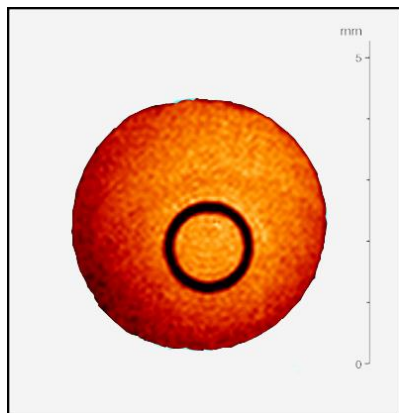


Figure 2.37. ^{19}F NMR image of vesicles of sucrose octaoleate-F104, obtained from four scans using the spin–echo technique with echo delay of 6 ms and repetition time of 1.2 s. The internal diameter of the 5 mm NMR tube and the 1 mm capillary tube can be estimated from the dimension bar on the right hand side of the image.

image and very high planar resolution, it should be possible to employ much smaller concentrations of the imaging agent when working *in vivo* [266].

3. CONCLUSIONS

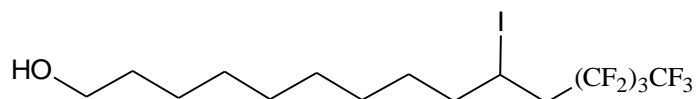
1. In the bromination of 4-aryl-6-methyl-3,4-dihydropyridones with NBS in dry methanol the bromine adds across the double bond or to carbon 5 and MeO adds to carbon 6 in a cis geometry. Furthermore, due to steric effects the bromine adds to the opposite face with respect to the aryl group, as has been proved by single crystal X-ray diffraction analysis.
2. In the bromination of 4 unsubstituted 6-methyl-3,4-dihydropyridones with NBS in dry methanol the bromine adds to carbon 5 and MeO adds to carbon 6 in a trans fashion (proved by X-ray diffraction) just like in the classical bromohydrin reaction which proceeds through a bromonium ion intermediate.
3. Bromination of N-benzyl-6-methyl-3,4-dihydropyridone with NBS in dry methanol the bromine adds to the 6-methyl group, giving the 6-bromomethyl DHPOD exclusively.
4. Optimized bromination of the three different types of DHPODs listed above, with bromine in dry chloroform solution give high yields of 6-bromomethyl DHPODs.
5. The standard reduction potential of bromine is +1.09 V and the oxidation potentials of various 1,4-DHP derivatives determined by cyclic voltammetry are in the -1.07 V to -1.15 V range and for this reason they would oxidize to the pyridines if bromine is used as brominating agent.
6. The oxidation potentials of 3,4-dihydropyridones are -1.63 V to -1.65 V and thus they can be brominated with bromine without any oxidation to the pyridones taking place.
7. The 1,4-DHP bispyridinium diperchlorates and DHPOD pyridinium perchlorates being positively charged have oxidation potentials still higher or at -1.57 V to -1.70 V and -2.04 V to -2.35 V respectively.
8. X-ray diffraction has provided data on the DHPOD hydrogen bonding with 4-phenyl-3,4-dihydropyridones crystallizing as dimers with $\text{NH}\cdots\text{O}$ distance about 1.893 Å and the oxidized 4-phenyl-pyridones with a smaller $\text{NH}\cdots\text{O}$ distance of 1.810 Å.
9. An ultra short $\text{NH}\cdots\text{N}$ hydrogen bond was observed in the X-ray structure of a compound which was obtained through a Wittig reaction with a DHPOD triphenylphosphine derivative and a pyridine-2-carboxaldehyde with a bond distance of 1.765 Å and a large $^1\text{H-NMR}$ downfield shift from 8 ppm in the parent DHPOD to 14 ppm in the product.

10. The DHPOD heterocycle was elaborated through the 6-methyl group by a Wittig reaction and through copper catalyzed “Click-chemistry” providing a means to large libraries of original DHPODs with a double bond or triazole linkage respectively.
11. A recently published work (2011) on the room temperature synthesis of 2-amino-DHP derivatives was proved wrong by providing unequivocal X-ray diffraction data establishing that in fact 4*H*-pyrans had been synthesized.
12. A reaction intermediate with an internal hydrogen bond of the above reaction was isolated which couldn't be cyclized to the DHP heterocycle in room temperature conditions, providing evidence for the reaction mechanism i.e., the acetoacetate (not the enamine) reacts with arylmethylenemalononitrile and cyclizes to the 4*H*-pyrans.
13. A series of novel 1,4-DHP based fluorous cationic amphiphiles were synthesized, some of which are non-toxic i.e., (LD₅₀ > 2000 mg/kg) however, their gene transfection efficiency is minimal.
14. A series of novel 3,4-DHPOD based fluorous cationic amphiphiles were synthesized, some of which exhibited >50% gene transfection efficiency at the same time some of these amphiphiles proved highly cytotoxic to cancer cell lines while being only marginally cytotoxic to normal cells.
15. These fluorous cationic amphiphiles have the added advantage that their movement through an organism can be tracked by the non-invasive ¹⁹F-MRI technology. A high resolution ¹⁹F-MR image of a capillary tube was obtained in sucrose octaoleate-F104 emulsion.

4. EXPERIMENTAL

4.1. General

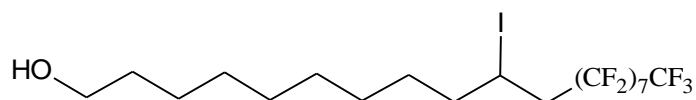
All reagents were purchased from Aldrich, Acros, Fluka or Merck and used without further purification. TLC was performed on 20 cm \times 20 cm Silica gel TLC-PET F254 foils (Fluka). The onedimensional ^1H (400 MHz), ^{19}F (376.2 MHz), ^{31}P (161.86 MHz) and ^{13}C (100.61 MHz) and two dimensional ^1H – ^1H COSY, ^{19}F – ^{19}F COSY, ^{13}C – ^1H HMBC, ^{13}C – ^1H HSQC NMR spectra of compounds were recorded on a Varian-Mercury BB 400 MHz. The ^1H – ^{13}C -HMBC spectra were recorded with the evolution time of 62.5 s delay for the generation of long-range correlations. For all two dimensional ^{13}C – ^1H HMBC, ^{13}C – ^1H HSQC spectra 4096 \times 1024 data matrix was used, which ensured $t_{2\text{max}} = 100$ ms for ^1H and $t_{2\text{max}} = 50$ ms for ^{13}C along the F1 and F2 axes, correspondingly. In order to improve the signal-noise ratio, the data matrix before Fourier transformation was zero-filled twice and multiplied with a cosine function. The chemical shifts of the hydrogen and carbon atoms are presented in parts per million and referred to the residual signals of the CDCl_3 solvent 7.25 (^1H) and 77.0 ppm (^{13}C) ppm respectively. The chemical shifts of fluorine and phosphorus atoms were referred to internal software standards CFCl_3 and H_3PO_4 correspondingly. Mass spectral data were determined on an Acquity UPLC system (Waters) connected to a Q-TOF micro hybrid quadrupole time of flight mass spectrometer (Micromass) operating in the ESI positive or negative ion mode on an Acquity UPLC BEH C18 column (1.7 mm, 2.1 mm \times 50 mm) using a gradient elution with acetonitrile/phosphate buffer (pH 2.2; 0.05 M) in water (10:90 by volume) at a flow rate of 1 mL/min. Peak areas were determined electronically with a DP-800 (GBC Scientific Equipment). Melting points were determined on an OptiMelt (SRS Stanford Research Systems). The nanoaggregates were prepared by dispersing the compounds in water using a Cole Parmer probe type ultrasonic processor CPX 130W, U.S.A. and observed with MFP-3DBIOTM atomic force microscope in dynamic mode using Olympus AC240TM tips. The characteristics of the formed nanoaggregates were determined by the Dynamic Light Scattering technique (DLS). For DLS measurements, we employed a Zetasizer Nano instrument. Nano–Nano S90: size range 1 nm–3 μm . Laser 633 nm and software of Malvern Instruments Ltd.



12,12,13,13,14,14,15,15,15-Nonafluoro-10-iodopentadecan-1-ol (**1**)

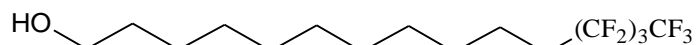
To a solution of 10-undecen-1-ol 3.43 g (0.02 mol) in CH_3CN (20 mL) and deionized H_2O (20 mL) was added perfluorbutyl iodide, 8.24 g (0.024 mol) NaHCO_3 1.72 g (0.02 mol) and 85% $\text{Na}_2\text{S}_2\text{O}_4$ 4.12 g (0.02 mol) at 0 $^\circ\text{C}$, and then this mixture was stirred for 4 h at room temperature. The mixture was diluted with deionized H_2O , and then extracted with CH_2Cl_2 . The organic layers were washed with satd NaCl aq, and then dried over MgSO_4 . After filtration and evaporation of the solvent, there was obtained 9.54 g of **1** as a light yellow oil in 92% yield.

^1H NMR (CDCl_3) δ : 1.16–1.48 (12H, m, H3–H8), 1.48–1.68 (2H, m, H2), 1.70–1.90 (2H, m, H9), 2.68–2.83, 2.83–3.00 (1H, 1H, m, m, H11), 3.65 (2H, t, $J = 6.71$ Hz, H1), 4.33 (1H, tt, $J = 4.41, 8.88, 17.60$ Hz, H10).



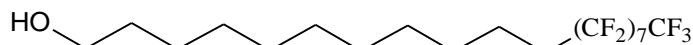
12,12,13,13,14,14,15,15,16,16,17,17,18,18,19,19,19-Heptafluoro-10-iodononadecan-1-ol (2)

This compound was synthesized using the same procedure as for compound **2** giving an oily solid in 94% yield. ¹H NMR (CDCl₃) d: 1.16–1.48 (12H, m, H3–H8), 1.48–1.68 (2H, m, H2), 1.70–1.90 (2H, m, H9), 2.68–2.83, 2.83–3.00 (1H, 1H, m, m, H11), 3.65 (2H, t, J = 6.71 Hz, H1), 4.33 (1H, tt, J = 4.41, 8.88, 17.60 Hz, H10).



12,12,13,13,14,14,15,15,15-Nonafluoropentadecan-1-ol (3)

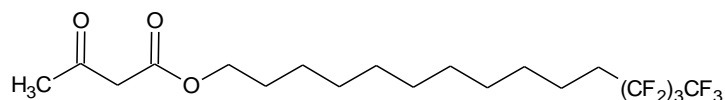
1 9.5 g (18.5 mmol) was added to a mixture of Zn powder 3.9 g and NiCl₂·6H₂O 0.75 g in dry THF (45 mL) and deionized H₂O (77 drops). This mixture was stirred for 4 h at room temperature. The mixture was quenched with satd NaHCO₃ aq, and was extracted with CH₂Cl₂. The organic layers were washed with satd NaCl aq, and then was dried over MgSO₄. After filtration and evaporation of the solvent, the residue was purified by a column chromatography (EtOAc/n-hexane, 30%) to give **3** 5.63 g as a white solid mp. 33.5°C, 78%. ¹H NMR (CDCl₃) d: 1.26–1.45 (12H, m, H3–H9), 1.52–1.65 (4H, m, H2, H10), 2.05 (2H, tt, J = 8.24, 18.87 Hz, H11), 3.65 (2H, t, J = 6.46 Hz, H1).



12,12,13,13,14,14,15,15,16,16,17,17,18,18,19,19,19-Heptafluorononadeca-1-ol (4)

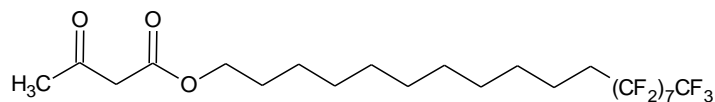
Compound **4** was synthesized using the same procedure as for compound **3** giving a white solid mp. 77.2°C in 86% yield.

¹H NMR (CDCl₃) d: 1.29 (m, 14 H, (CH₂)₇ and s, 1H, OH); 1.56 (m, 4H, CH₂CH₂OH and CH₂CH₂CF₂); 2.05 (m, 2H, CH₂CF₂); 3.64 (t, 2H, J=6.6 Hz, CH₂OH).



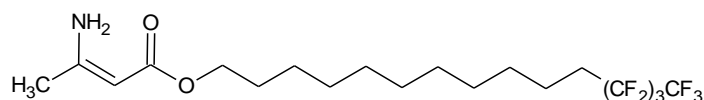
12,12,13,13,14,14,15,15-Nonafluoropentadecyl 3-oxobutanoate (5)

To a 20 mL round bottomed flask was added (5.30 g, 14 mmol) of **3** and (2.0 g, 14 mmol) 2,2,6-trimethyl-4H-1,3-dioxin-4-one in 5 mL xylene. The mixture was stirred and refluxed for 2 h. After the xylene was removed on the rotary evaporator and the residue eluted through a silica gel column with CH₂Cl₂ there was obtained 5.3 g of a white oily solid in 80% yield. ¹H NMR (CDCl₃) d: 1.26–1.45 (14H, m, H3–H9), 1.52–1.65 (4H, m, H2, H10), 2.04 (2H, tt, J = 8.24, 18.87 Hz, H11), 2.25 (2H, s, CH₃), 3.44 (2H, s, CH₂) 4.13 (2H, t, J = 7.00 Hz, H1). ¹³C NMR (CDCl₃) d: 200.52, 167.16, 122-108 (4m, CF₂CF₂CF₂CF₃), 65.52, 50.11, 31-28.6 (11 C's).



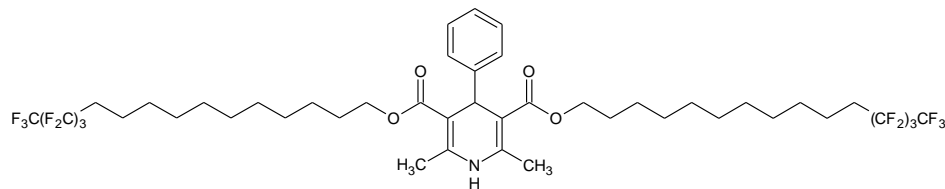
12,12,13,13,14,14,15,15,16,16,17,17,18,18,19,19,19-Heptadecafluorononadecyl 3-oxobutanoate (6) **3-**

Compound **6** was obtained by the same procedure as for compound **5** as a white solid mp. 50-51°C in 96% yield. ¹H NMR (CDCl₃) d: 1.26–1.45 (14H, m, H3–H9), 1.52–1.68 (4H, m, H2, H10), 2.04 (2H, tt, J = 8.24, 18.87 Hz, H11), 2.26 (3H, s, CH₃), 3.44 (2H, s, CH₂) 4.13 (2H, t, J = 7.00 Hz, H1).



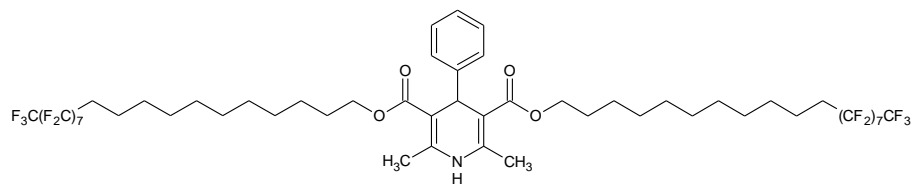
12,12,13,13,14,14,15,15,15-Nonafluoropentadecyl 3-aminobut-2-enoate (7)

To a 50 mL round bottomed flask was added **5** (5.3 g, 0.01 mol) in 10 ml ethanol and to this solution was added 7 mL 25% aqueous ammonia solution (0.05 mol). The solution was stirred at room temperature for 2 days and after cooling in the refrigerator the precipitated white solid was filtered and washed with cold ethanol giving 3.4 g of a white flaky solid mp. 33-35°C in 65% yield. ¹H NMR (CDCl₃) d: 1.26–1.45 (12H, m, H3–H9), 1.52–1.65 (4H, m, H2, H10), 1.89 (3H, s, CH₃), 2.04 (2H, tt, J = 8.24, 18.87 Hz, H11), 4.03 (2H, t, J = 6.06 Hz, H1), 4.52 (1H, s, CH), 7.87 (2H, bs, NH₂).



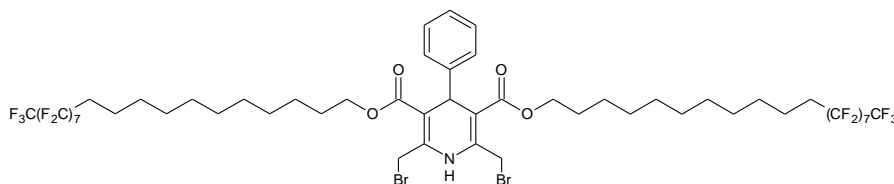
Bis(12,12,13,13,14,14,15,15,15-nonafluoropentadecyl) 1,4-dihydro-2,6-dimethyl-4-phenylpyridine-3,5-dicarboxylate (8)

To a 25 mL round bottom flask was added **7** (1.5 g, 3 mmol) in 10 mL ethanol and to this solution was added benzaldehyde (0.17 g, 1.5 mmol) and 3 drops of glacial acetic acid. The solution was stirred at room temperature for 6 days. The solvent was removed on a rotary evaporator and the residue eluted with 10% EtAc/Hexane to give 230 mg of a clear oil in 15% yield. ¹H NMR (CDCl₃) d: 1.26–1.45 (28H, m, H3–H9), 1.52–1.68 (8H, m, H2, H10), 1.98 (4H, tt, J = 8.24, 18.87 Hz, H11), 2.27 (6H, s, CH₃), 3.96 (4H, t, J = 6.46 Hz, H1), 4.92 (1H, s, CH), 5.51 (1H, bs, NH), 7.04-7.22 (5H, m, Arom). ¹³C NMR (CDCl₃) d: 167.70, 147.70, 143.0, 127.80, 126.04, 122-108 (4m, CF₂CF₂CF₂CF₃), 104.08, 63.89, 39.52, 30.74 (t) 29.45-28.68 (m), 26.04, 19.46.



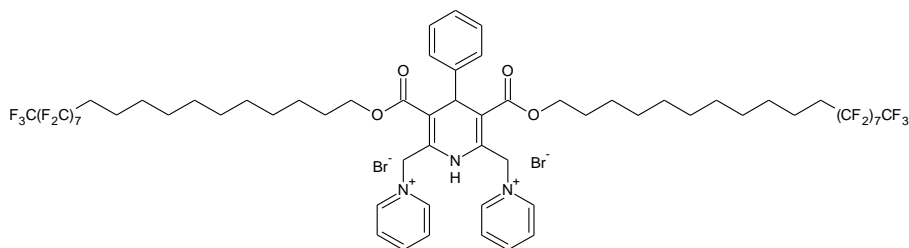
Bis(12,12,13,13,14,14,15,15,16,16,17,17,18,18,19,19,19-heptafluorononadecyl) 1,4-dihydro-2,6-dimethyl-4-phenylpyridine-3,5-dicarboxylate (9)

To a 15 mL glass pressure tube was added **6** (1.5 g, 2 mmol) and freshly distilled benzaldehyde (0.12 g, 1 mmol) and ammonium acetate (0.08 g, 1 mmol) in 5 mL ethanol. The tube was capped and placed in a temperature controlled microwave oven and heated at 120°C for 30 min. The tube was cooled and the precipitated yellowish solid filtered and washed with cold ethanol. The product was recrystallized from ethanol and ethyl acetate to give a light yellow solid 350 mg with a broad mp. 82-87°C in 25% yield. ¹H NMR (CDCl₃) δ: 1.26–1.45 (28H, m, H3–H9), 1.52–1.68 (8H, m, H2, H10), 2.04 (4H, tt, J = 8.24, 18.87 Hz, H11), 2.33 (6H, s, CH₃), 4.01 (4H, t, J = 6.46 Hz, H1), 4.99 (1H, s, CH), 5.63 (1H, bs, NH), 7.10-7.28 (5H, m, Arom).



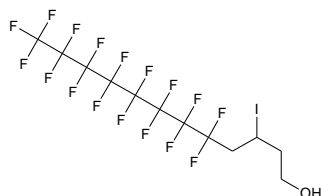
Di-12,12,13,13,14,14,15,15,16,16,17,17,18,18,19,19,19-heptafluorononadecyl 2,6-bis(bromomethyl)-4-phenyl-1,4-dihydropyridine-3,5-dicarboxylate (12)

The dihydropyridine **9** (0.7g, 0.5mmol) was suspended in 20 ml methanol and carbontetrachloride was added until the solid dissolved then (0.18g, 1mmol) NBS was added and the solution was stirred overnight. The solvent was removed using rotary evaporation and most of the solid dissolved in carbontetrachloride and the succinic acid was filtered off. The solvent was removed by rotary evaporation to yield a yellowish solid 0.6g or 80% yield of **12**. The compound was used in the next reaction without purification since it is unstable in solution. ¹H NMR (CDCl₃) δ: 1.26–1.45 (28H, m, H3–H9), 1.52–1.68 (8H, m, H2, H10), 2.04 (4H, tt, J = 8.24, 18.87 Hz, H11), 4.01 (4H, t, J = 4.03, 6.46 Hz, H1), 4.61 (2H, d, J=11.4 Hz, CH₂Br), 4.92 (2H, d, J=11.4 Hz, CH₂Br), 5.01 (1H, s, CH), 6.46 (1H, bs, NH), 7.10-7.28 (5H, m, Arom).



Bis(12,12,13,13,14,14,15,15,16,16,17,17,18,18,19,19,19-heptafluorononadecyl)1,4-dihydro-2,6-dimethyl-4-phenylpyridine-3,5-dicarboxylate-2,6-dipyridinium bromide (13)

The bisbromodihydropyridine (**7**) (0.19g, 0.12mmol) was dissolved in dry acetone and dry pyridine (0.025g, 0.3mmol) was added. The solution was stirred over the weekend by which time the dipyridiumbromide (**8**) had precipitated as a light yellow solid 0.14g or 70% yield mp. 85-105 °C. ¹H NMR (CDCl₃) d: 1.26–1.45 (28H, m, H3–H9), 1.52–1.68 (8H, m, H2, H10), 2.04 (4H, tt, J = 8.24, 18.87 Hz, H11), 4.01 (4H, t, J = 4.03, 6.46 Hz, H1), 5.08 (1H, s, CH), 5.88 (2H, d, J=13.8 Hz. CHBrPy), 6.39 (2H, d, J=13.8 Hz. CHBrPy), 7.10-7.28 (5H, m, Arom), 8.18 (4H, t, J=7.6, 6.6 Hz, Py), 8.57 (2H, t, J=7.8, 7.8 Hz, Py), 9.33 (4H, d, J=5.8 Hz, Py), 10.93 (1H, bs, NH).

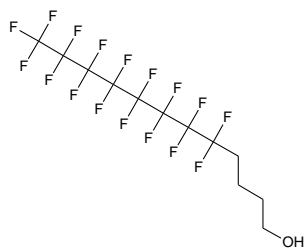


5,5,6,6,7,7,8,8,9,9,10,10,11,11,12,12,12-Heptafluoro-3-iodododecan-1-ol (**15**)

In a 250 ml 1 neck round bottomed flask in 40 ml acetonitrile added 10.92 g (0.02 mol) 1-Iodoperfluorooctane and 1.44 g (0.02 mol) 3-Buten-1-ol. To this solution was added 1.72 g NaHCO₃ (0.02 mol) dissolved in 20 ml DI water whereby two layers were formed. The solution was cooled in an ice bath with magnetic stirring and 4.12 g (0.02 mol) of Na₂S₂O₄ (85%) was added slowly. After all of the sodium dithionite was added the flask was removed from the ice-bath and left to stir overnight. The white suspension was diluted with 100 ml DI water and extracted with ethylacetate 3X50 ml and the organic fractions were dried with MgSO₄, filtered and the solvent removed on the rotary evaporator to give 11.37 g of a white solid in 92% yield.

C₁₂H₈F₁₇IO MW. 618.07 Mp. 82-83 °C. ¹H NMR (CDCl₃): δ=4.56-4.47 (m, 1 H, CHI), 3.91-3.73 (m, 2 H), 3.07-2.75 (m, 2H), 2.10-1.94 (m, 2 H), 1.46 (br s, 1 H, HO).

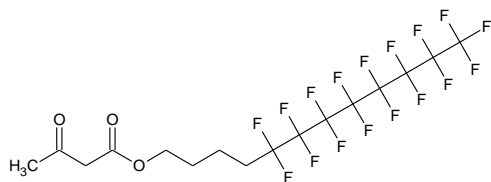
¹⁹F NMR (CDCl₃): δ= -81.3 (t, ³J_{FF} = 9.2 Hz, 3 F, CF₃), -111.8 (dm, ²J_{FF} = 272 Hz, 1 F), -114.6 (dm, ²J_{FF} = 272 Hz, 1 F), -122.1 (m, 2 F), -123.2 (m, 4 F), -124.1 (m, 2 F), -126.6 (m, 2 F), -122.4 (m, 2 F). MS (EI); m/z (%): 618 (3) [M⁺], 491 (100) [M⁺ - I], 473 (32) [M⁺ - I, - H₂O], 441 (32), 395 (5), 219 (1) [CF₃(CF₂)₃⁺], 169 (4) [CF₃(CF₂)₂⁺], 119 (6) [CF₃CF₂⁺], 69 (1) [CF₃⁺]. - C₁₂H₈F₁₇OI (618.06): calcd. C 23.32, H 1.30; found C 23.95, H 1.38.



5,5,6,6,7,7,8,8,9,9,10,10,11,11,12,12,12-heptafluorododecan-1-ol (**16**)

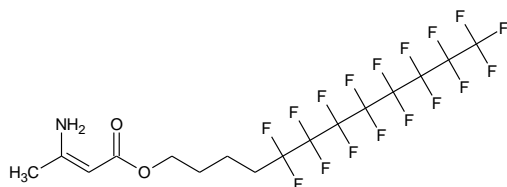
A 250 mL round bottomed flask was charged with **15** (9.74 g, 15.76 mmol), Bu₃SnH (9.27 g, 31.86 mmol), AIBN (0.26 g, 1.61 mmol, 10 mol-%) and toluene (40 mL). The solution was stirred at 70 °C. After 4 h, the solvent was removed by rotary evaporation. The residue was dissolved in hexane (10 mL) and cooled to -20 °C. The resulting white crystals were collected on

a frit. The filtrate was concentrated (10 mL) and cooled to -20 °C. A second crop of crystals was similarly collected. The crops were combined and dried by oil pump vacuum to give 7.42g. C₁₂H₉F₁₇O MW. 492.17 ¹H NMR (CDCl₃): δ = 3.68 (t, ³J_{HH} = 6.0 Hz, 2 H, HOCH₂), 2.19-2.01 (m, 2 H, CH₂CF₂), 1.75-1.61 (m, 4 H, CH₂CH₂CH₂CF₂), 1.36 (br s, 1 H, HO). ¹⁹F NMR (CDCl₃): δ = -81.3 (t, ³J_{FF} = 9.2 Hz, 3 F, CF₃), -115.0 (m, 2 F), -122.2 (m, 2 F), -123.2 (m, 4 F), -124.0 (m, 2 F), -126.6 (m, 2 F), -122.4 (m, 2 F).



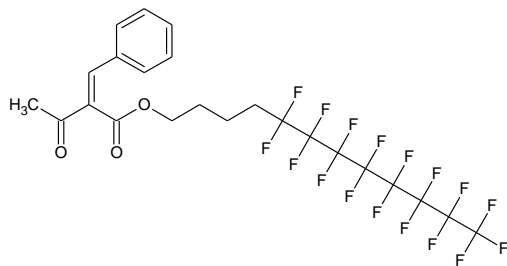
5,5,6,6,7,7,8,8,9,9,10,10,11,11,12,12,12-Heptafluorododecyl 3-oxobutanoate (17)

In 100 mL round bottom flask equipped with a water cooled condenser a CaCl₂ guard tube and a magnetic stir bar was placed 6.45 g (0.0131 mol) **16** and 2,2,6-Trimethyl-4H-1,3-dioxin-4-one 1.86 g (0.0131 mol) in 50 mL p-Xylene. The flask was heated in an oil bath while stirring at 160°C for 2 hours. The solvent was removed on a rotary evaporator to give 6.89 g of a light yellow oil. The oil was purified by a silica gel column using EtAc/Hexane as eluent 800 mL 5% and 500 mL 10% in EtAc, the fractions were monitored on TLC plates with phosphomolybdic acid developer. Fractions with R_f=0.1 were collected and concentrated to give 4.43 g 64% yield of oil which solidified. C₁₆H₁₃F₁₇O₃ MW. 576.25. ¹H NMR 400 MHz (CDCl₃): δ = 4.13 (t, J = 6.2 Hz, 2H, OCH₂), 3.42 (s, 2H, COCH₂CO), 2.21 (s, 3H, COCH₃), 2.12-1.99 (m, 2H, CH₂CF₂), 1.75-1.61 (m, 4H, CH₂CH₂). ¹³C-NMR 100.3 MHz (CDCl₃): δ = 200.15, 166.95, 123-105 (m, CF), 64.34, 49.74, 30.28 (t, J = 16.5 Hz, CH₂CF₂), 29.81, 27.81, 16.81 ppm.



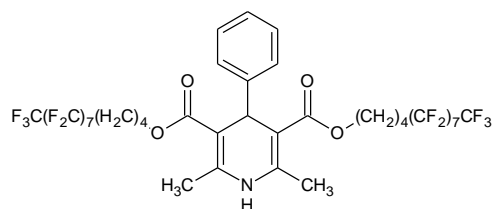
5,5,6,6,7,7,8,8,9,9,10,10,11,11,12,12,12-Heptafluorododecyl 3-aminobut-2-enoate (18)

In a 10 mL RB was weighed 1.50g (0.0026mol) compound **18** and dissolved in 2 mL EtOH, then 3 mL of concentrated aqueous ammonia was added and the flask was stoppered. The mixture was stirred magnetically overnight and the flask was put in the fridge to cool. The precipitated solid was filtered and washed with DI water. After drying in air there was obtained 0.94 g of a white powder in 63% yield. Mp. 75-76°C. C₁₆H₁₄F₁₇NO₂ MW 575.26 Composition C(33.41) H(2.45) F(56.14) N(2.43) O(5.56) ¹H NMR 200 MHz (CDCl₃): δ = 4.46 (s, 1H, -CH=C-), 4.02 (t, J = 6 Hz, OCH₂), 2.11-2.00 (m, 2H, -CH₂CF₂-), 1.85 (s, 3H, -CH₃), 1.66-1.65 (m, 4H, CH₂CH₂). LC/MS: MS(+ESI) m/z (rel.intensity): 598 ([M+Na]⁺, 100).



5,5,6,6,7,7,8,8,9,9,10,10,11,11,12,12,12-Heptadecafluorododecyl 2-benzylidene-3-oxobutanoate (E/Z mix) (19)

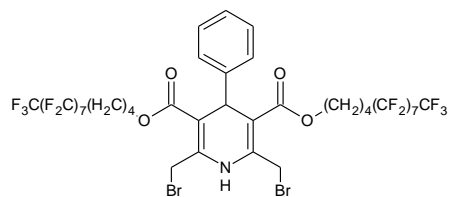
Compound **17**, 2.88 g (0.005mol) and benzaldehyde 0.53 g (0.005mol) were dissolved in 40 mL benzene and 3 drops of glacial acetic acid and 5 drops of piperidine were added. The mixture was stirred magnetically overnight. The solvent was removed on a rotary evaporator and the residue was purified by silica gel chromatography (eluent: 10% EtOAc / Hexane) providing 2.47 g of a yellow oil in 74% yield. $C_{23}H_{17}F_{17}O_3$, MW 664.35. 1H NMR 200 MHz ($CDCl_3$): δ = 7.60 (s, 1H, $-CH=C-$), 7.41 (m, 5H, Ph), 4.28 (t, J = 6.2 Hz, 2H, $-OCH_2-$), 2.44 (s, 3H, CH_3CO), 2.02 (m, 2H, $-CH_2CF_2-$), 1.49-1.79 (m, 4H, $-CH_2CH_2-$).



Bis(5,5,6,6,7,7,8,8,9,9,10,10,11,11,12,12,12-heptafluorododecyl) 1,4-dihydro-2,6-dimethyl-4-phenylpyridine-3,5-dicarboxylate (20)

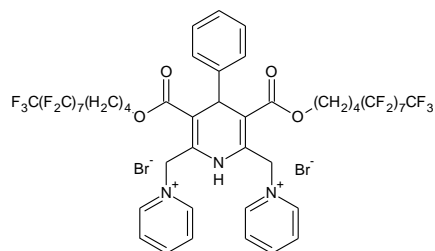
In a round bottomed flask was weighed 1.33 g (0.002mol) compound **19** and 1.15 g (0.002 mol) compound **18** then 11 mol % or 0.038 g 1-butylpyridinium chloride was added and the mixture was dissolved in diethyleneglycol 10 mL. The flask was stoppered and placed in an oil bath and was stirred magnetically at 80°C for 6 h. The flask was left stirring overnight (without heating) and the contents were poured in ice-water. The mixture was extracted with EtOAc 3x40 mL. The organic extract was dried with anh. Na_2SO_4 , filtered and the solvent was removed at reduced pressure on a rotary evaporator. The yellow residue (2.57 g) was recrystallized from EtOH to give 1.10 g of a pale yellow compound in 45% yield. Mp. 107-108°C

1H NMR 400 MHz ($CDCl_3$): δ = 7.20-7.04 (m, 5H, Ph), 5.60 (br s, 1H, NH), 4.89 (s, 1H, 4-CH), 4.06-3.95 (m, 4H, 3,5- CO_2CH_2-), 2.28 (s, 6H, 2,6- CH_3), 2.04-1.91 (m, 4H, 3,5- CH_2CF_2-), 1.63-1.52 (m, 8H, 3,5- CH_2CH_2-). ^{13}C -NMR 100.3 MHz ($CDCl_3$): δ = 167.34, 147.51, 144.31, 127.95, 127.81, 126.32, 107.30-120.86 [(CF_2) $_7$ CF $_3$], 103.99, 62.88, 39.54, 30.43 (t, J = 21.6 Hz, CH_2CF_2), 28.22, 19.54, 17.01 ppm.



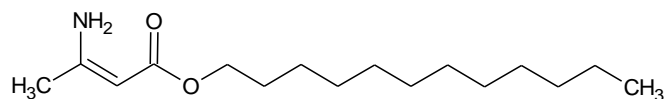
Di-5,5,6,6,7,7,8,8,9,9,10,10,11,11,12,12,12-heptafluorododecyl 2,6-bis(bromomethyl)-4-phenyl-1,4-dihydropyridine-3,5-dicarboxylate (21)

0.62 g (0.0005 mol) of compound **20** was dissolved in 6 mL chloroform and 4 mL MeOH solution. The solution was cooled in ice bath and 0.18 g (0.001 mol) NBS was added in small portions. After all the NBS was added the reaction was left stirring overnight. The solvent was removed at reduced pressure on the rotary evaporator. The residue was triturated with carbon tetrachloride and filtered from the solid succinimide. The solvent was removed in vacuum providing 0.53 g of a yellow solid in 75% yield. $^1\text{H NMR}$ 200 MHz (CDCl_3): δ = 7.26 (m, 5H, Ph), 6.93 (br s, 1H, NH), 4.98 (s, 1H, -CHPh), 4.78 (dd, 4H, J =11.6 and Hz, J =56.4 Hz, -CH₂Br), 4.12 (m, 4H, -OCH₂-), 2.22-1.99 (m, 4H, -CH₂CF₂-), 1.62-1.56 (m, 8H, -CH₂CH₂-).



Bis(5,5,6,6,7,7,8,8,9,9,10,10,11,11,12,12,12-heptafluorododecyl) 1,4-dihydro-2,6-dimethyl-4-phenylpyridine-3,5-dicarboxylate-2,6-dipyridinium bromide (22)

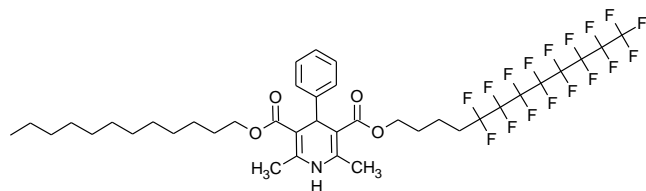
In a 10 mL RB was placed 0.45 g (0.33mmol) compound **21** and dissolved in dry acetone 2 mL then was added dry pyridine 0.05 g (0.66mmol) and left stirring overnight. The precipitate was filtered and washed with diethyl ether to provide 0.30 g of a pale yellow powder in 60% yield. Mp. 172-177°C. $^1\text{H NMR}$ 400 MHz (DMSO-d_6): δ = 10.30 (br s, 1H, NH), 8.98 (d, 4H, J =6 Hz, Py), 8.59 (t, J =8.4 Hz, 2H, Py), 8.11 (m, 4H, Py), 7.28-7.22 (m, 5H, Ph), 5.85 (dd, J =100.8 and 15.2 Hz, 4H, CH₂PyBr), 5.00 (s, 1H, CHPh), 4.04 (m, 4H, OCH₂), 2.35-2.05 (m, 4H, CH₂CF₂), 1.81-1.58 (m, 8H, CH₂CH₂)



Dodecyl 3-aminobut-2-enoate (26)

In a 10 mL RB was weighed 1.30 g (0.0048mol) of dodecyl 3-oxobutanoate then 2 mL EtOH and 3 mL conc. aqueous ammonium hydroxide solution were added. The flask was stoppered and stirred overnight. The flask was then placed in the fridge and the cold precipitate was filtered and washed with DI water. After drying in air the white product weighed 0.90 g or 70% yield.

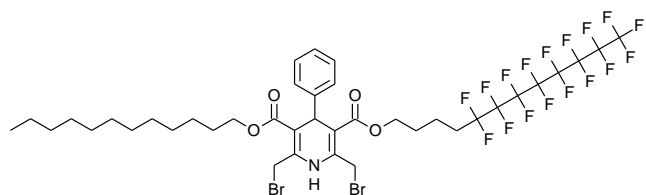
^1H NMR 200 MHz (CDCl_3): δ = 4.53 (s, 1H, $-\text{CH}=\text{C}-$), 4.04 (t, J = 6.6 Hz, 2H, $-\text{OCH}_2-$), 1.90 (s, 3H, $-\text{CH}_3$), 1.64-1.25 (m, 23H, $(\text{CH}_2)_{10}\text{CH}_3$).



Dodecyl 5,5,6,6,7,7,8,8,9,9,10,10,11,11,12,12,12-heptafluorododecyl 1,4-dihydro-2,6-dimethyl-4-phenylpyridine-3,5-dicarboxylate (27)

In a round bottomed flask was weighed 1.88 g (0.003 mol) compound **26** and 0.75 g (0.003 mol) compound **19**. The compounds were dissolved in diethyleneglycol 0.038 g 1-butylpyridinium chloride (11 mol%) was added and the flask was heated in an oil bath at 80°C for 5 hours. The heat was turned off and the flask was left stirring overnight. The contents were poured into ice-water and extracted with EtOAc 3x40 mL. The organic extract was dried with Na_2SO_4 , filtered and the solvent distilled off under reduced pressure leaving an oily residue 2.63g which was recrystallized from EtOH giving 1.10g of a pale yellow compound in 43% yield.

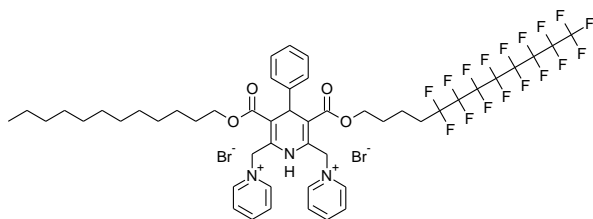
^1H NMR 400 MHz (CDCl_3): δ = 7.20-7.03 (m, 5H, Ph), 5.63 (br s, 1H, NH), 4.91 (s, 1H, 4-CH), 4.07-3.91 (m, 4H, 3,5- CO_2CH_2-), 2.28 (s, 3H, 2- CH_3), 2.26 (s, 3H, 6- CH_3), 2.03-1.89 (m, 2H, CH_2CF_2-), 1.62-1.49 (m, 6H, $\text{OCH}_2\text{CH}_2\text{CH}_2-$), 1.86 (m, 18H, $(\text{CH}_2)_9$), 0.81 (t, J = 6.2 Hz, 3H, CH_3). ^{13}C -NMR 100.3 MHz (CDCl_3): δ = 167.62, 167.45, 147.60, 144.46, 143.64, 127.89, 127.80, 126.20, 121.58-107.20 [$(\text{CF}_2)_7\text{CF}_3$], 104.43, 103.74, 64.03, 62.80, 39.57, 30.45 (t, J = 21.8 Hz, CH_2CF_2), 19.59, 14.05 ppm.



Dodecyl 5,5,6,6,7,7,8,8,9,9,10,10,11,11,12,12,12-heptafluorododecyl 2,6-bis(bromomethyl)-4-phenyl-1,4-dihydropyridine-3,5-dicarboxylate (28)

0.60 g (0.0007 mol) of compound **27** was dissolved in chloroform 6 mL and 4 mL MeOH and cooled in ice-bath. While the mixture was stirring magnetically during 10 min. was added 0.24 g (0.0014 mol) NBS. The mixture was left stirring overnight and then the solvent was removed under reduced pressure. The residue was triturated with carbontetrachloride and filtered to remove the precipitated succinimide. The solvent was removed on the rotary evaporator to provide 0.52 g of a yellow compound in 69% yield which was not further purified.

$\text{C}_{39}\text{H}_{44}\text{Br}_2\text{F}_{17}\text{NO}_4$ MW 1073.55 ^1H NMR 200 MHz (CDCl_3): δ = 7.26 (m, 5H, Ph), 6.93 (br s, 1H, NH), 4.98 (s, 1H, $-\text{CHPh}$), 4.95-4.60 (dd, 4H, J = 11.6 Hz, J = 56.4 Hz, $-\text{CH}_2\text{Br}$), 4.12 (m, 4H, $-\text{OCH}_2-$), 2.22-1.99 (m, 4H, $-\text{CH}_2\text{CF}_2-$), 1.62-1.52 (m, 6H, $\text{OCH}_2\text{CH}_2\text{CH}_2-$), 1.86 (m, 18H, $(\text{CH}_2)_9$), 0.81 (t, J = 6.2 Hz, 3H, CH_3).

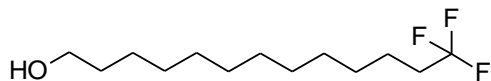


Dodecyl 5,5,6,6,7,7,8,8,9,9,10,10,11,11,12,12,12-heptafluorododecyl 1,4-dihydro-2,6-dimethyl-4-phenylpyridine-3,5-dicarboxylate-2,6-dipyridinium dibromide (29)

In a round bottom flask in 2 mL dry acetone was dissolved 0.50 g (0.047 mmol) of compound **28** and after adding 0.07 g (0.93 mmol) dry pyridine the flask was stoppered and stirred magnetically. After 1h some precipitate started forming. The flask was left stirring overnight. The solid was filtered and washed with diethyl ether to give a pale yellow solid 0.28 g in 49% yield. Mp. 140-147°C. C₄₉H₅₄Br₂F₁₇N₃O₄ MW 1231.75.

¹H NMR 400 MHz (CDCl₃): δ =10.92 (s, 1H, NH), 10.18 (d, 4H, *J*=9.2 Hz, Py), 9.55 (t, *J*=6.4 Hz, 2H, Py), 9.30 (m, 4H, Py), 7.22-7.16 (m, 5H, Ph), 6.12 (dd, *J*=194 and 14 Hz, 4H, CH₂PyBr), 5.03 (s, 1H, CHPh), 4.06-3.98 (m, 4H, OCH₂), 1.98-1.95 (m, 4H, CH₂CF₂), 1.63-1.51 (m, 6H, OCH₂CH₂CH₂-), 1.86 (m, 18H, (CH₂)₉), 0.81 (t, *J*= 6.2 Hz, 3H, CH₃).

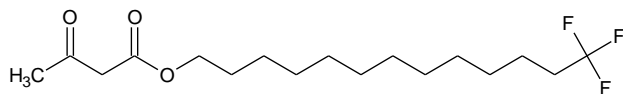
LC/MS: MS(+ESI) *m/z* (rel.intensity): 1151 ([M-Br]⁺, 100).



13,13,13-Trifluoro-1-tridecanol (31)

10-Undecenyl acetate 10.6 g (50 mmol) and trifluoroethyl iodide 12.6 g (60 mmol) were placed in a pressure tube with a magnetic stir bar and 0.32 g (1.0 mmol) of 75% benzoyl peroxide was added. The tube was sealed with a screw cap and placed in an oil bath. While stirring magnetically the temperature was raised to 80°C and the reaction continued for 3h. The tube was cooled in an ice bath and a fresh portion of benzoyl peroxide was added. The cycle was repeated until an H-NMR probe indicated that most of the double bond had reacted (six cycles) giving an orange solution. NaBH₄ 4.75 g (125 mmol) in 255 mL DMF was cooled to 0°C (ice bath) and the crude iodoalkane in 45 mL DMF was slowly added within 45 min. After 3h at 0°C the reaction mixture was allowed to warm to RT and was stirred a further 2h and cooled again to 0°C and 100 mL of H₂O was added to hydrolyze the excess borohydride. The deiodinated trifluorotridecyl acetate was extracted with petroleum ether 3x100 mL dried, filtered and concentrated and then hydrolyzed in aqueous ethanolic NaOH and after acidification with HCl there was obtained a clear oil in 86% yield. C₁₃H₂₅F₃O, MW 254.33

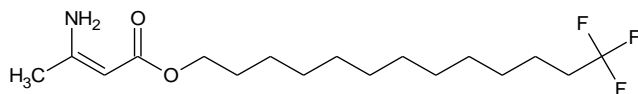
¹H NMR 400 MHz (CDCl₃): δ =3.61 (t, *J*= 6.6 Hz, 2H, OCH₂), 2.12-1.95 (m, 2H, CH₂CF₃), 1.65 (br s, OH), 1.58-1.47 (m, 4H, CH₂CH₂), 1.36-1.22 (m, 16H, (CH₂)₈).



13,13,13-Trifluorotridecyl 3-oxobutanoate (32)

10.00 g (0.039 mol) of alcohol **31** was dissolved in p-xylene with warming then 2,2,6-trimethyl-4H-1,3-dioxin-4-one 5.59 g (0.039 mol) was added and the mixture was refluxed 2h in an oil bath. The reaction mixture was cooled and the xylene removed on a rotary evaporator. The residue was purified on a silica gel chromatography column (EtOAc / hexane 1:3 eluent) providing 11.86g (89%) of an orange oil. C₁₇H₂₉F₃O₃ MW 338.41.

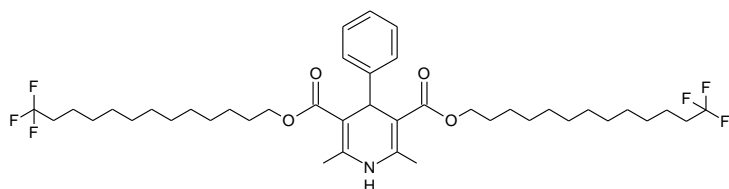
¹H NMR 200 MHz (CDCl₃): δ = 4.12 (t, *J* = 7.4 Hz, 2H, OCH₂), 3.44 (s, 2H, COCH₂CO), 2.26 (s, 3H, -CH₃), 2.11-1.94 (m, 2H, -CH₂CF₃), 1.54-1.44 (m, 4H, OCH₂CH₂ and CH₂CH₂CF₃), 1.31-1.18 (m, 16H (CH₂)₈).



13,13,13-Trifluorotridecyl 3-aminobut-2-enoate (**33**)

In a 10 mL RB was weighed 1.40 g (0.0041 mol) compound **32** and 2 mL EtOH was added and then 3 mL concentrated aqueous ammonium hydroxide was added. The flask was stoppered and vigorously magnetically stirred overnight. The flask was placed in the fridge to cool. The precipitated product was filtered and washed with DI water to provide a white compound 1.06 g in 77 % yield. C₁₇H₃₀F₃NO₂ MW 337.42.

¹H NMR 200 MHz (CDCl₃): δ = 4.52 (s, 1H, CH=), 4.03 (t, *J* = 6.6 Hz, 2H, OCH₂), 2.13-1.94 (m, 2H, -CH₂CF₃), 1.89 (s, 3H, CH₃), 1.64-1.46 (m, 4H, OCH₂CH₂ and CH₂CH₂CF₃), 1.26 (s, 16H, (CH₂)₈).

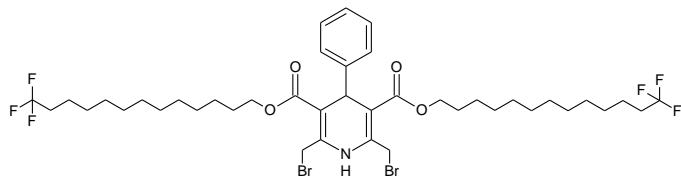


Bis(13,13,13-Trifluorotridecyl)1,4-dihydro-2,6-dimethyl-4-phenylpyridine-3,5-dicarboxylate (**34**)

0.99 g (0.0029 mol) of compound **33** was dissolved in 12 mL n-propanol, then 0.16 g (0.0015 mol) benzaldehyde was added and 1 mL glacial acetic acid. The reaction mixture was refluxed for 4h, the heating was stopped and left stirring overnight. The solvent was removed under reduced pressure and the residue weighed 1.17g. The compound was recrystallized twice from EtOH, filtered and washed with cold EtOH. After air drying there was obtained 0.35 g of a pale yellow compound in 32% yield. Mp. 49-53°C. C₄₁H₆₁F₆NO₄ MW 745.92.

¹H NMR 400 MHz (CDCl₃): δ = 7.21-7.02 (m, 5H, Ph), 5.50 (br s, 1H, NH), 4.93 (s, 1H, CHPh), 4.01-3.90 (m, 4H, OCH₂), 2.27 (s, 6H, CH₃), 2.05-1.93 (m, 4H, CH₂CF₃), 1.53-1.44 (m, 8H, OCH₂CH₂ and CH₂CH₂CF₃), 1.31-1.18 (m, 32H (CH₂)₁₆). ¹³C-NMR 100.3 MHz (CDCl₃): δ = 167.62, 147.65, 143.78, 127.88, 127.83, 126.07, 104.23, 63.92, 39.53, 33.71 (q, *J* = 28.5 Hz, CH₂CF₃), 29.52, 29.51, 29.34, 29.27, 29.18, 28.68, 26.06, 21.87, 21.84, 21.81, 19.64 ppm.

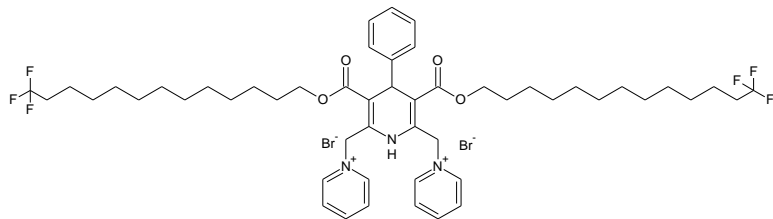
LC/MS: MS(-ESI) m/z (rel.intensity): 744 ([M-H]⁻, 40).



Di-13,13,13-Trifluorotridecyl 2,6-bis(bromomethyl)-4-phenyl-1,4-dihydropyridine-3,5-dicarboxylate (35)

0.45 g (0.60 mmol) of compound **34** was dissolved in 3 mL chloroform and 2 mL MeOH. The solution was cooled in an ice bath and during 10 min. 0.21g (1.20 mmol) of NBS was added in small portions. After all the NBS was added the reaction was stirred for 4h at RT and put in the fridge overnight. The solvent was removed on the rotary evaporator and to the residue was added hexane to precipitate the succinimide. The mixture was filtered and the hexane was distilled off under reduced pressure to give the dibromide 0.54g in 99% yield which was not purified further.

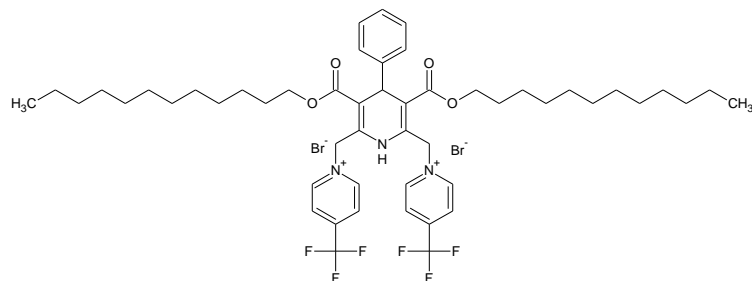
¹H NMR 200 MHz (CDCl₃): δ =9.25 (br s, 1H, NH), 7.23-7.09 (m, 5H, Ph), 5.01 (s, 1H, CHPh), 4.83 (d, *J*= 10.4 Hz, 1H, CH₂Br), 4.54 (d, *J*= 10.4 Hz, 1H, CH₂Br), 4.06 (t, *J*=6.8 Hz, 4H, OCH₂), 2.10-1.96 (m, 4H, CH₂CF₂), 1.59-1.44 (m, 8H, OCH₂CH₂ and CH₂CH₂CF₃), 1.31-1.18 (m, 32H (CH₂)₁₆).



Bis(13,13,13-trifluorotridecyl)1,4-dihydro-2,6-dimethyl-4-phenylpyridine-3,5-dicarboxylate-2,6-dipyridinium bromide (36)

In a 10 mL RB was weighed 0.54g (0.60 mmol) of compound **35** and dissolved in 1.5 mL dry acetone. Pyridine 0.09 g (1.20 mmol) was added and the reaction mixture was left stirring overnight. The reaction mixture was triturated with diethyl ether to precipitate the product. The precipitate was filtered and washed with diethyl ether to give 0.33g of a pale yellow compound in 52% yield.

¹H NMR 400 MHz (CDCl₃): δ =10.95 (s, 1H, NH), 9.33 (d, 4H, *J*=6.2 Hz, 4H, Py), 8.62 (t, *J*=7.8 Hz, 2H, Py), 8.20 (m, 4H, Py), 7.26 (m, 5H, Ph), 6.36 (d, *J*=13.5 Hz, 4H, CH₂PyBr), 5.93 (d, *J*=13.5 Hz, 4H, CH₂PyBr) 5.07 (s, 1H, CHPh), 4.05 (t, *J*=6.8 Hz, 4H, OCH₂), 2.12-1.98 (m, 4H, CH₂CF₂), 1.58-1.24 (m, 40H, (CH₂)₁₀). ¹³C-NMR 100.3 MHz (CDCl₃): δ=166.43, 146.61, 145.51, 144.88, 138.01, 128.86, 128.60, 128.05, 127.50, 126.85 (q, *J*=27.3 Hz, CF₃), 110.41, 65.52, 57.32, 39.76, 33.69 (q, *J*=28 Hz, CH₂CF₃), 29.54, 29.34, 29.25, 29.18, 28.66, 28.39, 25.94, 21.83, 21.80 ppm. ¹⁹F NMR (CDCl₃): δ= -66.42 (t, *J*=11.6 Hz, 3F, CF₃).

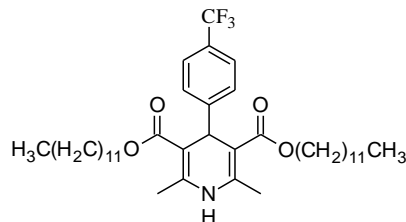


1,1'-[(3,5-Bis(dodecyloxycarbonyl)-4-phenyl-1,4-dihydropyridin-2,6-diyl)bis(methylene)]bis(4-(trifluoromethyl)pyridinium) bromide (38)

Dibromomethyl DHP **37** 0.40g (0.52 mmol) was dissolved in 3 mL dry acetone and 0.16 g (1.1 mmol) of 4-trifluoropyridine was added. The RB was stoppered and stirred overnight. The precipitated product was filtered and washed with diethyl ether to give 0.16 g of a pale yellow compound in 29% yield.

$C_{51}H_{69}Br_2N_3O_4$ MW 1061.91 Mp. 159-161°C

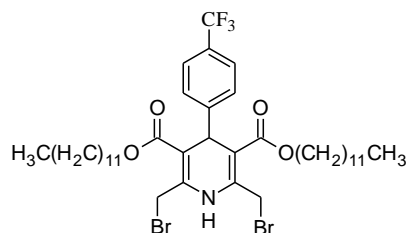
1H NMR 400 MHz ($CDCl_3$): δ = 10.75 (br s, 1H, NH), 9.81 (d, J =6.4 Hz, 4H, Py), 8.27 (d, J =6.4 Hz, 4H, Py), 7.37-7.21 (m, 5H, Ph), 6.49 (d, J =13.8 Hz, 2H, HCPy), 5.19 (d, J =13.8 Hz, 2H, HCPy), 5.16 (s, 1H, CHPh), 4.05-4.01 (m, 4H, OCH_2), 1.59-1.56 (m, 4H OCH_2CH_2), 1.32-1.23 (m, 36H, $(CH_2)_9CH_3$), 0.88 (t, J =6.8 Hz, 6H, CH_3). ^{13}C -NMR 100.3 MHz ($CDCl_3$): δ = 164.61, 145.77, 143.89, 143.52, 143.15, 134.17, 126.54, 125.49, 122.99, 120.15, 117.41, 109.99, 63.70, 56.77, 29.99 27.76, 27.71, 27.64, 27.44, 27.37, 26.43, 24.02, 20.76, 12.18 ppm. ^{19}F NMR ($CDCl_3$): δ = -65.25 ppm. LC/MS: MS(+ESI) m/z (rel. intensity): 899 ($[M-2Br]^+$, 30).



Didodecyl 2,6-dimethyl-4-[4-(trifluoromethyl)phenyl]-1,4-dihydropyridine-3,5-dicarboxylate (39).

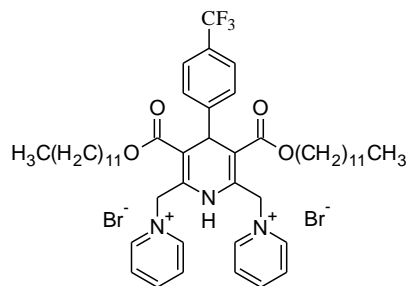
p-Trifluoromethylbenzaldehyde 1.75g (0.01 mol) was weighed in a 100 mL RB then dodecyl 3-aminobut-2-enoate (**26**) 5.39 g (0.02 mol) was added and 3 drops of glacial acetic acid with 25 mL n-propanol. The reaction mixture was refluxed 6 hours and the heat turned off. The reaction mixture was left stirring at RT overnight and poured in ice water. The precipitated product was filtered and recrystallized from EtOH to yield a white powder 2.76 g in 41% yield. $C_{40}H_{62}F_3NO_4$ MW 677.92 Mp. 64-67°C.

1H NMR 400 MHz ($CDCl_3$): δ = 7.44 (d, J =8.4 Hz, 2H, Ar), 7.37 (d, J =8.4 Hz, 2H, Ar), 5.58 (br s, 1H, NH), 5.04 (s, 1H, CHAr), 4.06-3.98 (m, OCH_2), 2.34 (s, 6H, CH_3), 1.58-1.54 (m, 4H OCH_2CH_2), 1.32-1.23 (m, 36H, $(CH_2)_9CH_3$), 0.88 (t, J =6.8 Hz, 6H, CH_3). ^{13}C -NMR 100.3 MHz ($CDCl_3$): δ = 167.28, 151.49, 144.21, 128.20, 124.86, 124.82, 103.71, 64.11, 31.91, 29.64, 29.61, 29.55, 29.35, 29.28, 28.70, 26.08, 22.68, 19.68, 14.10 ppm. LC/MS: MS(-ESI) m/z (rel. intensity): 676 ($[M-H]^-$, 100).



Didodecyl 2,6-bis(bromomethyl)-4-[4-(trifluoromethyl)phenyl]-1,4-dihydropyridine-3,5-dicarboxylate (40).

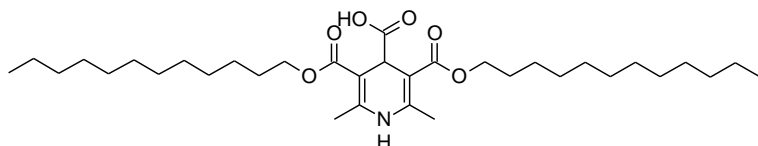
In a 10 mL RB was weighed 0.68 g (0.001 mol) of compound **39** and dissolved in 5 mL MeOH. NBS 0.36 g (0.002 mol) was added and the reaction mixture was sonicated in an ultrasonic bath for 14 min. The MeOH was removed on a rotary evaporator and the residue was triturated with carbon tetrachloride to precipitate succinimide. The solids were filtered and the solvent removed to give the crude dibromide as an orange oil 1.05 g in quantitative yield. $C_{40}H_{60}Br_2F_3NO_4$ MW 835.71. 1H NMR 200 MHz ($CDCl_3$): δ = 7.49 (d, J =9.0 Hz, 2H, Ar), 7.37 (d, J =9.0 Hz, 2H, Ar), 6.57 (br s, 1H, NH), 5.08 (s, 1H, CHAr), 4.86 (d, J =11.4 Hz, 1H, CH_2Br), 4.66 (d, J =11.4 Hz, 1H, CH_2Br), 4.07 (t, J =6.6 Hz, OCH_2), 1.58-1.54 (m, 4H OCH_2CH_2), 1.32-1.23 (m, 36H, $(CH_2)_9CH_3$), 0.87 (t, J =6.8 Hz, 6H, CH_3).



1,1'-[(3,5-Bis(dodecyloxycarbonyl)-4-[4-(trifluoromethyl)phenyl]-1,4-dihydropyridin-2,6-diyl)bis(methylene)] bis(pyridinium) bromide (41).

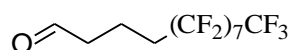
The above crude dibromide **40**, 1.05 g (0.001 mol) was dissolved in diethyl ether and 0.17 g (0.002 mol) pyridine was added. The mixture was stirred overnight and the precipitated product was filtered through a glass fritted funnel, washed with diethyl ether and dried to give 0.61 g of a white powder in 73% yield. Mp 174-186°C. $C_{50}H_{70}Br_2F_3N_3O_4$ MW 993.91.

1H NMR 400 MHz ($CDCl_3$): δ = 11.04 (br s, 1H, NH), 9.38 (d, 4H, J =6.1 Hz, 4H, Py), 8.56 (t, J =8.0 Hz, 2H, Py), 8.19 (m, 4H, Py), 7.55 (d, J =8.0 Hz, 2H, Ar), 7.46 (d, J =8.0 Hz, 2H, Ar), 6.39 (d, J =13.8 Hz, 4H, CH_2PyBr), 5.92 (d, J =13.8 Hz, 4H, CH_2PyBr), 5.17 (s, 1H, CHAr), 4.05 (t, J =6.9 Hz, OCH_2), 1.58-1.54 (m, 4H OCH_2CH_2), 1.32-1.23 (m, 36H, $(CH_2)_9CH_3$), 0.87 (t, J =6.9 Hz, 6H, CH_3). ^{13}C -NMR 100.3 MHz ($CDCl_3$): δ = 166.08, 149.30, 146.31, 145.08, 138.41, 128.84, 128.76, 125.53, 125.50, 125.37, 123.94 (q, J =272 Hz, CF_3), 109.91, 65.65, 57.34, 40.02, 31.89, 29.62, 29.56, 29.34, 29.26, 28.39, 25.98, 22.66, 14.09 ppm. ^{19}F NMR ($CDCl_3$): δ = -62.41. LC/MS: MS(+ESI) m/z (rel. intensity): 834 ($[M-2Br]^+$, 50).



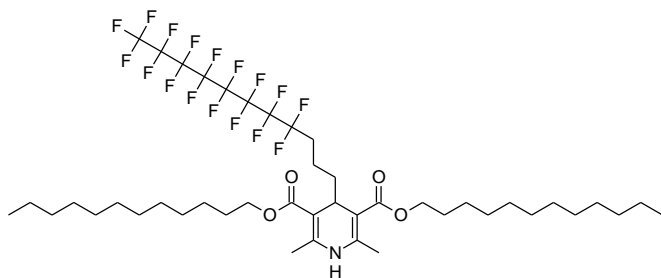
3,5-Bis(dodecyloxycarbonyl)-2,6-dimethyl-1,4-dihydropyridine-4-carboxylic acid (42).

In a 100 mL RB flask was placed glyoxylic acid monohydrate 0.92 g (0.01 mol) and dodecyl 3-aminobut-2-enoate (**26**) 5.4 g (0.02 mol) the components were dissolved in glacial acetic acid, the flask was stoppered and the contents stirred magnetically for 3 days. The reaction mixture was poured into ice water and the precipitated product filtered and washed with ice cold water. The solid was recrystallized from EtOH and dried to give 1.37 g of a pale yellow powder in 24% yield. Mp. 57-64°C C₃₄H₅₉NO₆ MW 577.84 Composition C(70.67) H(10.29) N(2.42) O(16.61) ¹H NMR 200 MHz (CDCl₃): δ =6.74 (br s, 1H, NH), 4.62 (s, 1H, CHCO₂H), 4.16 (t, J=6.6 Hz, 4H, OCH₂), 2.24 (s, 6H, CH₃), 1.65 (m, 4H, OCH₂CH₂), 1.25 (m, 36H, (CH₂)₉), 0.87 (t, J=6.6 Hz, CH₃).



5,5,6,6,7,7,8,8,9,9,10,10,11,11,12,12,12-Heptadecafluorododecanal (44).

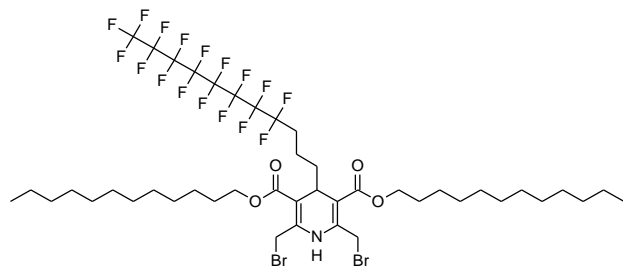
5,5,6,6,7,7,8,8,9,9,10,10,11,11,12,12,12-heptadecafluorododecan-1-ol (**16**) 3.59 g (0.0072 mol) was dissolved in 50 mL DCM and in about 10 min. added drop-wise with stirring to a 45 mL DCM solution containing Dess-Martin periodinane 3.71 g (0.0086 mol). After 2h 100 mL of diethyl ether was added and the solution passed through a silica plug. The solvent was removed using a rotary evaporator to give 3.29g of a yellow oil 93% which solidified in the fridge. C₁₂H₇F₁₇O MW 490.6. ¹H NMR 200 MHz (CDCl₃): δ =9.80 (s, 1H, CHO), 2.60 (t, J=7 Hz, 2H, OCHCH₂), 2.27-1.70 (m, 4H, CH₂CH₂CF₂). GC/MS : 490 [M-H]⁺.



4-(4,4,5,5,6,6,7,7,8,8,9,9,10,10,11,11,11-Heptafluoro-undecyl)-2,6-dimethyl-1,4-dihydropyridine-3,5-dicarboxylic acid didodecyl ester (45).

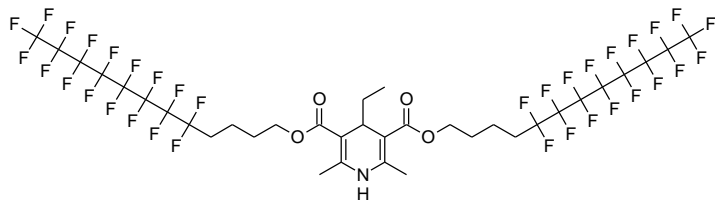
A solution of thionyl chloride 0.71g (6mmol) in 6 mL DCM was cooled to 0°C. Then a solution of pyridine 0.47g (6mmol) in 3 mL DCM was added dropwise followed by the aldehyde 2.45g (5mmol) in 3 mL DCM and the mixture was stirred for 1h –then 3.5g (13mmol) of the enamine was slowly added and reacted overnight. The DCM was evaporated using a rotary evaporator and the residue subjected to a silica gel column using 10% EtOAc in Hexane as eluant to provide a yellow oil 3.17g in 63.8% yield. C₄₄H₆₄F₁₇NO₄ MW 993.96 ¹H NMR 400 MHz (CDCl₃): δ =5.76 (br s, 1H, NH), 4.10 (t, J=6.4 Hz, 4H, OCH₂), 3.63 (t, J=6.4 Hz, 1H, CH), 2.29 (s, 6H, =CCH₃), 2.07-1.94 (m, 2H, CH₂CF₂), 1.67-1.61 (m, 6H, OCH₂CH₂ and CHCH₂), 1.54-1.48 (m, 2H, CH₂CH₂CF₂), 1.37-1.20 (m, 36H, (CH₂)₉), 0.87 (t,

$J=7.2$ Hz, CHCH_3). $^{13}\text{C-NMR}$ 100.3 MHz (CDCl_3): $\delta = 167.82, 145.24, 102.66, 63.97, 36.15, 32.50, 31.89, 30.96$ (t, $J=21.97$ Hz, CH_2CF_2), 29.63, 29.58, 29.34, 29.29, 28.76, 26.15, 22.65, 19.41, 14.03 ppm. LC/MS: MS(-ESI) m/z (rel. intensity): 993 ($[\text{M-H}]^-$, 100).



2,6-Bis-bromomethyl-4-(4,4,5,5,6,6,7,7,8,8,9,9,10,10,11,11,11,11-heptadecafluoroundecyl)-1,4-dihydropyridine-3,5-dicarboxylic acid didodecyl ester (46).

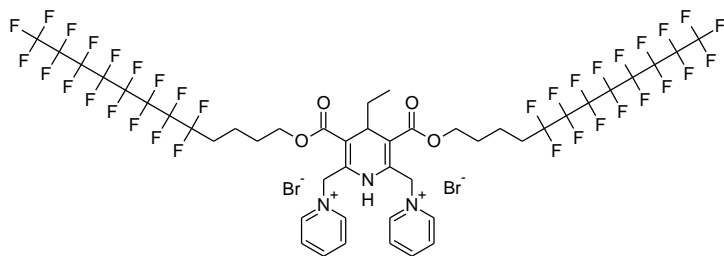
1.03g (1mmol) A dissolved in MeOH and CHCl_3 0.37g (2mmol) NBS added and sonicated for about 20min. The solvent was removed on the rotary evaporator and to the residue was added CCl_4 and filtered to remove the succinamide to give the dibromide as a yellow syrup 1.35g, theoretical 1.15. MW 1151.75 By spectra looks like got the oxidation product!!!



Bis(5,5,6,6,7,7,8,8,9,9,10,10,11,11,12,12,12-heptadecafluorododecyl) 1,4-dihydro-2,6-dimethyl-4-ethylpyridine-3,5-dicarboxylate (47).

In a 50 mL RB was placed 5,5,6,6,7,7,8,8,9,9,10,10,11,11,12,12,12-Heptadecafluorododecyl 3-oxobutanoate (17) 5.00 g (0.0087 mol), propionaldehyde 0.25 g (0.0043 mol) and ammonium acetate 0.50 g (0.0065 mol). The mixture was dissolved in 25 mL abs. EtOH and 5 drops of glacial acetic acid were added. The mixture was refluxed for 4 h and after cooling deposited a yellow precipitate. The precipitate was filtered and recrystallized from EtOH to give a white powder 2.85 g in 56% yield.

$\text{C}_{35}\text{H}_{29}\text{F}_{34}\text{NO}_4$ MW 1173.55. $^1\text{H NMR}$ 200 MHz (CDCl_3): $\delta = 5.53$ (br s, 1H, NH), 4.15-3.95 (m, 4H, 3,5- CO_2CH_2), 3.89 (t, $J=7.7$ Hz, 1H, 4-CH), 2.31 (s, 6H, 2,6- CH_3), 2.17-1.99 (m, 4H, 3,5- CH_2CF_2), 1.75 (m, 2H, 4- CHCH_2), 1.57-1.31 (m, 8H, 3,5- CH_2CH_2), 0.74 (t, $J=7.6$ Hz, 3H, CH_2CH_3).

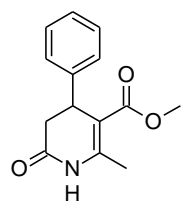


Bis(5,5,6,6,7,7,8,8,9,9,10,10,11,11,12,12,12-heptafluorododecyl) 1,4-dihydro-2,6-dimethyl-4-ethylpyridine-3,5-dicarboxylate-2,6-dipyridinium bromide (49).

In a 50 mL RB was weighed DHP **47** 1.20 g (0.0010 mol) and dissolved in dry chloroform. To this solution was added NBS 0.36 g (0.0020 mol) in portions. After all the NBS was added the reaction mixture was stirred for 1h. The solution was transferred to a separatory funnel and washed with water to remove the succinimide. The layers were separated and the chloroform phase was dried with MgSO_4 filtered and the chloroform removed on the rotary evaporator to give the dibrominated DHP **48** as a yellow compound 1.37 g in quantitative yield. The product was not purified further. In a 25 mL RB was placed 1.37 g (0.0010 mol) of compound **48**, dissolved in dry acetone and 0.15 g (0.0021 mol) of dry pyridine was added. The flask was stoppered and stirred magnetically overnight. The precipitated product was filtered and washed with diethyl ether to give 0.73 g of a pale yellow product in 48% yield.

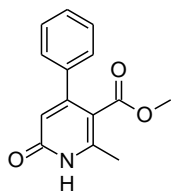
$\text{C}_{45}\text{H}_{37}\text{Br}_2\text{F}_{34}\text{N}_3\text{O}_4$ FW 1489.55

^1H NMR 200 MHz (CDCl_3): δ = 11.01 (br s, 1H, NH), 9.29 (d, 4H, J =5,8 Hz, 4H, Py), 8.57 (t, J =7.2 Hz, 2H, Py), 8.19 (m, 4H, Py), 6.38 (d, J =14 Hz, 4H, CH_2PyBr), 5.76 (d, J =14 Hz, 4H, CH_2PyBr), 4.29-4.02 (m, 4H, 3,5- CO_2CH_2), 3.89 (t, J =7.7 Hz, 1H, 4-CH), 2.17-1.99 (m, 4H, 3,5- CH_2CF_2), 1.75 (m, 2H, 4- CHCH_2), 1.58-1.31 (m, 8H, 3,5- CH_2CH_2), 0.73 (t, J =7.6 Hz, 3H, CH_2CH_3). LC/MS: MS(+ESI) m/z (rel. intensity): 1330 ($[\text{M}-2\text{Br}]^+$, 70).



5-Methoxycarbonyl-6-methyl-4-phenyl-3,4-dihydro-2(1H)-pyridone (50).

A mixture of benzaldehyde (40 mmol), Meldrum's acid (40 mmol), methyl acetoacetate (40 mmol), and ammonium acetate (42 mmol) in acetic acid (40 mL) was refluxed for 10 h. and then poured into ice-water. The solid that precipitated was collected by filtration. Further purification was accomplished by recrystallization from ethanol. 59 % yield, m.p, 197-198°C $\nu_{\text{max}}/\text{cm}^{-1}$ 3209 (NH), 1706 (C=O, ester), 1685 (C=O) and 1619 (C=C); ^1H -NMR(CDCl_3): δ = 8.66 (br s, 1H, NH), 7.50-7.22 (m, 5H, Ph), 4.25 (dd, 1H, H-4, J = 8.4 Hz, J = 1.5 Hz, X part of ABX), 3.64 (s, 3H, OCH_3), 3.01 (dd, 1H, H-3, J = 16.5 Hz, J = 8.4 Hz, A part of ABX), 2.70 (dd, 1H, H-3', J = 16.5 Hz, J = 1.9 Hz, B part of ABX) and 2.39 (s, 3H, CH_3). Anal Calcd. for $\text{C}_{14}\text{H}_{15}\text{NO}_3$ (245.28) C, 68.56; H, 6.16; N, 5.71. Found: C, 68.62; H, 6.21; N 5.92.

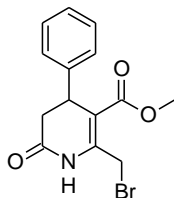


Methyl 2-methyl-6-oxo-4-phenyl-1,6-dihydropyridine-3-carboxylate (95).

This compound was synthesized by oxidation electrolytically of the above compound by passing 2.2 V in acetonitrile for 24 h. The solvent was evaporated and the residue recrystallized from EtOH providing almost quantitative yield of white crystals.

C₁₄H₁₃NO₃ MW 243.26 Composition C(69.12) H(5.39) N(5.76) O(19.73)

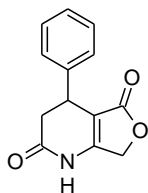
¹H-NMR 400 MHz (CDCl₃): δ= 7.42-7.27 (m, 5H, Ph), 6.44 (s, 1H, =CH), 3.48 (s, 3H, OCH₃), 2.55 (s, 1H, CH₃). ¹³C-NMR 100.3 MHz (CDCl₃): δ=167.43, 164.61, 154.69, 147.54, 139.02, 128.64, 128.47, 126.90, 116.90, 112.70, 51.84, 18.14 ppm.



5-Methoxycarbonyl-6-bromomethyl-4-phenyl-3,4-dihydro-2(1H)-pyridone (74).

1.5g (0.006 mol) of 5-Methoxycarbonyl-6-methyl-4-phenyl-3,4-dihydro-2(1H)-pyridone in 50 ml RB was dissolved in 25 ml chloroform and while being stirred 4.20 ml of 0.232 g/ml solution of Br₂ in chloroform (0.006 mol) was added drop-wise. The flask was stoppered and stirred for 30 min. The solvent was removed on a rotary evaporator and the residual 1.98g orange syrup was dissolved in MeOH and left to crystallize. After several days the deposited crystals were washed with cold MeOH to give a yellowish compound 1.51g in 76% yield. Mp.237-240°C.

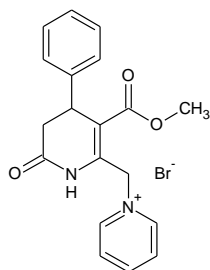
¹H-NMR 400 MHz (CDCl₃): δ= 8.63 (br s, 1H, NH), 7.29-7.17 (m, 5H, Ph), 4.75 (d, J=10.7 Hz, 1H CHBr), 4.61 (d, J=10.7 Hz, 1H CHBr), 4.30 (dd, J= 8.1 and 1.9 Hz, 1H, CHPh), 3.69 (s, 3H, OCH₃), 2.95 (dd, J=16.7 and 8.01 Hz, 1H, CHHCO), 2.73 (dd, J=16.7 and 1.9 Hz, 1H, CHHCO). ¹³C-NMR 100.3 MHz (CDCl₃): δ=170.62, 166.16, 144.68, 140.91, 128.98, 127.32, 126.629, 109.45, 52.04, 37.90, 26.20 ppm.



5-Oxo-4-phenyl-1,2,3,4,5,7-hexahydrofuro[3,4-b]-2(1H)-pyridone (97).

A solution of 5-methoxycarbonyl-6-methyl-4-phenyl-3,4-dihydro-2(1H)-pyridone (1,15g, 5 mmol), N-bromosuccinimide (0.89g, 5 mmol), in 10 ml of dry chloroform was refluxed for 12 hours. The reaction mixture was cooled and the solid that precipitated was collected by

filtration. Further purification was accomplished by recrystallization from ethanol. 55 % yield, m.p.239-240°C; ¹H-NMR (DMSO-d6) δ= 10.74 (s, 1H, NH); 7.35-7.18 (m, 5H, aryl protons), 4.91 (dd, 2H, OCH2), 4.01 (dd, 1H, H-4 *J*= 8.9 Hz, *J*= 3.8 Hz, X part of ABX), 3.12 (dd, 1H, H-3a, *J*= 16.7 Hz, *J*= 8.9 Hz, A part of ABX), 2.57 (dd, H-3b, *J*= 16.6 Hz, *J*= 3.7 Hz, B part of ABX); ¹³C-NMR (DMSO-d6) δ= 170.9 (C2), 169.6 (C5), 160.7 (C7a), 144.8, 128.7(2C), 126.9, 126.5 (2C) (aryl), 101.7(C4a), 65.3(C7), 38.5(C3), 33.3 (C4).
 Anal Calcd. for C₁₃H₁₁NO₃ (229.24) C, 68.05; H, 4.80; N, 6.11. Found: C, 68.22; H, 4.92; N 5.99.

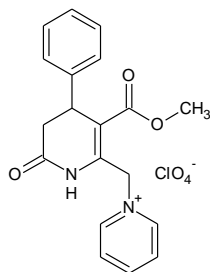


1-((3-Methoxycarbonyl)-6-oxo-4-phenyl-1,4,5,6-tetrahydropyridin-2-yl)methylpyridinium bromide (79).

5-Methoxycarbonyl-6-bromomethyl-4-phenyl-3,4-dihydro-2(1H)-pyridone 0.33g (0.001mol) was dissolved in 5 mL dry acetone in a 10 mL RB and 0.08g (0.001mol) pyridine was added. The flask was stoppered and stirred for 2 days. The solid was filtered on a glass fritted funnel and washed with diethyl ether to give a white fine powder 0.41g in 58.5% yield.

C₁₉H₁₉BrN₂O₃ MW. 403.27, Mp. 189-191°C.

¹H-NMR 400 MHz (CDCl₃): δ= 10.67 (br s, 1H, NH), 9.55 (d, *J*=5.6 Hz, 2H, Py), 8.55 (t, *J*=7.6 Hz, 1H, Py), 8.14 (t, *J*=7.2 Hz, 2H, Py), 7.30-7.23 (m, 5H, Ph), 6.42 (d, *J*=13.6 Hz, 1H, HCPy), 6.19 (d, *J*=13.6 Hz, 1H, HCPy), 4.24 (dd, *J*=2 Hz and *J*=8.4 Hz, 1H, CHPh), 3.67 (s, 3H, OCH₃), 3.02 (dd, *J*=7.6 Hz and 16.4 Hz, 1H, CH₂CO), 2.62 (dd, *J*=1.6 Hz and *J*=16.4 Hz, 1H, CH₂CO). ¹³C-NMR 100.3 MHz (CDCl₃): δ= 168.93, 166.60, 145.77, 145.13, 141.24, 140.51, 128.77, 128.12, 127.13, 126.23, 112.42, 57.21, 52.14, 37.82, 37.61ppm. LC/MS: MS(+ESI) m/z (rel.intensity): 323 ([M-Br]⁺, 100).



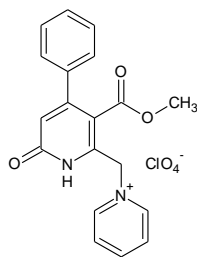
1-((3-Methoxycarbonyl)-6-oxo-4-phenyl-1,4,5,6-tetrahydropyridin-2-yl)methylpyridinium perchlorate (79b).

In a 25 mL RB flask was weighed the above DHPOD pyridinium bromide 0.45g (0.0011 mol) and dissolved in abs. EtOH. While the mixture was stirred conc. HClO₄ was added by drops (15

drops). The white solid was filtered and washed with diethyl ether to give 0.26g of a white powder in 55% yield.

C₁₉H₁₉ClN₂O₇ MW 422.82 Composition C(53.97) H(4.53) Cl(8.38) N(6.63) O(26.49)

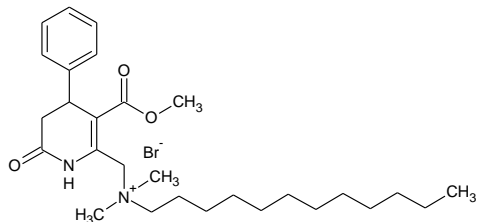
¹H-NMR 200 MHz (CDCl₃): δ= 10.15 (br s, 1H, NH), 9.32 (d, J=6.0 Hz, 2H, Py), 8.39 (t, J=8.0 Hz, 1H, Py), 8.03 (t, J=6.0 Hz, 2H, Py), 7.30-7.14 (m, 5H, Ph), 6.35 (d, J=14.0 Hz, 1H, HCPy), 5.98 (d, J=14.0 Hz, 1H, HCPy), 4.23 (d, J=8 Hz, 1H, CHPh), 3.63 (s, 3H, OCH₃), 3.09 (dd, J=8.0 Hz and 16.0 Hz, 1H, CH₂CO), 2.58 (d, J=16.0 Hz, 1H, CH₂CO).



1-[[3-(Methoxycarbonyl)-6-oxo-4-phenyl-1,6-dihydropyridin-2-yl]methyl]pyridinium perchlorate (96).

C₁₉H₁₇ClN₂O₇ MW 420.80 Composition C(54.23) H(4.07) Cl(8.43) N(6.66) O(26.61)

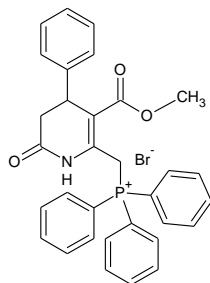
¹H-NMR 400 MHz (CDCl₃): δ= 10.15 (br s, 1H, NH), 9.22 (d, J=6.0 Hz, 2H, Py), 8.44 (t, J=7.0 Hz, 1H, Py), 8.11 (t, J=7.0 Hz, 2H, Py), 7.41-7.37 (m, 5H, Ph), 6.65 (s, 1H, =CH), 5.86 (s, 2H, H₂CPy), 3.49 (s, 3H, OCH₃). ¹³C-NMR 100.3 MHz (CDCl₃): δ=167.67, 163.70, 153.61, 146.11, 145.48, 145.03, 138.07, 128.76, 128.47, 128.21, 126.98, 118.04, 115.84, 61.45, 52.59 ppm. LC/MS: MS(+ESI) m/z (rel.intensity): 321 ([M-ClO₄]⁺, 100).



N-((3-(methoxycarbonyl)-6-oxo-4-phenyl-1,4,5,6-tetrahydropyridin-2-yl)methyl)-N,N-dimethyldodecan-1-aminium bromide (87).

Following the general synthesis there was obtained 79% yield of a white solid. C₂₈H₄₅BrN₂O₃ MW 537.57

¹H-NMR 400 MHz (CDCl₃): δ=10.18 (br s, 1H, NH), 7.29-7.12 (m, 5H, Ph), 5.46 (d, J=12 Hz, 1H, CHN⁺), 5.15 (d, J=12 Hz, 1H, CHN⁺), 4.28 (m, 1H, CHPh), 3.62 (s, 3H, OCH₃), 3.60-3.34 (m, 2H, NCH₂ and 6H, N(CH₃)₂), 2.58-2.54 (m, 2H, NCOCH₂), 1.36-1.27 (m, 20H, (CH₂)₁₀), 0.89 (t, J=8 Hz, 6H, CH₃). ¹³C-NMR 100.3 MHz (CDCl₃): δ=167.08, 164.73, 138.83, 136.99, 127.08, 125.32, 124.73, 114.42, 66.33, 56.49, 50.28, 36.50, 29.97, 27.66, 27.65, 27.52, 27.39, 20.75, 12.19 ppm. LC/MS: MS(+ESI) m/z (rel.intensity): 457 ([M-Br]⁺, 100).

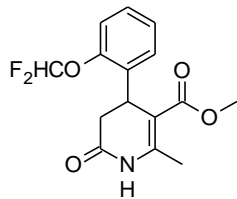


1-((3-Methoxycarbonyl)-6-oxo-4-phenyl-1,4,5,6-tetrahydropyridin-2-yl)methyltriphenylphosphonium bromide (93).

5-Methoxycarbonyl-6-bromomethyl-4-phenyl-3,4-dihydro-2(1H)-pyridone 2.12g (0.0065mol) was dissolved in 25 mL dry acetonitrile and 1.72 g (0.0066mol) of triphenylphosphine was added. The reaction mixture was stirred at 40°C for 2h by which time the whole mixture solidified. The mixture was put in fridge to cool and then filtered and washed with cold EtOH. After drying the white powder weighed 3.16g or 82.3% of theoretical yield.

$C_{32}H_{29}BrNO_3P$ MW. 586.46, Mp. 211-213°C.

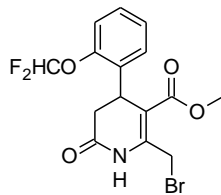
1H -NMR 400 MHz ($CDCl_3$): δ = 10.08 (br s, 1H, NH), 7.88-7.61 (m, 15H, PPh_3), 7.25-7.07 (m, 5H, Ph), 5.98 (t, J =14.4 Hz, 1H, CHP), 5.70 (t, J =14.4 Hz, 1H, CHP) 3.97 (dd, J =4.4 Hz, 1H, CHPh), 3.24 (s, 3H, OCH_3), 2.70 (dd, J =8.4 Hz and 8 Hz, 1H, CH_2CO), 2.49 (d, J =16.4 Hz, 1H, CH_2CO). ^{13}C -NMR 100.3 MHz ($CDCl_3$): δ = 168.02, 166.49, 135.19 (d, J =3.2 Hz, CP), 134.63, 134.52, 130.03, 129.90, 128.95, 127.21, 126.77, 117.83, 116.96, 111.45 (d, J =9.2 Hz, CP), 51.54, 37.80, 37.39, 27.45, 26.98 ppm. TLC silica, 5%EtOH/ $CHCl_3$ R_f =0.6. LC/MS: MS(+ESI) m/z (relat. intensity): 506 ([M-Br], 100).



Methyl 4-[2-(difluoromethoxy)phenyl]-2-methyl-6-oxo-1,4,5,6-tetrahydropyridine-3-carboxylate (52).

$C_{15}H_{15}F_2NO_4$ MW 311.28 Mp. 206-208°C. Composition C(57.88) H(4.86) F(12.21) N(4.50) O(20.56)

1H -NMR 400 MHz ($CDCl_3$): δ =8.03 (br s, 1H, NH), 7.23 (m, 1H, Ar), 7.12 (m, 3H, Ar), 6.57 (t, J =74.1 Hz, 1H, $OCHF_2$), 4.63 (d, J =8.4 Hz, 1H, CHAr), 3.61 (s, 3H, OCH_3), 2.90 (dd, J =8.5 and 16.6 Hz, 1H, CHHCO), 2.64 (ddd, J =16.6, 1.9, and 1.0 Hz, 1H, CHHCO), 2.45 (s, 3H, CH_3). ^{13}C -NMR 100.3 MHz ($CDCl_3$): δ =170.50, 167.02, 149.00, 147.42, 132.51, 128.48, 127.64, 125.61, 118.77, 116.41 (t, J =258.2 Hz, CF_2), 105.67, 51.44, 36.86, 31.94, 19.13 ppm.

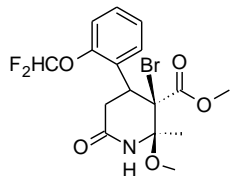


Methyl 2-(bromomethyl)-4-[2-(difluoromethoxy)phenyl]-6-oxo-1,4,5,6-tetrahydropyridine-3-carboxylate (67).

$C_{15}H_{14}BrF_2NO_4$ MW 390.18

Composition C(46.17) H(3.62) Br(20.48) F(9.74) N(3.59) O(16.40)

1H -NMR 400 MHz ($CDCl_3$): δ =7.83 (br s, 1H, NH), 7.25 (m, 1H, Ar), 7.15 (m, 3H, Ar), 6.58 (t, J =73.9 Hz, 1H, OCHF₂), 5.04 (d, J = 11.06 Hz, 1H, CH₂Br), 4.69 (dd, J =8.41 and 1.64 Hz, 1H, CHAr), 4.49 (d, J = 11.06 Hz, 1H, CH₂Br), 3.65 (s, 3H, OCH₃), 2.95 (dd, J =8.3 and 16.5 Hz, 1H, CHHCO), 2.68 (ddd, J =16.8, 1.7, and 0.83 Hz, 1H, CHHCO). ^{13}C -NMR 100.3 MHz ($CDCl_3$): δ =169.44, 165.90, 148.86, 145.26, 131.61, 128.79, 127.33, 125.81, 118.70, 116.30 (t, J =258.6 Hz, CF₂), 108.42, 52.06, 36.64, 31.93, 26.15 ppm.

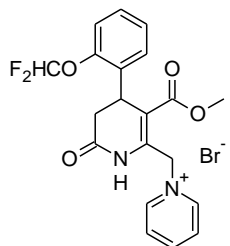


Methyl (2R,3R)-3-bromo-4-[2-(difluoromethoxy)phenyl]-2-methoxy-2-methyl-6-oxopiperidine-3-carboxylate and (2S, 3S) racemate (66).

$C_{16}H_{18}BrF_2NO_5$ MW 422.22

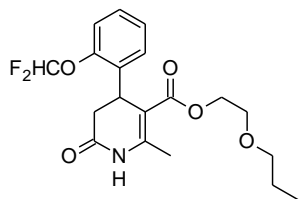
1H -NMR 200 MHz ($CDCl_3$): δ =7.81 (br s, 1H, NH), 7.35-6.90 (m, 4H, Ar), 6.55 (t, J =71.4 Hz, 1H, OCHF₂), 4.97 (dd, J =11 and 8.2 Hz, CHAr), 3.84 (s, 3H, CO₂CH₃), 3.48 (s, 3H, OCH₃), 3.07 (dd, J =18.4, and 11.2 Hz, 1H, CH₂), 2.72 (dd, J =18.4, and 8 Hz, 1H, CH₂), 2.48 (s, 3H, CH₃).

LC/MS: MS(+ESI) m/z (relative intensity): 392 ($[M-OCH_3]^+$ 100).



1-({4-[2-(Difluoromethoxy)phenyl]-3-(methoxycarbonyl)-6-oxo-1,4,5,6-tetrahydropyridin-2-yl}methyl)pyridinium bromide (80).

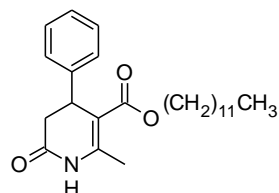
$C_{20}H_{19}BrF_2N_2O_4$ MW 469.28 Mp. 181-183°C Composition C(51.19) H(4.08) Br(17.03) F(8.10) N(5.97) O(13.64)



2-Propoxyethyl 4-[2-(difluoromethoxy)phenyl]-2-methyl-6-oxo-1,4,5,6-tetrahydropyridine-3-carboxylate (53).

$C_{19}H_{23}F_2NO_5$ MW 383.9 Mp. 136-138°C.

1H -NMR 400 MHz ($CDCl_3$): δ =7.89 (br s, 1H, NH), 7.22 (m, 1H, Ar), 7.09 (m, 3H, Ar), 6.58 (t, J =72.8 Hz, 1H, OCHF₂), 4.64 (d, J =8.4 Hz, 1H, CHAr), 4.14 (t, J =4.8 Hz, 2H, CO₂CH₂), 3.47 (m, 2H, CH₂O), 3.24 (t, J =6.8 Hz, 2H, OCH₂), 2.91 (dd, J =8.4 and 16.8 Hz, 1H, CHHCO), 2.63 (dd, J =16.8, and 2.0 Hz, 1H, CHHCO), 2.45 (s, 3H, CH₃), 1.47 (m, 2H, CH₂CH₃), 0.83 (t, J =7.6 Hz, 3H, CH₂CH₃). ^{13}C -NMR 100.3 MHz ($CDCl_3$): δ =170.45, 166.60, 149.22, 147.62, 132.84, 128.58, 127.81, 125.83, 119.24, 116.76 (t, J =271.0 Hz, CF₂), 105.82, 72.94, 68.54, 63.67, 37.01, 32.17, 22.86, 19.35, 10.56 ppm.

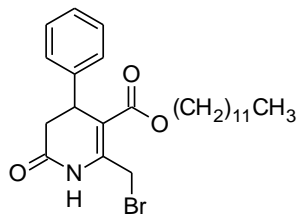


Dodecyl 2-methyl-6-oxo-4-phenyl-1,4,5,6-tetrahydropyridine-3-carboxylate (55).

In a 100 mL RB flask was placed Meldrum's acid 2.88g (0.02 mol), benzaldehyde 2.12g (0.02 mol), dodecyl acetoacetate 5.41g (0.02 mol), and ammonium acetate 2.1g (0.025 mol) in 25 mL glacial acetic acid. The contents was stirred magnetically and refluxed for 8 hours. The solution was cooled and left stirring overnight then poured in ice-water which gave an orange syrup. The reaction mixture was extracted with EtOAc 3X60 mL, washed with brine, dried with MgSO₄, filtered and the solvent removed with a rotary evaporator which left an orange syrup (9.77g). The syrup was transferred to an Erlenmeyer flask with EtOH and put in the freezer to crystallize. The precipitated solid was filtered and washed with cold EtOH and after drying in air gave a light yellow flakes 1.84g, 23% yield, m.p. 79-80°C.

$C_{25}H_{37}NO_3$ MW 399.57 Composition C (75.15) H(9.33) N(3.51). Found: C(75.01) H(9.49) N(3.41).

1H -NMR 400 MHz ($CDCl_3$): δ = 7.99 (br s, 1H, NH), 7.27-7.14 (m, 5H, Ph), 4.23 (d, J =7.2 Hz, 1H, HCPh), 4.07-3.99 (m, 2H CO₂CH₂), 2.92 (dd, J =8.0 Hz and 16.4 Hz, 1H, CH₂CO), 2.68 (d, J =16.2 Hz, 1H, CH₂CO), 2.40 (s, 3H, CH₃), 1.52-1.47 (m, 2H, CO₂CH₂CH₂), 1.24-1.15 (m, 18H, (CH₂)₉), 0.87 (t, J =6.4 Hz, 3H, CH₂CH₃). ^{13}C -NMR 100.3 MHz ($CDCl_3$): δ =170.72, 166.88, 145.95, 142.09, 128.70, 126.91, 126.62, 107.29, 64.35, 38.13, 37.99, 31.90, 29.61, 29.54, 29.46, 29.33, 29.17, 28.57, 25.91, 22.67, 19.10, 14.10 ppm.

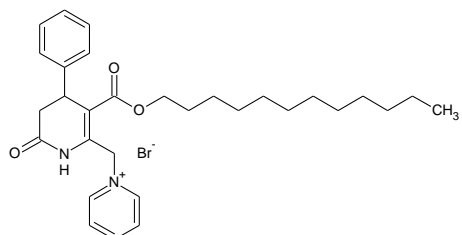


Dodecyl 2-(bromomethyl)-6-oxo-4-phenyl-1,4,5,6-tetrahydropyridine-3-carboxylate (75).

In a 10 mL RB was placed 1g(0.0025mol) of the above dodecyl dihydropyridone and dissolved in 5 mL dry chloroform. The flask was cooled in ice and while stirring 0.4g (0.0025mol) Br₂ in 1 mL dry chloroform was added drop-wise and the mixture was left stirring for 1h. The chloroform was removed using a rotary evaporator and the residue was dissolved in MeOH and left in the freezer to crystallize. The precipitate was filtered and washed with cold MeOH and dried in air to give a white product 1.04g in 87% yield. Mp. 48-54°C. MW. 478.46

Anal Calcd. for C₂₅H₃₆BrNO₃ (478.46), Composition C(62.76), H(7.58), N(2.93). Found: C(63.15), H(7.50), N(2.85). LC/MS: MS(+ESI) m/z (relative intensity): 478 ([M+H]⁺ 50).

¹H-NMR 200 MHz (CDCl₃): δ= 8.10 (br s, 1H, NH), 7.28-7.14 (m, 5H, Ph), 4.83 (d, J=10.2 Hz, 1H, CHBr), 4.59 (d, J=10.2 Hz, 1H, CHBr), 4.27 (d, J=8.2 Hz, 1H, CHPh), 4.06 (t, J=6.4 Hz, 2H CO₂CH₂), 2.96 (dd, J=8.0 Hz and 17.0 Hz, 1H, CH₂CO), 2.70 (d, J=16.6 Hz, 1H, CH₂CO), 1.55-1.49 (m, 2H, CO₂CH₂CH₂), 1.24-1.15 (m, 18H, (CH₂)₉), 0.87 (t, J=6.4 Hz, 3H, CH₃).

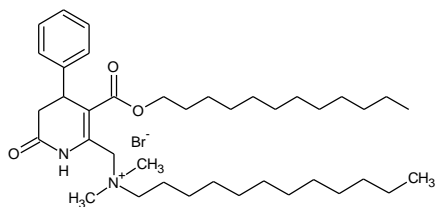


1-[3-(Dodecyloxycarbonyl)-6-oxo-4-phenyl-1,4,5,6-tetrahydro-pyridin-2-ylmethyl]-pyridinium bromide (81).

Dodecyl 2-(bromomethyl)-6-oxo-4-phenyl-1,4,5,6-tetrahydropyridine-3-carboxylate 0.48g (0.001mol) was dissolved in dry acetone 10 mL and pyridine 0.09g (0.0011mol) was added. The RB flask was stoppered and the mixture was stirred over the weekend, by which time a white solid had precipitated. After filtration and washing the solid with ethyl ether there was obtained 0.46g of a white powder in 82% yield.

C₃₀H₄₁BrN₂O₃ MW. 557.56, Mp. 147-149°C. Composition C(64.62) H(7.41) Br(14.33) N(5.02) O(8.61), Found N(4.92) C(64.55) H(7.54).

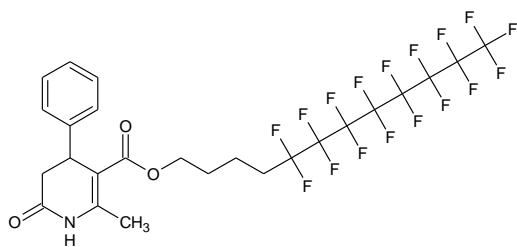
¹H-NMR 400 MHz (CDCl₃): δ= 10.60 (br s, 1H, NH), 9.56 (d, J=6 Hz, 2H, Py), 8.49 (t, J=8.0 Hz, 1H, Py), 8.14 (dd, J=6.0 Hz and J=8.0 Hz, 2H, Py), 7.30-7.13 (m, 5H, Ph), 6.40 (d, J=13.9 Hz, 1H, HCPy), 6.30 (d, J=13.9 Hz, 1H, HCPy), 4.18 (d, J=5.8 Hz, 1H, CHPh), 4.00 (t, J=6.4 Hz, 2H CO₂CH₂), 3.13 (dd, J=8.2 Hz and 16.6 Hz, 1H, CH₂CO), 2.59 (d, J=16.6 Hz, 1H, CH₂CO), 1.52-1.40 (m, 2H, CO₂CH₂CH₂), 1.24-1.15 (m, 18H, (CH₂)₉), 0.87 (t, J=6.4 Hz, 3H, CH₃). ¹³C-NMR 100.3 MHz (CDCl₃): δ= 169.22, 166.66, 145.83, 145.36, 141.38, 141.25, 128.98, 128.46, 127.30, 126.64, 113.08, 65.44, 57.25, 38.46, 38.05, 31.90, 29.61, 29.54, 29.44, 29.34, 29.13, 28.31, 25.76, 22.67, 14.10 ppm. LC/MS: MS(+ESI) m/z (relat. intensity): 477 ([M-Br]⁺, 100).



***N*-((3-(dodecyloxycarbonyl)-6-oxo-4-phenyl-1,4,5,6-tetrahydropyridin-2-yl)methyl)-*N,N*-dimethyldodecan-1-aminium bromide (88).**

A general synthesis for obtaining these salts follows: in a 25 mL RB flask was placed 0.25g (0.00052 mol) of 5-methoxycarbonyl-6-bromomethyl-4-phenyl-3,4-dihydro-2(1H)-pyridone and dissolved in dry acetone (10 mL). While stirring 0.12 g (0.00052 mol) of *N,N*-dimethyldodecyl-1-amine was added and the flask was stoppered. The mixture was stirred overnight and the precipitated solid was filtered and washed with diethyl ether to give 0.28g of a white solid in 78% yield. C₃₉H₆₇BrN₂O₃ MW 691.86 Mp 152.8-154.0°C

¹H-NMR 200 MHz (CDCl₃): δ= 10.26 (br s, 1H, NH), 7.27-7.09 (m, 5H, Ph), 5.47 (d, *J*=12 Hz 1H, CHN⁺), 5.20 (d, *J*=12 Hz, 1H, CHN⁺), 4.20 (d, *J*=5.8 Hz, 1H, CHPh), 4.15 (t, *J*=6 Hz, 2H, OCH₂), 3.58-3.46 (m, 2H, NCH₂), 3.41 (s, 6H, N(CH₃)₂), (2.82-2.55 (m, 2H, NCOCH₂CH₂), 1.52-1.40 (m, 2H, CO₂CH₂CH₂) 1.34-1.25 (m, 20H, (CH₂)₁₀), 1.24-1.15 (m, 18H, (CH₂)₉), 0.87 (t, *J*=6 Hz, 6H, CH₃). LC/MS: MS(+ESI) *m/z* (rel. intensity): 612 ([M-Br]⁺, 100).

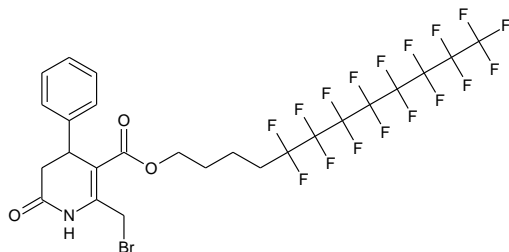


C₂₅H₂₀F₁₅NO₃ MW.705.4

5,5,6,6,7,7,8,8,9,9,10,10,11,11,12,12,12-heptafluorododecyl 2-methyl-6-oxo-4-phenyl-1,4,5,6-tetrahydropyridine-3-carboxylate (56).

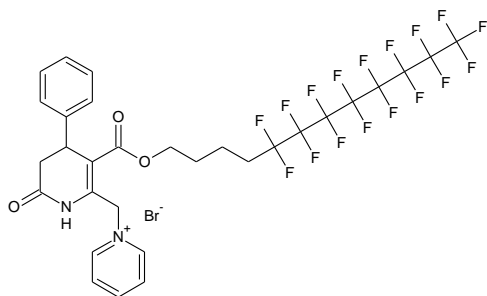
An RB flask fitted with a water cooled condenser and a CaCl₂ guard tube was charged with Meldrum's acid 1.03 g (7.2 mmol), benzaldehyde 0.76 g (7.2 mmol), the above perfluoroalkyl acetoacetate 4.13 g (7.2 mmol), ammonium acetate 0.83 g (10 mmol), and 12 mL glacial acetic acid. The reaction mixture was stirred magnetically and heated to reflux in an oil bath for 6.5 h, after which the heating was stopped and left stirring overnight. The reaction mixture was poured into ice water and extracted with 3x50 mL EtOAc, and washed with brine, dried with Na₂SO₄ filtered and concentrated on the rotary evaporator to a light brown mass and after addition of 10 mL EtOH was left in the fridge to crystallize. The crystals were filtered on a glass frit and washed with cold EtOH to yield a light yellow compound 1.59 g 31% yield with R_f 0.36 on a silica TLC in 9:7:1 chloroform:petroleum ether:acetone under UV light mp 114-120°C. ¹H NMR, 400 MHz (CDCl₃): δ =7.53 (br s 1H, NH), 7.26 (t, ³*J*_{HH}=7,8 Hz, 2H, m-Ph), 7.19 (t, ³*J*_{HH}=7.8Hz, 1H, p-Ph), 7.15 (d, ³*J*_{HH}=7,8 Hz, 2H, o-Ph), 4.23 (dm, ³*J*_{HH}=8.1 Hz, 1H, C₄H), 4.11 and 4.03 (dt, ²*J*_{HH}=11.5, ³*J*_{HH}=6.0 Hz, 2H, AB-sys, OCH₂) 2.71 (dd, ²*J*_{HH}=16.5, ³*J*_{HH}=8, C₅H_A), 2.94 (ddd, ²*J*_{HH}=16.5, ³*J*_{HH}=2, ⁴*J*_{HH}=0.9, C₅H_B), 2.43 (s, 3H, CH₃), 1.96 (m, 2H, CH₂CF₂), 1.59

(m, 2H, OCH₂CH₂), 1.47 (m, 2H, CH₂CH₂CF₂). ¹³C NMR, 100.6 MHz (CDCl₃): δ=170.04 (C₆), 166.65 (COO), 146.40 (C₂), 141.95 (i-Ph), 128.79 (m-Ph), 127.05 (p-Ph), 126.50 (o-Ph), 120-108 (6m, 8CF's), 106.84 (C₃), 63.21 (OCH₂), 38.23(C₄), 38.16(C₅), 30.50 (t, ²J_{CF}=23Hz, CH₂CF₂), 28.10(OCH₂CH₂), 19.23 (CH₃), 16.93 (CH₂CH₂CF₂). ¹⁹F NMR (CDCl₃): δ= -80.76 (t, ³J_{FF} = 10.4 Hz, 3F, CF₃), -114.4 (m, 2F CH₂CF₂), -121.72 (m, 2F CH₂CF₂CF₂), -121.91 (m, 4F CF₂C₂F₅ and CH₂C₂F₄CF₂), -122.69 (m, 2F CF₃CF₂), -123.51 (m, 2F C₃F₇CF₂), -126.1 (m, 2F C₄F₉CF₂). LC-MS: MS(+ESI) m/z (relative intensity): 728 ([M+Na]⁺ 100) actual C₂₅H₂₀F₁₅NO₃ MW 705.40.



5,5,6,6,7,7,8,8,9,9,10,10,11,11,12,12,12-heptafluorododecyl 2-(bromomethyl)-6-oxo-4-phenyl-1,4,5,6-tetrahydropyridine-3-carboxylate (76).

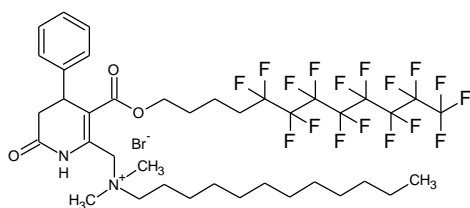
The above dihydropyridone 0.71 g (1mmol) was dissolved in 5 mL chloroform. While stirring magnetically 0.7 mL of a 0.232 g/mL Br₂ solution in chloroform (1mmol) was added drop-wise and the flask was stoppered and stirred 30 min. Then the flask contents were transferred to a 100 mL round bottom flask with an additional chloroform wash and the solvent was removed on a rotary evaporator (foaming) and dissolved in about 1 mL MeOH and left to crystallize in the dark. The precipitated solid was filtered after 3 days as a light yellow solid powder 0.57 g, 72% yield and mp 100-104°C. ¹H NMR 400 MHz (CDCl₃): δ =7.95 (bs, 1H, NH), 7.28 (t, ³J_{HH}=7.8 Hz, 2H, m-Ph), 7.21 (t, ³J_{HH}=7.8Hz 1H, p-Ph), 7.15 (d, ³J_{HH}=7.8 Hz, 2H, o-Ph), 4.88 (d, ²J_{HH}=11.2 Hz, 1H, CH_ABr), 4.57 (dd, ²J_{HH}=11.2, ⁴J_{HH}=0.7 Hz, 1H, CH_BBr), 4.26 (dd, ³J_{HH}=8, ³J_{HH}=1.8 Hz, C₄H), 4.15 and 4.07 (two dt, ²J_{HH}=11.3, ³J_{HH}=6.1 Hz, 2H, OCH₂) 2.95 (dd, ²J_{HH}=16.5, ³J_{HH}=8.3 Hz, C₅H_A), 2.72 (ddd, ²J_{HH}=16.5, ³J_{HH}=2.1, ⁴J_{HH}=0.9 Hz, C₅H_B), 1.96 (m, 2H, CH₂CF₂), 1.60 (m, 2H, OCH₂CH₂), 1.47 (m, 2H, CH₂CH₂CF₂). ¹³C NMR 100 MHz (CDCl₃): δ=169.60 (C₆), 165.57 (COO), 144.46 (C₂), 141.01 (i-Ph), 129.02 (m-Ph), 127.38 (o-Ph), 126.44 (o-Ph), 120-108 (6br m, 8CF's), 109.41 (C₃), 63.95 (OCH₂), 38.33 (C₄), 38.04 (C₅), 30.34 (t, ²J_{CF}=22.5 Hz, CH₂CF₂), 27.93 (OCH₂CH₂), 26.16 (CH₂Br), 16.90 (CH₂CH₂CF₂). ¹⁹F NMR 376.2 MHz (CDCl₃): δ= -80.78 (t, ³J_{FF} = 10.4 Hz, 3F, CF₃), -114.34 (m, 2F, CH₂CF₂), -121.73 (m, 2F, CH₂CF₂CF₂), -121.91 (m, 4F, CF₂C₂F₅ and CH₂C₂F₄CF₂), -122.71 (m, 2F, CF₃CF₂), -123.51 (m, 2F, C₃F₇CF₂), -126.1 (m, 2F, C₄F₉CF₂). LC-MS: MS(+ESI) m/z (relative intensity): 806 ([M+Na]⁺ 100) actual C₂₅H₁₉BrF₁₅NO₃ MW 784.30.



1-[3-(5,5,6,6,7,7,8,8,9,9,10,10,11,11,12,12,12-Heptafluoro-dodecyloxy)carbonyl]-6-oxo-4-phenyl-1,4,5,6-tetrahydropyridin-2-ylmethyl]pyridinium bromide (82).

0.30g (0.38 mmol) of the above compound (**3**) was dissolved in 0.5mL dry acetone and while stirring magnetically 2-3 drops (> 2 equiv.) dry pyridine were added and the flask was stoppered. The reaction mixture was left stirring overnight, filtered and the solid was washed with diethyl ether to provide 0.26g of a white powder in 79% yield, mp 145-151°C.

¹H NMR 400 MHz (CDCl₃): δ = 10.56 (bs, 1H, NH), 9.51 (d, ³J_{HH}=5.6 Hz, 2H, o-Py), 8.42 (t, ³J_{HH}=7.6 Hz, 1H, p-Py), 8.12 (dd, ³J_{HH}=7.6, ³J_{HH}=5.6 Hz, 2H, m-Py), 7.25 (t, ³J_{HH}=7.6 Hz, 1H, m-Ph), 7.21 (t, ³J_{HH}=7.6 Hz, 1H, p-Ph), 7.14 (d, ³J_{HH}=7.6 Hz, 2H, o-Ph), 6.39 and 6.25 (two d, ²J_{HH}=13.5 Hz, 2H, AB-syst, CH₂Py), 4.18 (dd, ³J_{HH}=6.4 Hz, ⁴J_{HH}=1.5, 1H, C₄H), 4.06 and 4.02 (two dt, ²J_{HH}=11.3, ³J_{HH}=5.4 Hz, 2H, AB-syst, OCH₂), 3.16 (dd, ²J_{HH}=16.1, ³J_{HH}=7.7 Hz, 1H, CH_ACOO), 2.57 (d, ²J_{HH}=16.1 Hz, 1H, CH_BCOO), 1.94 (m, 2H, CH₂CF₂), 1.54 (m, 2H, CH₂CH₂O), 1.37 (m, 2H, CH₂CH₂CF₂). ¹³C NMR, 100 MHz (CDCl₃): δ=169.29 (C₆), 166.47 (COO), 145.97 (p-Py), 145.40 (o-Py), 141.74 (C₂), 141.14 (i-Ph), 129.05 (m-Ph), 128.56 (m-Py), 127.39 (p-Ph), 126.53 (o-Ph), 120-108 (6bm, 8CF's), 112.78 (C₃), 64.33 (OCH₂), 57.42 (C₂CH₂), 38.59 (C₄), 38.29 (C₅), 30.28 (t, ²J_{CF}=22.3Hz, CH₂CF₂), 27.87 (OCH₂CH₂), 16.83 (CH₂CH₂CF₂). ¹⁹F NMR, 376.2 MHz (CDCl₃): δ= -80.78 (t, ³J_{FF} = 9.3 Hz, 3F, CF₃), -114.32 (m, 2F, CH₂CF₂), 121.73 (m, 2F, CH₂CF₂CF₂), -121.91 (m, 4F, CF₂C₂F₅ and CH₂C₂F₄CF₂), -122.71 (m, 2F, CF₃CF₂), -123.51 (m, 2F, C₃F₇CF₂), -126.11 (m, 2F, C₄F₉CF₂). LC-MS: MS(+ESI) m/z (relative intensity): 784 ([M-Br]⁺ 100) actual C₃₀H₂₄BrF₁₇N₂O₃ MW 863.40.

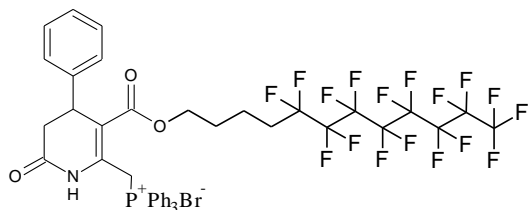


N-((3-((5,5,6,6,7,7,8,8,9,9,10,10,11,11,12,12,12-heptafluorododecyloxy)carbonyl)-6-oxo-4-phenyl-1,4,5,6-tetrahydropyridin-2-yl)methyl)-N,N-dimethyldodecan-1-aminium bromide (89).

Using the general synthesis there was obtained a white solid in 63% yield. C₃₉H₅₀BrF₁₇N₂O₃ MW 997.70 Mp. 173.1-174.1°C.

¹H NMR 400 MHz (CDCl₃): δ = 10.26 (br s, 1H, NH), 7.27-7.09 (m, 5H, Ph), 5.47 (d, J=12 Hz 1H, CHN⁺), 5.20 (d, J=12 Hz, 1H, CHN⁺), 4.20 (d, J=5.8 Hz, 1H, CHPh), 4.15 (t, J=6 Hz, 2H, OCH₂), 3.58-3.46 (m, 2H, NCH₂), 3.41 (s, 6H, N(CH₃)₂), 2.82-2.55 (m, 2H, NCOCH₂CH₂),

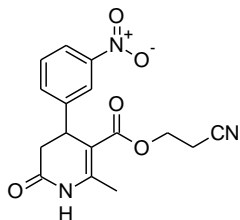
2.25-1.80 (m, 2H, CH₂CF₂), 1.78-1.69 (m, 4H, CH₂, CH₂), 1.34-1.25 (m, 20H, (CH₂)₁₀), 0.87 (t, *J*=6 Hz, 3H, CH₃) LC-MS: MS(+ESI) *m/z* (relative intensity): 918 ([M-Br]⁺ 100).



1-[3-(5,5,6,6,7,7,8,8,9,9,10,10,11,11,12,12,12-Heptafluoro-dodecyloxycarbonyl)-6-oxo-4-phenyl-1,4,5,6-tetrahydro-pyridin-2-ylmethyl]-triphenyl-phosphonium bromide (94).

0.50g (0.64mmol) of compound (3) and 0.17g (0.64mmol) triphenylphosphine were dissolved in 5mL of dry acetonitrile. The yellow solution was stirred magnetically at 40°C for 2h and then cooled in the fridge. The precipitated product filtered and washed with diethyl ether to give 0.55g (82%) of a yellowish powder mp 162-167°C.

¹H NMR 400 MHz (CDCl₃): δ = 10.06 (bs, 1H, NH), 7.85 (dd, ³*J*_{HH}=7.6, ³*J*_{HP}=13.5 Hz, 6H, o-Ph), 7.76 (td, ³*J*_{HH}=7.6, ⁵*J*_{HP}=1.7 Hz, 3H, p-Ph), 7.63 (td, ³*J*_{HH}=7.6, ⁴*J*_{HP}=3.7 Hz, 6H, m-Ph), 7.20 (t, ³*J*_{HH}=7.6 Hz, 2H, m-Ph), 7.16 (t, ³*J*_{HH}=7.6 Hz, 1H, p-Ph), 7.04 (d, ³*J*_{HH}=7.6 Hz, 2H, o-Ph), 5.86 and 5.66 (two dt, ²*J*_{HH}=14.9, ²*J*_{HP}=14.7 Hz, 2H, AB-syst., C₂CH₂), 3.90 (m, 1H, C₄H), 3.75 and 3.52 (two dt, ²*J*_{HH}=11, ³*J*_{HH}=6.2 Hz, 2H, OCH₂), 2.70 (dd, ²*J*_{HH}=16, ³*J*_{HH}=8.7 Hz, 1H, C₅H_A), 2.42 (dd, ²*J*_{HH}=16, ²*J*_{HF}=1.9 Hz, 1H, C₅H_B), 1.87 (m, 2H, CH₂CF₂), 1.35 (m, 2H, OCH₂CH₂), 1.27 (m, 2H, CH₂CH₂CF₂). ¹³C NMR 100 MHz (CDCl₃): δ=167.92 (C₆), 165.96 (d, ³*J*_{CP}=3 Hz, COO), 141.21 (d, ⁵*J*_{CP}=3.9 Hz, i-Ph), 140.96 (d, ²*J*_{CP}=11.3 Hz, C₂), 135.24 (d, ⁴*J*_{CP}=3.3 Hz, 3C, p-Ph), 134.62 (d, ²*J*_{CP}=10.4 Hz, 6C, o-Ph), 130.01 (d, ³*J*_{CP}=13.2 Hz, 6C, m-Ph), 128.9 (m-Ph), 127.26 (p-Ph), 126.62 (o-Ph), 117.43 (d, ¹*J*_{CP}=86.6 Hz, 3C, i-Ph), 111.41 (d, ³*J*_{CP}=9.3 Hz, C₃), 120-108 (6bm, 8CF's), 63.57 (OCH₂), 38.33 (d, ⁴*J*_{CP}=2.4 Hz, C₄), 38.04 (C₅), 30.21 (t, ²*J*_{CF}=23.2 Hz, CH₂CF₂), 27.73 (OCH₂CH₂), 27.32 (d, ¹*J*_{CP}=48.9 Hz, CH₂Br), 16.78 (CH₂CH₂CF₂). ¹⁹F NMR 376.2 MHz (CDCl₃): δ= -80.79 (t, ³*J*_{FF} = 9.74 Hz, 3F, CF₃), -114.32 (m, 2F, CH₂CF₂), -121.72 (m, 2F, CH₂CF₂CF₂), -121.92 (m, 4F, CF₂C₂F₅ and CH₂C₂F₄CF₂), -122.71 (m, 2F, CF₃CF₂), -123.52 (m, 2F, C₃F₇CF₂), -126.11 (m, 2F, C₄F₉CF₂). ³¹P NMR 161.86 MHz (CDCl₃) δ= 24.77 ppm. LC-MS: MS(+ESI) *m/z* (relative intensity): 966 ([M-Br]⁺ 100) actual C₄₃H₃₄BrF₁₇NO₃P MW. 1046.59.

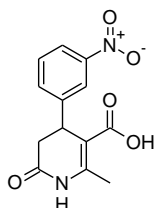


2-cyanoethyl 2-methyl-4-(3-nitrophenyl)-6-oxo-1,4,5,6-tetrahydropyridine-3-carboxylate (54).

m-Nitrobenzaldehyde 9.74 g (0.06 mol) was dissolved in 80 mL glacial acetic acid and to this solution was added 10.0 g (0.06 mol) 2-cyanoethyl-3-oxobutanoate, 9.29 g (0.06 mol) Meldrum's acid, and 6.13 g (0.06 mol) ammonium acetate. The reaction mixture was refluxed

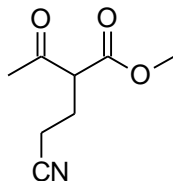
for 12h and the solvent was removed under reduced pressure. The brown syrupy residue was crystallized from ethanol to give 6.61 g of a yellowish powder in 33% yield. Mp. 165-168°C.

^1H NMR 400 MHz (DMSO- d_6): δ =10.12 (br s, 1H, NH), 8.08 (m, 1H, Ar), 8.00 (t, J =2.0 Hz, Ar), 7.62 (m, 2H, Ar), 4.29 (d, 1H, CHAr), 3.04 (m, 2H, OCH₂), 2.67 (m, 2H, CH₂CO), 2.37 (s, 3H, CH₃), 2.33 (m, 2H, CH₂CN). ^{13}C -NMR 100.3 MHz (DMSO- d_6): δ = 206.0, 169.1, 165.5, 150.0, 147.9, 144.8, 133.2, 130.0, 121.7, 121.0, 118.2, 102.9, 58.6, 30.2, 18.3, 17.2 ppm. LC/MS: MS(+ESI) m/z (relative intensity): 330 ([M+H]⁺ 97) actual C₁₆H₁₅N₃O₅ MW 329.31.



2-methyl-4-(3-nitrophenyl)-6-oxo-1,4,5,6-tetrahydropyridine-3-carboxylic acid

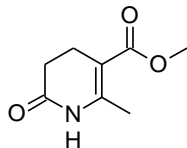
The above 2-cyanoethyl 2-methyl-4-(3-nitrophenyl)-6-oxo-1,4,5,6-tetrahydropyridine-3-carboxylate 5.0g (15 mmol) was dissolved in 50 mL EtOH and 1.11 g (20 mmol) KOH which was dissolved in 10 mL H₂O was added. The reaction mixture was stirred at room temperature for 6h. The EtOH was removed under reduced pressure and the residue was dissolved in water. The solution was cooled and made acidic with dilute HCl. The precipitate was filtered and washed with minimal amount of cold EtOH to give 4.0g of a yellow powder in 98% yield. Mp. 197-200°C. ^1H NMR 400 MHz (DMSO- d_6): δ =12.11 (br s, 1H, CO₂H), 9.93 (br s, 1H, NH), 8.08 (m, 1H, Ar), 7.99 (m, 1H, Ar), 7.62 (m, 2H, Ar), 4.26 (d, J =7.1 Hz, 1H, CHAr), 2.99 (m, 2H, CH₂CO), 2.08 (s, 3H, CH₃). ^{13}C -NMR 100.3 MHz (DMSO- d_6): δ = 169.1, 167.8, 148.2, 147.7, 145.0, 133.4, 130.0, 121.5, 121.0, 104.3, 37.6, 37.0, 17.8 ppm. LC/MS: MS(+ESI) m/z (relative intensity): 277 ([M+H]⁺ 98) actual C₁₃H₁₂N₂O₅ MW 276.24.



Methyl 2-(2-cyanoethyl)-3-oxobutanoate (57).

In a 500 mL RB was added 250mL dry MeOH, methyl 3-oxobutanoate 58g (0.57mol) and 2g MeONa. While stirring magnetically and cooling in an ice-bath acrylonitrile 26.5g (0.57mol) was added dropwise. After all the acrylonitrile was added the stirring was continued overnight at room temperature. The reaction mixture was cooled to precipitate out the bis-ethylcyano addition product and after filtration the MeOH was removed on the rotary evaporator. The residue was washed with water containing acetic acid and then vacuum (0.1mm Hg) distilled and the fraction boiling at 120-125°C (oil bath 170°C) collected to provide a clear liquid 26.8g in 28% yield. MW. 169.18

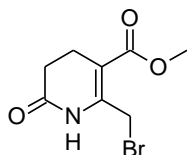
^1H NMR 200 MHz (CDCl₃): δ =3.78 (s, 3H, OCH₃), 3.67 (t, J =7 Hz, 1H, COCHCO), 2.45 (t, J =7 Hz, 2H, CH₂CN), 2.30 (s, 3H, CH₃), 2.23-2.10 (m, 2H, CHCH₂CH₂).



Methyl 6-methyl-3,4-dihydro-2(1H)-pyridone-5-carboxylate (59).

In a 100 mL Erlenmeyer flask was added 5 mL conc. H_2SO_4 and a magnetic stirrer. While stirring methyl 2-(2-cyanoethyl)-3-oxobutanoate 5g(0.03mol) was added dropwise. When the solution became warm and started bubbling, it was cooled in ice-water. After all of the oxobutanoate was added the stirring was continued for 0.5h at room temperature and poured into ice-water whereby a white compound precipitated. After filtering and drying there was obtained a white powder 3.1g in 62% yield. MW. 169.18, mp. 149-152°C. Comp. C(56.80) H(6.55) N(8.28) Found: C(56.83) H(6.54) N(8.22).

^1H NMR 400 MHz (CDCl_3): δ = 7.88 (br s, 1H, NH), 3.72 (s, 3H, OCH_3), 2.65 (t, J = 8 Hz, 2H, CH_2C), 2.48 (t, J = 8 Hz, 2H, CH_2CO), 2.30 (s, 3H, CH_3). ^{13}C NMR 100 MHz (CDCl_3): δ = 172.02, 167.55, 145.62, 104.01, 51.31, 30.13, 21.36, 18.82. LC/MS: MS(+ESI) m/z (relative intensity): 170 ($[\text{M}+\text{H}]^+$ 100).

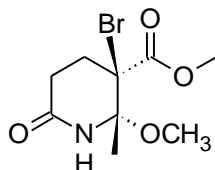


Methyl 6-bromomethyl-3,4-dihydro-2(1H)-pyridone-5-carboxylate (72).

In a 50 mL RB was weighed 2.20g (0.0130 mol) of methyl 6-methyl-3,4-dihydro-2(1H)-pyridone-5-carboxylate and dissolved in dry CHCl_3 . To the stirred solution was added a Br_2 CHCl_3 solution drop by drop via a dropping funnel. When all the Br_2 (0.014 mol) was added the reaction mixture was left stirring overnight. The solvent was removed and the residue crystallized from MeOH to give a white solid 2.10g and an additional 0.41g was deposited after concentrating the mother liquors for a total of 78% yield.

$\text{C}_8\text{H}_{10}\text{BrNO}_3$ MW. 248.07, Mp. 140°C (changes appearance) ~200° dec. Comp. C(38.73) H(4.06) N(5.65) Found: C(38.74) H(3.89) N(5.53).

^1H NMR 400 MHz (CDCl_3): δ = 7.66 (br s, 1H, NH), 4.62 (s, 2H, CH_2Br), 3.78 (s, 3H, OCH_3), 2.72 (t, J = 7.8 Hz, 2H, CH_2C), 2.52 (t, J = 7.8 Hz, 2H, CH_2CO). ^{13}C NMR 100.3 MHz (CDCl_3): δ = 170.90, 166.35, 143.25, 106.96, 51.96, 29.71, 26.20, 21.79 ppm. LC/MS: MS(+ESI) m/z (relative intensity): 248 ($[\text{M}+\text{H}]^+$ 100).

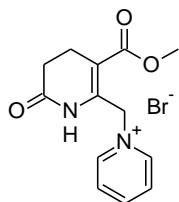


Methyl (2S,3R)-3-bromo-2-methoxy-2-methyl-6-oxopiperidine-3-carboxylate and the (2R,3S) racemate (71).

Methyl 6-methyl-3,4-dihydro-2(1H)-pyridone-5-carboxylate 0.5 g (0.003 mol) was dissolved in dry MeOH and NBS 0.55g (0.003 mol) was added to the stirred suspension. After addition of NBS all the solids went into solution and the reaction mixture was stirred for 1h. The solvent was removed on the rotary evaporator and the residue recrystallized from EtOH to give a white crystalline solid 0.77g in 92% yield. C₉H₁₄BrNO₄ MW 280.12 Mp. 99-101°C.

Composition C(38.59) H(5.04) N(5.00) Found: C(38.60) H(4.93) N(4.94)

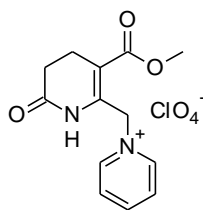
¹H NMR 400 MHz (CDCl₃): δ=8.06 (br s, 1H, NH), 3.79 (s, 3H, CO₂CH₃), 3.25 (s, 3H, OCH₃), 2.89 (ddd, *J*=14.9, 11.9, and 6.7 Hz, 1H, CH₂), 2.66 (ddd, *J*=14.9, 11.9, and 6.7 Hz, 1H, CH₂), 2.47 (ddd, *J*=15.1, 7.7, and 1.1 Hz, 1H CH₂), 2.28 (ddd, *J*=15.1, 7.7, and 1.1 Hz, 1H CH₂). ¹³C NMR 100.3 MHz (CDCl₃): δ=172.44, 168.71, 88.32, 62.58, 53.22, 50.37, 28.68, 28.43, 21.50 ppm. LC/MS: MS(+ESI) m/z (relative intensity): 289 ([M-OCH₃+K]⁺ 100).



1-[[3-(Methoxycarbonyl)-6-oxo-1,4,5,6-tetrahydropyridin-2-yl]methyl]pyridinium bromide (83).

In a 10 mL RB was weighed methyl 6-bromomethyl-3,4-dihydro-2(1H)-pyridone-5-carboxylate 0.25g (0.0010 mol) and dissolved in dry acetone. Pyridine 0.10g (0.001 mol) was added and the flask was stoppered and stirred overnight. The precipitated salt was filtered and washed with diethyl ether to give 0.28g of a white solid in 85% yield. C₁₃H₁₅BrN₂O₃ MW 327.17 Mp. 179-181°C. Composition C(47.72) H(4.62) N(8.56) Found: C(47.72) H(4.54) N(8.51).

¹H NMR 400 MHz (CDCl₃): δ = 10.52 (br s, 1H, NH), 9.65 (d, *J*=5.6 Hz, 2H, Py), 8.51 (t, *J*=7.6 Hz, 1H, Py), 8.14 (dd, *J*=6.0 Hz and *J*=7.4 Hz, 2H, Py), 6.28 (s, 2H, CH₂Py), 3.78 (s, 2H, OCH₃), 2.75 (t, *J*=8.0 Hz, 2H, CH₂C), 2.51 (t, *J*= 8.0 Hz, 2H, CH₂CO). ¹³C NMR 100.3 MHz (CDCl₃): δ= 170.16, 167.35, 145.67, 145.45, 141.35, 128.39, 109.96, 56.84, 52.32, 29.73, 21.59 ppm.

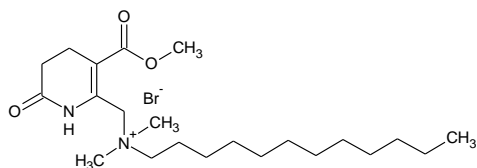


1-[[3-(Methoxycarbonyl)-6-oxo-1,4,5,6-tetrahydropyridin-2-yl]methyl]pyridinium perchlorate (83b).

In a 10 mL RB was placed 0.10g (0.31mmol) of the above DHPOD pyridinium bromide and dissolved in abs. EtOH. With stirring conc. HClO₄ was added drop by drop until no more precipitate formed (13 drops). The solid was filtered and washed with diethyl ether to give .09g as white powder in 83% yield.

C₁₃H₁₅ClN₂O₇ MW 346.72 Composition C(45.03) H(4.36) Cl(10.23) N(8.08) O(32.30)

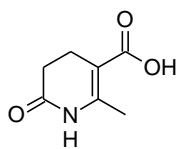
^1H NMR 200 MHz (DMSO- d_6): δ = 10.16 (br s, 1H, NH), 9.03 (d, $J=6.0$ Hz, 2H, Py), 8.65 (t, $J=7.4$ Hz, 1H, Py), 8.17 (dd, $J=7.0$ Hz and $J=7.4$ Hz, 2H, Py), 5.67 (s, 2H, CH_2Py), 3.69 (s, 2H, OCH_3), 2.68 (t, $J=7.8$ Hz, 2H, CH_2C), 2.50 (t, $J=7.8$ Hz, 2H, CH_2CO).



N-((3-(methyloxycarbonyl)-6-oxo-1,4,5,6-tetrahydropyridin-2-yl)methyl-N,N-dimethyldodecan-1-aminium bromide (90).

Following the general synthesis there was obtained a white solid in 79% yield. $\text{C}_{22}\text{H}_{41}\text{BrN}_2\text{O}_3$
MW 461.48

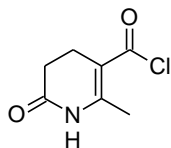
^1H NMR 400 MHz (CDCl_3): δ = 10.08 (br s, 1H, NH), 5.15 (s, 2H, CH_2N^+), 3.75 (s, 3H, OCH_3), 3.57-3.53 (m, 2H, NCH_2), 3.45 (s, 6H, $\text{N}(\text{CH}_3)_2$), 2.76 (br s, 2H, NCOCH_2), 2.67 (br s, 2H, $\text{NCOCH}_2\text{CH}_2$), 1.89 (br s, 2H, NCH_2CH_2), 1.38-1.27 (m, 20H, $(\text{CH}_2)_{10}$), 0.89 (t, $J=8$ Hz, 6H, CH_3). ^{13}C NMR 100.3 MHz (CDCl_3): δ = 168.21, 164.81, 136.34, 111.96, 66.15, 56.94, 50.23, 29.97, 27.66, 27.64, 27.52, 27.48, 27.39, 27.22, 24.46, 21.03, 20.74, 12.18 ppm. LC/MS: MS(+ESI) m/z (relative intensity): 382 ($[\text{M}-\text{Br}]^+$ 100).



6-Methyl-3,4-dihydro-2(1H)-pyridone-5-carboxylate (60).

The above dihydropyridone methyl ester 2.85g(0.017mol) was placed in a 100mL RB and a 50% solution of MeOH/ H_2O containing 1.2g(0.03mol) NaOH. The mixture was heated at 60°C for 3h and after cooling in ice acidified with conc. HCl. The white precipitate was filtered and washed with cold water and dried to give 2.08g, 80% yield of a white powder. MW. 155.15.

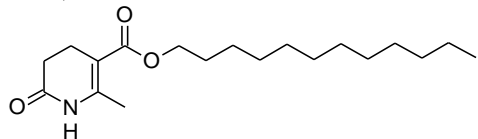
^1H NMR 400 MHz (DMSO- d_6): δ = 11.90 (br s, 1H, CO_2H), 9.60 (br s, 1H, NH), 2.49 (t, $J=6.0$ Hz, 2H, $\text{CH}_2\text{C}=\text{O}$), 2.30 (t, $J=6.0$ Hz, CH_2CO), 2.16 (s, 3H, CH_3). ^{13}C NMR 100.3 MHz (DMSO- d_6): δ = 170.84, 168.34, 146.28, 102.64, 29.96, 21.34, 17.77 ppm.



6-Methyl-3,4-dihydro-2(1H)-pyridone-3-carbonyl chloride (61).

In a 50mL RB was added 25mL anhydrous DCM and 2 drops of DMF and the above dihydropyridone carboxylic acid 1.7g (0.011mol) and while stirring oxalyl chloride 1.95g (0.015 mol) was added drop-wise and the solution stirred for 1h at RT. The DCM was evaporated on a rotary evaporator and 25ml toluene was added and again the solvent was evaporated on the rotary evaporator giving an orange residue in quantitative yield of the crude acid chloride, which was not further purified. MW. 173.6.

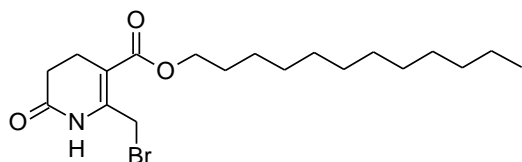
^1H NMR 200 MHz (CDCl_3): δ = 8.00 (br s, 1H, NH), 2.86-2.54 (m, 4H, CH_2CH_2), 2.29 (s, 3H, CH_3).



Dodecyl 6-methyl-3,4-dihydro-2(1H)-pyridone-3-carboxylate (62).

In a 50 mL RB flask was added dihydropyridone carboxylic acid 0.80g(0.0052mol) and thionyl chloride 6 mL and the mixture refluxed for 1h the resulting black solution was evaporated on the rotary evaporator which gave a dark residue 1.24g of the acid chloride. To the residue was added 25 mL toluene, dodecanol 0.96g(0.0052mol), and pyridine 0.41g(0.0052mol) after stirring for 2h the solution was transferred to a separatory funnel and washed with 50 mL saturated Na_2CO_3 aqueous solution and brine, dried with MgSO_4 and the toluene removed on the rotary evaporator giving a light brown compound 1.7g and recrystallized from ethanol. MW. 323.47, calcd. anal. for $\text{C}_{19}\text{H}_{33}\text{NO}_3$ = C(70.55), H(10.28), N(4.33), O(14.8)

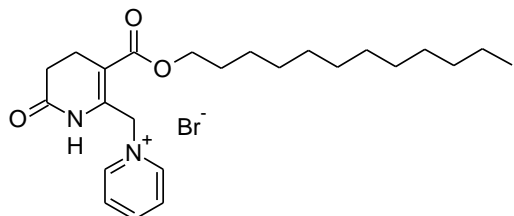
^1H NMR 200 MHz (CDCl_3): δ = 7.56 (br s, 1H, NH), 4.12 (t, J = 6.6 Hz, 2H, OCH_2), 2.65 (t, J =7 Hz, 2H, CH_2C), 2.47 (t, J = 7 Hz, 2H, CH_2CO), 2.29 (s, 3H, CH_3), 1.65 (m, 2H, OCH_2CH_2), 1.25 (m, 18H, $(\text{CH}_2)_9$), 0.87 (t, J = 6 Hz, 3H, CH_2CH_3). ^{13}C NMR 100.3 MHz (CDCl_3): δ =170.67, 166.00, 142.68, 107.44, 65.16, 31.90, 29.74, 29.62, 29.55, 29.50, 29.33, 29.23, 28.57, 26.31, 26.04, 22.67, 21.87, 14.10 ppm.



Dodecyl 6-bromomethyl-3,4-dihydro-2(1H)-pyridone-3-carboxylate (77).

MW 402.37, Calcd. anal. for $\text{C}_{19}\text{H}_{32}\text{BrNO}_3$ C(56.72), H(8.02), Br(19.86), N(3.48), O(11.93)

^1H NMR 400 MHz (CDCl_3): δ = 7.35 (br s, 1H, NH), 4.62 (s, 2H, CH_2Br), 4.16 (t, J = 6.6 Hz, 2H, OCH_2), 2.72 (t, J =7 Hz, 2H, CH_2C), 2.52 (t, J = 7 Hz, 2H, CH_2CO), 1.71-1.57 (m, 2H, OCH_2CH_2), 1.25 (m, 18H, $(\text{CH}_2)_9$), 0.87 (t, J = 6 Hz, 3H, CH_2CH_3).



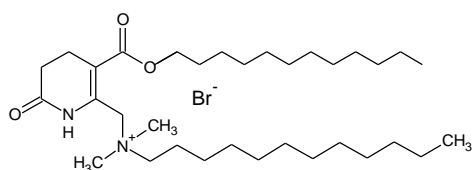
1-[3-(Dodecyloxycarbonyl)-6-oxo-1,4,5,6-tetrahydro-pyridin-2-ylmethyl]-pyridinium bromide (85).

In a 10 mL RB was placed dodecyl 6-bromomethyl-3,4-dihydro-2(1H)-pyridone-3-carboxylate 0.2g (0.0005mol) and dissolved in 5 mL dry acetone then pyridine 0.04g (0.0005mol) was added

and the flask stoppered. The mixture was stirred magnetically overnight and the precipitated solid was filtered and washed with diethyl ether to give white flakes 0.22g in 92% yield. Mp. the compound softened 127-131°C and melted completely at 156°C.

C₂₄H₃₇BrN₂O₃ MW 481.47 Composition C(59.87) H(7.75) Br(16.60) N(5.82) O(9.97) found C(59.88) H(7.79) N(5.76).

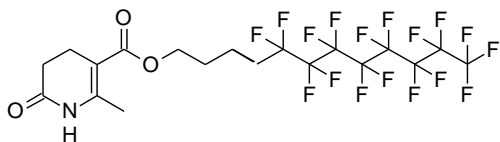
¹H NMR 400 MHz (CDCl₃): δ = 9.62 (d, *J*=6.0 Hz, 2H, o-Py), 8.53(t, *J*=8.0 Hz, 1H, p-Py), 8.16 (m, 2H, m-Py), 6.26 (s, 2H, CH₂Py), 4.14 (t, *J*=6.4 Hz, 2H, OCH₂), 2.74 (t, *J*=8.0 Hz, 2H, CH₂C=), 2.52 (t, *J*= 8.0 Hz, 2H, CH₂CO), 1.69-1.62 (m, 2H, OCH₂CH₂), 1.25 (m, 18H, (CH₂)₉), 0.87 (t, *J*= 6.8 Hz, 3H, CH₂CH₃). ¹³C NMR 100.3 MHz (CDCl₃): δ=170.31, 166.94, 145.81, 145.36, 140.97, 128.47, 110.42, 65.54, 56.85, 31.88, 29.77, 29.60, 29.55, 29.49, 29.32, 29.21, 28.48, 25.99, 22.66, 21.63, 14.10 ppm. LC/MS: MS(+ESI) m/z (relative intensity): 402 ([M-Br]⁺ 100).



***N*-((3-(dodecyloxycarbonyl)-6-oxo-1,4,5,6-tetrahydropyridin-2-yl)methyl)-*N,N*-dimethyldodecan-1-aminium bromide (91).**

Following the general procedure there was obtained a white solid in 87% yield. C₃₃H₆₁BrN₂O₃ MW 615.77 Mp. 157.3-158.2°C.

¹H NMR 200 MHz (CDCl₃): δ = 10.26 (br s, 1H, NH), 5.18 (br s, 2H, CH₂N⁺), 4.15 (t, *J*=6 Hz, 2H, OCH₂), 3.58-3.46 (m, 2H, ⁺NCH₂), 3.41 (s, 6H, ⁺N(CH₃)₂), 2.82-2.55 (m, 2H, NCOCH₂CH₂), 1.52-1.40 (m, 2H, CO₂CH₂CH₂) 1.34-1.25 (m, 20H, (CH₂)₁₀), 1.24-1.15 (m, 18H, (CH₂)₉), 0.87 (t, *J*=6 Hz, 6H, CH₃). LC/MS: MS(+ESI) m/z (relative intensity): 536 ([M-Br]⁺ 100).

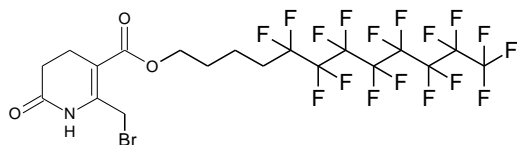


5,5,6,6,7,7,8,8,9,9,10,10,11,11,12,12,12-Heptafluorododecyl 6-methyl-3,4-dihydro-2(1H)-pyridone-3-carboxylate (63).

In a 50 mL RB was placed dihydropyridone-3-carbonyl chloride 0.71g (0.0041 mol), dry toluene 25 mL, 5,5,6,6,7,7,8,8,9,9,10,10,11,11,12,12,12-heptafluorododecanol 2.00g (0.0041 mol) and pyridine 0.32g (0.0041mol) and the reaction mixture was stirred for 2h. Added chloroform to the mixture for complete dissolution and transferred to a separatory funnel and washed with an aqueous solution of saturated Na₂CO₃ and brine. The organic layer was separated and dried with Na₂SO₄ filtered and the solvent was removed on a rotary evaporator to give a yellow compound 1.30g in 50% yield. After recrystallization from ethanol was a light yellow powder.

MW. 629.31 Anal calcd. for C₁₉H₁₆F₁₇NO₃ C(36.26), H(2.56), F(51.32),N(2.23), O(7.63)

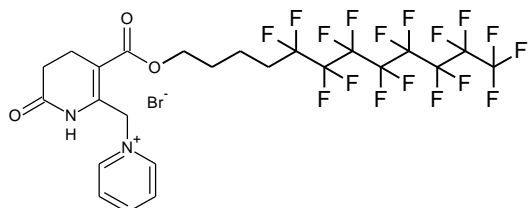
^1H NMR 400 MHz (CDCl_3): δ = 7.01 (br s, 1H, NH), 4.17 (t, J = 6.2 Hz, 2H, OCH_2), 2.65 (t, J =8.0 Hz, 2H, $\text{CH}_2\text{C}=\text{O}$), 2.49 (t, J =8.0 Hz, 2H, CH_2CO), 2.28 (s, 3H, CH_3), 2.18-2.03 (m, 2H, CH_2CF_2), 1.79-1.69 (m, 4H, CH_2CH_2). ^{13}C NMR 100.3 MHz (CDCl_3): δ =171.18, 166.93, 145.51, 103.98, 63.40, 30.53 (t, J =20.3 Hz, CH_2CF_2), 30.10, 28.18, 21.38, 19.74, 19.06, 17.19 ppm.



5,5,6,6,7,7,8,8,9,9,10,10,11,11,12,12,12-Heptadecafluorododecyl 6-bromomethyl-3,4-dihydro-2(1H)-pyridone-3-carboxylate (78).

$\text{C}_{19}\text{H}_{15}\text{BrF}_{17}\text{NO}_3$ MW 708.20 Composition C(32.22) H(2.13) Br(11.28) F(45.60) N(1.98) O(6.78)

^1H NMR 400 MHz (CDCl_3): δ = 7.35 (br s, 1H, NH), 4.41 (s, 2H, CH_2Br), 4.21 (t, J = 6.0 Hz, 2H, OCH_2), 2.72 (t, J =8.0 Hz, 2H, $\text{CH}_2\text{C}=\text{O}$), 2.53 (t, J =8.0 Hz, 2H, CH_2CO), 2.18-2.06 (m, 2H, CH_2CF_2), 1.82-1.70 (m, 4H, CH_2CH_2). ^{13}C NMR 100.3 MHz (CDCl_3): δ =170.48, 165.81, 143.30, 64.10, 30.50, 29.68, 28.07, 26.16, 21.80, 17.16, 17.13 ppm.

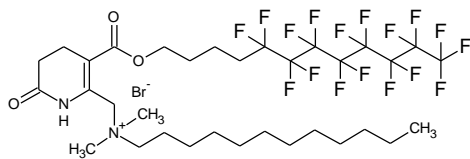


1-[3-(5,5,6,6,7,7,8,8,9,9,10,10,11,11,12,12,12-Heptafluoro-dodecyloxycarbonyl)-6-oxo-1,4,5,6-tetrahydro-pyridin-2-ylmethyl]-pyridinium bromide (86).

In a 10 mL RB was weighed 5,5,6,6,7,7,8,8,9,9,10,10,11,11,12,12,12-heptafluorododecyl 6-bromomethyl-3,4-dihydro-2(1H)-pyridone-3-carboxylate 0.1g (0.00014mol) and dissolved in 5 mL dry acetone. While the solution was being stirred magnetically pyridine 0.02g (0.00014mol) was added, the flask was stoppered and left stirring overnight. The precipitated solid was filtered and washed with diethyl ether to give 0.08g of a grey powder in 72% yield. The compound softened at 168-171°C and melted at 187°C.

$\text{C}_{24}\text{H}_{20}\text{BrF}_{17}\text{N}_2\text{O}_3$ MW 787.30

^1H NMR 400 MHz (CDCl_3): δ = 9.68 (d, J =5.6 Hz, 2H, o-Py), 8.48 (t, J =8 Hz, 1H, p-Py), 8.13 (m, 2H, m-Py), 6.30 (s, 2H, CH_2PyBr), 4.20 (t, J = 6.0 Hz, 2H, OCH_2), 2.74 (t, J =8.2 Hz, 2H, $\text{CH}_2\text{C}=\text{O}$), 2.52 (t, J =8.2 Hz, 2H, CH_2CO), 2.19-2.06 (m, 2H, CH_2CF_2), 1.82-1.69 (m, 4H, CH_2CH_2). 170.03, 145.52, 128.36, 109.73, 64.48, 29.74, 28.00, 21.60, 17.11 ppm. LC/MS: MS(+ESI) m/z (relative intensity): 708 ($[\text{M}-\text{Br}]^+$ 100).

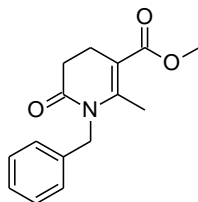


***N*-((3-((5,5,6,6,7,7,8,8,9,9,10,10,11,11,12,12,12-heptafluorododecyloxy)carbonyl)-6-oxo-1,4,5,6-tetrahydropyridin-2-yl)methyl-*N,N*-dimethyldodecan-1-aminium bromide (92).**

Following the general procedure there was obtained a white solid in 76% yield.

$C_{33}H_{46}BrF_{17}N_2O_3$ MW 921.61 Mp.158-159.6°C.

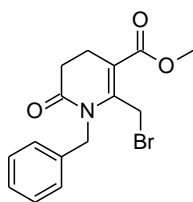
1H NMR 200 MHz ($CDCl_3$): δ =10.17 (br s, 1H, NH), 5.18 (br s, 2H, CH_2N^+), 4.15 (t, $J=6$ Hz, 2H, OCH_2), 3.58-3.46 (m, 2H, NCH_2), 3.41 (s, 6H, $N(CH_3)_2$), 2.82-2.55 (m, 4H, $NCOCH_2CH_2$), 2.25-1.80 (m, 2H, CH_2CF_2), 1.78-1.69 (m, 4H, CH_2 , CH_2), 1.34-1.25 (m, 20H, $(CH_2)_{10}$), 0.87 (t, $J=6$ Hz, 3H, CH_3). LC/MS: MS(+ESI) m/z (relative intensity): 842 ($[M-Br]^+$ 100).



Methyl 1-benzyl-2-methyl-6-oxo-1,4,5,6-tetrahydropyridine-3-carboxylate (65).

Methyl 6-methyl-3,4-dihydro-2(1H)-pyridone-5-carboxylate 5.07 g (0.03 mol) was placed in a 100 mL RB and dissolved in 50 mL of dry THF under an Ar atmosphere. The flask was cooled in an ice-bath add 1 mol equiv. or 1.20 g (0.03 mol) NaH (60% in oil) was added by portions. The reaction mixture was stirred for 30 min and benzyl bromide 5.13 g (0.03 mol) was added and the mixture stirred for 2 h at room temperature. Cold water was slowly added and the organic layer was separated via a separatory funnel. The organic layer was washed with brine and dried with $MgSO_4$. The THF was removed on a rotary evaporator to give the product as a yellow syrup. After silica gel chromatography there was obtained 6.61 g of a yellow oil in 85% yield. $C_{15}H_{17}NO_3$ MW 259.30 Composition C(69.48) H(6.61) N(5.40) O(18.51)

1H NMR 200 MHz ($CDCl_3$): δ = 7.34-7.10 (m, 5H, Ph), 5.01 (s, 2H, CH_2Ph), 3.71 (s, 3H, OCH_3), 2.62 (m, 4H, CH_2CH_2), 2.34 (s, 3H, CH_3). LC/MS: MS(+ESI) m/z (relative intensity): 260 ($[M+H]^+$ 100).



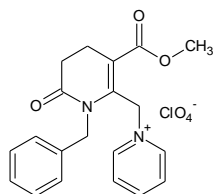
Methyl 1-benzyl-2-(bromomethyl)-6-oxo-1,4,5,6-tetrahydropyridine-3-carboxylate (73).

Method A: In a 25 mL RB was weighed 0.51g (0.00020mol) of the above N-benzlydihydropyridone and dissolved in dry $CHCl_3$. While stirring a Br_2 solution in $CHCl_3$ (0.00020 mol) was added drop-wise and stirred an additional 30 min. The $CHCl_3$ was evaporated using a rotary evaporator to give 0.77g of an orange syrup in quantitative yield. The syrup was passed through a silica gel plug with 10% EtOAc in pet.ether and after removing the solvent there was obtained 0.31g of a yellow oil in 50% yield.

Method B: In a 10 mL RB was weighed 0.51g (0.00020mol) of the above *N*-benzyl dihydropyridone and dissolved in dry MeOH and while stirring NBS 0.36g (0.0020 mol) was added after 1h the solvent was removed and the solids filtered and washed with CHCl₃. After removing the solvent there was obtained a dark colored oil 0.46g in 70% yield.

C₁₅H₁₆BrNO₃ MW 338.20 Composition C(53.27) H(4.77) Br(23.63) N(4.14) O(14.19)

¹H NMR 200 MHz (CDCl₃): δ = 7.35-7.10 (m, 5H, Ph), 5.18 (s, 2H, CH₂Ph), 4.61 (s, 2H, CH₂Br), 3.76 (s, 3H, OCH₃), 2.72-2.03 (m, 4H, CH₂CH₂). LC/MS: MS(+ESI) m/z (relative intensity): 279 ([M+K]⁺ 100).

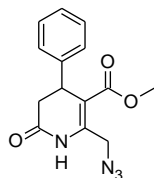


1-[[1-Benzyl-3-(methoxycarbonyl)-6-oxo-1,4,5,6-tetrahydropyridin-2-yl]methyl]pyridinium perchlorate (84b).

In a 25 mL RB flask was weighed the above *N*-benzyl DHPOD methylbromide 0.38g (0.0011 mol) and the oil was dissolved in dry acetone. Pyridine 0.09g (0.0011 mol) was added and the reaction mixture was stirred overnight. No pyridinium bromide salt precipitated so the solvent was removed to give a brown syrup which was dissolved in abs. EtOH and conc. HClO₄ was added by drops. Again no precipitate formed. The solvent was removed and after addition of diethethyl ether the oil solidified to give a pink solid 0.41g in 77% yield.

C₂₀H₂₁ClN₂O₇ MW 436.84 Composition C(54.99) H(4.85) Cl(8.12) N(6.41) O(25.64)

¹H NMR 400 MHz (CDCl₃): δ = 8.56 (d, 2H, *J*=4 Hz, Py), 8.22-8.18 (m, 1H, Py), 7.73-7.70 (m, 2H, Py), 7.07-6.93 (m, 5H, Ph), 5.92 (s, 2H, CH₂Ph), 5.12 (s, 2H, CH₂Py), 3.84 (s, 3H, OCH₃), 2.91-2.80 (m, 4H, COCH₂CH₂). ¹³C NMR 100.3 MHz (CDCl₃): δ = 168.73, 164.80, 143.27, 141.65, 138.38, 134.27, 127.15, 126.09, 125.61, 123.99, 117.72, 55.53, 50.86, 43.09, 28.23, 19.43 ppm. LC/MS: MS(+ESI) m/z (relative intensity): 382 ([M-Br]⁺ 100).



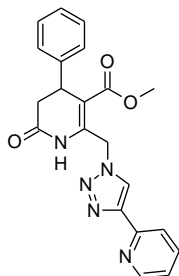
Methyl 2-(azidomethyl)-6-oxo-4-phenyl-1,4,5,6-tetrahydropyridine-3-carboxylate (98).

In a 50 mL RB was placed 0.06 g (0.85 mmol) of NaN₃ and dissolved in 10 mL DMSO then 2-bromomethyl-4-phenyl-3,4-dihydropyridone 0.26 g (0.8 mmol) was added and the solution was stirred overnight. To the orange solution was added 25 mL DI water and the stirring was continued until a solid precipitated. The solid was filtered and washed with water and dried to give 0.22g of a white solid in 96% yield.

C₁₄H₁₄N₄O₃ MW 286.29 Composition C(58.73) H(4.93) N(19.57) O(16.77)

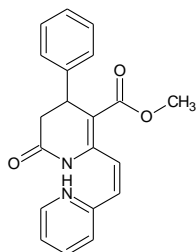
¹H-NMR 200 MHz (CDCl₃): δ = 7.79 (br s, 1H, NH), 7.32-7.14 (m, 5H, Ph), 4.91 (d, *J*=16.8 Hz, 1H CHN₃), 4.77 (d, *J*=17 Hz, 1H CH N₃), 4.26 (d, *J*= 7.4, 1H, CHPh), 3.67 (s, 3H, OCH₃), 2.93

(dd, $J=16.4$ and 7.6 Hz, 1H, *CHHCO*), 2.72 (dd, $J=16$ Hz, 1H, , *CHHCO*). LC/MS: MS(+ESI) m/z (relat. intensity): 285 ($[M-H]^+$, 100).



Methyl 6-oxo-4-phenyl-2-[[4-(pyridin-2-yl)-1H-1,2,3-triazol-1-yl]methyl]-1,4,5,6-tetrahydropyridine-3-carboxylate (99).

In a 25 mL RB was placed $\text{Cu}(\text{OAc})_2$ 0.01g and dissolved in 5 mL acetonitrile (blue color) to this was added 0.5 mL aqueous solution containing 0.1 g sodium ascorbate (the solution went yellow). Then 0.09g (0.30 mmol) of the azide **98** was added and 2-ethynylpyridine 0.03g (0.30 mmol). The solution was stirred magnetically overnight and the acetonitrile was removed under reduced pressure. The residue was dissolved in DCM and washed with conc. NH_4OH and water then dried with Na_2SO_4 filtered and the solvent removed to give a tan solid 0.11g or 94% yield. $\text{C}_{21}\text{H}_{19}\text{N}_5\text{O}_3$ MW 389.41 $^1\text{H-NMR}$ 200 MHz (CDCl_3): $\delta=8.53$ (br s, 1H, *NH*), 8.36 (d, $J=6.0$ Hz, 1H, *Py*), 7.76 (m, 1H, *Py*), 7.62 (m, 1H, *Py*), 7.47 (d, $J=7.2$ Hz, 1H, *Py*), 7.25-7.08 (m, 5H, *Ph*), 5.98 (d, $J=15$ Hz, 1H, *CHN*), 5.77 (d, $J=15$ Hz, 1H, *CHN*), 5.28 (s, 1H, *CH=*), 4.27 (d, $J=6.8$ Hz, 1H, *CHPh*), 3.70 (s, 3H, *OCH}_3*), 2.90 (dd, $J=6.8$; 16 Hz, 1H, *OCHH*), 2.67 (d, $J=16$ Hz, 1H, *OCHH*).

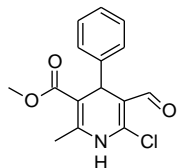


Methyl 6-oxo-4-phenyl-2-[(Z)-2-(pyridin-2-yl)ethenyl]-1,4,5,6-tetrahydropyridine-3-carboxylate (100).

In a 50 mL RB was placed 0.59g (0.001 mol) of the DHPOD 6-methyltriphenylphosphonium bromide and dissolved in 25 mL dry THF. Under an Ar atmosphere while stirring magnetically 0.22g (0.001 mol) of *t*BuOK was added. The orange solution was stirred for 30 min and 0.11g (0.001 mol) of 2-pyridinecarboxaldehyde was added. The solution was allowed to stir at RT overnight, 3 mL of aqueous solution containing 0.6 g NH_4Cl was added and after stirring 15 min the layers were separated. The THF was removed under reduced pressure and the sticky reaction product was dissolved in min. EtOAc. After addition of hexane the precipitated triphenylphosphine oxide was filtered off and the solvent removed to leave 0.55 g of product. The product was purified using prep. HPLC with 50% EtOAc / DCM as eluent. The solvent was

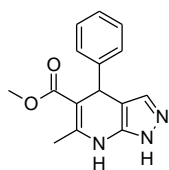
removed providing 0.21 g of product (62% yield) which was recrystallized from EtOH giving 100 mg of light green needles. $C_{20}H_{18}N_2O_3$ MW 334.37 Mp. 136-138°C.

1H -NMR 400 MHz ($CDCl_3$): δ =13.90 (br s, 1H, NH), 8.68 (ddd, J =5.0; 1.7; 0.82 Hz, 1H, Py), 7.77 (td, J =7.8; 1.82 Hz, 1H, Py), 7.72 (d, J =14.1 Hz, CH=), 7.37 (dt, J =7.9; 1.2 Hz, 1H, Py), 7.28-7.23 (m, 5H, Ph), 7.20-7.17 (m, 1H, Py), 6.62 (d, J =14.1 Hz, 1H, CH=), 4.35 (dd, J =7.79; 2.19 Hz, 1H, CHPh), 3.67 (s, 3H, OCH_3), 2.91 (dd, J =16.1; 7.6 Hz, 1H, COCH), 2.70 (ddd, J =16.3; 2.4; 0.8 Hz, 1H, COCH). ^{13}C -NMR 100.3 MHz ($CDCl_3$): δ =170.51, 167.37, 153.12, 147.61, 144.74, 141.76, 138.01, 132.06, 128.73, 126.99, 126.87, 126.43, 123.13, 110.41, 51.74, 51.72, 38.87, 37.65 ppm.



Methyl 4-aryl-6-chloro-5-formyl-2,1,4-dihydropyridine-3-carboxylate

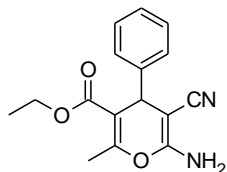
General procedure for synthesis. A solution of anhydrous *N,N*-dimethylformamide 3.1 mL (40 mmol) in dry chloroform 10 mL was added dropwise to a stirred solution of $POCl_3$ 3.85 mL (40 mmol) under a nitrogen atmosphere at RT. After 30 min. a solution of the methyl 4-aryl-6-methyl-2-oxo-1,2,3,4-tetrahydropyridine-5-carboxylate (10 mmol) in 40 mL dry chloroform was added. After 18 h stirring at RT, a solution of sodium acetate (40g) in water (60mL) was slowly added. After 0.5 h the mixture was partitioned between water and chloroform, and the aqueous phase was extracted with EtOAc. The organic phase was dried with $MgSO_4$. The organic solvent was removed *in vacuo* and the solid recrystallized from EtOH to give a pale yellow solid in 80% yield. $C_{15}H_{14}ClNO_3$ FW 291.73 Mp. 181-182°C Calcd. Comp. C(61.76) H(4.84) N(4.80) Found: C(61.9) H(4.9) N(4.9). 1H -NMR 400 MHz ($DMSO-d_6$): δ =10.36 (br s, 1H, NH), 9.69 (s, 1H, HCO), 7.23-7.12 (m, 5H, Ph), 4.95 (s, 1H, CHPh), 3.55 (s, 3H, OCH_3), 2.34 (s, 3H, CH_3). ^{13}C -NMR 100.3 MHz ($DMSO-d_6$): δ =186.5 (CHO), 166.6 (CO_2), 145.6 (C6), 142.7 (C2), 145.5, 128.3 (2C), 127.1 (2C), 126.5 (Ar), 111.2 (C5), 104.5 (C3), 51.1 (OCH_3), 37.6 (C4), 17.7 (CH_3).



Methyl 4-aryl-6-methyl-4,7-dihydro-1H-pyrazolo[3,4-b]pyridine-5-carboxylates

General procedure for synthesis: A mixture of the corresponding 6-chloro-5-formyl-DHP (2 mmol) and hydrazine hydrate 99% (2 mmol) in ethanol 20 mL was heated at reflux for 6 h. The reaction mixture was then cooled to 0°C and the solid that precipitated was collected by filtration. Further purification was accomplished by recrystallization from ethanol. Thus employing the procedure 61% yield of the product was obtained. $C_{15}H_{15}N_3O_2$, FW 269.30, Mp. 278-279°C. Calcd. Comp. C(66.90), H(5.61), N(15.60). Found: C(67.0), H(5.8), N(15.7). 1H -NMR 400 MHz ($DMSO-d_6$): δ =10.01 (s, 1H, NH), 9.98 (s, 1H, NH), 8.35 (s, 1H, CH=N), 7.22-7.13 (m, 5H, Ph), 5.18 (s, 1H, CHPh), 3.55 (s, 3H, OCH_3), 2.31 (s, 3H, CH_3). ^{13}C -NMR 100.3

MHz (DMSO- d_6): δ =166.9 (CO₂), 156.4 (C3), 146.2 (C6), 133.0 (C7a), 146.0, 128.0 (2C), 127.2 (2C), 126.2 (Ph), 107.7 (C3a), 102.5 (C5), 50.8 (OCH₃), 38.4 (C4), 18.0 (CH₃).



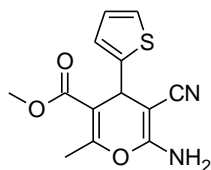
Preparation of Ethyl 6-Amino-5-cyano-2-methyl-4-phenyl-4H-pyran-3-carboxylate

Typical Procedure

A mixture of benzaldehyde (10 mmol, 1 ml), malononitrile (10 mmol, 0.66 g), and ammonium acetate (15 mmol, 1.15 g) was thoroughly mixed in a mortar by grinding until the completion of reaction as indicated by thin-layer chromatography (TLC) (15 min). The mixture solidified during the grinding. Then, ethyl acetoacetate (10 mmol, 1.26 ml) was added to the same vessel. The mixture, which initially was in a partial liquid state, solidified during the process of grinding (15 min). The pure product was obtained by recrystallized from ethanol (2.21 g, 78%).

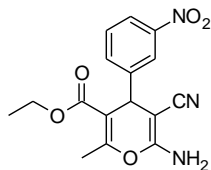
Mp 190–192 °C; IR (KBr) ν = 3402 (s), 3328 (s), 3223 (m), 2966 (w), 2189 (s),

1693 (s), 1259 (s), 1060 (s) cm^{-1} ; ¹H NMR (300 MHz, CDCl₃): δ =1.10 (t, J =7.20 Hz, 3H, CH₃ ester), 2.38 (s, 3H, CH₃₋₂), 4.05 (m, 2H, CH₂ ester), 4.45 [s, 1H, C(4)-H], 4.50 (br, s, 2H, NH₂), 7.17–7.35 (m, 5H, Ar-H) ppm; ¹³C NMR (75 MHz, CDCl₃): δ =13.86 (CH₃ ester), 18.37 (CH₃₋₂), 38.75 (C-4), 60.64 (CH₂ ester), 62.58 (C-5), 108.00 (C-3), 118.80 (CN), 127.17 (C-4'), 127.50 (C-3',5'), 128.56 (C-2',6'), 143.72 (C-1'), 156.76, 157.39 (C-2, 6), 165.83 (CO) ppm.



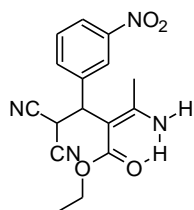
Methyl 6-amino-5-cyano-2-methyl-4(thiophen-2-yl)-4H-pyran-3-carboxylate (110)

This compound was synthesized by the above procedure except 1.12g (10mmol) thiophene-2-carbaldehyde was used and 1.16g (10mmol) methyl acetoacetate instead of ethyl acetoacetate. At the end of the grinding procedure the sticky yellow substance was recrystallized from ethanol to give white crystals (1.98 g, 72%). Mp 142-144°C; ¹H NMR (400 MHz, DMSO- d_6): δ =2.28 (s, 3H, CH₃), 3.64 (s, 3H, CH₃ ester), 4.65 [s, 1H, C(4)-H], 6.85 (d, J =3.6 Hz, 1H, Ar), 6.93 (dd, J =5.1, 3.5, 1H, Ar), 7.05 (br, s, 2H, NH₂), 7.36 (d, J =5.1, 1H, Ar) ppm; ¹³C NMR (100 MHz, DMSO- d_6): δ = 18.22, 33.81, 51.69, 56.93, 107.61, 119.55, 123.55, 124.78, 126.97, 149.34, 156.90, 159.09, 165.76 ppm.



Ethyl 6-amino-5-cyano-2-methyl-4-(3-nitrophenyl)-4H-pyran-3-carboxylate (112)

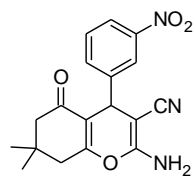
Mp 187–188°C; IR (KBr) ν =3402 (s), 3328 (s), 3221 (m), 2987 (w), 2190 (s), 1672 (s), 1531 (s), 1344 (s), 1063 (s) cm^{-1} ; ^1H NMR (400 MHz, CDCl_3): δ =1.12 (t, J =7.20 Hz, 3H, CH_3 ester), 2.41 (s, 3H, CH_{3-2}), 4.05 (m, 2H, CH_2 ester), 4.58 (s, 1H, C(4)-H), 4.69 (br, s, NH_2), 7.49 (t, J =8.00Hz, 1H, Ar- $\text{H}5'$), 7.58 (td, J_1 =8.00 Hz, J_2 =0.80 Hz, Ar- $\text{H}6'$), 8.06 (t, J =1.60 Hz, 1H, Ar- $\text{H}2'$), 8.11 (md, J =8.00 Hz, 1H, Ar- $\text{H}4'$) ppm; ^1H NMR (400 MHz, DMSO-d_6): δ =1.01 (t, J =7.20 Hz, 3H, CH_3 ester), 2.07 (s, 2H, NH_2), 2.34 (s, 3H, CH_{3-2}), 3.95 (m, 2H, CH_2 ester), 4.52 [s, 1H, C(4)-H], 7.60–7.70 (m, 2H, Ar- $\text{H}5'$, $\text{H}6'$), 7.98 (s, 1H, Ar- $\text{H}2'$), 8.10 (dt, J_1 =7.50Hz, J_2 =1.92Hz, 1H, Ar- $\text{H}4'$) ppm; ^{13}C NMR (100MHz, CDCl_3): δ =12.90 (CH_3 ester), 17.64 (CH_{3-2}), 37.75 (C-4), 59.95 (CH_2 ester), 63.50 (C-5), 105.93 (C-3), 117.33 (CN), 121.39 (C-4'), 121.55 (C-2'), 128.51 (C-5'), 133.01 (C-6'), 145.10 (C-1'), 147.47 (C-3'), 159.77, 156.95 (C-2, 6), 164.26 (CO) ppm.



(Z)-Ethyl 3-amino-2-(2,2-dicyano-1-(3-nitrophenyl)ethyl)but-2-enoate (113)

This intermediate was synthesized according to the typical grinding procedure using 3-nitrobenzaldehyde 1.52 g (10mmol) and (Z)-ethyl 3-aminobut-2-enoate (1.29g 10mmol) instead of ethyl acetoacetate. The yellow sticky mixture was washed with ethanol and recrystallized to give light green needles (1.9 g, 58%).

Mp 142-144°C; ^1H NMR(400 MHz, DMSO-d_6): δ =1.02 (t, J =7.0 Hz, 3H, CH_3 , ester), 2.17 (s, 3H, CH_3), 3.67-4.12 (m, 2H, CH_2 , ester), 4.75 (d, J =11.4 Hz, 1H, $\text{CH}(\text{CN})_2$), 5.73 (d, J =11.4 Hz, 1H, CH-Ar), 7.46 (br, s, 1H, NH), 7.58 (t, J =7.9 Hz, 1H, Ar- $\text{H}5$), 7.73 (d, J =7.6 Hz, 1H, Ar- $\text{H}6$), 8.07 (d, J =8.0 Hz, 1H, Ar- $\text{H}4$), 8.14 (s, 1H, Ar- $\text{H}2$), 8.61 (br, s, 1H, $\text{NH}\cdots\text{O}$) ppm; ^{13}C NMR (100 MHz, DMSO-d_6): δ =13.99, 20.92, 26.69, 43.34, 58.45, 88.97, 113.79, 114.38, 121.92, 122.24, 129.47, 135.03, 141.99, 147.38, 163.10, 167.55 ppm.



2-Amino-7,7-dimethyl-4-(3-nitrophenyl)-5-oxo-5,6,7,8-tetrahydro-4H-chromene-3-carbonitrile (115)

A mixture of m-nitrobenzaldehyde 0.76 g (5.0 mmol), dimedone 0.70 g (5.0 mmol), malononitrile 0.33 g (5.0 mmol), and NH_4OAc 0.6 g (7.5 mmol) was mixed thoroughly in a mortar with pestle followed by grinding till the completion of reaction as indicated by TLC (10-20 min). The resultant material was washed with water to remove any unreacted ammonium acetate and was air-dried to afford the crude product. The pure product was obtained by recrystallization from EtOH to give 1.06 g of a white crystalline compound in 67% yield. Mp 214-216°C. ^1H NMR(400 MHz, DMSO-d_6): δ =8.06-8.04 (m, 2H, Ph), 7.65-7.62 (m, 1H, Ph),

7.52-7.48 (m, 1H, Ph), 6.30 (s, 2H, NH₂), 4.47 (s, 1H, CHPh), 2.52 (s, 2H, CH₂), 2.26 (d, *J*=16 Hz, 1H, H-6a), 2.17 (d, *J*=16 Hz, 1H, H-6b), 1.12 (s, 3H, CH₃), 1.03 (s, 3H, CH₃).

Representative single crystal X-ray diffraction experiments and data

For ethyl 6-amino-5-cyano-2-methyl-4-(3-nitrophenyl)-4H-pyran-3-carboxylate (**112**), methyl 6-amino-5-cyano-2-methyl-4-(thiophen-2-yl)-4H-pyran-3-carboxylate (**110**) and intermediate **113** diffraction data were collected at -100°C (for **112** and **110**) and at room temperature for **113** on a Bruker-Nonius KappaCCD diffractometer using graphite monochromated Mo-K α radiation ($\lambda = 0.71073 \text{ \AA}$). Both crystal structures were solved by the direct method and refined by full-matrix least squares. All non-hydrogen atoms were refined anisotropically.

Crystal data for 110: C₁₃H₁₂N₂O₃S, triclinic, *a* = 8.6311(2), *b* = 9.0785(3), *c* = 9.6055(3) Å, $\alpha = 96.548(2)$, $\beta = 115.097(2)$, $\gamma = 95.679(2)^\circ$; *V* = 668.02(3) Å³, *Z* = 2, $\mu = 0.250 \text{ mm}^{-1}$, *D*_{calc} = 1.374 g·cm⁻³, space group is *P* $\bar{1}$. A total of 3256 independent reflection intensities were collected at room temperature. For structure refinement, 2055 reflections with *I* > 3 σ (*I*) were used. The final *R*-factor is 0.059.

Crystal data for 112: C₁₆H₁₅N₃O₅, triclinic, *a* = 8.3621(2), *b* = 8.4736(3), *c* = 12.0001(5) Å, $\alpha = 82.192(1)$, $\beta = 71.039(2)$, $\gamma = 76.176(2)^\circ$; *V* = 779.29(5) Å³, *Z* = 2, $\mu = 0.106 \text{ mm}^{-1}$, *D*_{calc} = 1.403 g·cm⁻³, space group is *P* $\bar{1}$. A total of 3911 independent reflection intensities were collected at room temperature. For structure refinement, 2546 reflections with *I* > 3 σ (*I*) were used. The final *R*-factor is 0.047.

Crystal data for 113: C₁₆H₁₆N₄O₄, monoclinic, *a* = 19.8757(7), *b* = 8.4327(3), *c* = 20.637(1) Å, $\beta = 106.330(1)^\circ$; *V* = 3319.3(2) Å³, *Z* = 8, $\mu = 0.097 \text{ mm}^{-1}$, *D*_{calc} = 1.314 g·cm⁻³, space group is *P*2₁/*n*. A total of 8959 independent reflection intensities were collected at room temperature. For structure refinement, 3496 reflections with *I* > 3 σ (*I*) were used. The final *R*-factor is 0.074. For further details, see crystallographic data for these structures deposited with the Cambridge Crystallographic Data Centre as Supplementary Publication Number CCDC 865274 (for **1**), 865275 (for **3c**) and 870203 (for 'intermediate'). Copies of the data can be obtained, free of charge, on application to CCDC, 12 Union Road, Cambridge CB2 1EZ, UK.

Publications

1. **Rufus Smits**, Sergey Belyakov, Aiva Plotniece, Gunars Duburs, Synthesis of 4*H*-pyran derivatives under solvent-free and grinding conditions, Submitted to: *Synthetic Communications*, manuscript ID is 2012 LSYC 716484, Published on line 22. Aug. 2012. DOI:10.1080/00397911.2012.716484
2. **Rufus Smits**, Yelena Goncharenko, Iveta Vesere, Baiba Skrivele, Oksana Petrichenko, Brigita Vigante, Marina Petrova, Aiva Plotniece, Gunars Duburs, Synthesis and self-assembly of novel fluorous cationic amphiphiles with a 3,4-dihydro-2(1*H*)-pyridone spacer, *Journal of Fluorine Chemistry* 132 (2011) 414–419
3. Buchanan, Gerald W.; **Smits, Rufus**; Munteanu, Elena; Santyr, Giles; Wallace, Julia; Gherase, Mihai-Raul. Ottawa-Carleton Chemistry Institute, Department of Chemistry, Carleton University, Ottawa, Can., Synthesis and dissolved hyperpolarized xenon NMR studies of sucrose octaoleate-F104. *Journal of Fluorine Chemistry* (2004), 125(10), 1457-1460.
4. Buchanan, Gerald W.; **Smits, Rufus**; Munteanu, Elena. Ottawa-Carleton Chemistry Institute, Department of Chemistry, Carleton University, Ottawa, Can., Synthesis and 19F NMR study of RF-oleic acid-F13, *Journal of Fluorine Chemistry* (2003), 123(2), 255-259.
5. Buchanan, Gerald W.; **Smits, Rufus**; Munteanu, Elena. Ottawa-Carleton Chemistry Institute, Department of Chemistry, Carleton University, Ottawa, Can., Synthesis of a highly fluorinated fatty acid analog, *Journal of Fluorine Chemistry* (2003), 119(2), 207-209.

International conferences

1. **Smits, R.**; Vigante, B.; Duburs, G., Bromination of 6-methyl-3,4-dihydropyridinone-5-carboxylates. In *Program and Abstract Book*, International Conference on Organic Synthesis Balticum Organicum Syntheticum (BOS-2008), June 29 - July 2, 2008: PO129. Vilnius, Lithuania, 2008; 176.
2. Vigante, B.; Mekss, K; Neider, Z; **Smits, R.**; Belyakov, S; Sobolev, A.; Duburs G. Synthesis of 3-substituted nitrodienamines- versatile synthons for heterocyclization. In *Program and Abstract Book*, International Conference on Organic Synthesis Balticum Organicum Syntheticum (BOS-2008), June 29 - July 2, 2008: PO119. Vilnius, Lithuania, 2008; 166.
3. **Smits, R.**; Goncareno, J.; Skrivele, B.; Turovska, B.; Vigante, B.; Duburs, G. Synthesis of charged fluorinated alkyl 6-methyl-3,4-dihydropyridone-5-carboxylates, In *Program and Abstract Book*, International Conference on Organic Synthesis Balticum Organicum Syntheticum (BOS-2010), June 27 - 30, 2010: PO139. Riga, Latvia, 2010; 185.

4. **Smits, R.**; Goncharenko, Y.; Vesere, I.; Skrivele, B.; Petrichenko, O.; Vigante, B.; Petrova, M.; Plotniece, A.; Duburs, G., Self-assembly of novel fluorous cationic amphiphiles with a 3,4-dihydro-2(1H)-pyridone spacer for possible drug delivery applications, *In Program and Abstract Book*, Helsinki Drug Research 2011 Tools for Admet and Pharmaceutical Nanotechnology, September 18-20, 2011: Poster 29. Helsinki, Finland, 2011; 34.

5. Gunars Duburs, **Rufus Smits**, Zenta Kalme, Brigita Vigante, Iveta Vesere, Dihydropyridones as derivatives of unsaturated cyclic β -amino acids, *In Program and Abstract Book*, Bordeaux 2012 Symposium on Foldamers January 30 – February 2 2012, poster 27.

REFERENCES

- [1] Tristan Montier, Thierry Benvegno, Paul-Alain Jaffrès, Jean-Jacques Yaouanc, Pierre Lehn, *Current Gene Therapy*, **2008**, 8, 296-312.
- [2] Zanna Hyvönen; Seppo Rönkkö; Marjo-Riitta Toppinen; Ilpo Jääskeläinen; Aiva Plotniece; Arto Urtti, *Journal of controlled release : official journal of the Controlled Release Society* **2004**; 99(1):177-90.
- [3] K. Pajuste, Ph.D. thesis, *Amfifilo katjono piridīna atvasinājumu sintēze jaunu gēnu transporta formu izveidei*, Riga, Latvia **2010**.
- [4] Krafft, M. P. *Advanced Drug Delivery Reviews* 47, **2001**, 209 –228.
- [5] X. Liu, Z-X. Jiang, Y. B. Yu, and E-K. Jeong, *Proc. Intl. Soc. Mag. Reson. Med.* 16 (2008) 1739.
- [6] Kok MB, de Vries A, Abdurrachim D, Prompers JJ, Grüll H, Nicolay K, Strijkers GJ., *Contrast Media Mol Imaging*. **2011** Jan-Feb; 6(1):19-27
- [7] Yla-Herttuala, S.; Martin, J. F. *Lancet*, **2000**, 355, 213-222.
- [8] Check, E. *Nature* **2003**, 423, 573-574.
- [9] Haccin-Bey-Abina, S. et al. *Science* **2003**, 401, 415-419.
- [10] Karmali, P. P.; Chaudhuri, A. *Med. Res. Rev.* **2007**, 27, 696-722.
- [11] Mishra, S.; Heidel, J. D.; Webster, P.; Davis, M. E. *J. Control. Rel.* **2006**, 116, 179-191.
- [12] Luo, D.; Haverstick, K.; Belcheva, N.; Han, E.; Saltzman, W. M. *Macromolecules* **2002**, 35, 3456-3462.
- [13] Prata, C. A.; H.; Zhao, Y.; Barthelemy, P.; Li, Y.; Luo, D.; McIntosh, T. J.; Lee, S. J.; Grinstaff, M. W. *J. Am. Chem. Soc.* **2004**, 126, 12196-12197.
- [14] Karmali, P. P.; Majeti, B. K.; Bojja, S.; Chaudhuri, A. *Bioconjugate Chem.* **2006**, 17, 159-171.
- [15] Zabner J, Fasbender AJ, Moninger T, Poellinger KA, Welsh MJ. Cellular and Molecular Barriers to Gene-Transfer by a Cationic Lipid. *J Biol Chem* **1995**; 270(32): 18997-19007.
- [16] Behr JP. Synthetic Gene-Transfer Vectors. *Acc Chem Res* **1993**; 26(5): 274-278.
- [17] Gao X, Huang L. Cationic liposome-mediated gene transfer. *Gene Ther* **1995**; 2(10): 710-22.
- [18] Labat-Moleur F, Steffan AM, Brisson C, Perron H, Feugeas O, Furstenberger P, *et al.* An electron microscopy study into the mechanism of gene transfer with lipopolyamines. *Gene Ther* **1996**; 3(11): 1010-1017.
- [19] Friend DS, Papahadjopoulos D, Debs RJ. Endocytosis and intracellular processing accompanying transfection mediated by cationic liposomes. *Biochim Biophys Acta* **1996**; 1278(1): 41-50.
- [20] Mislick KA, Baldeschwieler JD. Evidence for the role of proteoglycans in cation-mediated gene transfer. *Proc Natl Acad Sci USA* **1996**; 93(22): 12349-12354.
- [21] Mukherjee S, Ghosh RN, Maxfield FR. Endocytosis. *Physiol Rev* **1997**; 77(3): 759-803.
- [22] Hasegawa S, Hirashima N, Nakanishi M. Microtubule involvement in the intracellular dynamics for gene transfection mediated by cationic liposomes. *Gene Ther* **2001**; 8(21): 1669-1673.
- [23] Martin B, Aissaoui A, Sainlos M, Oudrhiri N, Hauchecorne M, Vigneron J-P, *et al.* Advances in Cationic Lipid-Mediated Gene Delivery. *Gene Ther Mol Biol* **2003**; 7: 273-289.

- [24] Aissaoui A, Oudrhiri N, Petit L, Hauchecorne M, Kan E, Sainlos M, *et al.* Progress in gene delivery by cationic lipids: Guanidiniumcholesterol- based systems as an example. *Curr Drug Targets* **2002**; 3(1): 1-16.
- [25] Miller AD. Cationic liposomes for gene therapy. *Angew Chem Int Ed* **1998**; 37(13-14): 1769-1785.
- [26] Roth JA, Cristiano RJ. Gene therapy for cancer: what have we done and where are we going? *J Natl Cancer Inst* **1997**; 89(1): 21-39.
- [27] Hersh EM, Stopeck AT. Cancer gene therapy using nonviral vectors: preclinical and clinical observations. In: Kabanov AV, Felgner PL, Seymour LW, editor. *Self-assembling Complexes for Gene Delivery*. Chichester, UK: John Wiley and Sons **1998**; p.421-436.
- [28] Alton EFWF, Stern M, Farley R, Jaffe A, Chadwick SL, Phillips J, *et al.* Cationic lipid-mediated CFTR gene transfer to the lungs and nose of patients with cystic fibrosis: a double-blind placebocontrolled trial. *Lancet* **1999**; 353(9157): 947-954.
- [29] Griesenbach U, Geddes DM, Alton EFWF. Cystic fibrosis gene therapy. In: Huang L, Hung MC, Wagner E, editor. *Nonviral Vectors for Gene Therapy*. San Diego, USA, Academic Press. **1999**; p. 337-356.
- [30] Davies JC, Geddes DM, Alton EW. Gene therapy for cystic fibrosis. *J Gene Med* **2001**; 3(5): 409-17.
- [31] Boucher RC. Status of gene therapy for cystic fibrosis lung disease. *J Clin Invest* **1999**; 103(4): 441-445.
- [32] B. Martin, M. Sainlos, A. Aissaoui, N. Oudrhiri, M. Hauchecorne, J.-P. Vigneron, J.-M. Lehn and P. Lehn, *Current Pharmaceutical Design*, **2005**, 11, 375-394.
- [33] Fire,A., Xu,S., Montgomery,M.K., Kostas,S.A., Driver,S.E. and Mello,C.C. Potent and specific genetic interference by doublestranded RNA in *Caenorhabditis elegans*. *Nature*, (1998) 391, 806–811.
- [34] Medema,R.H. Optimizing RNA interference for application in mammalian cells. *Biochem. J.*, (2004) 380, 593–603.
- [35] Mittal,V. Improving the efficiency of RNA interference in mammals. *Nature Rev. Genet.*, (2004) 5, 355–365.
- [36] Sioud,M. On the delivery of small interfering RNAs into mammalian cells. *Expert Opin. Drug Deliv.*, (2005) 2, 639–651.
- [37] Ryther,R., Flynt,A., Phillips,J.,III and Patton,J. siRNA therapeutics: big potential from small RNAs. *Gene Ther.*, (2005) 12, 5–11.
- [38] Hannon,G.J. and Rossi,J.J. Unlocking the potential of the human genome with RNA interference. *Nature*, (2004) 431, 371–378.
- [39] Dorsett,Y. and Tuschl,T. siRNAs: applications in functional genomics and potential as therapeutics. *Nature Rev. Drug Discov.*, (2004) 3, 318–329.
- [40] Caplen,N.J. and Mousses,S. Short interfering RNA (siRNA)-mediated RNA interference (RNAi) in human cells. *Ann. NY Acad. Sci.*, (2003) 1002, 56–62.
- [41] Elbashir,S.M., Harborth,J., Lendeckel,W., Yalcin,A., Weber,K. And Tuschl,T. Duplexes of 21-nucleotide RNAs mediate RNA interference in cultured mammalian cells. *Nature*, (2001) 411, 494–498.
- [42] Scherer,L.J. and Rossi,J.J. Approaches for the sequence-specific knockdown of mRNA. *Nat. Biotechnol.*, (2003) 21, 1457–1465.

- [43] Stark,G.R., Kerr,I.M., Williams,B.R.G., Silverman,R.H. and Schreiber,R.D. How cells respond to interferons. *Annu. Rev.Biochem.*, (1998) 67, 227–264.
- [44] Overhoff,M., Wunsche,W. and Sczakiel,G. Quantitative detection of siRNA and single-stranded oligonucleotides: relationship between uptake and biological activity of siRNA. *Nucleic Acids Res.*, (2004) 32, e170.
- [45] Lingor,P., Michel,U., Scholl,U., Bahr,M. and Kugler,S. Transfection of ‘naked’ siRNA results in endosomal uptake and metabolic impairment in cultured neurons. *Biochem. Biophys. Res. Commun.*, (2004) 315,1126–1133.
- [46] Hu-Lieskovan,S., Heidel,J.D., Bartlett,D.W., Davis,M.E. and Triche,T.J. Sequence-specific knockdown of EWS-FLI1 by targeted, nonviral delivery of small interfering RNA inhibits tumor growth in a murine model of Ewing’s sarcoma. *Cancer Res.*, (2005) 65, 8984–8992.
- [47] Derek W. Bartlett and Mark E. Davis, *Nucleic Acids Research*, 2006, Vol. 34, No. 1322–333.
- [48] D. Bumcrot, M. Manoharan, V. Kotliansky, D.W. Sah, RNAi therapeutics: a potential new class of pharmaceutical drugs, *Nat. Chem. Biol.* 2 (2006) 711–719.
- [49] R. Juliano, M.R. Alam, V. Dixit, H. Kang, Mechanisms and strategies for effective delivery of antisense and siRNA oligonucleotides, *Nucleic Acids Res.* 36 (2008) 4158–4171.
- [50] A. Aigner, Nonviral in vivo delivery of therapeutic small interfering RNAs, *Curr. Opin. Mol. Ther.* 9 (2007) 345–352.
- [51] Yu-Kyoung Oh, Tae Gwan Park, *Advanced Drug Delivery Reviews* 61 (2009) 850–862.
- [52] H. Lv, S. Zhang, B. Wang, S. Cui, J. Yan, Toxicity of cationic lipids and cationic polymers in gene delivery, *J. Control. Release*, 114 (2006) 100–109.
- [53] H.S. Kim, I.H. Song, J.C. Kim, E.J. Kim, D.O. Jang, Y.S., *J. Control. Release* 115 (2006) 234–241.
- [54] Y. Obata, D. Suzuki, S. Takeoka, Evaluation of cationic assemblies constructed with amino acid based lipids for plasmid DNA delivery, *Bioconjug. Chem.* 19 (2008)1055–1063.
- [55] A. Akinc, A. Zumbuehl, M. Goldberg, E.S. Leshchiner, V. Busini, N. Hossain, S.A. Bacallado, D.N. Nguyen, J. Fuller, R. Alvarez, A. Borodovsky, T. Borland, R. Constien, A. de Fougères, J.R. Dorkin, K. Narayanannair, M. Jayaraman, M. John, V. Kotliansky, M. Manoharan, L. Nechev, J. Qin, T. Racie, D. Raitcheva, K.G. Rajeev, D.W. Sah, J. Soutschek, I. Toudjarska, H.P. Vornlocher, T.S. Zimmermann, R.Langer, D.G. Anderson, A combinatorial library of lipid-like materials for delivery of RNAi therapeutics, *Nat. Biotechnol.* 26 (2008) 561–569.
- [56] H.R. Kim, I.K. Kim, K.H. Bae, S.H. Lee, Y. Lee, T.G. Park, Cationic solid lipid nanoparticles reconstituted from low density lipoprotein components for delivery of siRNA, *Mol. Pharm.* 5 (2008) 622–631.
- [57] D.V. Morrissey, J.A. Lockridge, L. Shaw, K. Blanchard, K. Jensen, W. Breen, K. Hartsough, L. Machemer, S. Radka, V. Jadhav, N. Vaish, S. Zinnen, C. Vargeese, K. Bowman, C.S. Shaffer, L.B. Jeffs, A. Judge, I. MacLachlan, B. Polisky, Potent and persistent in vivo anti-HBV activity of chemically modified siRNAs, *Nat.Biotechnol.* 23 (2005) 1002–1007.
- [58] T.W. Geisbert, L.E. Hensley, E. Kagan, E.Z. Yu, J.B. Geisbert, K. Daddario-DiCaprio, E.A. Fritz, P.B. Jahrling, K. McClintock, J.R. Phelps, A.C. Lee, A. Judge, L.B. Jeffs, I. MacLachlan, Postexposure protection of guinea pigs against a lethal ebola virus challenge is conferred by RNA interference, *J. Infect. Dis.* 193 (2006) 1650–1657.

- [59] Majeti, B. K.; Singh, R. S.; Yadav, S. K.; Reddy, S. B.; Ramkrishna, S.; Diwan, P. V.; Madhavendra, S. S.; Chaudhuri, A. *Chem. Biol.* **2004**, *11*, 427-437.
- [60] Heyes, J. A.; Duvaz, D. N.; Cooper, R. G.; Springer, C. J. *J. Med. Chem.* **2002**, *45*, 99-114.
- [61] Banerjee, R.; Mahidhar, Y. V.; Chaudhuri, A.; Gopal, V.; Rao, N. M. *J. Med. Chem.* **2001**, *44*, 4176-4185
- [62] Singh, R. S.; Chaudhuri, A. *FEBS Lett.* **2004**, *556*, 86-90
- [63] Karmali, P. P.; Kumar, V. V.; Chaudhuri, A. *J. Med. Chem.* **2004**, *47*, 2123-2132.
- [64] M. Rajesh, J. Sen, M. Srujan, K. Mukherjee, B. Sreedhar, A. Chaudhuri, *J. Am. Chem. Soc.*, **2007**, *129* (37), 11408-11420.
- [65] Nicolau C, Sene C. Liposome-mediated DNA transfer in eukaryotic cells. Dependence of the transfer efficiency upon the type of liposomes used and the host cell cycle stage. *Biochim Biophys Acta* **1982**; *721*(2): 185-90.
- [66] Nicolau C, Le Pape A, Soriano P, Fargette F, Juhel MF. *In vivo* expression of rat insulin after intravenous administration of the liposome-entrapped gene for rat insulin I. *Proc Natl Acad Sci USA* **1983**; *80*(4): 1068-72.
- [67] Felgner PL, Gadek TR, Holm M, Roman R, Chan HW, Wenz M, *et al.* Lipofection: a highly efficient, lipid-mediated DNA-transfection procedure. *Proc Natl Acad Sci USA* **1987**; *84*(21): 7413-17.
- [68] Behr JP, Demeneix B, Loeffler JP, Perez-Mutul J. Efficient gene transfer into mammalian primary endocrine cells with lipopolyamine-coated DNA. *Proc Natl Acad Sci USA* **1989**; *86*(18): 6982-6.
- [69] Gao X, Huang L. A novel cationic liposome reagent for efficient transfection of mammalian cells. *Biochem Biophys Res Commun* **1991**; *179*(1): 280-5.
- [70] Farhood H, Serbina N, Huang L. The Role of Dioleoyl Phosphatidylethanolamine in Cationic Liposome-Mediated Gene-Transfer. *Biochim Biophys Acta* **1995**; *1235*(2): 289-295.
- [71] Vidal M, Hoekstra D. *In vitro* fusion of reticulocyte endocytic vesicles with liposomes. *J Biol Chem* **1995**; *270*(30): 17823-9.
- [72] Ellens H, Bentz J, Szoka FC. Fusion of phosphatidylethanolamine-containing liposomes and mechanism of La-HII phase transition. *Biochemistry* **1986**; *25*(14): 4141-7.
- [73] Wang J, Guo X, Xu Y, Barron L, Szoka FC, Jr. Synthesis and Characterization of Long Chain Alkyl Acyl Carnitine Esters. Potentially Biodegradable Cationic Lipids for Use in Gene Delivery. *J Med Chem* **1998**; *41*(13): 2207-2215.
- [74] Obika S, Yu W, Shimoyama A, Uneda T, Miyashita K, Doi T, *et al.* A symmetrical and biodegradable cationic lipid. Synthesis and application for efficient gene transfection. *Bioorg Med Chem Lett* **1997**; *7*(14): 1817-1820.
- [75] Roosjen A, Smisterova J, Driessen C, Anders JT, Wagenaar A, Hoekstra D, *et al.* Synthesis and characteristics of biodegradable pyridinium amphiphiles used for *in vitro* DNA delivery. *Eur J Org Chem* **2002**; (7): 1271-1277.
- [76] Pijper D, Bulten E, Smisterova J, Wagenaar, Hoekstra D, Engberts JBFN, *et al.* Novel Biodegradable Pyridinium Amphiphiles for Gene Delivery. *Eur J Org Chem* **2003**; (22): 4406-4412.
- [77] Ioan, P.; Carosati, E.; Micucci, M.; Cruciani, G.; Broccatelli, F.; S. Zhorov, B.; Chiarini, A.; Budriesi, R. *Current Medicinal Chemistry*, Volume 18, Number 32, November **2011**, pp. 4901-4922(22)

- [78] Khadilkar, B.; Borkar, S. Silica gel supported ferric nitrate: A convenient oxidizing reagent. *Synth. Commun.*, **1998**, *28*, 207-212.
- [79] (a) Buhler, F.R.; Kiowski, W. Calcium antagonists in hypertension. *J. Hypertens. Suppl.*, **1987**, *S3* 10; (b) Zolfigol, M.A.; Salehi, P.; Safaiee M. An efficient and eco-friendly procedure for the synthesis of Hantzsch ethyl 1,4-dihydro-2,6-dimethylpyridine-3,5-dicarboxylates under mild and green conditions. *Lett. Org. Chem.*, **2006**, *3*, 153-156.
- [80] Vo, D.; Matowe, W.C.; Ramesh, M.; Iqbal, N.; Wolowyk, M.W.; Howlett, S.E.; Knaus, E.E. Syntheses, calcium channel agonist-antagonist modulation activities, and voltage-clamp studies of iso-propyl 1,4-dihydro-2,6-dimethyl-3-nitro-4-pyridinylpyridine-5-carboxylate racemates and enantiomers. *J. Med. Chem.*, **1995**, *38*, 2851-2859.
- [81] Klusa V (**1995**) *Drugs Fut* 20:135.
- [82] Godfraind T, Miller R, Wibo M (**1986**) *Pharmacol Rev* 38:321.
- [83] Sausins A, Duburs G (**1988**) *Heterocycles* 27:269.
- [84] Gaudio AC, Korolkovas A, Takahata Y (**1994**) *J Pharm Sci* 83:1110.
- [85] Cooper K, Fray M J, Parry M J, Richardson K, Steele J (**1992**) *J Med Chem* 35:3115.
- [86] Yadav JS, Reddy VS, Reddy PT (**2001**) *Synth Commun* 31:425.
- [87] Kumar R, Malik S, Chandra R (**2009**) *Ind J Chem* 48B:718-724.
- [88] Böcker RH, Guengerich FP (**1986**) *J Med Chem* 29:1596-1603.
- [89] Krechl, J.; Smrčková, S. Biomimetic models of lactate dehydrogenase. *Tetrahedron Lett.*, **1989**, *30*, 5315-5318.
- [90] Rueping, M.; Antonchick, A.P.; Theissmann, T. A Highly enantioselective brønsted acid catalyzed cascade reaction: organocatalytic transfer hydrogenation of quinolines and their application in the synthesis of alkaloids. *Angew. Chem. Int. Ed. Engl.*, **2006**, *45*, 3683-3686.
- [91] Hoffmann, S.; Nicoletti, M.; List, B. Catalytic asymmetric reductive amination of aldehydes via dynamic kinetic resolution. *J. Am. Chem. Soc.*, **2006**, *128*, 13074-13075.
- [92] (a) Yang, J.W.; Fonseca, M.T.H.; List, B. A metal-free transfer hydrogenation: Organocatalytic conjugate reduction of α,β -unsaturated aldehydes. *Angew. Chem. Int. Ed. Engl.*, **2004**, *43*, 6660-6662; (b) Martin, N.J.A.; List, B. Highly enantioselective transfer hydrogenation of α,β -unsaturated ketones. *J. Am. Chem. Soc.*, **2006**, *128*, 13368-13369.
- [93] Hantzsch, A. Condensationprodukte aus Aldehydammoniak und ketoniartigen Verbindungen. *Chem. Ber.* **1881**, *14*, 1637-1638.
- [94] Love, B.; Snader, K.M. The Hantzsch Reaction. I. oxidative dealkylation of certain dihydropyridines. *J. Org. Chem.*, **1965**, *30*, 1914-1916.
- [95] (a) Anniappan, M.; Muralidharan, D.; Perumal, P.T. Synthesis of Hantzsch 1,4-dihydropyridines under microwave irradiation. *Synth. Commun.*, **2002**, *32*, 659-663; (b) Khadikar, B. M.; Gaikar, V. G.; Chitnavis, A. A. Aqueous hydrotrope solution as a safer medium for microwave enhanced hantzsch dihydropyridine ester synthesis. *Tetrahedron Lett.* **1995**, *36*, 8083-8086; (c) Öhberg, L.; Westman, J. An efficient and fast procedure for the Hantzsch dihydropyridine synthesis under microwave conditions. *Synlett*, **2001**, 1296-1298; (d) Agarwal, A.; Chauhan, P. M. S. Solid supported synthesis of structurally diverse dihydropyrido[2,3-d]pyrimidines using micro-wave irradiation. *Tetrahedron Lett.*, **2005**, *46*, 1345-1348; (e) Kuraitheerthakumaran, A.; Pazhamalai, S.; Gopalakrishnan M. An efficient and solvent-free one-

- pot synthesis of 1,4-dihydropyridines under microwave irradiation. *Chin. Chem. Lett.*, **2011**, 22, 1199-1202.
- [96] Ko, S.; Sastry, M.N.V.; Lin, C.; Yao, C.-F. Molecular iodine-catalyzed one-pot synthesis of 4-substituted-1,4-dihydropyridine derivatives *via* Hantzsch reaction. *Tetrahedron Lett.*, **2005**, 46, 5771-5774.
- [97] Sharma, G.V.M.; Reddy, K.L.; Lakshmi, P.S.; Krishna, P.R. *In situ* Generated HCl - An efficient catalyst for solvent-free Hantzsch re-action at room temperature: Synthesis of new dihydropyridine gly-coconjugates. *Synthesis*, **2006**, 1, 55-58.
- [98] Yadav, J.S.; Reddy, B.V.S.; Basak, A.K.; Narsaiah, A.V. Three-component coupling reactions in ionic liquids: An improved proto-col for the synthesis of 1,4-dihydropyridines. *Green Chem.*, **2003**, 5, 60-63.
- [99] Chari, M.A.; Syamasundar, K. Silica gel/NaHSO₄ catalyzed one-pot synthesis of Hantzsch 1,4-dihydropyridines at ambient tempera-ture. *Catal. Commun.*, **2005**, 6, 624-626.
- [100] Sabitha, G.; Reddy, G.S.K.K.; Reddy, Ch.S.; Yadav, J.S. A novel TMSI-mediated synthesis of Hantzsch 1,4-dihydropyridines at am-bient temperature. *Tetrahedron Lett.*, **2003**, 44, 4129-4131.
- [101] Wang, L.M.; Sheng, J.; Zhang, L.; Han, J.W.; Fan, Z.; Tian, H.; Qian, C.T. Facile Yb(OTf)₃ promoted one-pot synthesis of polyhy-droquinoline derivatives through Hantzsch reaction. *Tetrahedron*, **2005**, 61, 1539-1543.
- [102] (a) Guo, S.; Yuan, Y. One-Pot Synthesis of 1,4-Dihydropyridine and Polyhydroquinoline Derivatives *via* *L*-Proline catalyzed Hantzsch multicomponent reaction under ultrasound irradiation. *Chin. J. Chem.*, **2010**, 28, 811-817; (b) Ruiz, E.; Rodríguez, H.; Coro, J.; Niebla, V.; Rodríguez, A.; Martínez-Alvarez, R.; Novoa de Armas, H.; Suárez, M.; Martín N. Efficient sonochemical syn-thesis of alkyl 4-aryl-6-chloro-5-formyl-2-methyl-1,4-dihydropyridine-3-carboxylate derivatives. *Ultrason. Sonochem.*, **2012**, 19, 221-226.
- [103] Mirela Filipan-Litvić, Mladen Litvić, Ivica Cepanec, Vladimir Vinković, *Molecules* **2007**, 12, 2546-2558.
- [104] Loev, B.; Goodman, M. M.; Snader, K. M.; Tedeschi, R.; Macko, E. "Hantzsch-Type" Dihydropyridine Hypotensive Agents. *J. Med. Chem.* **1974**, 17, 956-965.
- [105] Meyer, H.; Bossert, F.; Horstmann, H. Dihydropyridine, II. Synthese Von 1,4-Dihydropyridinen mit Brückenkopf-N-atom. *Liebigs Ann. Chem.* **1977**, 1888-1894.
- [106] Phillips, A. P. Hantzsch's Pyridine Synthesis. *J. Am. Chem. Soc.* **1949**, 71, 4003-4007.
- [107] Meyer, H.; Bossert, F.; Wehinger, E.; Stoepel, K.; Vater, W. Synthese und vergleichende pharmakologische Untersuchungen von 1,4-Dihydro-2,6-dimethyl-4-(3-nitrophenyl)pyridin-3,5-dicarbonsäureestern mit nicht-identischen Esterfunktionen. *Arzneim. Forsch. (Drug Res.)* **1981**, 31, 407-409.
- [108] Wong, W. C.; Chiu, G.; Wetzel, J. M.; Marzabadi, M. R.; Nagarathnam, D.; Wang, D.; Fang, J.; Miao, S. W.; Hong, X.; Forray, C.; Vaysse, P. J. J.; Brancheck, T. A.; Gluchowski, C. Identification of a Dihydropyridine as a Potent α_{1a} Adrenoreceptor-Selective Antagonist That Inhibits Phenylephrine-Induced Contraction of the Human Prostate. *J. Med. Chem.* **1998**, 41, 2643-2650.
- [109] Nagarathnam, D.; Wetzel, J. M.; Miao, S. W.; Marzabadi, M. R.; Chiu, G.; Wong, W. C.; Hong, X.; Fang, J.; Forray, C.; Brancheck, T. A.; Heydorn, W. E.; Chang, R. S. L.; Broten, T.; Schorn, T. W.; Gluchowski, C. Design and Synthesis of Novel α_{1a} Adrenoreceptor-Selective

- Antagonist for the Treatment of Benign Prostatic Hyperplasia. *J. Med. Chem.* **1998**, *41*, 5320–5333.
- [110] Khadilkar, B. M.; Jaisinghani, H. G.; Saraf, M. N.; Desai, S. K. *Ind.J. Chem.* **2001**, *40B*, 82–86.
- [111] Wang, G.-W.; Miao, *Green Chem.* **2006**, *8*, 1080-1095.
- [112] Angeles, E.; Santillán, H.; Martínez, I.; Ramírez, A.; Velásquez, A.; López-Castañares, R.; Martínez, R. *Molecules* **2001**, *6*, 683-693.
- [113] Görlitzer, K.; Fabian, J.; Trittmacher, J. *Pharmazie* **2005**, *60*, 571-573.
- [114] Dong, D., X. Bi, Q. Liu and F. Cong, **2005**. *Chem. Commun.*, 3580-3582.
- [115] Elias, R.S., B.A. Saeed, K.Y. Saour and N.A. Al-Masoudi, **2008**. *Tet. Lett.*, *49*: 3049-3051.
- [116] Magedov, I.V., M. Manapadi, M.A. Ogasawara, A.S. Dhwan and S. Rogdi *et al.*, **2008**. *J. Med. Chem.*, *51*: 2561-2570.
- [117] Goodman, K.B., H. Cui, S.E. Dowdell, D.E. Giatanopoulos and R.L. Ivy *et al.*, **2007**. *J. Med. Chem.*, *50*: 6-9.
- [118] Hu, E., A. Tasker, R.D. White, R.K. Kunz and J. Hutman *et al.*, **2008**. *J. Med. Chem.*, *51*: 3065-3068.
- [119] Goodman K. B. *et. al.* *J. Med. Chem.* **2007** Jan 11:50(1):6-9.
- [120] Nichols R. J. *et. al.* *Biochem. J.* **2009**, Oct 23:424(1):47-60,
- [121] Yeats, C.L., J.F. Betchelor, E.C. Capon, N.J. Cheesman and M. Fry *et al.*, **2008**. *J. Med. Chem.*, *51*: 2845-2852.
- [122] Revas, F.M., J.P. Stables, L. Murphree, R.V. Edwanker and C.R. Edwanker *et al.*, **2009**. *J. Med. Chem.*, *52*: 1795-1798.
- [123] Jones G. In *Comprehensive Heterocyclic Chemistry*; Katritzky, A. R., Rees, C. W. Eds. Pergamon Press, New York, **1984**, Vol. 2, Part 2A, p.395.
- [124] Meislich, H. In *Pyridine and Its Derivatives, Part 3*; Klingsberg, E. Ed.; John Wiley & Sons Inc., New York, **1962**, p 509.
- [125] Kametani T., Nemoto H., Takeda H., Tekano S., *Tetrahedron* **1970**, *26*, 5753.
- [126] Banerjee, D. K.; Sengupta, P.; Das Gupta, S. K. *J. Org. Chem.* **1954**, *19*, 1516.
- [127] Hortensia Rodríguez, Osvaldo Reyes, Margarita Suarez, Hilda E. Garay, Rolando Pe´rez, Luis Javier Cruz, Yamila Verdecia, Nazario Marti´n, Carlos Seoane, *Tetrahedron Letters* **43** (2002) 439–441
- [128] Hortensia Rodríguez, Margarita Suarez, Rolando Pe´rez, Alain Petit, Andre´ Loupy, *Tetrahedron Letters* **44** (2003) 3709–3712.
- [129] Ruiz E, Rodríguez H, Coro J, Salfrán E, Suárez M, Martínez-Alvarez R, Martín N., *Ultrason Sonochem.* **2011** Jan;18(1):32-6.
- [130] M. Olivia Noguez, Vanessa Marcelino, Hortensia Rodríguez, Osneski Martín, Joel O. Martínez, Gabriel A. Arroyo, Francisco J. Pérez, Margarita Suárez, René Miranda, *Int. J. Mol. Sci.* **2011**, *12*, 2641-2649.
- [131] Krafft, M. P. In *Handbook of Fluorous Chemistry*; Gladysz, J. A., Curran, D. P., Horvath, I. T., Eds.; Wiley-VCH: Weinheim, **2004**; Chapter 12.
- [132] Kissa, E. *Fluorinated Surfactants and Repellents*, 2nd ed.; Surfactant Science Series; Marcel Dekker: New York, **2001**; Vol. 97.
- [133] D. Simberg, D. Hirsch-Lerner, R. Nissim, Y. Barenholz, *J. Liposome Res.* **10** (2000) 1–13.

- [134] C. Nicolazzi, M. Garinot, N. Mignet, D. Scherman, M. Bessodes, *Curr. Med. Chem.* 10 (2003) 1263–1277.
- [135] B. Martin, M. Sainlos, A. Aissaoui, N. Oudrhiri, M. Hauchecorne, J.-P. Vigneron, J.-M. Lehn, P. Lehn, *Curr. Pharm. Des.* 11 (2005) 375–394.
- [136] T. Montier, T. Benvegna, P.-A. Jaffre`s, J.-J. Yaouanc, P. Lehn, *Curr. Gene Ther.* 8 (2008) 296–312.
- [137] M. Morille, C. Passirani, A. Vonarbourg, A. Clavreul, J.-P. Benoit, *Biomaterials* 29 (2008) 3477–3496.
- [138] S. Bhattacharya, A. Bajaj, *Chem. Commun.* (2009) 4632–4656.
- [139] D. Zhi, S. Zhang, B. Wang, Y. Zhao, B. Yang, S. Yu, *Bioconjug. Chem.* 21 (2010) 563–577.
- [140] E. Klein, C. Leborgne, M. Ciobanu, J. Klein, B. Frisch, F. Pons, G. Zuber, D. Scherman, A. Kichler, L. Lebeau, *Biomaterials* 31 (2010) 4781–4788.
- [141] J. Gaucheron, C. Santaella, P. Vierling, *Bioconjug. Chem.* 12 (2001) 569–575.
- [142] P. Vierling, C. Santaella, J. Greiner, *J. Fluorine Chem.* 107 (2001) 337–354.
- [143] J. Gaucheron, C. Santaella, P. Vierling, *Bioconjug. Chem.* 12 (2001) 114–128.
- [145] J. Gaucheron, C. Boulanger, C. Santaella, N. Sbirrazzuoli, O. Boussif, P. Vierling, *Bioconjug. Chem.* 12 (2001) 949–963.
- [146] C. Boulanger, C. Di Giorgio, J. Gaucheron, P. Vierling, *Bioconjug. Chem.* 15 (2004) 901–908.
- [147] K. Fabio, C. Di Giorgio, P. Vierling, *Biochim. Biophys. Acta* 1724 (2005) 203–214.
- [148] L. Le Gourrie´rec, C. Di Giorgio, J. Greiner, P. Vierling, *New J. Chem.* 32 (2008) 2027–2042.
- [149] S. Denoyelle, A. Polidori, M. Brunelle, P.Y. Vuillaume, S. Laurent, Y. ElAshari, B. Pucci, *New J. Chem.* 30 (2006) 629–646.
- [150] E. Klein, M. Ciobanu, J. Klein, V. Machi, T. Vandamme, C. Leborgne, B. Frisch, F. Pons, A. Kichler, G. Zuber, L. Lebeau, *Bioconjug. Chem.* 21 (2010) 360–371.
- [151] Nicolas Dupuy, Andreea Pasc, Stephane Parant, Stephane Fontanay, Raphael E. Duval, Christine Gerardin, *Journal of Fluorine Chemistry* 135, 2012, 330–338.
- [152] G. M. Lanza, P. M. Winter, S. D. Caruthers, M. S. Hughes, Grace Hu, A. H. Schmieder, S. A. Wickline, *Angiogenesis*, 2010, 13:189–202.
- [153] Bachert P, Pharmacokinetics using fluorine NMR in vivo. *Prog Nucl Magn Reson Spectrosc*, 1998, 33:1–56.
- [154] Wolf W et. al. 19F-MRS studies of fluorinated drugs in humans. *Adv. Drug. Deliv. Rev.*, 2000, 41:55–74.
- [155] Kaneda MM et. al. Perfluorocarbon nanoemulsions for quantitative molecular imaging and targeted therapeutics. *Ann. Biomed. Eng.* 2009, 37:1922–1933.
- [156] Jesús Ruiz-Cabelloa, Brad P. Barnetta, Paul A. Bottomleya, Jeff W.M. Bulte, *NMR Biomed.* 2011 February ; 24(2): 114–129.
- [157] Gesa Weise, Thomas C. Basse-Lusebrink, Christoph Kleinschnitz, Thomas Kampf, Peter M.Jakob, Guido Stol, *PLoS ONE* 2011, 6(12): 1-8: e28143.
- [158] Denoyelle, S.; Polidori, A.; Brunelle, M.; Vuillaume, P. Y.; Laurent, S.; ElAzharyb, Y.; Pucci, B. Synthesis and preliminary biological studies of hemifluorinated bifunctional bolaamphiphiles designed for gene delivery. *New J. Chem.* 2006, 30, 629-646.

- [159] Tanford C. *The hydrophobic effect: formation of micelles and biological membranes*. New York, John Wiley and Sons, Inc. **1973**.
- [160] Israelachvili JN, Mitchell DJ, Ninham BW. Theory of self-assembly of hydrocarbon amphiphiles into micelles and bilayers. *J Chem Soc Faraday Trans II*, **1976**, **72**: 1525–1568.
- [161] Israelachvili JN, Mitchell DJ, Ninham BW. Theory of self-assembly of lipid bilayers and vesicles. *Biochim Biophys Acta*, **1977**, 470: 185–201.
- [162] Gebicki JM, Hicks M. Ufasomes are stable particles surrounded by unsaturated fatty acid membranes. *Nature*, **1973**, 243: 232–234.
- [163] C. Rocaboy, W. Bauer, J. A. Gladysz, *Eur. J. Org. Chem.* **2000**, 2621–2628.
- [164] M.F. Strozhev, I.E. Lielbriedis, O.Ya. Neiland, *Chem. Heterocycl. Compd.* 26 (1990) 655–657.
- [165] A. Morales, E. Ochoa, M. Suarez, Y. Verdecia, L. Gonzalez, *J. Heterocycl. Chem.* **33** (**1996**) 103–107.
- [166] E. De Clercq, *Farmaco* 54 (**1999**) 26–45.
- [167] R.L.T. Parreira, O. Abrahao, S.E. Galembeck, *Tetrahedron* 57 (**2001**) 3243–3253.
- [168] G. Pastelin, R. Mendez, E. Kabela, A. Farah, *Life Sci.* **33** (**1983**) 1787–1796
- [169] W.K. Anderson, D.C. Dean, T. Endo, *J. Med. Chem.* **33** (**1990**) 1667–1675.
- [170] S.B. US Patent 5,962,478 (**1999**).
- [171] Q. Li, L.A. Mitscher, L.L. Shen, *Med. Res. Rev.* **20** (**2000**) 231–293.
- [172] P.S. Dragovich, T.J. Prins, R. Zhou, E.L. Brown, F.C. Maldonado, S.A. Fuhrman, L.S. Zalman, T. Tuntland, C.A. Lee, A.K. Patick, D.A. Matthews, T.S. Hendrickson, M.B. Kosa, B. Liu, M.R. Batugo, J.P.R. Gleeson, S.K. Sakata, L. Chen, M.C. Guzman, J.W. Meador III, R.A. Ferre, S.T. Worland, *J. Med. Chem.* **45** (**2002**) 1607–1623.
- [173] P.S. Dragovich, T.J. Prins, R. Zhou, T.O. Johnson, E.L. Brown, F.C. Maldonado, S.A. Fuhrman, L.S. Zalman, A.K. Patick, D.A. Matthews, X. Hou, J.W. Meador, R.A. Ferre, S.T. Worland, *Bioorg. Med. Chem. Lett.* **12** (**2002**) 733–738.
- [174] S.J. Patankar, P.C. Jurs, *J. Chem. Inf. Comput. Sci.* **42** (**2002**) 1053–1068.
- [175] Z. Hyvonen, A. Plotniece, I. Reine, B. Chekavichus, G. Duburs, A. Urtti, *Biochim. Biophys. Acta, Biomembranes* 1509 (**2000**) 451–466.
- [176] M.P. Krafft, F. Giulieri, J.G. Riess, *Angew. Chem. Int. Ed. Engl.* **32** (**1993**) 741–743.
- [177] M.P. Krafft, *J. Polym. Sci. Part A: Polym. Chem.* **44** (**2006**) 4251–4258.
- [178] Verdecia, Y.; Suárez, M.; Morales, A.; Rodríguez, E.; Ochoa, E.; González, L.; Martín, N.; Quinteiro, M.; Seoane, C.; Soto, J.L. Synthesis of methyl 4-aryl-6-methyl-4,7-dihydro-1H-pyrazolo[3,4-b]pyridine-5-carboxylates from methyl 4-aryl-6-methyl-2-oxo-1,2,3,4-tetrahydropyridine-5-carboxylates. *J. Chem. Soc. Perkin Trans. 1* **1996**, 947–951.
- [179] Hans-Joachim Lehmler, Rama Rao V.V.V.N.S., Dhananjaya Nauduri, John D. Vargo, Sean Parkin, *Journal of Fluorine Chemistry* **128**, **2007**, 595–607.
- [180] H.-J. Lehmler, S. Parkin, C.P. Brock, *Acta Cryst. B* **60** (**2004**) 325–332.
- [181] C.W. Bunn, E.R. Howells, *Nature* **174** (**1954**) 549–551.
- [182] Banerjee, S. D.; Sengupta, P.; Das Gupta, S. K. Investigation on the by-product obtained in the copecknoevenagel condensation of ethyl α -acetoglutarate with ethyl cyanoacetate. *J. Org. Chem.* **1954**, **19**, 1516–1517.
- [183] Carla Andréia Miranda da Costa and Ângela Maria Moraes, *Acta Scientiarum. Technology*, v. 25, no. 1, p. 53–61, **2003**.

- [184] Z.A. Kalme, R.A. Zhalubovskis, A. Shmidlers, J. Celmins, G. Duburs, *Chem. Heterocycl. Compd.* **40** (2004) 862–868.
- [185] A Guide to Organic Chemistry Mechanisms,
<http://orgo.curvedarrow.com/punbb/viewtopic.php?id=198>.
- [186] (a) Morales, A.; Ochoa, E.; Suarez, M.; Verdecia, Y.; Gonzales, L.; Martin, N.; Quinteiro, M.; Seoane, C.; Soto, J. L. Novel hexahydrofuro[3,4-*b*]-2(1*H*)-pyridones from 4-aryl substituted 5-alkoxycarbonyl-6-methyl-3,4-dihydropyridones. *J. Heterocycl. Chem.* **1996**, *33*, 103–107.
 (b) Ochoa, E.; Suarez, M.; Verdecia, Y.; Pita, B.; Martin, N.; Quinteiro, M.; Seoane, C.; Soto, J. L.; Duque, J.; Pomes, R. Structural study of 3,4-dihydropyridones and furo[3,4-*b*]-2(1*H*)-pyridones as potential calcium channel modulators. *Tetrahedron.* **1998**, *54*, 12409–12420.
- [187] Kalme, Z. A.; Zhalubovskis, R. A.; Shmidlers, A.; Celmins, J.; Duburs, G. Synthesis of 6-Bromomethyl-substituted Derivatives of Pyridin-2(1*H*)-ones and Their Reaction with Nucleophiles *Chem. Heterocycl. Compd.* **2004**, *40*, 862–868.
- [188] Petrova, M.; Muhamadejev, R.; Vigante, B.; Cekavicus, B.; Plotniece, A.; Duburs, G.; Liepinsh, E. Intramolecular C-H···O Hydrogen Bonding in 1,4-Dihydropyridine Derivatives. *Molecules.* **2011**, *16*, 8041–8052.
- [189] J. Sitterberg, A. Ozcetin, C. Ehrhardt, U. Bakowsky, *Eur. J. Pharm. Biopharm.* **74** (2010) 2–13.
- [190] E.I. Goksu, J.M. Vanegas, C.D. Blanchette, W.C. Lin, M.L. Longo, *Biochim. Biophys. Acta* **1788** (2009) 254–266.
- [191] S.K. Brar, M. Verma, *Trends Anal. Chem.* **30** (2011) 4–17.
- [192] K. Matsuoka, Y. Moroi, *Curr. Opin. Colloid Interface Sci.* **8** (2003) 221–235.
- [193] Bocker, R. H.; Guengerich, P. J. *Med. Chem.* **1986**, *29*, 1596–1603.
- [194] Itoh, T.; Nagata, K.; Matsuya, Y.; Miyazaki, M.; Ohsawa, A. *J. Org. Chem.* **1997**, *62*, 3582–3585.
- [195] Turovska, B.; Stradins, J.; Turovskis, I.; Plotniece, A.; Shmidlers, A.; Duburs, G. *Chem. Heterocycl. Comp.* **2004**, *40*, 753–758.
- [196] Baumane, L.; Krauze, A.; Belyakov, S.; Sile, L.; Chernova, L.; Griga, M.; Duburs, G.; Stradins, J. *Chem. Heterocycl. Comp.* **2005**, *41*, 362–373.
- [197] Garcí'a Rosales, A.; Ruiz Montoya, M.; Mari'n Galvi'n, R.; Rodr'iguez Mellado, J. M. *Electroanalysis* **1999**, *11*, 32–36.
- [198] Stradins, J.; Ogle, J.; Kadysh, V.; Baumane, L.; Gavars, R.; Duburs, G. *J. Electroanal. Chem.* **1987**, *226*, 103–116.
- [199] Ogle, J.; Stradins, J.; Baumane, L. *Electrochim. Acta* **1994**, *39*, 73–79.
- [200] El Jemal, A.; Vire', J. C.; Patriarche, G. J.; Nieto Palmeiro, O. *Electroanalysis* **1992**, *4*, 57–64.
- [201] Ludvik, J.; Turecek, F.; Volke, J. J. *Electroanal. Chem.* **1985**, *188*, 105–109.
- [202] J. Nuñez-Vergara, L.; Sturm, J. C.; Alvarez-Lueje, A.; Olea-Azar, C.; Sunkel, C.; Squella, J. A. *J. Electrochem. Soc.* **1999**, *146*, 1478–1485.
- [203] Nuñez-Vergara, L. J.; Ortiz, M. E.; Bollo, S.; Squella, J. A. *Chem. Biol. Interact.* **1997**, *106*, 1–14.
- [204] López-Alarco'n, C.; Squella, J. A.; Miranda-Wilson, D.; Nuñez-Vergara, L. J. *Electroanalysis* **2004**, *16*, 539–546.

- [205] Lo'pez-Alarco' n, C.; Nu'nez-Vergara, L. J.; Squella, J. A. *Electrochim. Acta* **2003**, *48*, 2505–2516.
- [206] Nu'nez-Vergara, L. J.; Lo'pez-Alarco' n, C.; Navarrete-Encina, P. A.; Atria, A. M.; Camargo, C.; Squella, J. A. *Free Radic. Res.* **2003**, *37*, 109–120.
- [207] Sobal, G.; Menzel, E. J.; Sinzinger, H. *Biochem. Pharmacol.* **2001**, *61*, 373–379.
- [208] Berkels, R.; Breitenbach, Th.; Bartels, H.; Taubert, D.; Rosenkranz, A.; Klaus, W.; Roesen, R. *Vas. Pharmacol.* **2005**, *42*, 145–152.
- [209] Cominacini, L.; Pasini, A. F.; Garbin, U.; Pastorino, A. M.; Davoli, A.; Nava, C.; Campagnola, M.; Rossato, P.; Lo Cascio, V. *Biochem. Biophys. Res. Commun.* **2003**, *302*, 679–684.
- [210] Yan'ez, C.; Lo'pez-Alarco' n, C.; Camargo, C.; Valenzuela, V.; Squella, J. A.; Nu'nez-Vergara, L. J. *Bioorg. Med. Chem.* **2004**, *12*, 2459–2468.
- [211] Tong Mak, I.; Zhang, J.; Weglicki, W. B. *Pharmacol. Res.* **2002**, *45*, 27–33.
- [212] van Amsterdam, F. T. M.; Roveri, A.; Maiorino, M.; Ratti, E.; Ursini, F. *Free Radic. Biol. Med.* **1997**, *12*, 183–187.
- [213] Luis J. Nu'nez-Vergara, R. Salazar, C. Camargo, J. Carbajo, B. Conde, P. A. Navarrete-Encinac and J. A. Squella, *Bioorganic & Medicinal Chemistry* *15*, **2007**, 4318–4326.
- [214] Liu, Q.; Li, J.; Shen, X.-X.; Xing, R.-G.; Yang, J.; Liu, Z.; Zhou, B. *Tetrahedron Lett.* **2009**, *50*, 1026-1028.
- [215] J. Arguello, L.J. Nu'nez-Vergara, J.C. Sturm, J.A. Squella. *Electrochimica Acta* Volume 49, Issue 27, 30 October **2004**, Pages 4849–4856.
- [216] A. Plotniece, K. Pajuste, D. Kaldre, B. Cekavicus, B. Vigante, B. Turovska, S. Belyakov, A. Sobolev, G. Duburs, *Tetrahedron* *65* (**2009**) 8344-8349.
- [217] Kadysh, V.P.; Stradyn, Ya. P.; Ogle, Ya. V.; Pelcher Yu. E.; Dubur Ya. G. *Electrochemical Oxidation of Substituted 3,4-Dihidro-2-Pyridones at a Rotating Graphite Electrode with a Ring. J. Khim. Geterocikl. Soed.* **1984**, 73-77.
- [218] Aleksandra Simić, Dragan Manojlović *, Dejan Šegan and Marija Todorović, *Molecules* **2007**, *12*, 2327-2340.
- [219] F. Himo, T. Lovell, R. Hilgraf, V. V. Rostovtsev, L. Noodleman, K. B. Sharpless, V. V. Fokin, *J. Am. Chem. Soc.*, **2005**, *127*, 210-216.
- [220] M. Pietrzak, A.C. Try, B. Andrioletti, J.L. Sessler, P. Anzenbacher Jr., H-H. Limbach, *Angew Chem Int Ed Engl.* **2008** ; *47*(6): 1123–1126.
- [221] a) Black CB, Andrioletti B, Try AC, Ruiperez C, Sessler JL. *J Am Chem Soc* **1999**; *121*:10438–10439. b) Sessler JL, Pantos GD, Katayev E, Lynch VM. *Org Lett* **2003**; *5*:4141–4144. c) Sessler JL, Maeda H, Mizuno T, Lynch VM, Furuta H. *J Am Chem Soc* **2002**; *124*:13474–13479. d) Sessler JL, Maeda H, Mizuno T, Lynch VM, Furuta H. *Chem Commun* **2002**:862–863.
- [222] Vilsmeier, A.; Haack, A. *Berichte* **1927**, *60*, 119.
- [223] (a) Massa, C. M. *Tetrahedron* **1992**, *48*, 3659. (b) Jutz, C. In *Advances in Organic Chemistry*, 9; Taylor, E. C., Ed.; Wiley: New York, **1976**, 225. (c) Seshadri, S. *J. Sci. Ind. Res.* **1973**, *32*, 128.
- [224] Ramesh, E.; Sree Vidhya, T. K.; Raghunathan, R. *Tetrahedron Lett.* **2008**, *49*, 2810.
- [225] Kidwai, M.; Negi, N. *Monatsh. Chem.* **1997**, *128*, 85.
- [226] Cohen, B. W.; Polyansky, D. E.; Zong, R.; Zhou, H.; Ouk, T.; Cabelli, D. E.; Thummel, R.P.; Fujita, E. *Inorganic Chem.* **2010**, *49*, 8034.

- [227] Rajakumar, P.; Raja, R. *Tetrahedron Lett.* **2010**, *51*, 4365.
- [228] Venkatesan, P.; Sumathi, S. *J. Heterocycl. Chem.* **2010**, *47*, 81.
- [229] Srivastava, A.; Singh, R. M. *Indian J. Chem.* **2005**, *44B*, 1868.
- [230] Nyerges, M.; Pinter, A.; Viranyi, A.; Gabor, B.; Toke, L. *Tetrahedron* **2005**, *61*, 8199.
- [231] Krishnan, V. S. H.; Dubey, P. K.; Rao, S. S.; Aparna, V. *Indian J. Heterocycl. Chem.* **2003**, *13*, 11.
- [232] Krishnan, V. S. H.; Dubey, P. K.; Rao, S. S.; Reddy, P. V. P. *Indian J. Heterocycl. Chem.* **2003**, *13*, 5.
- [233] Dubey, P. K.; Rao S. S.; Reddy, P. V. P. *Indian Heterocycl. Commun.* **2003**, *9*, 411.
- [234] Mogilaiah, K.; Reddy, N. V.; Rao, R. B. *Indian J. Heterocycl. Chem.* **2002**, *11*, 253.
- [235] Ali, M. M.; Sana, S.; Tasneem, R. K. C.; Saiprakash, P. K. *Synth. Commun.* **2002**, *32*, 1351.
- [236] Álvarez, A.; Suárez, M.; Verdecia, Y.; Ochoa, E.; Barrie, B.; Pérez, R.; Díaz, M.; Martínez-Álvarez, R.; Molero, D.; Seoane, C.; *et al.* Synthesis and structural study of semicarbazone-containing 1,4-dihydropyridine. *Heterocycles* **2006**, *68*, 1631-1649.
- [237] Suárez, M.; Verdecia, Y.; Illescas, B.; Martínez-Alvarez, R.; Álvarez, A.; Ochoa, E.; Seoane, C.; Kayali, N.; Martin, N. Synthesis and study of novel fulleropyrrolidines bearing biologically active 1,4-dihydropyridines. *Tetrahedron* **2003**, *59*, 9179-9186.
- [238] Suárez, M.; Martin, N.; Martínez, R.; Verdecia, Y.; Molero, D.; Alba, L.; Seoane, C.; Ochoa, E. *Magn. Reson. Chem.* **2002**, *40*, 303-306.
- [239] Hortensia Rodríguez, Osneski Martin, Margarita Suarez, Nazario Martín and Fernando Albericio, *Molecules* **2011**, *16*, 9620-9635.
- [240] Suárez, M., Novoa, H., Verdecia, Y., Ochoa, E., Alvarez, A., Perez, R., Martin, N., *Tetrahedron* **2006**, *62*, 1365-1371.
- [241] Zonouz, A. M.; Moghani, D. Synthesis of 1,4-dihydropyridine derivatives under solvent-free and grinding conditions. *Syn. Commun.* **2011**, *41*, 2152-2160.
- [242] (a) Foye, W. O. *Principi di Chemico Farmaceutica*; Piccin: Padora, Italy, **1991**, p 416; (b) Andreani, L. L.; Lapi, E. On some esters of coumarin-3-carboxylic acid with balsamic bronchodilator action. *Bull. Chim. Farm.* **1960**, *99*, 583-586; (c) Zhang, Y. L.; Chen, B. Z.; Zeng, K. Q.; Xu, M. L.; Lei, X. H.; Yaoxue, X. B. *Chem. Abstr.* **1982**, *17*, 17. *Chem. Abstr.* **1982**, *96*, 135383e; (d) Bonsignore, L; Loy, G.; Secci, D.; Calignano, A. Synthesis and pharmacological activity of 2-oxo-(2H) 1-benzopyran-3-carboxamide derivatives. *Eur. J. Med. Chem.* **1993**, *28*, 517-520.
- [243] Kuthan, J. Pyrans, Thiopyrans, and Selenopyrans. *Adv. Heterocycl. Chem.* **1983**, *34*, 145-303.
- [244] Hatakeyama, S.; Ochi, N.; Numata, H.; Takano, S. A new route to substituted 3-methoxycarbonyldihydropyrans enantioselective synthesis of (-)-methyl enolate. *J. Chem. Soc. Chem. Commun.* **1988**, 1202-1204.
- [245] Witte, E. C.; Neubert, P.; Roesch, A. *Ger. Offen.* DE3427985 **1986**.
- [246] Wang, J.L.; Liu, D.; Zhang, Z. J.; Shan, S.; Han, X.; Srinivasula, S. M.; Croce, C. M.; Alnemri, E. S.; Huang, Z. Structure-based discovery of an organic compound that binds Bcl-2 protein and induces apoptosis of tumor cells. *Proc. Natl. Acad. Sci. U.S.A.* **2000**, *97*, 7124-7129.
- [247] El-Saghier, A. M. M.; Naili, M. B.; Rammash, B. Kh.; Saleh, N. A.; Kredan, K. M. Synthesis and antibacterial activity of some new fused chromenes. *Arkivoc* **2007**, xvi, 83-91.
- [248] Kumar, R. R.; Perumal, S.; Senthilkumar, P.; Yogeewari, P.; Sriram, D. *Bioorg. Med. Chem. Lett.* **2007**, *17*, 6459-6462.

- [249] Kumar, D.; Reddy, V. B.; Sharad, S.; Dube, U.; Kapur, S. A facile one-pot green synthesis and antibacterial activity of 2-amino-4*H*-pyrans and 2-amino-5-oxo-5,6,7,8-tetrahydro-4*H*-chromenes. *Eur. J. Med. Chem.* **2009**, 44, 3805-3809.
- [250] Suarez, M.; Slafran, E.; Verdecia, Y.; Ochoa, E.; Alba, L.; Martin, N.; Martinez, R.; Quinteiro, M.; Seoane, C.; Novoa, H.; Blaton, N.; Peeters, O. M.; De Ranter, C. *Tetrahedron* **2002**, 58, 953-960.
- [251] Banerjee, S.; Horn, A.; Khatri, H.; Sereda, G. *Tet. Lett.* **2011**, 52, 1878-1881.
- [252] Heravi, M. M.; Beheshtiha, Y. S.; Piernia, Z.; Sadjadi, S.; Adibi, M. *Syn. Commun.* **2009**, 39, 3663-3667.
- [253] Sobczyk, L.; Grabowski, S.J.; Krygowski, T.M. *Chem. Rev.* **2005**, (105), 3513.
- [254] Perrin, C.L.; Nielson, J.B. *Annu. Rev. Phys. Chem.* **1997**, (48), 511.
- [255] Hargis, J.C.; Evangelista, F.A.; Ingels, J.B.; Schaefer, H.F. *J. Am. Chem. Soc.* **2008**, (130), 17471-17478.
- [256] Suarez, M.; Verdecia, Y.; Ochoa, E.; Martin, N.; Martinez, R.; Quinteiro, M.; Seoane, C.; Soto, J. L.; Novoa, H.; Blaton, N.; Peeters, O. M.; De Ranter, C. Synthesis and structural study of novel 1,4,5,6,7,8-hexahydroquinolones. *J. Heterocyclic Chem.* **2000**, 37, 735-742.
- [257] Shujiang Tu, Jinpeng Zhang, Xiaotong Zhu, Yan Zhang, Qian Wang, Jianing Xu, Bo Jiang, Runhong Jia, Junyong Zhang, Feng Shi, *J. Heterocyclic Chem.* **2006**, 43, 985-988.
- [258] F.H. Matteson, R.A. Volpenheim, *J. Lipid Res.* 13 (**1972**) 325.
- [259] C.C. Akoh, *Crit. Rev. Food Sci. Nutr.* 35 (**1995**) 405.
- [260] G.W. Buchanan, R. Smits, E. Munteanu, *J. Fluorine Chem.* (**2003**), 119(2), 207-209.
- [261] G.W. Buchanan, R. Smits, E. Munteanu, *J. Fluorine Chem.* 123 (**2003**) 255-259.
- [262] G.W. Buchanan, R. Smits, E. Munteanu, G. Santyr, J. Wallace, M.-R. Gherase, *J. Fluorine Chem.* 125 (**2004**) 1457.
- [263] M. Albert, G. Cates, B. Driehuys, W. Happer, B. Saam, C.S. Springer, A. Wishnia, *Nature* 370 (**1994**) 199.
- [264] H.E. Moller, M.S. Chawla, X.J. Chen, B. Driehuys, K.C. Hasson, L.W. Hedlund, C.T. Wheeler, G.A. Johnson, *Magn. Reson. Med.* 41 (**1999**) 1058.
- [265] R. Schwartz, M. Schuurmans, J. Seelig, B. Kunnecke, *Magn. Reson. Med.* 41 (**1999**) 80.
- [266] G.W. Buchanan, I. Moudrakosvski, *J. Fluorine Chem.* 129 (**2008**) 137-138.

Additions

APLIECINĀJUMS

Ar šo es apliecinu, ka šodien iesniegto promocijas darbu esmu veicis pats izmantojot tikai tajā norādītos informācijas avotus.

Rīga (27. 08. 2012)

Promocijas darbs izstrādāts Latvijas Organiskās sintēzes institūtā Membrānaktīvo savienojumu un β -diketonu laboratorijā.

Autors:

Rufs Šmits

Zinātniskā vadītāja:

Brigita Vīgante

Darbs iesniegts Latvijas Universitātes Ķīmijas nozares promocijas padomei
2012. gada 27. Augustā.

Darbu pieņēma: